THE EFFECTS AND MECHANISMS OF THERAPEUTIC HYPOTHERMIA ON INTRACRANIAL PRESSURE REGULATION FOLLOWING ISCHAEMIC STROKE IN RATS

Lucy Anne Murtha

BBiomedSci (Hons)

Thesis by publication submitted for the degree of

Doctor of Philosophy (Human Physiology)

School of Biomedical Sciences and Pharmacy

Faculty of Health and Medicine

University of Newcastle

September, 2014

I, Lucy Murtha, hereby declare that this thesis contains no material which has been accepted for the award of any other degree or diploma in any university or other tertiary institution and, to the best of my knowledge and belief, contains no material previously published or written by another person, except where due reference has been made in the text. I give consent to the final version of my thesis being made available worldwide when deposited in the University's Digital Repository, subject to the provisions of the Copyright Act 1968.

I hereby certify that the work embodied in this thesis has been done in collaboration with other researchers, or carried out in other institutions. I have included as part of my thesis a statement clearly outlining the extent of collaboration, with whom and under what auspices.

I hereby certify that this thesis is submitted in the form of a series of published papers of which I am a joint author. I have included as part of the thesis a written statement from each co-author, endorsed by the Faculty Assistant Dean (Research Training), attesting to my contribution to the joint publications.

Lucy Murtha

September, 2014

ACKNOWLEDGEMENTS

I would like to thank my supervisors Dr. Neil Spratt and Dr. Damian McLeod. I thank Neil for his invaluable support and wealth of medical and physiological knowledge. His dedication and passion for his work is to be truly admired. I thank him for his tireless efforts to constantly improve this project with fantastic ideas. Damian's knowledge and enthusiasm for science is truly inspiring and I sincerely thank him for his support and encouragement. Damian's help throughout this candidature could not be more greatly appreciated. To the Spratt Lab Team: I thank you all for keeping me sane, and for your continuous and immeasurable help and support. I thank you for all the laughs, the 'interesting' lunch time discussions and for helping me procrastinate so well! This project would not have been possible without you!!

I would sincerely like to thank Prof. Mhairi Macrae for allowing me to study with her in Scotland and for all her invaluable ideas and support. I would also like to thank all involved in making the Scottish component of this thesis a success, in particular Lindsay Gallagher, Chris McCabe, William Holmes and Jim Mullin for all their help. Special thanks must go to the men in the University of Newcastle workshop. This thesis would not have been possible without their creative genius. I also thank Emlyn and Jennie Thomas for the generous scholarship, hugs and lovely family morning teas!!

Finally I would like to thank my friends, family and the wonderful Ben Burton for their unwavering support throughout this ambitious project. You all helped to make these years as stress-free as possible and it is truly appreciated!

PUBLICATIONS INCLUDED IN THIS THESIS

Publication 1

Murtha L, McLeod D, Spratt N. Epidural intracranial pressure measurement in rats using a fiber-optic pressure transducer. *J Vis Exp*. e3689, doi:10.3791/3689. (2012).

Publication 2

Murtha L, McLeod D, McCann S, Pepperall D, Chung S, Levi C, Calford M, Spratt N. Short-duration hypothermia after ischemic stroke prevents delayed intracranial pressure rise. *Int J Stroke.* 9, 553-559, doi:10.1111/ijs.12181. (2014).

Publication 3

Murtha L, McLeod D, Beard D, Pepperall D, McCann S, Tomkins A, Holmes W, McCabe C, Macrae I.M, Spratt N. Intracranial pressure elevation following ischemic stroke in rats: Cerebral edema is not the only cause, and short-duration mild hypothermia is a highly effective preventive therapy. Submitted to *JCBFM* - Awaiting Review. (2014).

Publication 4

Beard D, McLeod D, Logan C, **Murtha L**, Imtiaz M, van Helden D, Spratt N. Intracranial pressure elevation reduced flow through collateral vessels and the penetrating arterioles they supply. A possible explanation for 'Collateral Failure' in Stroke-in-Progression. Submitted to *JCBFM* - Awaiting Review. (2014).

PUBLICATIONS INCLUDED IN THE APPENDIX OF THIS THESIS

Publication 5

Murtha L, Yang Q, Parsons M, Levi C, Beard D, Spratt N, McLeod D. Cerebrospinal fluid is drained primarily via the spinal canal and olfactory route in young and aged spontaneously hypertensive rats. *Fluids Barriers CNS*. 11:12, doi:10.1186/2045-8118-11-12. (2014).

Publication 6

McLeod D, Parsons M, Hood R, Hiles B, Allen J, McCann S, **Murtha L**, Calford M, Levi C, Spratt N. Perfusion computed tomography thresholds defining ischemic penumbra and infarct core: studies in a rat stroke model. *Int J Stroke*. doi: 10.1111/ijs.12147. (2013). [E-Pub ahead of print]

CONFERENCE PUBLICATIONS AND PRESENTATIONS ARISING FROM THIS THESIS

Murtha L, McLeod D, Beard D, McCabe C, Holmes W, Macrae IM, Spratt N. Is cerebral oedema really the primary cause of intracranial pressure elevation following stroke? Conference: Seminar Series, School of Biomedical Sciences and Pharmacy. University of Newcastle, Australia, August 2014. (Oral Presentation)

Murtha L, McLeod D, Beard D, McCabe C, Holmes W, Macrae IM, Spratt N. Is cerebral oedema really the primary cause of intracranial pressure elevation following stroke? Conference: Australian Society for Medical Research NSW Conference. Sydney, Australia, June 2014. (Oral Presentation)

Beard D, McLeod D, **Murtha L**, Spratt N. Elevation of intracranial pressure reduces leptomeningeal collateral and watershed blood flow during experimental stroke. *Cerebrovasc Dis*. 37:1–4. DOI: 10.1159/000357550. Conference: European Stroke Society. Nice, France, May 2014. (Oral Presentation)

Murtha L, McLeod D, Beard D, Pepperall D, Spratt N. Short duration mild hypothermia prevents delayed intracranial pressure rise following experimental ischaemic stroke. *Cerebrovasc Dis*. 37:1–4. DOI: 10.1159/000357550. Conference: European Stroke Society. Nice, France, May 2014. (E-Poster Presentation)

McLeod D, **Murtha L**, Logan C, Beard D, Hood R, Pepperall D, Spratt N. Intracranial pressure elevation 24 hours after minor stroke is not caused by oedema and is triggered by factor(s) is cerebrospinal fluid. Conference: 8th International Symposium of Neuroprotection and Neurorepair. Magdeburg, Germany, March 2014. (Poster Presentation)

Murtha L, McLeod D, McCabe C, Holmes W, Macrae IM, Spratt N (2014). Is cerebral oedema really the primary cause of intracranial pressure elevation following stroke? Conference: 8th International Symposium of Neuroprotection and Neurorepair. Magdeburg, Germany, March 2014. (Poster Presentation)

Murtha L, McLeod D, Beard D, McCabe C, Holmes W, Macrae IM, Spratt N. Is cerebral oedema really the primary cause of intracranial pressure elevation following stroke? Conference: Australian Society for Medical Research Newcastle Conference. Newcastle, Australia, March 2014. (Oral Presentation)

Murtha L, McLeod D, McCabe C, Holmes W, Macrae IM, Spratt N (2014). Cerebral oedema: Not the primary cause of ICP elevation following ischaemic stroke. Conference: Australian Neuroscience Society Annual Meeting. Adelaide, Australia, January 2014. (Oral Presentation)

McLeod D, **Murtha L**, Bourke J, Pitsillides K. Biotelemetry of intracranial pressure in freely moving rats: a detailed description of surgical implantation for chronic studies. *FASEB Journal.* 27:700.11. Conference: Experimental Biology. Boston, USA, April 2013. (Poster Presentation)

Murtha L, McLeod D, Spratt N. Effects of short duration hypothermia on intracranial pressure following ischaemic stroke. Conference: 7th International Symposium on Neuroprotection and Neurorepair. Potsdam, Germany, May 2012. (Poster Presentation)

Tomkins A, **Murtha L**, McCann S, Pepperall D, Levi C, Spratt N. Thromboembolic stroke with site-specific delivery of platelet rich clots. Conference: 7th International Symposium on Neuroprotection and Neurorepair. Potsdam, Germany, May 2012. (Poster Presentation)

McLeod D, **Murtha L**, Pitsillides K. A new method of attaching a solid-state pressure sensor for measurement of chronic intracranial pressure in freely moving rats using biotelemetry. *FASEB Journal.* 26:1098.14. Conference: Experimental Biology. San Diego, USA, April 2012. (Poster Presentation)

Murtha L, McLeod D, Spratt N. The effects of therapeutic hypothermia on intracranial pressure after experimental ischaemic stroke. Conference: Australian Neuroscience Society Annual Meeting. Gold Coast, Australia, January 2012. (Poster Presentation)

Murtha L, McLeod D, Spratt N. The effects of therapeutic hypothermia on intracranial pressure after experimental ischaemic stroke in rats. Conference: Centre for Brain and Mental Health Conference. Newcastle, Australia, November 2011. (Oral Presentation)

Murtha L, McCann S, Pepperall D, McLeod D, Spratt N. Short duration hypothermia results in sustained prevention of intracranial pressure elevation following experimental stroke. *Int J Stroke*. 6(Suppl 1):31. Conference: 22nd Annual Scientific Meeting of the Stroke Society of Australasia. Adelaide, Australia, September 2011. (Oral Presentation)

WORK ARISING FROM COLLABORATIONS ASSOCIATED WITH THIS THESIS

Ariana Arulampalam. The fluid compartments of the brain after ischaemic stroke in rats and humans. School of Medicine and Public Health, Faculty of Health and Medicine, University of Newcastle; Bachelor of Medical Science, Honours; 2011

Rebecca Hood. The role of cerebrospinal fluid in intracranial pressure regulation after stroke. School of Biomedical Sciences and Pharmacy, Faculty of Health and Medicine, University of Newcastle; Bachelor of Biomedical Science, Honours; 2012

Julia Bourke. The effect of short-duration hypothermia on intracranial pressure after stroke in aged rats. School of Medicine and Public Health, Faculty of Health and Medicine, University of Newcastle; Bachelor of Medical Science, Honours; 2012

Caitlin Logan. The effects of cerebrospinal fluid factors on intracranial pressure regulation following ischaemic stroke. School of Biomedical Sciences and Pharmacy, Faculty of Health and Medicine, University of Newcastle; Bachelor of Biomedical Science, Honours; 2013

Jacqueline Montano. Investigating the effect of intracranial compliance on intracranial pressure rise in ischaemic and subarachnoid haemorrhage stroke. Department of Biomedicine, Karolinska Institute, Sweden; Bachelor of Medical Science Majoring in Biomedicine, Honours; 2014 (Co-supervisor)

AWARDS, SCHOLARSHIPS AND GRANTS ARISING FROM WORK ASSOCIATED WITH THIS THESIS

Awarded to Lucy Murtha

Best student oral presentation, ASMR Conference- Sydney: $500; 2014. **Lucy Murtha**. *Is cerebral oedema really the primary cause of intracranial pressure elevation following stroke?*

Emlyn & Jennie Thomas Postgraduate Medical Research Scholarship: $25,000; 2012. **Lucy Murtha.** *The effects and mechanisms of therapeutic hypothermia on intracranial pressure following ischaemic stroke.*

UoN School of Biomedical Sciences and Pharmacy top-up Scholarship: $14,000; 2011. **Lucy Murtha**. T*he effects and mechanisms of therapeutic hypothermia on intracranial pressure regulation following ischaemic stroke in rats.*

Grants to Spratt Laboratory Based Largely on Work from this Thesis

National Stroke Foundation Research Grant: $19,275; 2014. Damian McLeod, Neil Spratt. *Cooling the brain via the skin to prevent intracranial pressure elevation after stroke.*

University of Newcastle Near Miss Grant: $10,000; 2014. Neil Spratt. *Effects of intracranial pressure on collateral blood flow after stroke: a new pathophysiological mechanism and potential therapy.*

John Hunter Charitable Trust Grant: $20,218; 2013. Ferdinand Miteff, Neil Spratt, **Lucy Murtha**, Peter Stanwell. *Skin cooling to reduce intracranial pressure: a paradigm shift in understanding and therapy?*

National Stroke Foundation Research Grant: $20,000; 2013. Damian McLeod, Neil Spratt. *Novel mechanisms of 'Stroke-in-Progression': Intracranial pressure elevation and collateral blood vessel failure after minor stroke.*

National Health and Medical Research Council: $429,453; 2012. Neil Spratt. *Short duration hypothermia to prevent subsequent intracranial pressure rise.*

Hunter Medical Research Institute Research Grant: $20,000; 2012. Damian McLeod, Neil Spratt, Mark Parsons, Christopher Levi. *Experimental brain imaging to investigate novel protective mechanisms of short duration body cooling after stroke.*

Hunter Medical Research Institute Research Grant: $15,000; 2012. Neil Spratt. *Telemetry measurement of Intracranial Pressure in Stroke and Hypothermia.*

TABLE OF CONTENTS ***Page***

DECLARATION *i*

ACKNOWLEDGEMENTS *ii*

THESIS PUBLICATIONS *iii*

APPENDIX PUBLICATIONS *iv*

CONFERENCE PRESENTATIONS *v*

COLLABORATIONS *viii*

AWARDS, SCHOLARSHIPS & GRANTS *ix*

ABSTRACT *1*

CHAPTER 1: LITERATURE REVIEW *3*

1.1 Introduction *3*
1.2 Current Acute Stroke Therapies *4*
1.3 Intracranial Pressure *6*
1.3.1 Intracranial Pressure and Cerebral Oedema *7*
1.3.2 Intracranial Pressure and Cerebrospinal Fluid *9*
1.3.3 Intracranial Pressure and Cerebral Blood Volume *10*
1.4 Leptomeningeal Collateral Vessels *11*
1.5 Hypothermia *15*
1.6 Hypothermia and Intracranial Pressure *19*
1.7 Animal models of Stroke and ICP *20*
1.8 Rationale *22*

CHAPTER 2: RESEARCH AIMS AND HYPOTHESES *25*

CHAPTER 3: PUBLICATION 1 *26*

3.1 Introduction *26*
3.2 Contributions *28*
3.3 Publication: Epidural ICP measurement methodology *29*

CHAPTER 4: PUBLICATION 2 *36*

4.1 Introduction *36*
4.2 Contributions *38*
4.3 Publication: Hypothermia prevents ICP rise post-stroke *40*

CHAPTER 5: PUBLICATION 3 *47*

5.1 Introduction *47*
5.2 Contributions *49*
5.3 Publication: Oedema is not the cause of ICP rise post-stroke *51*

CHAPTER 6: PUBLICATION 4 *86*

6.1 Introduction *86*
6.2 Contributions *88*
6.3 Publication: ICP rise reduces collateral blood flow *90*

CHAPTER 7: DISCUSSION *127*

CHAPTER 8: CONCLUSIONS *141*

CHAPTER 9: REFERENCES *143*

APPENDIX A: PUBLICATIONS *157*

APPENDIX B: COPYRIGHT PERMISSIONS *175*

ABSTRACT

Background: Intracranial pressure (ICP) rises to dangerous levels 2-5 days after large ischaemic stroke. ICP following small stroke is not routinely monitored, although animal data suggests ICP rises 24 hours following small experimental stroke. Cerebral oedema has been thought to be the primary cause for ICP elevation. This assumption may have risen because ICP has only been monitored in patients with large infarct and oedema volumes. Since small ischaemic infarcts cause less cerebral swelling, ICP elevation may be the result of a different mechanism(s). Recent human imaging data indicates that patients deteriorating soon after minor stroke do so on the basis of cerebral collateral blood flow failure. Until now there has not been a plausible explanation for this 'collateral failure'. Long-duration hypothermia has been shown to lower ICP in patients. Long durations of cooling increase the risk of infection and rebound ICP during rewarming. Short-duration hypothermia has shown overwhelming efficacy in animal models of stroke but has not been tested in humans. I hypothesise: that ICP increases at 24 hours after small stroke; that this rise is not due to cerebral oedema; that ICP elevation reduces collateral blood flow; and that short-duration moderate or mild hypothermia prevents ICP elevation post-stroke.

Methods: An epidural ICP monitoring technique was developed. Experimental ischaemic stroke (middle cerebral artery occlusion) was performed in Long Evans, outbred Wistar and Sprague-Dawley rats and ICP was monitored. Infarct and oedema volumes were calculated using wet-dry weight calculations, histology or *in vivo* magnetic resonance imaging. Collateral blood flow was visualized using fluorescent microspheres through a closed cranial window and recorded using a high-speed

microscope-mounted recording camera. Short-duration moderate (32.5 °C) or mild (35 °C) hypothermia, or normothermia (37°C) was administered 1 hour post-stroke.

Results: Mean ICP was 9.1 ± 5.2 mmHg at baseline (pooled- all animals). ICP was significantly elevated 24 hours post-stroke in all normothermic animals (40.3 ± 16 mmHg, pooled normothermic animals, $p < 0.0001$ vs. baseline). Mean infarct volume was 22.6 ± 17.5% of contralateral hemisphere. Oedema volumes were small and were not correlated with ICP post-stroke ($r^2 = 0.09$, $p = 0.15$). There was a strong correlation between ICP elevation and collateral blood flow decrease ($r = - 0.62$, $p < 0.0001$). Early intervention of short-duration hypothermia completely prevented ICP rise post-stroke (10.3 ± 6.5 mmHg, pooled hypothermic animals at 24 hours, $p < 0.0001$ vs. normothermic animals at 24 hours).

Conclusions: In this thesis, I have presented data that contradicts the accepted wisdom in several ways and has important implications for patients with stroke. It suggests that ICP could be elevated in patients with small stroke and that a factor other than oedema is the primary cause of this ICP elevation. The data also suggest that ICP elevation following stroke is the likely mechanism of collateral failure leading to neurological deterioration in stroke patients. Finally, I have demonstrated that short-duration hypothermia is an effective ICP preventative treatment following experimental stroke, and suggests that short-duration hypothermia clinical studies in humans is warranted. These findings suggest that a fundamental rethink of ICP regulation post-stroke is necessary and have potentially important and exciting implications for the future treatment of stroke and stroke-in-progression.

CHAPTER 1

LITERATURE REVIEW

1.1 INTRODUCTION

Stroke results from a disruption in the blood supply to the brain. This disruption may be due to vessel occlusion (ischaemic stroke), or caused by a rupture to the vessel (haemorrhagic stroke). Ischaemic stroke accounts for approximately 80% of all strokes, and will be the focus of this thesis.

Fifteen million people worldwide suffer from stroke each year[1]. It is the second leading cause of adult death, and the leading cause of adult disability in Australia[2]. It is the third most common underlying cause of death for men and the second most common cause for women. Stroke deaths increase greatly with age, with 82% of deaths occurring in people aged 75 or over in 2011. In 2012, 50 000 Australians suffered new and recurrent strokes, costing the country an estimated $5 billion[3]. As our population ages, this burden is expected to increase greatly, with an estimation that in the next ten years more than half a million Australians will suffer from stroke.

The most beneficial preventative treatment for stroke is risk factor modification[1]. Major modifiable risk factors include high blood pressure, abnormal blood lipids, smoking, physical inactivity, obesity and diabetes mellitus. In 2011, a national stroke audit in Australia showed that these risk factors were common amongst patients

admitted to stroke units; 73% of patients had high blood pressure, 50% had high blood cholesterol, 31% were smokers, and 30% had diabetes[4]. Although each risk factor can occur separately, they often occur in combination. As such, the prevention of stroke primarily involves the reduction of modifiable risk factors by lifestyle changes and/or therapeutic agents. Age-specific incidence of stroke is believed to have fallen over the last 20 years in association with increased use of preventative treatments and reductions in pre-morbid risk factors[5].

1.2 CURRENT ACUTE STROKE THERAPIES

There are two significant regions of tissue injury as a result of an ischaemic insult: core and penumbra. The stroke core is an area of severe ischaemia (blood flow below 10-25% of normal). Cells in this region will die within minutes due to a severe deficiency in energy stores and subsequent ionic disruption and metabolic failure. The stroke core is therefore non-salvageable. Reduction of blood flow within the penumbra is less than that of the core, due to residual blood flow from collateral vessels. Over the years, there have been many definitions of the ischaemic penumbra, differing with new research; however the following definition is generally accepted today: *"ischaemic tissue which is functionally impaired and is at risk of infarction but has the potential to be salvaged by reperfusion and/or other strategies. If not salvaged this tissue is progressively recruited into the infarct core, which will expand with time into the maximal volume originally at risk"*[6].

The concept of neuroprotection is to salvage structurally intact penumbral tissue and limit irreversible ischaemic injury. Thousands of experimental papers have investigated neuroprotection in animals and provided proof-of-principle that protection in the ischaemic brain is achievable, however to date, clinical trials of neuroprotection have not been successful[7]. There are only four currently available acute stroke treatments that have demonstrated clinical evidence of benefit:

Aspirin: The individual patient benefit of aspirin is quite modest. For every 1000 people treated with aspirin, 13 people would avoid death or dependency (number needed to treat 79)[8]. However, aspirin is cost effective, low in toxicity and easy to administer and as such, is commonly administered post-stroke.

Stroke Care Units: The routine management of patients in stroke care units has proven highly successful and effective for all subtypes of stroke, reducing mortality and improving functional outcome by up to 20%[9,10]. However, in 2013, only 39% of Australian hospitals reported having a stroke unit[4].

Thrombolysis: The most biologically effective treatment for acute ischaemic stroke is recombinant tPA, an agent that breaks down clots (thrombolysis) to rapidly reperfuse the ischaemic brain. The therapeutic time window for tPA however, is limited to 4.5 hours from stroke onset, with earlier treatment associated with bigger proportional benefits[11]. This small therapeutic window limits the number of patients who can receive this therapy to roughly 5-10% of all strokes[10], although in some centres with highly organised pre-hospital stroke care rates >20% can be achieved[12].

Decompressive Surgery: One option for an extremely limited number of patients with large infarction and cerebral oedema is to surgically remove part of the skull to create space to accommodate the swollen brain, and consequently reduce intracranial pressure (ICP). Hemicraniectomy however, is not widely used. A recent meta-analysis of European hemicraniectomy trials demonstrated that, although a 59% reduction in case fatality was achieved, it came at the expense of an almost equivalent increase in the number of patients with severe disability[13].

The principle of reducing ICP to limit neurological injury is clinically important yet poorly understood and alternate less invasive ICP lowering approaches would be highly desirable. Hypothermia is one such treatment that has shown ICP lowering benefits, this modality will be discussed further in section 1.5.

1.3 INTRACRANIAL PRESSURE

Elevated ICP is a common complication of multiple neurological conditions including stroke. Following ischaemic stroke in humans and animals, ICP may rise to levels detrimental to cerebral perfusion and neurological outcome, typically peaking at 2-5 days[14-19]. The mechanisms behind this elevation in ICP are poorly understood. Sustained ICP greater than 20-25 mmHg in humans is associated with a poorer outcome[16,20]. The few studies that have demonstrated ICP elevation post-stroke, however, have predominantly investigated large 'malignant' strokes[14,15,18]. The levels of ICP in the majority of strokes that don't result in 'malignant' hemispheric infarction are largely unknown due to the invasiveness of the ICP measurement equipment.

ICP is an indication of both intracranial volume and the ability of the intracranial cavity to contain this volume[21]. The fundamental principles of ICP are condensed in the doctrine accredited to Monro (1823)[22] and Kellie (1824)[23]. The basis of this doctrine states that because the skull cannot expand and the brain parenchyma is almost incompressible, the total intracranial volume always remains constant under normal physiological conditions; consequently, any increase in volume of the intracranial contents (tissue (oedema), cerebrospinal fluid (CSF), and/or cerebral blood volume (CBV)) must be counteracted by a decrease in volume of the other components. Once these compensatory mechanisms are exhausted, ICP will rise dramatically[24,25].

1.3.1 Intracranial pressure and cerebral oedema

Cerebral oedema is the accumulation of fluid in brain tissue, causing detrimental swelling. Cytotoxic and vasogenic oedema are two types of oedema that occur post-stroke. Cytotoxic oedema is localised and will occur within minutes to hours. It involves extracellular water shifting to intracellular compartments following the failure of cellular ion pumps. The resultant accumulation of intracellular sodium with the influx of water causes cellular swelling. Vasogenic oedema occurs more slowly, over hours to days. This phenomenon is caused by the breakdown of the blood-brain-barrier resulting in intravascular water being shifted to extravascular compartments.

Cerebral oedema has traditionally been thought to be primarily responsible for ICP elevation post-stroke. After large strokes, pressure within the skull rises, associated with brain swelling (oedema), peaking at 48-72 hours[14-19]. This contributes to

secondary injury and death in these patients. Small strokes result in little oedema. Therefore it is generally assumed that pressure does not rise in patients with small strokes, but as far as I can ascertain, this has never been directly measured. The idea that cerebral oedema is the primary cause of ICP elevation post-stroke seems to have arisen due to the fact that it has only been looked for in patients with large strokes and large levels of oedema. The relationship between oedema and ICP may be more complicated than it appears. A small clinical study noted that of 39 stroke patients with 'malignant' middle cerebral artery occlusions, brain herniation actually preceded dramatic ICP elevations[16]. Another study noted that only 5 of 19 patients with large stroke and oedema had elevations in ICP[19]. This suggests that ICP elevation may be secondary to brain herniation in large stroke and is not its primary cause. Due to the invasiveness of the monitoring equipment, ICP is not routinely measured in the majority of stroke patients. It begs the question then- what is happening to the ICP of patients with small strokes?

The relationship between cerebral oedema and ICP in experimental animal models of ischaemic stroke is also uncertain. There are surprisingly few experimental studies that have investigated ICP post-stroke. The few studies that have reported ICP elevations have shown that ICP is increased 24 hours after small ischaemic stroke, however these studies did not report oedema volumes[26-28]. One study also demonstrated that only those with larger strokes had a later secondary peak 48-72 hours post stroke, which correlates well with the known time-course of oedema development[27]. Another experimental study also reported elevations in ICP at 24-48 hours following small to moderate stroke, however, oedema volumes reported in this study were taken from a

separate cohort of animals[29]. The idea that oedema is the primary cause of intracranial pressure has not been directly investigated in small ischaemic stroke, and deserves further investigation.

1.3.2 Intracranial pressure and cerebrospinal fluid

CSF is a clear fluid surrounding the brain and spinal cord. The majority of CSF is produced by the choroid plexus and ventricular ependymal cells at a rate of 0.3-0.4 ml/min in humans and 2-4 µL/min in rats[30-32]. Traditional interpretation of CSF drainage has been that CSF is absorbed into the venous sinuses via the arachnoid granulations[33-35]. This understanding has since been debated with recent human and experimental studies suggesting that olfactory perineural pathways and cervical lymphatics[36-39] may play a key role in CSF absorption and that arachnoid granulations may only come into play when intracranial pressures are elevated[40-42]. Altered CSF dynamics are thought to be associated with several neuropathologies including hydrocephalus[43,44], idiopathic intracranial hypertension[45,46], intracerebral haemorrhage[47], subarachnoid haemorrhage[48,49], traumatic brain injury[50] and in the aging brain[51,52]. The idea that CSF dynamics could be altered following stroke, potentially affecting ICP has not yet been investigated. However, since it plays a fundamental role in ICP regulation under normal circumstances (as stated in the Monro-Kellie Doctrine), further investigation into its association with ICP elevation post-stroke is warranted.

1.3.3 Intracranial pressure and cerebral blood volume

CBV is the total quantity of blood contained within the blood vessels of the brain and is important in the regulation of ICP. For continuous homeostasis of CBV, a continuous outflow of venous blood from the cranial cavity is required to make room for continuous incoming arterial blood. Should this homeostasis become unbalanced, so that the total CBV increases, an elevation in ICP would occur. This disturbance is seen in diseases involving cerebral venous obstruction or thrombosis[53-58] in which ICP is dramatically elevated following the reduction of venous outflow. The relationship between ICP elevation and total CBV post-stroke has not been directly investigated in humans. A recent preliminary study from our laboratory, however, suggests that CBV may not be the causative factor for increased ICP post-stroke. Using perfusion computed tomography in rats, this study demonstrated a significant decrease in total CBV ($p < 0.01$) at 24 hours post-stroke in both the ipsilateral and contralateral hemispheres (Figure 1; n = 4; unpublished data).

One of the most critical issues in stroke is the need to maintain sufficient perfusion to the ischaemic penumbra. Cerebral perfusion pressure (CPP) is governed by a relationship between mean arterial pressure (MAP) and ICP: CPP = MAP – ICP. Under normal circumstances cerebral blood flow is maintained by the process of local cerebral autoregulation, which involves local changes in the resistance of blood vessels in response to changes in pressure, and is not CPP-dependent except at extremes of CPP[59]. Cerebral autoregulation is able to maintain relatively constant cerebral blood

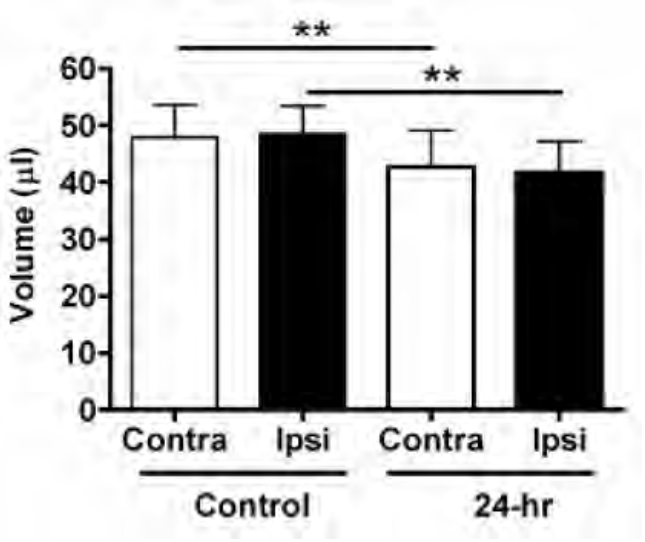

Figure 1. Total cerebral blood volume in the rat. Blood volumes of the contralateral (Contra) and ipsilateral (Ipsi) hemispheres were imaged using perfusion computed tomography scanning. Images were acquired before (Control) and at 24 hours following ischaemic stroke (n = 4). Mean ± SD; * $p < 0.05$; ** $p < 0.01$.

flow when CPP ranges between 50-140 mmHg. If CPP drops below 50 mmHg, autoregulation will fail and cerebral blood flow will be dramatically reduced. Following stroke, these autoregulatory mechanisms are exhausted within the ischaemic penumbra, and cerebral perfusion becomes CPP-dependent[60]. Therefore, in the absence of compensatory blood pressure elevation, ICP elevation will reduce CPP. This reduction in blood flow may have potentially devastating effects on the CPP-dependent leptomeningeal collateral vessels, which supply blood to the penumbral tissue.

1.4 LEPTOMENINGEAL COLLATERAL VESSELS

Leptomeningeal collateral vessels are pial vessels that connect the distal middle cerebral arterioles to the posterior and anterior arterial circulation. Under normal

circumstances, it is thought that these vessels supply the penetrating arterioles at the watershed region between vascular territories. The rate of blood flow required for this is low, relative to the diameter of the vessels. However, when major blood vessel routes fail following stroke, collateral vessels provide an alternate blood flow route to vital areas of the brain, increasing perfusion to tissue at risk of death. Leptomeningeal anastomoses provide residual perfusion to ischaemic penumbral tissue following stroke, slowing the progression of infarct core growth (Figure 2).

Good collateral supply has been strongly associated with better clinical outcome post-stroke[61-66]. Therapeutically improving the collateral blood supply post-stroke could therefore potentially improve stroke outcome. The idea that alterations in CPP can alter perfusion of the ischaemic penumbra is long-established[60]. There is also quite extensive literature on the effect of blood pressure manipulation after stroke and its effects on cerebral perfusion and patient outcomes[60]. Recent blood pressure manipulation approaches have been used to try to enhance collateral perfusion and improve stroke outcome in humans[67,68] and animals[69,70], and recent data suggests the possibility that nitric oxide may improve perfusion, likely through effects on collateral vessels[71]. However, these studies are preliminary and have not yet shown efficacy in improving stroke outcome in large clinical trials. To date, investigations into cerebral perfusion enhancement have primarily focused on the blood pressure aspect of the cerebral perfusion pressure equation, CPP = MAP - ICP. The effects of ICP on collateral perfusion are less often considered and have been much less studied.

Figure 2. Schematic representation of the left cerebral hemisphere arteries, with proximal MCA occlusion (indicated in black) and variable grades of retrograde distal MCA blood flow (arrows) via the leptomeningeal collaterals (white). This includes 'poor' retrograde flow in superficial vessels only (through the green vessel segments), 'moderate' flow into the Sylvian fissure (through the green and purple segments) or 'good' flow up to the occlusion (through the green, purple and yellow segments). Reproduced from Miteff *et al.* (2009)[65], by permission of Oxford University Press.

To date there have been relatively few animal studies investigating collateral supply post-stroke. Early investigations determined that the collateral vessels provide a compensatory capacity for alternate blood flow routes post-stroke[72-74]. These studies provided important data as to collateral vessel number and location. However, since they were conducted via post-mortem latex perfusion, they were unable to provide insight into the dynamic nature of the vessels. More recent studies have determined the *in vivo* physiology of the collateral vessels using flourescein isothiocyanate labelled red blood cells[75], fluorescent microspheres[76] and laser speckle imaging[77]. These studies demonstrated, for the first time, the velocity changes and bidirectional flow of

collateral vessels under normal conditions, post-stroke and post-reperfusion. The differing techniques used to study collateral dynamics, however, have led to confusing and sometimes conflicting results. For example, it has been reported that collateral vessels are functionally silent under normal conditions, demonstrating no blood flow, and that vessels are activated only after major occlusion[92,93]. In contrast, it has also been reported that collateral flow demonstrates slow bidirectional flow under normal conditions[75,76]. Furthermore, studies investigating blood flow through the penetrating vessels arising from collaterals are also conflicting, with one study demonstrating minimal flow[75] and another demonstrating a significant decrease in flow[78] during stroke. Interestingly, an element of collateral vessel dynamics that has currently been understudied is the importance of collateral vessel diameter versus blood flow velocity after stroke. Since collateral blood flow to the ischaemic penumbra is highly CPP-dependent, the velocity in which blood is supplied to this region seems an important factor to investigate. Understanding the fundamental dynamics of collateral blood flow pre- and post-stroke is essential to further develop post-stroke therapies.

Stroke-in-progression is a term used to describe a subset of stroke patients (10-40%[79]) who initially present with mild symptoms but suffer rapid clinical deterioration, typically over the first 24 hours in hospital[80,81]. The prognosis for these patients is poor. Until recently, it was assumed that the occluded vessel spontaneously reperfused, and that the subsequent deterioration was the result of a reformation of the clot[82]. Recent imaging studies have since demonstrated that the vessel does not spontaneously reperfuse in these patients, and that the neurological deterioration is associated with a reduced function of the leptomeningeal collateral vessels[83-85]. The cause of this

'collateral failure' is currently unknown. Proposed mechanisms include, collateral vessel thrombosis[86], venous steal[87], Reversed Robin Hood Syndrome[88] and blood pressure fluctuations secondary to autonomic dysfunction[89]. However evidence has not been strong for any of these mechanisms. Given the dependency of collateral vessels on CPP post-stroke, and the timing in which patients begin to deteriorate, investigations into the effects of ICP on collaterals is warranted.

1.5 HYPOTHERMIA

Therapeutic hypothermia has recently come to the forefront of neuroprotective research as the only neuroprotective modality to show overwhelming evidence for efficacy in animal models and the only strategy with proven efficacy in human brain ischaemia - following cardiac arrest[90,91] and neonatal hypoxia ischaemia[92]. The beneficial effect of deep therapeutic hypothermia (first termed 'human refrigeration') has been recognised since the 1940's[93]. The notion of protective body cooling led to the use of hypothermia in cerebral trauma[94], intracardiac surgery[95] and cerebral aneurysm surgery[96,97] in the 1950's. A lack of high-care facilities and severe side effects such as cardiac arrhythmia, shivering, infections and coagulation disorders, however, prevented therapeutic hypothermia from becoming a main-stream medical procedure. A renewed interest in hypothermia came as animal studies in the mid-1980's provided fresh insight into the underlying mechanisms of hypothermia and increasing evidence suggested that mild-moderate hypothermia (28-35°C) could provide neuroprotective benefits with fewer side-effects. In the 1990's, there appeared to be benefits of moderate hypothermia in small clinical trials to provide neuroprotective benefits in

traumatic brain injury patients[98,99]. The positive results of these studies led to multiple hypothermia trials in a variety of conditions causing neurological injuries, including cardiac surgery[90,91,100-102], perinatal asphyxia[103-106], traumatic brain injury[107-109], hepatic encephalopathy[110], and neonatal hypoxic ischaemia[92,111].

No large-scale randomised controlled trials have been completed using hypothermia as a treatment for ischaemic stroke. This may in part be due to the difficulties involved with cooling stroke patients. The major obstacles of hypothermia administration are shivering suppression, risk of pneumonia, and elevated ICP associated with rewarming. Shivering suppression is essential to achieving target temperatures <35 °C, but available therapies to suppress shivering are also sedating. In elderly, often drowsy, stroke patients who are already prone to pneumonia, this necessitates intensive care unit (ICU) admission. It should be noted that cardiac arrest patients are typically unconscious and ventilated in ICU facilities; stroke patients are not. Consequently, management of patient discomfort and shivering in cardiac arrest patients is simplified and thus hypothermic trials have been conducted in these conditions with positive results[103-105,112,113]. A recent collaborative group, the European Stroke Research Network for Hypothermia (EUROHYP), have begun a multicentre, randomised, Phase III clinical hypothermia trial in 80 hospitals over 21 European countries. The aim of EUROHYP is to determine whether cooling to 33-35 °C within 6 hours of symptom onset and maintained for 24 hours, improves functional outcome at 3 months following ischaemic stroke. The study is still in the early recruiting phase, and so data on efficacy is not yet available.

Over one hundred publications have demonstrated efficacy of therapeutic hypothermia in animal models of acute ischaemic stroke. A 2007 meta-analysis[114] revealed that in 3353 animals from 101 acute ischaemic stroke publications, induction of hypothermia reduced infarct sizes by 43.5% (95% CI, 40.1 - 47.0%). In a subgroup analysis, they found efficacy to be greatest when animals were cooled to lower temperatures (≤ 31 °C), and applied immediately following ischaemic insult, however mild hypothermia (35 °C) and a later hypothermic onset (90-180 minutes after ischaemia) still improved outcome by up to 33%[114] (Figure 3). Perhaps the most interesting result of this meta-analysis was that the median duration of cooling was 180 minutes, and that a small inverse relationship between duration of cooling and effect size was seen. Although this meta-analysis suggests that short-duration hypothermia may be more effective than long-duration, no studies have directly investigated it. Studies conducted by Colbourne *et al.*[115,116] suggested that long-duration hypothermia may be more effective than short, however 'short-duration' cooling in these studies was still 12 hours. It was also suggested by Markarian *et al.* (1996)[117] that longer durations of hypothermia resulted in better neuroprotection, however 'long-duration' in this study was 3-4 hours. Short-duration hypothermia is not at all the paradigm that has been tested in humans. In fact there is a large disconnect between animal and clinical studies. Therapeutic hypothermia has only been investigated in relatively few small-scale acute stroke trials. The vast majority of these trials cooled for 24-72 hours or longer. This concept of 'longer is better' is preserved amongst the neurological conditions, with recent meta-analyses of human therapeutic hypothermia in various neurological pathologies revealing that cooling for 12-48 hours was by far the norm[118-121]. Long periods of cooling inherently lead to systemic

complications such as pneumonia and sepsis[17,118,122,123]. In contrast, pneumonia and septicaemia was not reported in a single experimental study included in van der Worp's meta-analysis[114]. It is hard to judge whether the lack of infection in animal studies was due to short cooling periods or whether infection was just under-reported. In any case, the findings suggest that short-duration hypothermia, the dominant paradigm in successful experimental studies, should perhaps be investigated clinically.

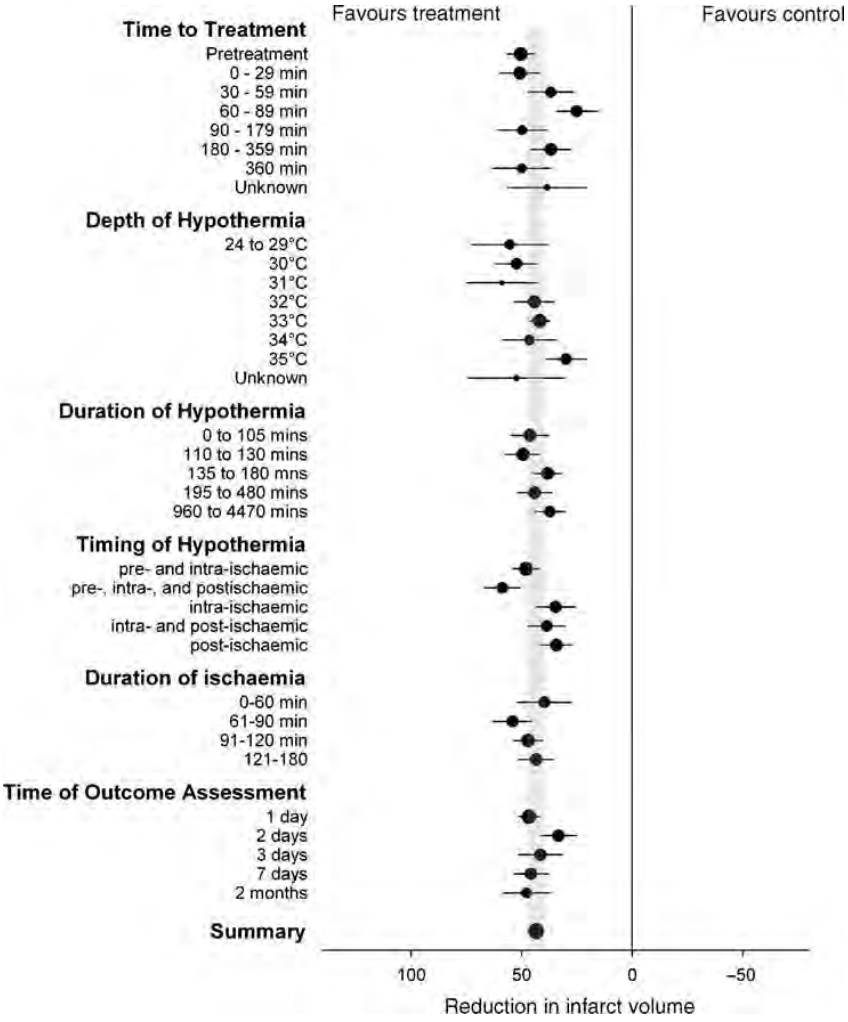

Figure 3. Point estimates of effect size on infarct size and 95% CI by duration of ischaemia in models of reperfusion, time to treatment, depth of hypothermia, duration of hypothermia, timing of hypothermia and time of outcome assessment. The grey band indicates the global estimate and its 95% CI. Reproduced from van der Worp *et al.* (2007)[114], by permission of Oxford University Press.

1.6 HYPOTHERMIA AND INTRACRANIAL PRESSURE

Therapeutic hypothermia has been used to decrease ICP following hepatic encephalopathy and traumatic brain injury[124-127]. A small clinical study of MCA infarction revealed that hypothermia (32 °C) produced a significant reduction in ICP when compared to normothermic controls[18]. This result was consistent with the findings of Marion *et al.* (1997)[99] and Metz *et al.* (1996)[128], who demonstrated similar results in clinical randomised controlled studies of traumatic brain injury. A major limitation of hypothermia therapy is that rewarming after 12–72 hours of cooling often results in rebound ICP elevation with subsequent neurological deterioration. This is more prevalent with rapid rewarming[17]. The rate of rewarming after therapeutic hypothermia in cerebral ischaemia appears to be critical for survival. Several small clinical trials have demonstrated a detrimental rebound increase in ICP during rapid rewarming[18,25]. An experimental animal study by Berger *et al.* (2007)[129] demonstrated that a slow and controlled rewarming phase reduced infarct volume by approximately 50% when compared to a rapid, uncontrolled rewarming phase. It should be noted that, like the majority of animal studies, hypothermia was only induced for a short duration (4 hours). Animals were rewarmed 'slowly' over 2 hours, or quickly over 20 minutes, however, authors acknowledged the possibility that rewarming may have actually resulted in brain hyperthermia. Despite convincing experimental data, short-duration whole-body hypothermia has not been tested in humans. If there was a way to avoid rebound ICP without the immunosuppressive effects of prolonged cooling, the outcome of patients may be greatly improved.

1.7 ANIMAL MODELS OF STROKE AND INTRACRANIAL PRESSURE MEASUREMENT

Animal models of ischaemia have provided a valuable contribution to the current knowledge and understanding of the neuropathogenesis of cerebral ischaemia. Rats and mice have very similar cerebral blood vessel anatomy to humans, and as such are the most widely used animals in stroke models. The middle cerebral artery (MCA) is the most commonly affected artery of acute ischaemic stroke. It is therefore the most commonly occluded artery in experimental ischaemic stroke models[130]. In experimental stroke research, the volume of infarcted tissue (often corrected for oedema) equates to the size of the stroke. The most widespread method of MCA occlusion in rats and mice is the intraluminal filament technique. When using the intraluminal filament model, there are differences in infarct volumes between different rat strains even when using identical occlusion durations[131]. These inter-species differences may be explained by differences in leptomeningeal collateral vessels supplying blood to the ischaemic penumbra, i.e. rat strains with better collaterals have smaller strokes than rats with poor collateral supply, despite identical occlusion durations. Because of these differences, investigators often describe the size of the stroke (infarcted tissue) in absolute terms (mm^3) or as a percentage of the ipsilateral or contralateral hemispheres. For example, Kotwika *et al.* (1991)[27] defined small and large strokes in Sprague-Dawley rats as 9-15% and 25-36% of the contralateral hemisphere, respectively. Variations within rat strains may also be observed. For example, infarct volumes in the Wistar rat strain are known to be dependent on the supplier[132-134]. In Wistar rats from our supplier, infarct volumes (absolute and relative) are not as large as in Wistar rats from other suppliers, after the

same duration of MCA occlusion. In this thesis, stroke size will be quantified and discussed. The relative percentages of infarcted tissue will demonstrate whether the stroke is 'small' or 'large'.

Monitoring ICP in animal models is difficult and as a result, there are no standard animal ICP monitoring methods. Fluid-filled systems are most frequently used[135-142]; however these systems can be prone to blockages and air bubbles, potentially leading to false ICP measurements. This is more of an issue in animal studies due to the very fine gauge catheters required. The most common placement locations for ICP catheters are intraventricular[139,143], intraparenchymal[28,144,145], subdural[137], cisterna magna[29,136,140], lumbar cannulation[138,141], or epidural[26,135,142]. Two recent studies have compared fluid-filled catheters placed in the epidural space versus intraventricular[142] or intraparenchymal[146] catheter placement and demonstrated that the correlation between recording sites was strong[142]. The intraventricular and intraparenchymal probes however, demonstrated safety and durability issues, including an increased risk of hydrocephalus, mechanical tissue damage and infection[142]. These issues confounded the ICP data. The epidural placement caused less injury and thus, was the placement of choice for subsequent studies[146]. These studies indicate that ICP catheters placed in the epidural space are less invasive, have a lower risk of infection, and cause less mechanical tissue damage. A solid-state probe placed in the epidural space would provide a less invasive, safer and more reliable ICP measurement.

1.8 RATIONALE

Following large 'malignant' ischaemic stroke, ICP elevation occurs, peaking 2-5 days post-stroke. In these patients, ICP elevation over 25 mmHg is a strong predictor of death. The effects of smaller strokes on ICP are less well known due to the invasive nature of the ICP monitoring equipment, however in animal models of ischaemic stroke, ICP has been shown to increase dramatically 24 hours after small stroke. The mechanisms regulating ICP elevations following ischaemic stroke are poorly understood. Traditional interpretation has been that cerebral oedema is the primary contributor to ICP elevation. This assumption, however, appears to have been based primarily on the fact that ICP changes have only been investigated in patients with large infarct and oedema volumes. To date, no studies have directly investigated the effects of oedema on ICP elevation. Since patients with smaller strokes have little cerebral swelling, it has also been assumed that these patients do not have ICP elevations. Although ICP elevations following small strokes have been reported in animals, it has not been considered to be of great importance and thus, is not widely known about. If this ICP rise occurs in the most commonly used animal model of ischaemic stroke, isn't it also likely to occur in patients with small stroke?

Elevations in ICP may be of particular importance to stroke outcome. Cerebral perfusion, which is vital to the poorly perfused region of the ischaemic penumbra, is governed by ICP and MAP through their effects on cerebral perfusion pressure (CPP = MAP - ICP). Perfusion of the penumbra is only sufficient to maintain cellular survival for a period of time – and without intervention this region is destined to die. Therefore

even minor reductions of perfusion pressure within this region may result in a larger region of infarction. Following stroke, perfusion to the penumbra can be partly maintained via leptomeningeal collaterals. In a subset of patients (10-40%), these collaterals fail. Typically, patients suffer this 'collateral failure' and subsequent clinical deterioration after 1 day in hospital (i.e. 24 hours). The cause of this 'collateral failure' is currently unknown. Several clinical trials have attempted to improve collateral blood flow by improving cerebral perfusion pressure. These trials have primarily focused on improving MAP. Although CPP is regulated by both MAP and ICP, to date, no studies have investigated ICP in relation to stroke-in-progression. ICP elevation may be a long-unrecognised pathophysiological derangement that accounts for collateral failure and late infarct progression. Certainly, the timing of neurological deterioration and the failure of blood pressure manipulation studies suggests that ICP may play a role in the 'collateral failure' seen in stroke-in-progression patients.

Therapeutic hypothermia has been shown to improve neurological outcome following cardiac arrest and neonatal hypoxia ischaemia, and small trials of hypothermia in stroke have demonstrated ICP lowering effects. Currently, hypothermia is a difficult and complicated therapeutic strategy to implement in the clinical setting. This is in part due to the long durations in which patients are cooled. Cooling patients for 24-72 hours has risks, including a higher risk of infection and rebound ICP elevations during rewarming. Short-duration therapeutic hypothermia following ischaemic brain injury has been shown to significantly improve neurological outcome in experimental animal models. Short-duration hypothermia is, by far, the most common paradigm used in experimental stroke, demonstrating overwhelming neuroprotective efficacy. In the

clinical setting, short-duration hypothermia would be easier to implement and would be less likely to result in serious complications. Despite this, short-duration hypothermia has never been tested in human stroke.

Understanding the mechanisms of intracranial pressure regulation and therapeutic hypothermia may contribute to improvements to the implementation and clinical testing of the most promising new therapeutic approach for stroke, and thereby prevent disability and save lives.

CHAPTER 2

RESEARCH AIMS AND HYPOTHESES

RESEARCH AIMS

1. To develop a reliable method for intracranial pressure measurement in the rat
2. To investigate the relationship between intracranial pressure and cerebral oedema following small ischaemic stroke.
3. To determine the effects of short-duration therapeutic hypothermia on intracranial pressure following ischaemic stroke.
4. To determine whether intracranial pressure rise causes collateral blood flow reduction.

HYPOTHESES

1. The use of an epidural fibre-optic pressure transducer is a reliable method for repeated intracranial pressure measurements in the rat.
2. Intracranial pressure increases 24 hours after small ischaemic stroke and a brief duration of hypothermia, administered shortly after stroke, will prevent this intracranial pressure elevation.
3. Cerebral oedema is not the primary contributor to intracranial pressure elevation post-stroke.
4. Intracranial pressure elevation causes collateral blood flow reduction.

CHAPTER 3

PUBLICATION 1

Murtha L, McLeod D, Spratt N. Epidural intracranial pressure measurement in rats using a fiber-optic pressure transducer. *J Vis Exp*. e3689, doi:10.3791/3689. (2012).

3.1 INTRODUCTION

Intracranial pressure (ICP) rises to levels detrimental to health following a number of neurological conditions including stroke. The measurement of ICP, however, is difficult and invasive. In the clinical setting, intraventricular cannulation is considered the 'gold standard'. The invasiveness of this procedure limits its use to those with large 'malignant' strokes. These limitations have hindered further understanding of ICP regulation. Consequently, there are few treatment options available for patients with elevated ICP. Although epidural cannulation is less invasive, this measurement has been shown to be less reliable in humans. This is most likely due to the previous use of older ICP pressure transducer technologies that suffer from signal drift when the catheter pressure sensor dries out; a situation which may occur with epidural placement of ICP catheters in humans. Furthermore, several recent studies have demonstrated good correlation between epidural measurement and intraventicular/intraparenchymal measurement in the rat, and noted less mechanical tissue damage with the epidural placement. To better understand the mechanisms underlying ICP elevation post-stroke and to develop viable treatments, a minimally

invasive and reliable animal model of ICP measurement that allowed for repeated measurements over time was needed.

The development of the following method originated from L. Murtha's honours project, 2010. The method was then refined and improved, and the following publication conceptualised, written and edited as part of L. Murtha's PhD candidature.

3.2 CONTRIBUTIONS

"As co-authors of the paper: Murtha L, McLeod D, Spratt N. Epidural intracranial pressure measurement in rats using a fiber-optic pressure transducer. *J Vis Exp*. e3689, doi:10.3791/3689. (2012), we confirm that Lucy Murtha has made the following contributions: 50% conception and design of research; 50% experimental procedures; 50% analysis and interpretation of the findings; 70% writing of the paper and critical appraisal of content."

Dr Damian McLeod

Signed Date: 05.08.2014

Dr Neil Spratt

Signed Date: 04.08.2014

FACULTY ASSISTANT DEAN (RESEARCH TRAINING)

Professor Robert Callister

Signed Date: 03.09.2014

Video Article

Epidural Intracranial Pressure Measurement in Rats Using a Fiber-optic Pressure Transducer

Lucy Murtha[1], Damian McLeod[1], Neil Spratt[1]

[1]Biomedical Sciences and Pharmacy, The University of Newcastle

Correspondence to: Neil Spratt at Neil.Spratt@newcastle.edu.au

URL: http://www.jove.com/video/3689
DOI: doi:10.3791/3689

Keywords: Medicine, Issue 62, Neuroscience, brain, rat, intracranial pressure, epidural, fibre-optic transducer, ischemic injury

Date Published: 4/25/2012

Citation: Murtha, L., McLeod, D., Spratt, N. Epidural Intracranial Pressure Measurement in Rats Using a Fiber-optic Pressure Transducer. *J. Vis. Exp.* (62), e3689, doi:10.3791/3689 (2012).

Abstract

Elevated intracranial pressure (ICP) is a significant problem in several forms of ischemic brain injury including stroke, traumatic brain injury and cardiac arrest. This elevation may result in further neurological injury, in the form of transtentorial herniation[1,2,3,4], midbrain compression, neurological deficit or increased cerebral infarct[2,4]. Current therapies are often inadequate to control elevated ICP in the clinical setting[5,6,7]. Thus there is a need for accurate methods of ICP measurement in animal models to further our understanding of the basic mechanisms and to develop new treatments for elevated ICP.

In both the clinical and experimental setting ICP cannot be estimated without direct measurement. Several methods of ICP catheter insertion currently exist. Of these the intraventricular catheter has become the clinical 'gold standard' of ICP measurement in humans[8]. This method involves the partial removal of skull and the instrumentation of the catheter through brain tissue. Consequently, intraventricular catheters have an infection rate of 6-11%[9]. For this reason, subdural and epidural cannulations have become the preferred methods in animal models of ischemic injury.

Various ICP measurement techniques have been adapted for animal models, and of these, fluid-filled telemetry catheters[10] and solid state catheters are the most frequently used[11,12,13,14,15]. The fluid-filled systems are prone to developing air bubbles in the line, resulting in false ICP readings. Solid state probes avoid this problem (**Figure 1**). An additional problem is fitting catheters under the skull or into the ventricles without causing any brain injury that might alter the experimental outcomes. Therefore, we have developed a method that places an ICP catheter contiguous with the epidural space, but avoids the need to insert it between skull and brain.

An optic fibre pressure catheter (420LP, SAMBA Sensors, Sweden) was used to measure ICP at the epidural location because the location of the pressure sensor (at the very tip of the catheter) was found to produce a high fidelity ICP signal in this model. There are other manufacturers of similar optic fibre technologies[13] that may be used with our methodology. Alternative solid state catheters, which have the pressure sensor located at the side of the catheter tip, would not be appropriate for this model as the signal would be dampened by the presence of the monitoring screw.

Here, we present a relatively simple and accurate method to measure ICP. This method can be used across a wide range of ICP related animal models.

Video Link

The video component of this article can be found at http://www.jove.com/video/3689/

Protocol

1. Skull Penetration

1. Anaesthetize rat with isoflurane (5% induction, 1.5-2% maintenance) in 70% N_2 and 30% O_2. Following induction of anaesthesia, place the rat prone on a warming plate, positioning the rat's nose in an anaesthetic nose cone.
2. Whilst maintaining anaesthesia, secure the head in a stereotaxic frame, inserting the ear-bars until head is stabilised. Ensure breathing is not impaired. (**Figure 2-A**).
3. Inject scalp subcutaneously with long lasting local anaesthetic, Bupivacaine 0.3 ml 0.5% (Pfizer, Australia) before making a 1.5 cm skin midline head incision. (Sterile instruments and gloves should be used.)
4. Blunt dissect the soft tissue and surrounding muscles to clearly locate Lambda and Bregma. Retract the skin and connective tissue.
5. Stem any bleeding by applying pressure to the exposed skull. Excessive skull bleeding may be cauterized.

6. Using a dental drill with a 1 mm tip burr, burr a hole 2 mm wide into the right parietal bone. Burr the hole 2 mm lateral and 2 mm posterior from Bregma to avoid the superior sagittal sinus and ensure the placement of the ICP sensor is over the ischemic territory, for stroke studies. Alternative locations would be equally suitable for other applications. Burr the hole to a depth where the skull above the dura becomes translucent. (**Figure 2-B**).
7. Replace the burr with a 0.5 mm tip burr to remove the skull at the base of hole.
8. When the skull begins to crack, use 45° forceps to remove all remaining skull, ensuring the base of the hole is cleared of debris. (**Figure 3**).

2. Screw Modification and Insertion

1. Drill a 0.7 mm hole through a hexagonal-headed screw using a lathe and 0.7 mm drill bit.
2. Insert the monitoring screw into the hole by turning it approximately 1.5 turns (use the minimum amount of turns needed to secure screw in skull so as not to damage underlying tissue). (**Figure 2-C** and **Figure 4**).
3. Burr a second hole for an anchoring screw in the left parietal bone, 2 mm lateral and 2 mm posterior from Bregma. This hole does not require complete penetration of the skull, so the 1 mm tip burr is used to thin the skull for screw insertion.
4. Insert a 2 x 4 mm hexagonal-headed screw into the second hole. This screw helps to anchor the dental cement and hence the monitoring screw to the skull.
5. Use a transfer pipette to mix and apply dental cement monomer and polymer to the base of the head of the screws.
6. Allow dental cement to dry for at least 10 minutes.

3. Intracranial Pressure Transducer Insertion

1. Using white correction fluid, mark the fibre-optic sensor 4 mm from the tip.
2. Fill the hole of the monitoring screw with sterile saline (0.9%) and ensure no air bubbles are present within the screw.
3. Insert the ICP probe 4 mm into the screw so that the tip of the probe is level with the end of the screw. Ensure the tip does not pierce the dura.
4. Adjust the tip of the probe within the screw until an ICP trace reflecting ventilation and blood pressure pulse waves can be observed. (**Figure 5**).

4. Forming an Airtight Seal

1. An airtight seal is imperative to an accurate ICP reading. Mix a viscous biocompatible caulking material monomer and polymer in the ratio of 1:1. Because the pressure sensor is at the tip of the probe, and this is within the hollowed out screw, application of caulking material to the shaft of the fibre-optic probe has no effect on pressure sensitivity of the sensor.
2. Apply a thin layer around the probe and the head of the monitoring screw. Avoid displacing the ICP probe.
3. Allow to set for 5 minutes.
4. Apply a second layer of caulking material around the entire monitoring screw and probe. Ensure that no liquid is leaking from any crevasses in the caulking material. (**Figure 2-D**).
5. Remove ear-bars.
6. The rat may remain in the prone position, or be carefully rotated into the supine position during ICP monitoring.
7. A schematic of the completed procedure is depicted in (**Figure 6**).

5. Intracranial Pressure Transducer Removal and Reinsertion

1. At the completion ICP monitoring, the ICP sensor may be removed by gently pulling the catheter from the screw and caulking material.
2. The SAMBA sensor should be immediately place into 1 % Terg-A-Zyme solution to prevent tip corrosion.
3. The hole remaining in the caulking material should be covered with an additional layer of caulking material. (Rat may be woken at this stage).
4. To reinsert the SAMBA catheter for additional monitoring, slice the caulking material at the level of the head of the screw.
5. Repeat steps 3.2 - 5.3.

6. Representative Results

Figure 5 is a representation of ICP readings over ten seconds. At baseline, the average ICP in a Wistar rat is 6 mmHg. The events of shorter periodicity depicted in **Figure 5** reflect blood pressure pulse waves. The events of longer periodicity show ventilation events. Note that the SAMBA sensor reflects a ventilation amplitude of 3-4 mmHg and pulse amplitude of 1-2 mmHg.

To validate the position of the SAMBA sensor in each experiment, ICP traces should be tested for responsiveness to abdominal compressions and respiratory events, such as periods of apnoea. An abdominal compression is depicted in **Figure 7**.

Periods of apnoea (illustrated in **Figure 8**) are observed in most experiments involving spontaneously breathing animals. These events are identified on physiological records by an absence of respiratory deflections on respiratory (diaphragm transducer) and arterial pressure traces. An equivalent alteration in the ICP trace validates the ICP probe positioning.

Figure 9 depicts a typical ICP trace after the removal of the ear-bars (step 4.6). The insertion of the ear-bars in step 1.2 results in a slight compression of the skull and consequent disruption in intracranial volume and hence an increased ICP. If the sensor is positioned correctly, ICP will drop at least 4 - 5 mmHg with the removal of the ear-bars.

Histological analysis may be used to check for any damage to the cortical area immediately under the pressure sensor and screw. An example of a traumatic and non-traumatic screw insertion is depicted in **Figure 4.**

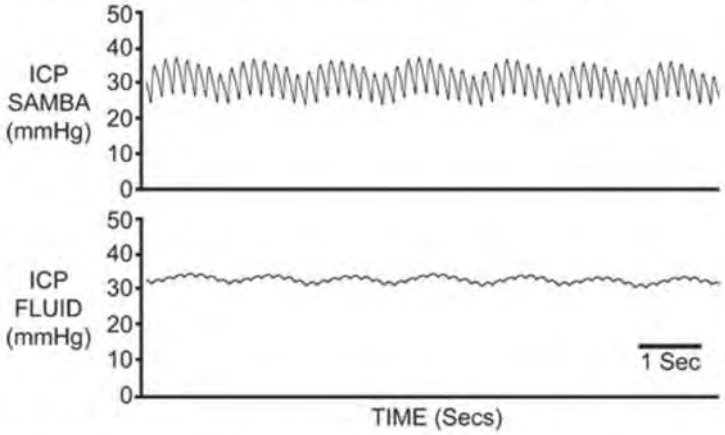

Figure 1. Fluid Filled Vs SAMBA ICP Traces. ICP was recorded simultaneously via the SAMBA fibre-optic catheter (*top*) and a fluid filled catheter (*bottom*). The mean ICP values were similar in both traces, however the fluid filled catheter signal was notably dampened compared to the clear respiratory and arterial pressure waveforms seen with the fibre-optic catheter.

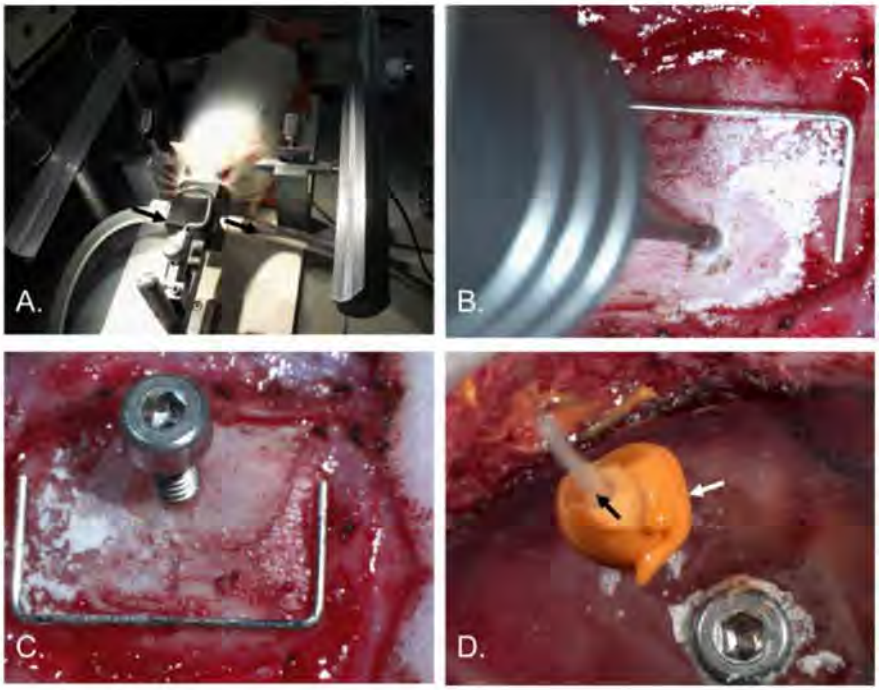

Figure 2. Intracranial Pressure Catheter Insertion Procedure. The rat's head was secured in a stereotaxic frame with ear-bars and an anaesthetic nose cone [A]. A hole, approximately 2 mm in diameter, was drilled into the right parietal bone [B]. A 2 x 4 mm screw with a 0.7 mm hole in the shaft was inserted [C]. An anchoring screw was inserted into the left parietal bone and the skull and surgical site covered in dental cement. The ICP catheter (*black arrow*) was then inserted into the screw-hole and an airtight seal made with the caulking material (*white arrow*) [D]. Staple (for scale) = 12 mm x 5 mm.

Figure 3. Monitoring Screw Burr Hole Orientation. The skull was cleared of connective tissue to locate Lambda (*black asterisk*) and Bregma (*white asterisk*) and the hole drilled 2 mm lateral and 2 mm posterior from Bregma. The hole was cleared of debris leaving the dura and pial vessels (*black arrow*) intact. Staple (for scale) = 12 mm x 5 mm.

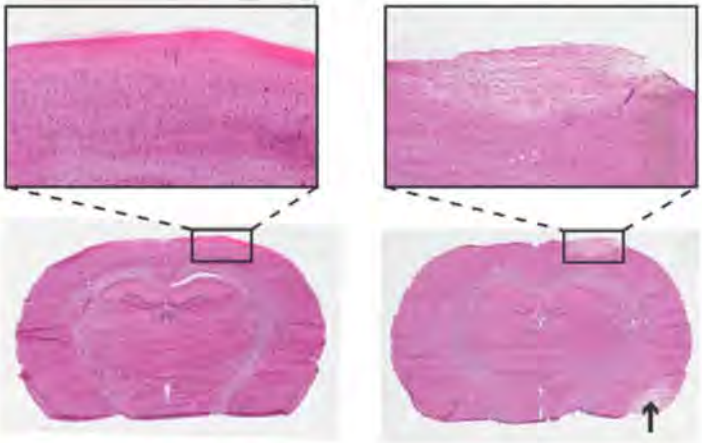

Figure 4. Histology of Rat Brain 24 Hours after Instrumentation of ICP Monitoring Screw. Haemotoxylin and Eosin staining, 6 µm coronal sections. Left: Non-traumatic screw insertion. Right: Traumatic screw insertion, area of pallor depicts damaged tissue with similar cellular morphology to stroke damaged area (*arrow*). Inserts at 4x objective.

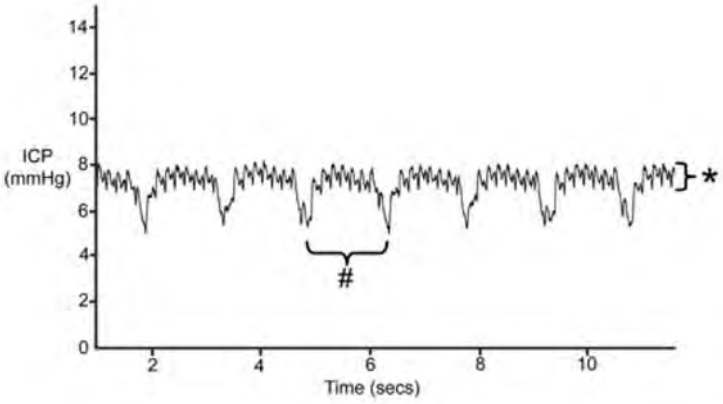

Figure 5. Typical ICP Trace. Pulse pressure waves are depicted by events of smaller amplitude (*). Ventilation is reflected by events of longer periodicity (#).

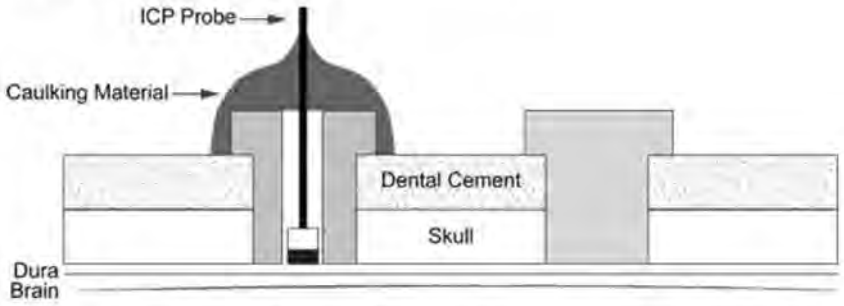

Figure 6. ICP Probe Insertion Schematic. Diagram illustrates placement of support screw (*right*) and caulking material coated ICP probe into screw (*left*).

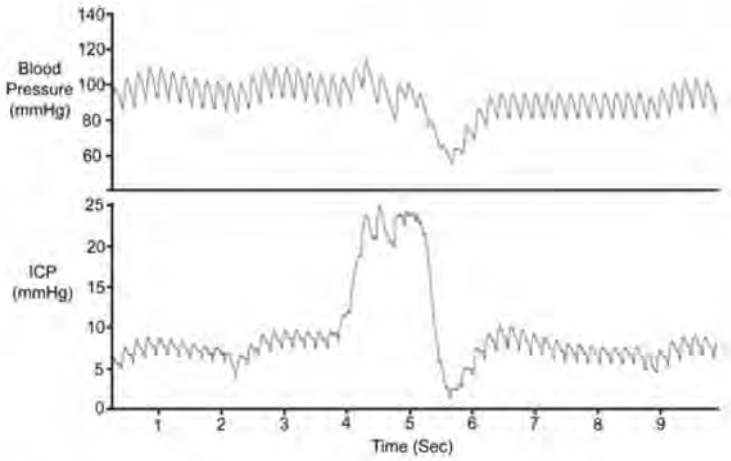

Figure 7. Abdominal Compression. The abdomen was temporarily compressed (~1 sec) to validate the viability of the ICP signal. Compression results in reduced cerebral venous return, increasing intracranial volume and thus increasing ICP. Arterial pressure (Pa) dropped only after the initial ICP rise.

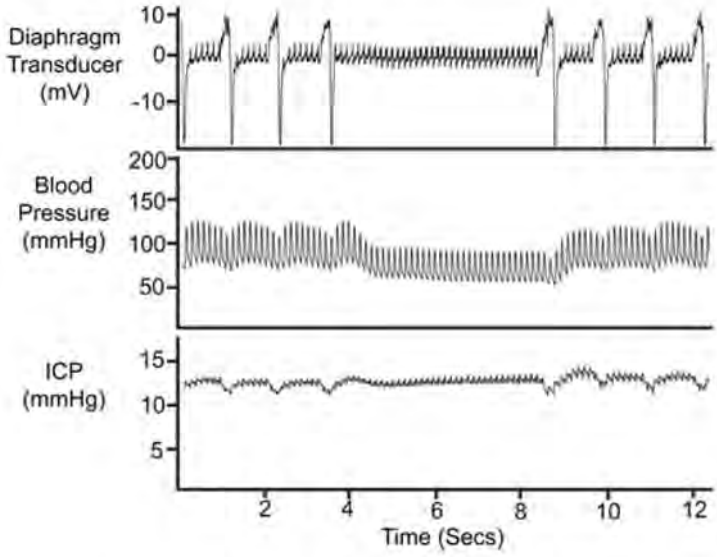

Figure 8. Period of Apnoea. The temporary cessation of breathing is reflected in the diaphragm transducer trace, the arterial pressure (Pa) trace and the ICP trace.

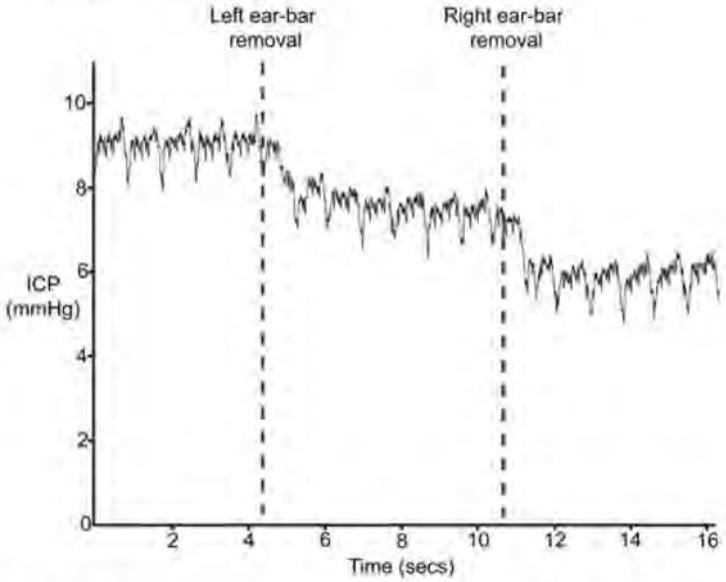

Figure 9. Ear-Bar Removal. ICP should drop with the removal of the stereotaxic frame ear-bars.

Discussion

The procedure presented here enables a very sensitive and accurate recording of intracranial pressure. This minimally invasive technique avoids significant brain trauma by positioning the pressure sensor in the epidural space and not the brain tissue or ventricles.

The critical steps include: 1) drilling through the skull – care must be taken not to pierce the dura or damage underlying brain tissue; 2) ensuring a tight seal with the caulking material – if there is any leak, the ICP trace will not be reliable. When the ICP sensor is appropriately positioned, the reading will give an accurate trace of not only ICP, but also respiratory and heart rate. With inspiration, the more negative intrathoracic pressure reduces downstream intravascular pressure, creating a greater pressure gradient and increasing cerebral venous return. The subsequent reduction in cerebral blood volume results in a decrease in ICP. Conversely, expiration increases the downstream venous pressure and increases ICP. Brief, one second abdominal compressions can be performed in every experimental animal to simulate a stimulus similar to a Valsalva manoeuvre. When applied, this physiological stimulus is known to reduce cerebral venous return and result in a transient rise in ICP. A lack of response to abdominal compression (no rise in ICP) suggests a leak in the airtight seal or blockage of the hollow screw. If a leak is apparent, a third layer of caulking material may be applied around the sensor to obtain an airtight seal. Note that the caulking material will not compress the optic fibre, so an additional layer will only ensure an adequate seal. If the screw is blocked, remove the caulking material and sensor, flush the screw gently with sterile saline and repeat steps 3.2 – 4.5. If the ICP trace is still weak, the fibre optic cable must be checked. The SAMBA optic fibre cable can tolerate a bend radius of 10 cm, if this is exceeded the ICP trace will be compromised.

The dura is in very close proximity to the skull, and therefore utmost care must be taken when removing the skull in step 1.8. When learning this technique, the dura may be accidently pierced and cerebrospinal fluid (CSF) will leak into the epidural space and into the monitoring screw. A knick in the dura, however, will not affect the ICP measurement because the cranial vault is sealed.

This method is suitable for use in animals under anaesthetic, however it is readily modifiable to perform recordings using a tether system in awake animals. The technique described has the potential to be used in many models of ICP measurement. The optic fibre used in this method is insensitive to any form of electro-magnetic fields and is therefore compatible with imaging technologies such as MR, CT, PET and SPECT. The quality of the recordings and reliability of measurements over time is superior to those obtained using commercially available fluid-filled catheter systems.

Disclosures

We have nothing to disclose.

Acknowledgements

This project was funded by the National Stroke Foundation, Hunter Medical Research Institute (HMRI) and National Health and Medical Research Council (NH&MRC), Australia. Special thanks to the Faculty of Health Workshop staff at The University of Newcastle for their technical expertise.

References

1. Ng, L.K. & Nimmannitya, J. Massive cerebral infarction with severe brain swelling: a clinicopathological study. *Stroke*. **1**, 158-163 (1970).
2. Plum, F. Brain swelling and edema in cerebral vascular disease. *Res. Publ. Assoc. Res. Nerv. Ment. Dis.* **41**, 318-348 (1966).
3. Ropper, A.H. & Shafran, B. Brain edema after stroke. Clinical syndrome and intracranial pressure. *Arch. Neurol.* **41**, 26-29 (1984).
4. Silver, F.L., Norris, J.W., Lewis, A.J., & Hachinski, V.C. Early mortality following stroke: a prospective review. *Stroke* **15**, 492-496 (1984).
5. Geraci, E.B. & Geraci, T.A. Hyperventilation and head injury: controversies and concerns. *J. Neurosci. Nurs.* **28**, 381-387 (1996).
6. Schwab, S., Aschoff, A., Spranger, M., Albert, F., & Hacke, W. The value of intracranial pressure monitoring in acute hemispheric stroke. *Neurology.* **47**, 393-398 (1996).
7. Adams, H.P., Jr., *et al.* Guidelines for the early management of patients with ischemic stroke: A scientific statement from the Stroke Council of the American Stroke Association. *Stroke.* **34**, 1056-1083 (2003).
8. Zhong, J., *et al.* Advances in ICP monitoring techniques. *Neurol. Res.* **25**, 339-350 (2003).
9. Aucoin, P.J., *et al.* Intracranial pressure monitors. Epidemiologic study of risk factors and infections. *Am. J. Med.* **80**, 369-376, doi:0002-9343(86)90708-4 [pii] (1986).
10. Silasi, G., MacLellan, C.L., & Colbourne, F. Use of telemetry blood pressure transmitters to measure intracranial pressure (ICP) in freely moving rats. *Curr. Neurovasc. Res.* **6**, 62-69 (2009).
11. Crutchfield, J.S., Narayan, R.K., Robertson, C.S., & Michael, L.H. Evaluation of a fiberoptic intracranial pressure monitor. *J. Neurosurg.* **72**, 482-487, doi:10.3171/jns.1990.72.3.0482 (1990).
12. Bolander, R., Mathie, B., Bir, C., Ritzel, D., & Vandevord, P. Skull Flexure as a Contributing Factor in the Mechanism of Injury in the Rat when Exposed to a Shock Wave. *Ann. Biomed. Eng.* doi:10.1007/s10439-011-0343-0 (2011).
13. Chavko, M., Koller, W.A., Prusaczyk, W.K., & McCarron, R.M. Measurement of blast wave by a miniature fiber optic pressure transducer in the rat brain. *J. Neurosci. Methods.* **159**, 277-281, doi:S0165-0270(06)00336-0 [pii] 10.1016/j.jneumeth.2006.07.018 (2007).
14. Chavko, M., *et al.* Relationship between orientation to a blast and pressure wave propagation inside the rat brain. *J. Neurosci. Methods.* **195**, 61-66, doi:S0165-0270(10)00655-2 [pii] 10.1016/j.jneumeth.2010.11.019 (2011).
15. Leonardi, A.D., Bir, C.A., Ritzel, D.V., & VandeVord, P. J. Intracranial pressure increases during exposure to a shock wave. *J. Neurotrauma.* **28**, 85-94, doi:10.1089/neu.2010.1324 (2011).

CHAPTER 4

PUBLICATION 2

Murtha L, McLeod D, McCann S, Pepperall D, Chung S, Levi C, Calford M, Spratt N. Short-duration hypothermia after ischemic stroke prevents delayed intracranial pressure rise. *Int J Stroke.* 9, 553-559, doi:10.1111/ijs.12181. (2014).

4.1 INTRODUCTION

Intracranial pressure (ICP) has been shown to rise dramatically following large ischaemic stroke; however the mechanisms behind ICP elevation post-stroke are poorly understood. Typically in large stroke, ICP peaks at 2-5 days. ICP is not routinely monitored in patients with small stroke; however ICP elevations at 24 hours have been shown following small experimental stroke. Hypothermia has been shown to decrease elevated ICP following several neurological disorders, including in several Phase II stroke clinical trials. These studies used long durations of cooling (24-72 hours), and often encountered problems of systemic infection and rebound ICP elevation during patient rewarming. Long-duration hypothermia typically requires admission into an intensive care unit (ICU). Although successful hypothermia studies have been conducted in cardiac arrest and neonatal hypoxia ischaemia patients, it should be noted that these patients are already admitted into ICU facilities, whereas stroke patients in the majority of hospitals are not. This severely limits the number of patients recruited into hypothermia stroke trials. In stark contrast to the clinical paradigm,

short-duration hypothermia has shown overwhelming evidence of neuroprotection in animal models of stroke. In the clinical setting, short-duration hypothermia would be safer, easier to implement and potentially more widely applicable. Despite this, short-duration hypothermia has not been tested in humans.

Pilot studies were initially conducted to investigate rebound ICP following short-duration cooling. This study used a strain of rat not previously used by our laboratory. The result that an inadvertent small stroke caused dramatic ICP elevations was not anticipated. This finding is investigated further in this publication. The aim of this study was to investigate whether short-duration hypothermia, administered shortly after stroke (before ICP is elevated), would prevent ICP elevation at 24 hours following small ischaemic stroke in rats using the method of epidural ICP probe placement developed in the previous publication.

The initial experiments of this publication were conducted as the basis of L. Murtha's honours project, 2010. The majority of the experiments and data analysis were completed for L. Murtha's PhD candidature. The following publication was conceptualised, written and edited as part of L. Murtha's PhD candidature.

4.2 CONTRIBUTIONS

"As co-authors of the paper: Murtha L, McLeod D, McCann S, Pepperall D, Chung S, Levi C, Calford M, Spratt N. Short-duration hypothermia after ischemic stroke prevents delayed intracranial pressure rise. *Int J Stroke.* 9, 553-559, doi:10.1111/ijs.12181. (2014), we confirm that Lucy Murtha has made the following contributions: 50% conception and design of research; 50% experimental procedures; 70% analysis and interpretation of the findings; 60% writing of the paper and critical appraisal of content."

Dr Damian McLeod

Signed Date: 05.08.2014

Dr Sarah McCann

Signed Date: 04.08.2014

Mrs Debbie-Gai Pepperall

Signed Date: 07.08.2014

Mrs Sun Young Chung

Signed Date: 06.08.2014

Dr Christopher Levi

Signed Date: 04.08.2014

Dr Mike Calford

Signed Date: 05.08.2014

Dr Neil Spratt

Signed Date: 04.08.2014

FACULTY ASSISTANT DEAN (RESEARCH TRAINING)

Professor Robert Callister

Signed Date: 03.09.2014

Short-duration hypothermia after ischemic stroke prevents delayed intracranial pressure rise

L. A. Murtha[1†], D. D. McLeod[1†], S. K. McCann[1], D. Pepperall[1], S. Chung[1], C. R. Levi[1,2], M. B. Calford[1], and N. J. Spratt[1,2]*

Background **Intracranial pressure elevation, peaking three to seven post-stroke is well recognized following large strokes. Data following small–moderate stroke are limited. Therapeutic hypothermia improves outcome after cardiac arrest, is strongly neuroprotective in experimental stroke, and is under clinical trial in stroke. Hypothermia lowers elevated intracranial pressure; however, rebound intracranial pressure elevation and neurological deterioration may occur during rewarming.**

Hypotheses **(1) Intracranial pressure increases 24 h after moderate and small strokes. (2) Short-duration hypothermia-rewarming, instituted before intracranial pressure elevation, prevents this 24 h intracranial pressure elevation.**

Methods **Long-Evans rats with two hour middle cerebral artery occlusion or outbred Wistar rats with three hour middle cerebral artery occlusion had intracranial pressure measured at baseline and 24 h. Wistars were randomized to 2·5 h hypothermia (32·5°C) or normothermia, commencing 1 h after stroke.**

Results **In Long-Evans rats ($n = 5$), intracranial pressure increased from 10·9 ± 4·6 mmHg at baseline to 32·4 ± 11·4 mmHg at 24 h, infarct volume was 84·3 ± 15·9 mm^3. In normothermic Wistars ($n = 10$), intracranial pressure increased from 6·7 ± 2·3 mmHg to 31·6 ± 9·3 mmHg, infarct volume was 31·3 ± 18·4 mm^3. In hypothermia-treated Wistars ($n = 10$), 24 h intracranial pressure did not increase (7·0 ± 2·8 mmHg, $P < 0·001$ vs. normothermia), and infarct volume was smaller (15·4 ± 11·8 mm^3, $P < 0·05$).**

Conclusions **We saw major intracranial pressure elevation 24 h after stroke in two rat strains, even after small strokes. Short-duration hypothermia prevented the intracranial pressure rise, an effect sustained for at least 18 h after rewarming. The findings have potentially important implications for design of future clinical trials.**

Key words: hypothermia, intracranial pressure, ischemic stroke

Correspondence: Neil Spratt*, Department of Neurology, John Hunter Hospital, Locked Bag 1, Hunter Region Mail Centre, NSW 2310, Australia.
E-mail: Neil.Spratt@newcastle.edu.au
[1]University of Newcastle and Hunter Medical Research Institute, School of Biomedical Sciences & Pharmacy, University of Newcastle, Callaghan, NSW, Australia
[2]Hunter New England Local Health District, Department of Neurology, John Hunter Hospital, Hunter Region M.C., NSW, Australia

Received: 27 May 2013; Accepted: 22 July 2013; Published online 12 September 2013

Conflict of interest: The authors declare no potential conflict of interest.

Funding: This work was supported by a NHMRC Program Grant #454417 and research support from the Hunter Medical Research Institute from funds donated by the Greater Building Society. N. Spratt received a NHMRC training fellowship, #455632. L. Murtha received a student grant from the National Stroke Foundation (Australia). D. McLeod and N. Spratt received a project grant from the National Stroke Foundation (Australia).

†These authors contributed equally to this work.

DOI: 10.1111/ijs.12181

Introduction

Stroke remains the third leading cause of death and a major cause of morbidity worldwide (1). Clearly, better widely applicable acute therapies are needed. Catastrophic intracranial pressure (ICP) elevation has been associated with death in large acute stroke (2,3). However, the association between size of stroke and degree of ICP elevation is not strong (4). Typically in large strokes, ICP peaks between two to five days post-stroke (2). Data on ICP in small stroke in humans are not available. In experimental stroke, there are surprisingly little data available on ICP changes; however, the work of Kotwica *et al.* (1991) (5) suggests that an initial ICP peak at 24 h is seen after both medium and large strokes (relative infarct size, % hemisphere, in large stroke: 25–36%, in small stroke: 9–15%). In the larger strokes, ICP had a secondary peak at three to four days, whereas in the medium-sized strokes, it normalized over this period.

Hypothermia results in reduction of ICP, and it has been used to achieve therapeutic ICP reduction in stroke, traumatic brain injury, and hepatic encephalopathy (6–8). A major limitation to hypothermia therapy is that rewarming after 12–72 h of cooling, often results in rebound ICP elevation with subsequent neurological deterioration. This is more prevalent with rapid rewarming (9). Consequently, most protocols rewarm over ≥12 h (10,11). However, prolonging the duration a patient is exposed to hypothermia increases the risk of adverse effects such as immunosuppression and pneumonia (9).

Therapeutic mild–moderate hypothermia is also a proven neuroprotective therapy in human global brain ischemia – post cardiac arrest and neonatal hypoxia ischemia (12–14); however, benefit has not yet been proven in focal brain ischemia (stroke). Importantly, hypothermia appears to have the strongest evidence base of any neuroprotective strategy in experimental stroke (15). However, clinical trials have been hampered by the logistical challenges of prolonged cooling (12–72 h) in stroke patients and concerns about iatrogenic complications (16). This extensive cooling period largely limits its use to centers with available intensive care facilities. In stark contrast to the clinical literature, the majority of studies in experimental stroke induce hypothermia for three hours or less (17). Somewhat surprisingly, there are very little data regarding the effect of hypothermia on ICP in experimental stroke.

Preliminary studies in our laboratory to investigate rebound ICP elevation following hypothermia treatment of stroke revealed some unanticipated results, leading to the hypotheses that: (1) ICP rises consistently at 24 h after any stroke, not only after large hemispheric stroke, and (2) a brief period of body cooling commenced soon after stroke may prevent subsequent ICP

elevation. Our aims were to measure ICP 24 h after stroke in two different rat strains and to determine the effect of a short duration of moderate hypothermia on ICP, and infarct and edema volumes 24 h post-stroke.

Materials and methods

Animals

Surgery was performed on male Long-Evans ($n = 6$, Client Service Centre, Monash University) and outbred Wistar rats ($n = 37$, Animal Services Unit, University of Newcastle) weighing 290–450 g. All experimental animal procedures used in this project were in accordance with the Australian Code of Practice for the Care and Use of Animals for Scientific Purposes and were approved by the Animal Care and Ethics Committee of the University of Newcastle.

Experimental protocols

A small study (Part I) was conducted in Long-Evans rats, a strain that has large infarcts with this model, to investigate the effect of two hour temporary middle cerebral artery occlusion (MCAo) on ICP. Since similar ICP effects were seen with small and large infarcts, for ethical reasons, we conducted pilot studies in Wistar rats, which have much smaller strokes. These data showed a similar dramatic ICP rise with smaller strokes than the Long-Evans (data not shown). Because similar results were obtained in Wistars, the prospective studies of the effects of hypothermia on ICP were performed in this strain (Part II).

ICP was monitored at baseline, during stroke surgery, and again at 24 h post-stroke before sacrifice for histology. Infarct volume in Wistar rats is known to be dependent on the supplier (18–20), and our previous data show small lesion sizes using rats from our supplier, even with permanent arterial occlusion (114 ± 50 mm^3) (20,21). Therefore, this strain was used to determine ICP following small strokes and the effects of short-duration hypothermia. Randomization to hypothermia, or normothermia under anesthetic, was performed one hour after stroke surgery in Wistar rats.

Anesthesia and monitoring

Anesthetic and surgical protocols were as previously reported (21). In brief, rats were anesthetized with isoflurane (5% induction, 2% maintenance) in 60: 40%, $N_2 : O_2$. Incision sites were injected subcutaneously (s.c.) with 2 mg/kg 0·05% Bupivacaine (Pfizer, Sydney, Australia). Core body temperature was regulated via a thermocouple rectal probe (RET-2, Physitemp Instruments Inc, Clifton, New Jersey, USA) and warming plate (HP-1M, Physitemp Instruments Inc). Temperature was also recorded every five minutes for 24 h post-stroke using a datalogger (SubCue, Calgary, Canada) inserted into the peritoneal cavity at the beginning of the surgery. Blood gases were monitored periodically from 0·1 ml blood samples taken from a right femoral arterial line. This line was also used for arterial blood pressure monitoring. Prior to recovery, an additional Bupivacaine injection (0·3 ml 0·05%, s.c) and rectal Panadol (250 mg/kg; GlaxoSmithKline, Brentford, UK) were administered for overnight pain relief and saline was administered ($2 \times 2{\cdot}5$ ml, s.c.) to replace fluid losses. Following surgery, the animals were returned to their cages with free access to food and water, with cages placed half over a heat mat to allow animals to self-thermoregulate during recovery.

ICP measurement

ICP was measured using a SAMBA microcatheter (SAMBA Sensors, Gothenburg, Sweden), as previously described (22). In brief, the catheter was sealed in an epidural position inside a fluid-filled hollow screw inserted in the parietal bone. Correct positioning was confirmed by observation of pulse and respiratory wave amplitudes and ICP response to abdominal compression. Cerebral perfusion pressure (CPP) was calculated using the formula CPP = Mean Arterial Pressure – Mean ICP. At 24 h post-MCAo, animals were re-anesthetized for one hour of ICP recording prior to sacrifice. The left femoral artery was cannulated, physiological monitoring equipment was reattached, and the ICP catheter was reinserted and sealed.

Experimental stroke and hypothermia

Thread occlusion of the middle cerebral artery was performed using a silicone-tipped monofilament passed via the external carotid artery, according to our established method (21,23), with a minor variation to shorten the length of the silicone tip of the occluding thread to 3–4 mm.

After one hour of MCAo, Wistars were randomized by sealed numbered envelope to hypothermia or normothermia. Hypothermia-treated animals were cooled to 32·5°C using 70% ethanol evaporation with a sprayer and a fan. Hypothermia was maintained for 2·5 h, followed by controlled rewarming to 37°C over 2·5 h. Normothermic animals were maintained at 37°C under anesthesia for the same time intervals.

Neurological testing

Prior to 24 h post-stroke monitoring, animals were tested for stroke-induced neurological deficits. The forelimb flexion, torso twist, and lateral push tests were used to assess this and a total neurological deficit score given out of six (higher score indicating greater deficit) (24,25).

Histological analysis

At 25 h, brains were processed for hematoxylin and eosin staining and histological analysis of infarct and edema volumes using standard methodology (21). Images were scanned at high resolution using a digital slide scanner (Aperio, Vista, CA, USA) and analyzed by an investigator blind to treatment. Infarct (corrected for edema) was calculated by subtracting the measured interhemispheric volume difference (edema volume, ipsilateral–contralateral) from the measured infarct volume for each slice. Edema was calculated by infarct volume minus the corrected infarct volume.

Exclusions and statistical analysis

Sample size calculations were performed using SPSS v21·0 (IBM, Armonk, New York, USA) prior to the commencement of the Long-Evans study (for a 15 mmHg difference in ICP) and the Wistar study (for a 30% difference in infarct volume) based on pilot data. Animals were excluded prior to randomization if there were major deviations from the protocol, such as significant intra-operative oxygen desaturation, blood loss, or temperature fluctuations. Additionally, evidence of subarachnoid hemorrhage (SAH) upon brain removal after perfusion fixation was a pre-

specified exclusion criterion, because this may alter both stroke outcome and ICP. Animals that died before final ICP measurement were by necessity excluded from outcome analyses but are fully reported. All physiological and histological data were analyzed by an investigator blinded to treatment allocation.

Analysis of covariance was performed using STATA/IC 11·1 for Windows (StataCorp, College Station, Texas, USA) to test whether treatment had a significant overall effect on the primary outcome of change in ICP at 24 h, and on the secondary outcome of CPP, adjusting for baseline values. Other statistical tests were performed using GRAPHPAD PRISM™ version 4·02 for Windows (GraphPad Software, La Jolla, CA, USA). Student's *t*-tests were used to compare differences in infarct volumes and edema volumes between groups. Significant differences were accepted at the $P < 0·05$ level. Student's *t*-tests were also performed on physiological parameters for illustrative purposes to highlight changes from baseline and between treatment groups; *P* values are reported with no correction for multiple comparisons. Unless otherwise stated, data are expressed as mean ± standard deviation.

Results

A total of 5 Long-Evans, 10 each of hypothermia-treated and normothermic control, and 2 normothermic sham surgical Wistar rats were included. A total of 16 animals were excluded: eight pre-randomization, six due to SAH detected at postmortem (one Long-Evans), and two post-randomization due to malfunction of homeothermic heat mat (one hypothermia and one normothermia Wistar). Of the six SAH animals, three normothermic animals died, and SAH was detected at postmortem (including the excluded Long-Evans rat). Three hypothermic-treated animals survived at 24 h; however, SAH was detected at postmortem. In these animals, there was no significant difference in ICP at 24 h compared with baseline values (8·3 ± 2·9 mmHg vs. 10·5 ± 4·7 mmHg, respectively).

Infarct volume and ICP 24 h post-stroke

In Long-Evans rats ($n = 5$), mean edema-corrected infarct volume was 84·3 ± 15·9 mm^3 (range 61–105 mm^3). ICP increased from 10·9 ± 4·6 mmHg at pre-MCAo baseline to 32·4 ± 11·4 mmHg at 24 h (Fig. 1). In normothermic Wistar rats, edema-corrected infarct volume was 31·3 ± 18·4 mm^3 (Fig. 2a). ICP increased from 6·7 ± 2·3 mmHg at baseline to 31·6 ± 9·3 mmHg at 24 h (Fig. 3b).

Short-duration hypothermia to 32·5°C prevents delayed ICP rise

Accurate temperature regulation was maintained in hypothermia-treated animals and controls (Fig. 3a). Heart rate and respiratory rate were lower during hypothermia (Table 1). ICP traces revealed consistent pulse and respiratory waveforms. There were no major changes in ICP during the initial six hour monitoring, including during hypothermia. One animal had an 8·0 mmHg ICP rise during rewarming, to 15·5 mmHg at 6 h. At 24 h, its ICP was 4·6 mmHg. There were dramatic increases in ICP at 24 h in all normothermic animals. ICP increased from 6·7 ± 2·3 mmHg at baseline to 31·6 ± 9·3 mmHg at 24 h, whereas the ICP in hypothermia-treated animals was 5·4 ± 2·1 mmHg at

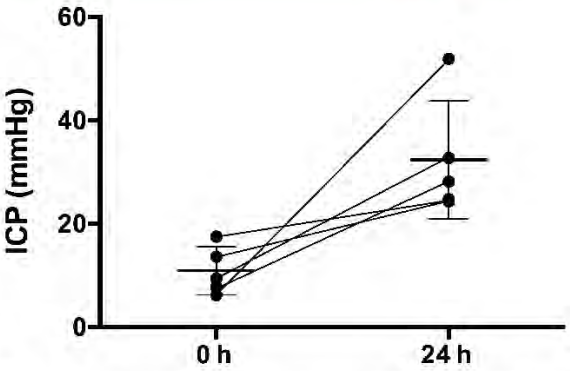

Fig. 1 Intracranial pressure (ICP) at 0 h and 24 h post-stroke in Long-Evans (individual data points, mean, and standard deviation).

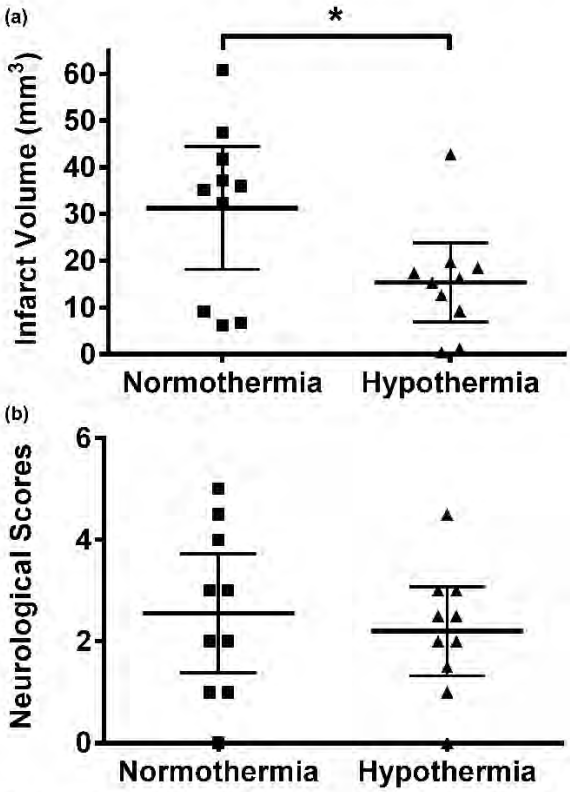

Fig. 2 (a) Infarct volume and (b) neurological scores in normothermia and hypothermia treatment groups in Wistar rats.

baseline and 7·0 ± 2·8 mmHg at 24 h. There was a significant main effect of treatment group, $F(2,17) = 31·87$, $P < 0·0001$ (Fig. 3b). There was no overlap in final ICP values between the two groups. This was despite equivalent core temperatures in the two groups at 24 h and for the preceding 18 h (Fig. 3a). Sham surgical animals showed no elevation of ICP.

There was no significant difference in mean arterial pressure between groups (Table 1). Therefore, as predicted, there was a significant main effect of treatment group on CPP at 24 h, $F(2,16) = 14·73$, $P = 0·0002$ (Fig. 3c). There was significantly

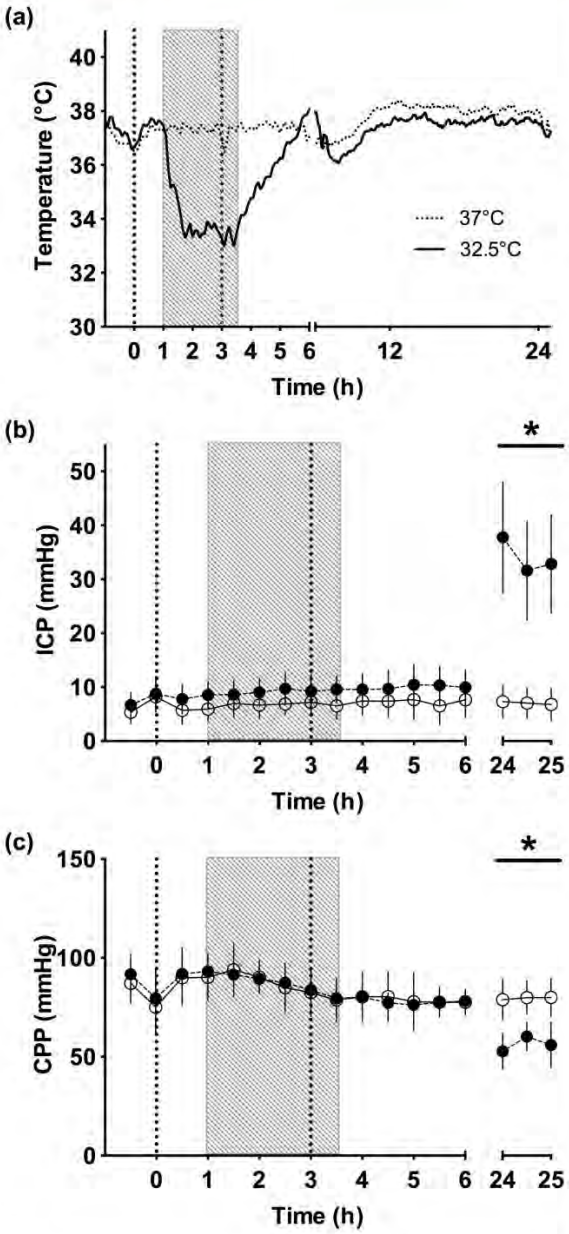

Fig. 3 Temperature, ICP, and CPP in Wistar rats. (a) Temperature profiles of experimental groups during hypothermia or normothermia. (b) Intracranial pressure (ICP) 0–6 and 24–25 h post-stroke in hypothermia-treated (open circles) and normothermic rats (filled circles). The shaded region represents the cooling interval. (c) Cerebral perfusion pressure (CPP) following stroke. CPP was calculated for each animal as arterial pressure minus ICP. *$P < 0{\cdot}0001$ for *t*-tests between respective hypothermia (open circles) and normothermia (filled circles) groups.

smaller mean edema-corrected infarct volume in hypothermia-treated animals compared to normothermics ($15{\cdot}4 \pm 11{\cdot}8$ mm^3 vs. $31{\cdot}3 \pm 18{\cdot}4$ mm^3, $P = 0{\cdot}03$). However, among the normothermia animals, there was no clear association between infarct volume and ICP. Edema volumes calculated from histological sections showed a non-significant trend to be lower in the hypothermia-treated animals ($2{\cdot}8 \pm 4{\cdot}6$ mm^3 vs. $17{\cdot}1 \pm 24{\cdot}2$ mm^3 in normothermic animals, $P = 0{\cdot}08$). Neurological deficit scores also showed a non-significant trend to be lower in the hypothermia-treated animals ($2{\cdot}5 \pm 1{\cdot}6$ vs. $2{\cdot}2 \pm 1{\cdot}2$ in normothermic animals, $P > 0{\cdot}05$) (Fig. 2b); however, there was no association between neurological deficit scores and ICP (Fig. 4).

Discussion

ICP is known to rise after large stroke, and hypothermia is well known to lower ICP (6). However, this study has revealed several important novel results. First, quite dramatic elevations in ICP were seen following only small stroke in normothermic animals. Second, a short period of hypothermia early post-stroke had a prolonged effect moderating subsequent ICP long after rewarming. Hypothermia treatment completely abolished the dramatic rise in ICP seen at 24 h in the normothermic animals, although no differences were seen between groups during the hypothermic interval.

The dramatic ICP elevations in normothermic animals were seen despite their small stroke sizes. Infarct and edema volumes resulting from temporary MCAo were approximately 1/6 of the maximal volume that can result from permanent occlusion in our hands, yet ICP elevation in the normothermic animals was dramatic. As already alluded to, we have been unable to find data reporting ICP measurement 24 h after small strokes, in either experimental animals or humans. Others have shown ICP elevation after moderate–large stroke in rat stroke models, peaking at 24–72 h (5,26). Baseline and post-stroke ICP values were similar to our results in the study that also monitored over the ipsilateral cortex (26) but lower in the study using infratentorial monitoring (5). ICP gradients between different cerebral compartments have been reported (27), so this may explain the apparent differences in measured pressures. Silasi *et al.* (26) reported ICP only in animals with massive infarction (228 ± 36 mm^3). Kotwica *et al.* (5) studied a mixture of infarct volumes, although even the group with the smallest strokes in their study had reported hemispheric lesion volumes larger than those calculated from our data. Interestingly, Kotwica *et al.* (5) reported similar ICPs at 24 h in the smaller and larger stroke groups, although some of the animals with larger strokes had a second, higher ICP peak at three to four days. The findings of the current study raise the question of whether the small volume of edema seen could be responsible for such dramatic ICP elevation in the normothermic animals.

Edema may have effects by increasing ICP post-stroke but may also have important effects through local swelling and mass effect, which may be associated with brain herniation and death after stroke (4). Schwab *et al.* (4) studied 48 patients with large hemispheric stroke and reported that although significantly elevated, ICP (>35 mmHg) reliably predicted death; clinical signs of brain herniation *preceded* ICP elevation in all 39 nonsurviving patients in their study. This suggests that in patients with large strokes, dramatic ICP elevation may be secondary to brain herniation (because of mass effect), not its primary cause. One may then ask, if ICP elevation does not cause brain herniation, is it important?

Table 1 Physiological parameters

		Pre-MCAo	2 h Post-MCAo	6 h Post-MCAo	24 h Post-MCAo
Temp (°C)	Normo.	37·2 ± 0·4	37·2 ± 0·1	37·3 ± 0·1	37·3 ± 0·2
	Hypo.	37·4 ± 0·3	32·7 ± 0·2*	37·2 ± 0·3	37·3 ± 0·3
RR (BPM)	Normo.	63·9 ± 13·8	58·4 ± 11·7	48·7 ± 14†	60·1 ± 12·9
	Hypo.	54·3 ± 15·4	47·7 ± 8·1*	51·2 ± 7·1	53·4 ± 8·6
HR (BPM)	Normo.	372 ± 42	454 ± 42†	382 ± 28	400 ± 27
	Hypo.	380 ± 28	347 ± 107*	380 ± 22	399 ± 31
MAP (mmHg)	Normo.	98·3 ± 9·3	100·4 ± 9·3	89·5 ± 7·3†	91·8 ± 4·6
	Hypo.	92·5 ± 9·9	96·9 ± 8·8	85 ± 7·2†	86·8 ± 8·2
pO_2 (mmHg)	Normo.	162 ± 30	187 ± 31†	173 ± 29	152 ± 30
	Hypo.	148 ± 29	167 ± 59	190 ± 70†	139 ± 13
SpO_2 (%)	Normo.	99·4 ± 0·6	99·4 ± 0·7	99·3 ± 0·5	99·4 ± 0·5
	Hypo.	99·1 ± 0·6	99 ± 1·4	99·5 ± 0·8	99 ± 0·0
pCO_2 (mmHg)	Normo.	49·6 ± 8·8	55·6 ± 7·3	59 ± 14·4	49·8 ± 4·3
	Hypo.	45·6 ± 6·3	56·6 ± 21·1	53·5 ± 11·3	46·4 ± 5
pH	Normo.	7·38 ± 0·04	7·35 ± 0·05	7·30 ± 0·09†	7·47 ± 0·07†
	Hypo.	7·40 ± 0·04	7·33 ± 0·11	7·4 ± 0·11*	7·47 ± 0·04†
Glu (mmol/l)	Normo.	10·4 ± 2·3	10 ± 1·5	8·5 ± 1·3	9·1 ± 1·9
	Hypo.	9·8 ± 1·1	11·6 ± 2·6	9·5 ± 1·6	9·5 ± 2·8

*$P < 0.05$ vs. normothermia; †$P < 0.05$ vs. pre-MCAo.
BPM, beats per minute; Glu, glucose; HR, heart rate; MCAo, middle cerebral artery occlusion; MAP, mean arterial pressure; pCO_2, partial pressure of carbon dioxide; pO_2, partial pressure of oxygen; RR, respiratory rate; SpO_2, oxygen saturation; Temp, temperature.

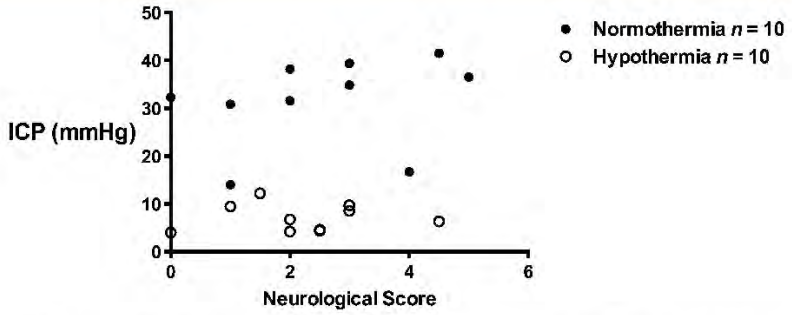

Fig. 4 Intracranial pressure (ICP) vs. neurological score in Wistar rats. Linear regression showed no significant correlation between ICP and neurological score for either group: normothermia $P = 0.44$, hypothermia $P = 0.94$.

We believe so, primarily because of potential effects on CPP: the difference between arterial pressure and ICP. Perfusion of peri-infarct regions supplied by collateral vessels is already compromised and normal autoregulation impaired, such that perfusion of the penumbra is CPP dependent. Because of its effect on CPP, ICP elevation post-stroke could well be the mechanism for secondary 'collateral failure' and stroke-in-progression. Clearly, this possibility requires further investigation.

Our second key finding was that a brief period of hypothermia exerts a prolonged effect on ICP. This is not an intuitive concept and has not previously been investigated. Studies in other brain injury models have shown minimal effect of hypothermia on ICP in the early phase post-injury (28), as also seen in our study. However, ICP was not measured at later times after rewarming. The effect of short-duration hypothermia that we observed appears to be a 'switch-like' mechanism, which completely prevented ICP elevation at 24 h. The exact mechanism has not yet been elucidated; however, it has obvious potential clinical importance.

The results raise the intriguing possibility that for the use of hypothermia after stroke, 'less may be more'. Therapeutic hypothermia in patients has traditionally been administered for 12–72 h and carries significant logistical and technical challenges. Rebound ICP elevation can be a significant problem, and prolonged rewarming protocols have been instituted in many studies to try to avoid this. Prolonged hypothermia is associated with a degree of immunosuppression. This and the sedative effects of shivering suppressant medication may be a particular problem in stroke patients because of their increased risk of pneumonia. A recent early phase trial reported very high rates of pneumonia in hypothermia-treated patients cooled for 24 h plus 12 h rewarming (11). Shorter duration cooling may reduce such complications, and most of the supportive experimental studies have shown neuroprotection with short-duration cooling (29). There is a wealth of data showing that infarct size and functional outcome are significantly improved by short-duration hypothermia at both early (24 h) and later (three days post-stroke) (30). In the large meta-analysis of animal experimental stroke

hypothermia studies, of 145 experiments, the median cooling duration was 180 min. Interestingly, in that study, a post hoc analysis indicated that shorter duration cooling may be associated with better neuroprotection (17). Despite being the only paradigm tried in human studies, prolonged hypothermia has only been investigated in relatively few experimental focal ischemia studies, and there are little easily interpretable data directly comparing short vs. long duration hypothermia. Yamamoto *et al.* (31) showed neuroprotection with either 3 h or 22 h cooling but only when this was begun prior to stroke induction (31,32). Colbourne *et al.* (32,33) have conducted several studies showing effectiveness of long-duration cooling, and one showing long-duration cooling was more effective than short; however, in that study, the short-duration group were cooled for 12 h, significantly longer than in the great bulk of experimental hypothermia research (33). In contrast, Markarian *et al.* (34) found greater neuroprotection with longer durations of hypothermia; however, the longest durations tested were three to four hours. The findings of the current study suggest that short-duration hypothermia, the dominant paradigm used in successful experimental studies, should perhaps be subject to trial in patients.

There were some unavoidable limitations to this study. There were differences in intraoperative physiological variables (particularly reduced heart and respiratory rates) during the cooling phase. This is largely unavoidable in hypothermia because heart and respiratory rates and anesthetic requirement drop considerably during this therapy. However, there is no known way these factors could account for the dramatic differences seen in final ICP. The measurement of ICP beyond 24 h, although desirable, was beyond the scope of this study and will be the focus of future investigations.

In conclusion, short-duration, moderate hypothermia commenced shortly after onset of experimental stroke had a profound, sustained, neuroprotective effect, preventing subsequent ICP elevation. This approach would be easier to apply in patients than most currently used protocols and would potentially avoid the problem of rewarming-induced ICP elevation. Further preclinical testing is required before clinical proof of concept studies. However, perhaps in the case of hypothermia following neurological injury, less is more?

Acknowledgements

We would like to thank the Faculty of Health Stores Workshop of the University of Newcastle for manufacture of bespoke surgical and anesthetic equipment.

References

1 Mackay J, Mensah G. Atlas of Heart Disease and Stroke. Geneva, Switzerland, World Health Organization, 2004.
2 Hacke W, Schwab S, Horn M, Spranger M, De Georgia M, von Kummer R. 'Malignant' middle cerebral artery territory infarction: clinical course and prognostic signs. *Arch Neurol* 1996; **53**:309–15.
3 Ropper AH, Shafran B. Brain edema after stroke. Clinical syndrome and intracranial pressure. *Arch Neurol* 1984; **41**:26–9.
4 Schwab S, Aschoff A, Spranger M, Albert F, Hacke W. The value of intracranial pressure monitoring in acute hemispheric stroke. *Neurology* 1996; **47**:393–8.
5 Kotwica Z, Hardemark HG, Persson L. Intracranial pressure changes following middle cerebral artery occlusion in rats. *Res Exp Med (Berl)* 1991; **191**:99–104.
6 Schwab S, Schwarz S, Spranger M, Keller E, Bertram M, Hacke W. Moderate hypothermia in the treatment of patients with severe middle cerebral artery infarction. *Stroke* 1998; **29**:2461–6.
7 Tokutomi T, Morimoto K, Miyagi T, Yamaguchi S, Ishikawa K, Shigemori M. Optimal temperature for the management of severe traumatic brain injury: effect of hypothermia on intracranial pressure, systemic and intracranial hemodynamics, and metabolism. *Neurosurgery* 2003; **52**:102–12.
8 Jalan R, Olde Damink SWM, Deutz NE, Lee A, Hayes PC. Moderate hypothermia for uncontrolled intracranial hypertension in acute liver failure. *Lancet* 1999; **354**:1164–8.
9 Schwab S, Georgiadis D, Berrouschot J, Schellinger PD, Graffagnino C, Mayer SA. Feasibility and safety of moderate hypothermia after massive hemispheric infarction. *Stroke* 2001; **32**:2033–5.
10 Guluma KZ, Hemmen TM, Olsen SE, Rapp KS, Lyden PD. A trial of therapeutic hypothermia via endovascular approach in awake patients with acute ischemic stroke: methodology. *Acad Emerg Med* 2006; **13**:820–7.
11 Hemmen TM, Raman R, Guluma KZ *et al.* Intravenous thrombolysis plus hypothermia for acute treatment of ischemic stroke (ICTuS-L): final results. *Stroke* 2010; **41**:2265–70.
12 Bernard SA, Gray TW, Buist MD *et al.* Treatment of comatose survivors of out-of-hospital cardiac arrest with induced hypothermia. *N Engl J Med* 2002; **346**:557–63.
13 Hypothermia after Cardiac Arrest Study Group. Mild therapeutic hypothermia to improve the neurologic outcome after cardiac arrest. *N Engl J Med* 2002; **346**:549–56.
14 Shankaran S, Laptook AR, Ehrenkranz RA *et al.* Whole-body hypothermia for neonates with hypoxic-ischemic encephalopathy. *N Engl J Med* 2005; **353**:1574–84.
15 van der Worp HB, Macleod MR, Kollmar R, European Stroke Research Network for Hypothermia (EuroHYP). Therapeutic hypothermia for acute ischemic stroke: ready to start large randomized trials? *J Cereb Blood Flow Metab* 2010; **30**:1079–93.
16 Den Hertog HM, van der Worp HB, Tseng MC, Dippel DW. Cooling therapy for acute stroke. *Cochrane Database Syst Rev* 2009; (1): CD001247.
17 van der Worp HB, Sena ES, Donnan GA, Howells DW, Macleod MR. Hypothermia in animal models of acute ischaemic stroke: a systematic review and meta-analysis. *Brain* 2007; **130**(Pt 12):3063–74.
18 Oliff HS, Weber E, Eilon G, Marek P. The role of strain/vendor differences on the outcome of focal ischemia induced by intraluminal middle cerebral artery occlusion in the rat. *Brain Res* 1995; **675**:20–6.
19 Oliff HS, Weber E, Miyazaki B, Marek P. Infarct volume varies with rat strain and vendor in focal cerebral ischemia induced by transcranial middle cerebral artery occlusion. *Brain Res* 1995; **699**:329–31.
20 McLeod D, Parsons M, Hood R *et al.* Perfusion computed tomography thresholds defining ischaemic penumbra and infarct core: studies in a rat stroke model. *Int J Stroke* 2013; DOI: 10.1111/ijs.12147.
21 McLeod DD, Parsons MW, Levi CR *et al.* Establishing a rodent stroke perfusion computed tomography model. *Int J Stroke* 2011; **6**:284–9.
22 Murtha L, McLeod D, Spratt N. Epidural intracranial pressure measurement in rats using a fiber-optic pressure transducer. *J Vis Exp* 2012; (62), e3689, doi:10.3791/3689.
23 Spratt NJ, Fernandez J, Chen M *et al.* Modification of the method of thread manufacture improves stroke induction rate and reduces mortality after thread-occlusion of the middle cerebral artery in young or aged rats. *J Neurosci Methods* 2006; **155**:285–90.
24 Petullo D, Masonic K, Lincoln C, Wibberley L, Teliska M, Yao DL. Model development and behavioral assessment of focal cerebral ischemia in rats. *Life Sci* 1999; **64**:1099–108.

25 Rewell SS, Fernandez JA, Cox SF *et al.* Inducing stroke in aged, hypertensive, diabetic rats. *J Cereb Blood Flow Metab* 2010; **30**:729–33.
26 Silasi G, MacLellan CL, Colbourne F. Use of telemetry blood pressure transmitters to measure intracranial pressure (ICP) in freely moving rats. *Curr Neurovasc Res* 2009; **6**:62–9.
27 Schaller B, Graf R. Different compartments of intracranial pressure and its relationship to cerebral blood flow. *J Trauma* 2005; **59**:1521–31.
28 Burger R, Bendszus M, Vince GH *et al.* Neurophysiological monitoring, magnetic resonance imaging, and histological assays confirm the beneficial effects of moderate hypothermia after epidural focal mass lesion development in rodents. *Neurosurgery* 2004; **54**:701–11; discussion 711–12.
29 Zgavc T, Ceulemans AG, Hachimi-Idrissi S, Kooijman R, Sarre S, Michotte Y. The neuroprotective effect of post ischemic brief mild hypothermic treatment correlates with apoptosis, but not with gliosis in endothelin-1 treated rats. *BMC Neurosci* 2012; **13**:105.
30 Kollmar R, Blank T, Han JL, Georgiadis D, Schwab S. Different degrees of hypothermia after experimental stroke: short- and long-term outcome. *Stroke* 2007; **38**:1585–9.
31 Yanamoto H, Nagata I, Nakahara I, Tohnai N, Zhang Z, Kikuchi H. Combination of intraischemic and postischemic hypothermia provides potent and persistent neuroprotection against temporary focal ischemia in rats. *Stroke* 1999; **30**:2720–6; discussion 2726.
32 Clark DL, Penner M, Orellana-Jordan IM, Colbourne F. Comparison of 12, 24 and 48 h of systemic hypothermia on outcome after permanent focal ischemia in rat. *Exp Neurol* 2008; **212**:386–92.
33 Corbett D, Hamilton M, Colbourne F. Persistent neuroprotection with prolonged postischemic hypothermia in adult rats subjected to transient middle cerebral artery occlusion. *Exp Neurol* 2000; **163**:200–6.
34 Markarian GZ, Lee JH, Stein DJ, Hong SC. Mild hypothermia: therapeutic window after experimental cerebral ischemia. *Neurosurgery* 1996; **38**:542–50; discussion 551.

CHAPTER 5

PUBLICATION 3

Murtha L, McLeod D, Beard D, Pepperall D, McCann S, Tomkins A, Holmes W, McCabe C, Macrae I.M, Spratt N. Intracranial pressure elevation following ischemic stroke in rats: Cerebral edema is not the only cause, and short-duration mild hypothermia is a highly effective preventive therapy. Submitted to *JCBFM* - Awaiting Review. (2014).

5.1 INTRODUCTION

Scientific interpretation of intracranial pressure (ICP) regulation has traditionally been that cerebral oedema is the primary cause of ICP elevation post-stroke. I have demonstrated in the previous publication, however, that ICP was dramatically increased following small ischaemic stroke despite relatively small oedema volumes. In fact, the data revealed that the animals with the largest oedema volumes, actually had some of the smallest ICP values, and those with the smallest oedema volumes had some of the highest ICP values. If a mechanism other than oedema is the primary cause of ICP elevation at 24 hours post-stroke, a fundamental rethink of ICP regulation following stroke is needed. It would also have potential implications for other neurological pathologies in which ICP elevation is common. Since this hypothesis challenges more than a century of accepted scientific wisdom, further investigations into the relationship between oedema and ICP elevations are needed.

Data in Publication 2 also indicated that cooling the core temperature to 32.5 °C prevented the subsequent rise in ICP. The effect size between the normothermic and hypothermia-treated groups was enormous. Short-duration hypothermia appears to act in a 'switch-like' manner, in which cooling for only 2.5 hours prior to ICP elevation, completely prevented the dramatic increases seen at 24 hours in the normothermic group. In the clinical setting, therapeutic hypothermia is typically induced over a period of 24-72 hours. Cooling for these longer durations increases the risk of infection, such as pneumonia. The data in Publication 2 suggested that short-duration moderate hypothermia was an effective ICP preventative treatment in rats. Cooling to 32.5 °C, however, is difficult in stroke patients. Shivering thermogenesis in humans is highly efficient, and prevents subsequent cooling. This is the major reason that sedation is needed in these patients. The issue with sedating stroke patients is that it increases the risk of pneumonia in an already high-risk population. Shivering tends to occur at core temperatures below 35 °C. If a short duration of mild hypothermia (35 °C) was all that was needed to prevent ICP, therapeutic hypothermia may become an easy, safe and effective treatment post-stroke. Understanding the fundamental mechanisms of post-stroke ICP elevation and the preventative effects of short-duration hypothermia is important in developing potential stroke treatments. The two aims of this study were therefore to determine the importance of cerebral oedema in ICP elevation post-stroke and to determine whether short-duration mild hypothermia prevents this ICP elevation.

5.2 CONTRIBUTIONS

"As co-authors of the paper: Murtha L, McLeod D, Beard D, Pepperall D, McCann S, Tomkins A, Holmes W, McCabe C, Macrae I.M, Spratt N. Intracranial pressure elevation following ischemic stroke in rats: Cerebral edema is not the only cause, and short-duration mild hypothermia is a highly effective preventive therapy. Submitted to *JCBFM* - Awaiting Review. (2014), we confirm that Lucy Murtha has made the following contributions: 50% conception and design of research; 95% experimental procedures; 70% analysis and interpretation of the findings; 70% writing of the paper and critical appraisal of content."

Dr Damian McLeod

Signed Date: 05.08.2014

Mrs Debbie-Gai Pepperall

Signed Date: 07.08.2014

Dr Sarah McCann

Signed Date: 04.08.2014

Mr Daniel Beard

Signed Date: 04.08.2014

Ms Amelia Tomkins

Signed Date: 07.08.2014

Dr William Holmes

Signed Date: 18.08.2014

Dr Christopher McCabe

Signed Date: 15.08.2014

Dr Mhairi Macrae

Signed Date: 16.08.2014

Dr Neil Spratt

Signed Date: 04.08.2014

FACULTY ASSISTANT DEAN (RESEARCH TRAINING)

Professor Robert Callister

Signed Date: 03.09.2014

Journal of
Cerebral Blood Flow
& Metabolism

Intracranial pressure elevation following ischemic stroke in rats: Cerebral edema is not the only cause, and short-duration mild hypothermia is a highly effective preventive therapy

Journal:	*Journal of Cerebral Blood Flow and Metabolism*
Manuscript ID:	Draft
Manuscript Type:	Original Article
Date Submitted by the Author:	n/a
Complete List of Authors:	Murtha, Lucy; University of Newcastle and Hunter Medical Research Institute, Australia, ; Glasgow Experimental MRI Centre, Institute of Neuroscience and Psychology, College of Medicine, Veterinary and Life Sciences, University of Glasgow, United Kingdom., McLeod, Damian; University of Newcastle and Hunter Medical Research Institute, Australia, Pepperall, Debbie; University of Newcastle and Hunter Medical Research Institute, Australia, McCann, Sarah; University of Newcastle and Hunter Medical Research Institute, Australia, Beard, Daniel; University of Newcastle and Hunter Medical Research Institute, Australia, Tomkins, Amelia; University of Newcastle and Hunter Medical Research Institute, Australia, Holmes, William; Glasgow Experimental MRI Centre, Institute of Neuroscience and Psychology, College of Medicine, Veterinary and Life Sciences, University of Glasgow, United Kingdom., McCabe, Chris; Glasgow Experimental MRI Centre, Institute of Neuroscience and Psychology, College of Medicine, Veterinary and Life Sciences, University of Glasgow, United Kingdom., Macrae, Iseabail; Glasgow Experimental MRI Centre, Institute of Neuroscience and Psychology, College of Medicine, Veterinary and Life Sciences, University of Glasgow, United Kingdom., Spratt, Neil; University of Newcastle and Hunter Medical Research Institute, Australia,
Keywords:	Brain edema, Hypothermia, Acute Stroke, Animal Models, MRI, Basic Science, Behavior (rodent), Blood brain barrier, Brain Imaging, Brain Ischemia, Focal Ischemia, Imaging, Magnetic Resonance, Microcirculation, Neuropathology, Neurophysiology, Neuroprotection, Physiology, Transcranial Doppler, Vascular Surgery

Intracranial pressure elevation following ischemic stroke in rats: Cerebral edema is not the only cause, and short-duration mild hypothermia is a highly effective preventive therapy

Lucy A. Murtha[1,2], Damian D. McLeod[1], Debbie Pepperall[1], Sarah K. McCann[1], Daniel J. Beard[1], Amelia J. Tomkins[1], William M. Holmes[2], Christopher McCabe[2], I. Mhairi Macrae[2], Neil J. Spratt[1]

1. University of Newcastle and Hunter Medical Research Institute, Australia
2. Glasgow Experimental MRI Centre, Institute of Neuroscience and Psychology, College of Medicine, Veterinary and Life Sciences, University of Glasgow, United Kingdom.

Corresponding author: Neil Spratt
Department of Neurology, John Hunter Hospital, Locked Bag 1, Hunter Region Mail Centre, NSW, 2310, Australia.
Ph: +61 2 49216171, fax: +61 2 49213481, email: Neil.Spratt@newcastle.edu.au

Acknowledgements/Funding: We would like to thank the Faculty of Health Stores Workshop of the University of Newcastle for manufacture of bespoke surgical and anesthetic equipment. We would also like to thank Jim Mullin, Lindsay Gallagher, and staff at the Wellcome Surgical Institute for technical assistance. This work was supported by a NHMRC Project Grant, APP1033461, and research support from the Hunter Medical Research Institute from funds donated by the Greater Building Society. N. Spratt received a NHMRC career development fellowship, APP1035465.

Conflicts of Interest/Disclosures: None

Running Title: **Edema not the only cause of ICP rise post-stroke**

Abstract

In both the human and animal literature it has largely been assumed that edema is the primary cause of intracranial pressure (ICP) elevation post-stroke, and that larger edema volumes equate to higher ICP. We recently demonstrated in rats that a dramatic elevation in ICP occurred 24 hours after small ischemic strokes with minimal edema. This ICP elevation was completely prevented by short-duration *moderate* hypothermia soon after stroke. Here, our aims were to determine the importance of edema in ICP elevation post-stroke and whether *mild* hypothermia prevented the ICP rise. Experimental stroke in rats was performed in three studies. ICP was monitored and short-duration mild (35 °C) or moderate (32.5 °C) hypothermia, or normothermia (37 °C) was induced post-stroke. Edema was measured using wet-dry weight calculations, T_2-weighted magnetic resonance imaging or histology. ICP increased significantly 24 hours post-stroke in all normothermic animals. Short-duration mild or moderate hypothermia prevented this rise. No correlation was seen between ΔICP and edema or infarct volumes. Calculated rates of edema growth were orders of magnitude less than normal cerebrospinal fluid production rates. These data challenge current concepts and suggest that factors other than cerebral edema are the primary cause of the ICP elevation 24 hours post-stroke.

Keywords: Cerebral edema, hypothermia, intracranial pressure, ischemic stroke, rats

Introduction

Dramatic elevations in intracranial pressure (ICP) may be associated with death following large ischemic stroke (1, 2). This elevation in ICP has been attributed to an increasing volume of cerebral edema, however there is a distinct lack of empirical evidence to support a causative relationship. The idea of edema as the primary cause of ICP elevation post-stroke appears to have become a self-fulfilling prophecy, as ICP rise seems only to have been investigated in subjects with large volumes of edema (2-4). Little is known about the levels of ICP in patients with smaller strokes and volumes of edema, due to the invasiveness of available methods for ICP monitoring in patients. Our group has recently shown that ICP is dramatically elevated 24 hours after relatively minor stroke in rats (5), raising doubts about the association between ICP and edema.

Hypothermia is the most promising neuroprotective modality currently available. It has shown overwhelming efficacy in experimental models (6) and cooling has been shown to reduce ICP in stroke and other neurological conditions such as traumatic brain injury and hepatic encephalopathy (7, 8). However rebound ICP elevation is a frequent complication during rewarming, particularly if this is rapid. Clinically, hypothermia is a difficult and complicated therapeutic strategy to implement. In particular, preventing shivering thermogenesis is difficult in awake patients if cooling to temperatures <35 °C. Prolonged cooling increases the risk of developing severe systemic complications such as pneumonia and immunosuppression (9, 10). Our recent study demonstrated that a short duration of moderate hypothermia (32.5 °C) administered shortly after stroke, did not affect ICP during the cooling interval, but completely prevented any subsequent rise in ICP 24 hours post-

stroke (5). If a short duration of mild hypothermia (35 °C) was able to limit post-stroke ICP elevation, this would be a more achievable target temperature in the clinical setting, and therefore a more widely applicable potential therapeutic strategy.

Understanding the fundamental mechanisms of post-stroke ICP elevation and the preventative effects of short-duration hypothermia is important in developing potential stroke treatments. The aims of this study were 1) to determine the importance of edema in the ICP elevation 24 hours post-stroke, and 2) to determine whether mild short-duration hypothermia prevents this ICP rise.

Materials and Methods

Animals

Surgery was performed on male outbred Wistar rats at the University of Newcastle, Australia (Studies I and III; n = 48, 315-497g, Animal Services Unit, University of Newcastle), and male Sprague-Dawley rats at the University of Glasgow, UK (Study II; n = 18, 282-372g, Harlan, Bicester, UK). Experimental animal procedures conducted in Australia were in accordance with the Australian Code for the Care and Use of Animals for Scientific Purposes (National Health and Medical Research Council, 2013) and were approved by the Animal Care and Ethics Committee of the University of Newcastle. Experiments performed in the United Kingdom were performed under license granted by the Home Office, UK, according to the UK Animals (Scientific Procedures) Act, 1986.

Experimental Protocols

Study I

In Study I we investigated the importance of edema in ICP elevation at 24 hours using the 'gold-standard' edema calculation, wet-dry weight. Wistar rats underwent experimental stroke (3 hour intraluminal Middle Cerebral Artery occlusion - MCAo). At 1 hour post-MCAo, rats were randomized by sealed numbered envelope to 2.5 hours hypothermia-treatment (32.5 °C, n = 6) or normothermia (37 °C, n = 6). Blood pressure and ICP were measured at baseline, throughout stroke, and at 24 hours post-stroke, before brains were removed for wet-dry weight calculation of brain edema.

Study II

In Study II our aim was to investigate the effect of moderate hypothermia on ICP post-stroke in a strain of rat known to have larger strokes, Sprague-Dawley, and to determine the importance of edema in an *in vivo*, intact skull model of edema calculation using magnetic resonance imaging (MRI). Animals underwent experimental stroke (45 min MCAo), followed by 2.5 hours hypothermia-treatment (32.5 °C, n = 6) or normothermia (37 °C, n = 6) commencing 30 minutes post-stroke. Blood pressure and ICP were measured at baseline, throughout stroke (blood pressure only), and at 24 hours post-stroke. Infarct volume, edema volume and blood-brain-barrier (BBB) breakdown were assessed using T_2- and T_1-weighted MRI scans.

Study III

Our aim in Study III was to determine whether early short-duration mild hypothermia prevents 24 hour ICP elevation, as is seen with moderate hypothermia (32.5 °C) (5), and to determine the importance of edema in ICP elevation post-stroke using histological methods. Wistar rats underwent experimental stroke (3 hour MCAo) and at 1 hour post-stroke, were randomized to 2.5 hours hypothermia-treatment (35 °C, n = 6) or normothermia (37 °C, n = 3 concurrent + n = 10 historical controls). Given the high consistency of the results of multiple previous experiments using the same paradigm, ten historical controls were included in this study, following the direction of the local ethical review committee. Data for historical controls used in Study III has previously been published (5). Blood pressure and ICP were measured at baseline, throughout stroke, and at 24 hours post-stroke, before brains were removed for histology.

Anesthesia and Monitoring

All animals were anesthetized with isoflurane (5% induction, 1.5-2% maintenance) in 70:30 N_2:O_2 (Studies I and III) or N_2O:O_2 (Study II). Animals spontaneously breathed through a laboratory-manufactured low dead-space nose cone in Studies I and III, and were intubated and artificially ventilated in Study II. A rectal thermocouple provided continual monitoring of core body temperature. Temperature was also recorded every 5 minutes for 24 hours using an intra-peritoneal datalogger (SubCue, Calgary, Canada) in Studies I and III. Blood pressure was continuously monitored under anesthesia via a right femoral arterial cannula. Blood samples from this line were periodically monitored for blood gases in Studies I and II. Heart rate, respiratory rate, and SpO_2 were also continuously monitored throughout surgery. Following stroke surgery, animals were injected subcutaneously with saline (2 x 2.5 mL) to prevent dehydration and returned to their cages with free access to softened laboratory chow and water.

Intracranial Pressure Measurement

ICP measurements were obtained whilst under anesthesia using a fibre-optic microcatheter (SAMBA Sensors, Gothenburg, Sweden), as previously described, with minor changes (11). Briefly, two polyether ether ketone, fluid-filled, hollow screws were inserted bilaterally into the parietal bone. The sensor was placed above the dura mater and sealed in place with a caulking material (Silagum, Gunz Dental, Sydney, Australia). Cerebral perfusion pressure (CPP) was calculated as mean arterial pressure – mean ICP.

Experimental Stroke and Hypothermia

Stroke surgery and hypothermia induction were performed as previously described (5, 12). Briefly, a 3 mm silicone-tipped monofilament was passed via the right external carotid artery to occlude the middle cerebral artery. The filament remained in place for 3 hours (Wistar rats, Studies I and III) or 45 minutes (Sprague-Dawley rats, Study II) before being retracted to allow reperfusion. Occlusion and reperfusion of the MCA were confirmed using a laser Doppler flowmetry probe (Studies II and III) that was placed above the MCA watershed area for the entire occlusion.

At 1 hour (Studies I and III) or 30 minutes (Study II) post-stroke, hypothermia-treated animals were cooled using 70% ethanol evaporation with a sprayer and a fan. Normothermia animals were maintained at 37 °C. Hypothermia/normothermia was maintained for 2.5 hours. ICP and blood pressure monitoring equipment was then removed, hollow skull screws were sealed with caulking material, and the animal was allowed to recover and self-thermoregulate by placing ½ the holding cage over a heat mat. At 24 hours post-MCAo, animals were re-anesthetized, the left femoral artery cannulated, physiological equipment reattached and ICP catheter reinserted and sealed for 1 hour.

Neurological Testing

Prior to 24 hour ICP and blood pressure monitoring, animals were tested for stroke induced neurological deficits. The forelimb flexion, torso twist and lateral push tests were used to assess this and a total neurological deficit score given out of 6 (higher score indicating greater deficit) by a blinded assessor (13, 14).

Wet–Dry Weight Calculations- Study I

Water content percentages of the brain tissue were evaluated using the wet-dry weight method. Rats were decapitated immediately under deep anesthesia with isoflurane. Brains were placed in a rat brain matrix, the cerebellum removed and the two hemispheres separated. Each hemisphere was weighed before being placed in an oven at 70 °C for 48 hours. The percentage of tissue water content was calculated using the formula: % water content = [(wet-dry weight) / wet weight] x 100. To allow comparisons with Studies II and III, water content was converted into percentage of contralateral hemisphere: [ipsilateral (wet-dry weight) – contralateral (wet-dry weight) / contralateral (wet weight)] x 100.

Magnetic Resonance Imaging and Analysis- Study II

The ICP probe was removed following the 24 hour ICP and blood pressure monitoring. Animals were then transferred under anesthesia to the MRI scanner. Body temperature was maintained at 37 ± 0.5 °C during the MRI scanning procedure by a closed circuit thermal jacket. All MRI data were acquired using a Bruker Pharmascan 7T/16cm system (Ettlingen, Germany) with a gradient coil (internal diameter = 90 mm, 300 mT/m). A 72 mm birdcage resonator was used to transmit and a 4-channel phased array rat head surface to receive the MRI signal.

Once a pilot sequence had been obtained to ensure correct geometry, a rapid acquisition with relaxation enhancement (RARE) T_2-weighted scan was performed (effective Te 46.6 ms, repetition time TR = 5000 ms, Rare factor 8, averages 2, matrix 256 x 256, FOV 3.0 cm x 3.0 cm, slice thickness 0.75 mm). A baseline T_1-weighted scan was acquired using a RARE sequence with 800 ms repetition time (Echo time Te= 13.5 ms, Rare factor 4, averages 8,

partial FT factor 1.6, matrix 256 x 256, FOV 3.0 cm x 3.0 cm, slice thickness 1.5 mm). Following this scan, 0.1 mL of MultiHance contrast (529 mg/mL, gadobenate dimeglumine, Bracco Diagnostics Inc. NJ, USA) and 0.5 mL of sterile saline were injected through a femoral venous cannula, and the T_1-weighted scan was repeated 5 minutes after contrast agent injection. When injected intravenously, the gadolinium-based contrast accumulates in regions with impairment of the BBB integrity.

Image J software (NIH, Maryland, USA) was used for image analysis. Infarct volume at 24 hours post-stroke was defined as the hyperintense area on T_2-weighted images. Hyperintensity was traced using Image J software on all slices and areas multiplied by the slice thickness to calculate volume. Contralateral and ipsilateral hemisphere volumes were also determined to assess brain swelling and for edema correction of infarct volume. All volumetric measurements were performed independently by 2 different investigators blinded to treatment allocation, any cases with >10% discrepancy were flagged for review. Infarct volume was corrected for edema using the formula: Corrected infarct volume (mm^3) = infarct volume x (contralateral volume/ipsilateral volume) (15). Edema was calculated by infarct volume minus corrected infarct volume.

Contrast agent enhancement maps were generated from the signal of the pre- and post-contrast T_1-weighted scans according to the formula: (post-contrast – pre-contrast)/pre-contrast x 100. Hyperintensity was traced using Image J software on all slices. Areas were then multiplied by the slice thickness to calculate the volume of contrast-induced hyperintensity.

Histological Analysis- Study III

Histological analysis followed the methodology described by McLeod *et al.* (15). Briefly, following the 24 hour ICP monitoring, animals were sacrificed and perfused transcardially with saline followed by 4% paraformaldehyde in 0.2M phosphate buffer. Brains were then fixed in neutral-buffered formalin before being processed, paraffin embedded, 5 μm coronal sections cut and stained with hematoxylin and eosin. Images were scanned using a digital slide scanner (Aperio Technologies Inc., Vista, CA, USA). Image J software was used for image analysis by two investigators blinded to treatment allocation. The edema-corrected infarct and edema volumes for both the concurrent animals and historical controls were calculated as per Study II.

Exclusion Criteria

Since subarachnoid hemorrhage (SAH) is a well-recognized complication using intraluminal thread occlusion models of stroke, and may have a profound effect on both ICP and infarct volume (vasospasm), any evidence of SAH was pre-specified as an exclusion criterion (5). Presence of SAH was assessed by: a) dramatic sudden ICP rise >50 mmHg at MCA occlusion/reperfusion, b) evidence of SAH at post-mortem in animals that died, or c) evidence of subarachnoid blood seen on saline/paraformaldehyde perfused brains post-mortem (blinded assessor).

Statistics

An *a priori* sample size calculation was performed for the mild hypothermia study based on our previously published ICP data (5, 16). Six animals per treatment group (hypothermia or normothermia) were required to detect a 15 mmHg difference in Δ ICP between the

treatment groups (Δ ICP = mean peak ICP – mean baseline ICP) with standard settings of alpha 0.05, power 0.8. Statistical analysis was performed using GraphPad Prism version 6.01 (GraphPad Software, Inc. La Jolla, CA, USA).

Intra-rater reliability of infarct volumes was determined in Study II and inter-rater reliability determined in Studies II and III. Intra-observer reliability was assessed by comparing two sets of measurements performed 4 months apart by the same investigator. Inter-rater reliability was assessed by comparing measurements of the same slices performed by two individual investigators. Investigator 2 was blinded to the results of investigator 1 and both investigators were blinded to treatment allocation. Pearson correlation analysis was used to determine reliability.

Student's *t*-tests were performed to compare differences between treatment groups (unpaired *t*-test) or changes from baseline (paired *t*-test). Mann-Whitney *U* tests were performed to compare neurological deficit scores between treatment groups. Neurological deficit scores are presented as median (25th – 75th interquartile range). Pearson correlation analysis was used to determine the relationship between ICP vs. infarct volume and edema volume. Spearman correlation analysis was used to compare ICP and neurological deficit scores. Significant differences were accepted at the $p < 0.05$ level. Data are presented as mean ± standard deviation unless otherwise stated.

Results

Study I- Effect of moderate hypothermia, wet-dry weight edema

Seven Wistar rats were excluded in total. Reasons for exclusion were: equipment difficulties (2 hypothermia; 1 normothermia; 1 prior to randomization), mortality during surgery (2 normothermia), or SAH (1 hypothermia). There were no significant differences in baseline or 24 hour physiological parameters between groups (Table 1). Mean temperature was 32.8 ± 1.3 °C during hypothermia-treatment and 38.1 ± 1.1 °C during equivalent normothermia period.

ICP increased from 9.7 ± 4.3 mmHg at baseline to 42.1 ± 7.0 mmHg at 24 hours in the normothermic group, $p < 0.0001$. There was no elevation in ICP in the hypothermia-treated group, 8.1 ± 2.1 mmHg at baseline vs. 7.7 ± 3.8 mmHg at 24 hours, $p = 0.24$ (Figure 1-A). ICP did not change significantly from baseline during hypothermia-treatment. CPP decreased significantly from baseline to 24 hours in the normothermic group (90.7 ± 12.1 mmHg vs. 70.7 ± 14.4 mmHg, $p < 0.0001$), and was significantly lower than in the hypothermia-treated group at 24 hours (70.7 ± 14.4 mmHg vs. 120 ± 13.7 mmHg, $p < 0.0001$). No significant change in CPP was seen from baseline to 24 hours in the hypothermia-treated group, $p = 0.10$ (Figure 1-B).

A trend to larger brain-water content was seen in the stroke (ipsilateral) hemisphere of the normothermic group compared to the contralateral hemisphere, 79.5 ± 1.5% vs. 78.4 ± 1.1%, $p = 0.08$. No difference in brain-water content was seen in the hypothermia-treated group, 78.5 ± 1.3% in the ipsilateral hemisphere vs. 78.4 ± 0.8% in the contralateral hemisphere, $p = 0.8$ (Figure 1-C). No difference was seen between normothermia and

hypothermia-treated edema volumes (expressed as percentage of contralateral hemisphere %HLV), 4.1 ± 8.5 vs. 7.4 ± 6.8%, p = 0.47. The growth rate of edema was calculated by dividing the edema volume by 1440 minutes (24 hours). There was no significant difference in edema growth rate between the normothermia and hypothermia-treated groups, 0.005 ± 0.006 μL/min vs. 0.002 ± 0.002 μL/min, p = 0.18. There was no significant difference in neurological deficit scores between the normothermia group, median score of 3 (0.75 - 5) and the hypothermia-treated group, median score 2.5 (1.0 - 3.5), p = 0.86.

***Study II- Effect of moderate hypothermia, "in vivo"* edema quantification**

Six Sprague-Dawley rats were excluded in total. Reasons for exclusion were: equipment difficulties (1 normothermia) or SAH (5 normothermia). Heart rate was significantly higher from baseline to 24 hours in the hypothermia-treated group, and was significantly higher than in the normothermic group. There was no significant difference in other physiological parameters (Table 1).

ICP increased from 10.2 ± 3.2 mmHg at baseline to 60.7 ± 21.1 mmHg at 24 hours in the normothermic group, p = 0.0025. There was no elevation of ICP in the hypothermia-treated group, 18.5 ± 8.5 mmHg at baseline vs. 15.5 ± 8.7 mmHg at 24 hours, p = 0.57 (Figure 2-A). CPP decreased significantly from baseline to 24 hours in the normothermic group (79.9 ± 10.9 mmHg vs. 33.1 ± 15.1 mmHg, p = 0.005), and was significantly lower than in the hypothermia-treated group at 24 hours (33.1 ± 15.1 mmHg vs. 79.5 ± 12.9 mmHg, p = 0.0002). No significant change in CPP was seen from baseline to 24 hours in the hypothermia-treated group, p = 0.66 (Figure 2-B).

There was no significant difference in infarct volume between the hypothermia-treated and normothermic group, 71.7 ± 41.7 mm^3 vs. 109.7 ± 65.6 mm^3, $p = 0.26$ (%HLV, 19.3 ± 11.5% vs. 21.1 ± 12.5%), Figure 2-C, (representative images in Supplementary Figure). Intra-rater and inter-rater reliability of infarct volume measurements was strong, r = 0.97 ($p < 0.0001$) and r = 0.99 ($p < 0.0001$), respectively. Similarly, there was no significant difference in edema between the hypothermia-treated group compared to the normothermic group, 9.6 ± 8.1 mm^3 vs. 17.8 ± 18.6 mm^3, $p = 0.34$ (%HLV, 2.6 ± 2.3% vs. 10.1 ± 7.5%), Figure 2-D. There was no significant difference in edema growth rate between the normothermia and hypothermia-treated groups, 0.012 ± 0.013 µL/min vs. 0.007 ± 0.006 µL/min, $p = 0.34$. No significant difference in volume of brain with BBB breakdown was detected between the groups, 0.4 ± 0.5 mm^3 in the normothermic group vs. 0.5 ± 0.4 mm^3 in the hypothermia-treated group, $p = 0.74$ (representative image, Figure 3). A trend towards a higher neurological deficit score was seen in the normothermia group, median score of 4.5 (2.8 - 5.3) when compared to the hypothermia-treated group, median score 2 (0.0 - 3.5), $p = 0.09$.

Study III- Effect of mild hypothermia, H&E edema

Ten animals were excluded in total. Reasons for exclusion were: equipment difficulties (1 hypothermia, 1 prior to randomization), mortality during surgery (1 hypothermia, 2 prior to randomization), or SAH (2 hypothermia, 1 normothermia, 2 prior to randomization). Core temperature was significantly higher at 24 hours compared to baseline in the hypothermia-treated group but was not different to normothermic group at 24 hours. There was no significant difference in other physiological parameters (Table 1). Mean temperature was 34.6 ± 0.8 °C during hypothermia-treatment and 37.4 ± 1.1 °C during equivalent normothermia period.

ICP increased from 7.0 ± 2.7 mmHg at baseline to 33.2 ± 8.6 mmHg at 24 hours in the normothermic group, $p < 0.0001$. There was no significant ICP rise in the animals that received 35 °C hypothermia-treatment, 8 ± 3.2 mmHg at baseline vs. 13 ± 7.1 mmHg at 24 hours, $p = 0.12$ (Figure 4-A). ICP did not change significantly from baseline during hypothermia-treatment. CPP decreased significantly from baseline to 24 hours in the normothermic group (90.3 ± 13.1 mmHg vs. 64.3 ± 13.8 mmHg, $p < 0.0001$), and was significantly lower than in the hypothermia-treated group at 24 hours (64.3 ± 13.8 mmHg vs. 95.2 ± 19.4 mmHg, $p = 0.02$). No significant change in CPP was seen from baseline to 24 hours in the hypothermia-treated group, $p = 0.75$ (Figure 4-B).

Infarct volume was significantly smaller in the hypothermia-treated group compared to normothermia group, 11.2 ± 11.5 mm^3 vs. 55.6 ± 45.9 mm^3, $p = 0.03$ (%HLV, 5.6 ± 6.0% vs. 14.8 ± 15.2%), Figure 4-C. Inter-rater reliability of infarct volume measurements was strong, $r = 0.99$ ($p < 0.0001$). Edema volumes were small in both groups, with a non-significant trend to lower values in hypothermia-treated rats, 3.1 ± 0.65 mm^3 vs. 27.9 ± 6.5 mm^3 in controls, $p = 0.15$ (%HLV, 0.3 ± 0.6% vs. 1.9 ± 2.8%), Figure 4-D. There was no significant difference in edema growth rate between the normothermia and hypothermia-treated groups, 0.005 ± 0.006 µL/min vs. 0.0004 ± 0.0008 µL/min, $p = 0.14$. There was no significant difference in neurological deficit scores between the normothermia group, median score of 3 (1.5 - 4.3) and the hypothermia-treated group, median score 2 (0.75 - 3.25), $p = 0.29$.

Correlations

No significant correlations were found between Δ ICP over 24 hours and infarct volume (%HLV), cerebral edema volume (%HLV) or neurological deficit scores in the normothermia and hypothermia-treated groups of each study (Table 2 and Figure 5). Pooled analysis of all

normothermia (n = 25) and hypothermia-treated (n = 18) animals across all three studies showed no correlation between Δ ICP and infarct volume (%HLV), edema volume (%HLV), or neurological deficit scores (Table 2 and Figure 5). Pooled analysis of all animals (n = 43) showed no correlation between Δ ICP and infarct volume (%HLV) (r^2 = 0.03, p = 0.35) or between Δ ICP and edema volume (%HLV) (r^2 = 0.04, p = 0.20). There was a significant correlation between pooled Δ ICP and neurological deficit scores (r = 0.36, p = 0.02).

Discussion

In these studies we have made several findings that challenge the conventional thinking about ICP post-stroke. We confirmed our previous findings that ICP is consistently and dramatically elevated 24 hours following even small strokes in Wistar rats and we showed even greater ICP elevation in the larger strokes induced in Sprague- Dawley rats. We also confirmed that a short duration of moderate hypothermia soon after the stroke prevents this later dramatic ICP elevation. We extended upon the latter finding by showing that mild hypothermia to 35 °C also prevented the ICP elevation. Finally, we have shown no correlation between ICP and volume of edema, indicating that there must be mechanisms other than edema contributing both to post-stroke ICP elevation, and to its prevention by hypothermia.

The data indicate that the 24 hour ICP elevation seen in these studies was not primarily caused by cerebral edema. Our previously published data demonstrated that animals with small strokes and little edema had a dramatic elevation in ICP (5). Using three separate methods of edema calculation, this study has confirmed those findings. The edema volumes that were observed in the normothermic groups of Studies I and III were small in

comparison to the dramatic ICP elevations. Furthermore, hypothermia-treated Sprague-Dawley rats had larger volumes of edema, but no ICP rise. This evidence suggests that while edema may be a contributory factor to ICP rise post-stroke, dramatic ICP elevation is possible in the absence of significant edema. Additionally, large volumes of edema were not accompanied by any ICP rise (in hypothermia-treated animals). Therefore edema appears neither necessary, nor sufficient to cause ICP rise (Figure 5-B). This was further confirmed by the lack of any correlation between ICP and edema in any of the individual studies or in the pooled comparison, even when hypothermia-treated animals were excluded. Furthermore, the rate of edema growth over 24 hours in each study was at least 2 orders of magnitude less than the natural rate of cerebrospinal fluid (CSF) production in rats, 2-3 μL/min (17). Even if we assumed that all of the edema growth occurred in the final 6 hours, the growth rate would still be < 0.05 μL/min. Previous investigators have shown that to artificially increase ICP to levels seen in this study (> 30 mmHg), a constant infusion rate of 4.8 μL/min into the spinal subarachnoid space was required (18). Our own data using lateral ventricular infusions suggests even higher flow rates may be required (unpublished). If ICP elevation is not primarily caused by cerebral edema, what then, is the mechanism involved? The Monro-Kellie doctrine states that since the cranial cavity is fixed, any increase in volume of an intracranial component (tissue, CSF or blood) must be compensated by a decrease in the other two (19, 20). ICP will elevate if this compensation fails. Blood volume and CSF are not parameters that have previously been considered important in ICP elevation post-stroke. Our data suggest that they are definitely worthy of further investigation.

Do patients with small strokes have a similar transient ICP elevation at 24 hours as we have seen in the rats? Despite the wealth of studies using rat experimental stroke, including

hypothermia (6), this has gone largely unrecognized until our recent work. The idea that cerebral edema is the cause of ICP elevation appears to have become a self-fulfilling prophecy – with ICP elevation only being looked for in big strokes. Other papers have reported an early ICP peak in animals with smaller strokes, but the authors chose to focus on the secondary peak at day 3 in those with significant edema (21, 22). Could a similar ICP rise also have gone unnoticed in stroke patients? To some, this idea may seem absurd. However we believe it is quite possible, since in the absence of invasive monitoring data, there would be no easy way to detect this (as is the case in rats with experimental stroke). Papilloedema (optic disc swelling) occurs in response to ICP elevation, but takes days to develop. Headache may be reported, but is a common enough phenomenon post-stroke that a self-limited headache of 4-6 hours would not be remarked upon. If a similar rise in ICP does occur following small human strokes, the implications would be very important to the outcome of those patients. Blood flow to the ischemic penumbra is known to be CPP-dependent since normal cerebral blood flow autoregulation is lost in the ischemic penumbra (23), so ICP elevation would be predicted to reduce penumbral perfusion. The principle of increasing CPP to enhance collateral flow and penumbral perfusion has been exploited in several clinical trials (24-30), however to date these have all focused on mean arterial pressure (MAP) rather than intracranial pressure (CPP = MAP- ICP).

Another key finding was that treatment with mild hypothermia also prevents subsequent ICP elevation. This has important implications in terms of clinical relevance, since cooling below 35 °C in conscious patients becomes progressively more difficult due to the need to prevent shivering thermogenesis. One fascinating aspect of these findings with great potential clinical importance was that neither mild nor moderate hypothermia influenced

ICP at the time of cooling. Our previous work also showed no effect during rewarming (5). Hypothermia is well known to lower ICP, and is used to treat otherwise uncontrollable ICP elevation in a number of conditions. A major problem in this setting is rebound ICP elevation during attempted rewarming. This has also been problematic in clinical trials of hypothermia in stroke (3, 10). Our recent data suggest that if cooling/rewarming is completed before the ICP elevation begins, it acts in a "switch-like" manner to prevent subsequent ICP increase even many hours after restoration of normothermia.

Hypothermia is the best studied neuroprotectant in experimental stroke. However, the significant logistical difficulties and risk of iatrogenic complications from long duration, deep hypothermia, are hindering its potential as a post-stroke treatment. There has been a paradox in the attempted clinical translation to date. The vast majority of animal studies have cooled for <6 hours (6), yet all the clinical trials to date have cooled for >12 hours, and the majority for >24 hours (3, 9, 10, 31, 32). Do we know that short and long duration cooling are equivalent, or that long duration is superior? If a short duration, mild hypothermia therapy is all that is needed, it may become much more clinically achievable and deserves further pre-clinical investigation.

This study had some unavoidable limitations. First, the use of the wet-dry weight technique for edema calculation in Study I prevented infarct volume from being calculated in these animals. Confirmation of ischemic insult, however, was determined with the use of laser Doppler flowmetry during MCAo and reperfusion, and from 24 hour neurological deficit scores. Second, the studies were powered to detect ICP reduction, not infarct reduction, since there have already been >100 studies and a meta-analysis of hypothermia-induced

neuroprotection in experimental stroke (6). The point estimates of infarct volumes were all consistent with that from the meta-analysis (6).

In conclusion, mild and moderate hypothermia prevented the dramatic ICP elevation that was observed at 24 hours after minor stroke, and this elevation in ICP was not primarily caused by cerebral edema. This challenges orthodoxy of nearly a century regarding the control of ICP elevation and begs the question about whether similar (as yet unknown) mechanisms also occur in other neurological conditions associated with ICP elevation? Edema has been considered to be the major contributor to ICP elevation in several other forms of acute neurological injury. As in stroke, cerebral edema as the causative mechanism of ICP elevation has been the 'accepted wisdom' and other possibilities may not have been considered. The current findings suggest that perhaps we should entertain other possibilities since, if an alternative mechanism is at play, the therapeutic options may be greater. This study not only suggests that a fundamental rethinking of the mechanisms elevating ICP following neurological injury is warranted, but also has important implications for the use of therapeutic hypothermia to treat ICP elevation in a range of neurological diseases.

Supplementary information is available at the Journal of Cerebral Blood Flow & Metabolism website- www.nature.com/jcbfm

References

1. Hacke W, Schwab S, Horn M, Spranger M, De Georgia M, von Kummer R. 'Malignant' middle cerebral artery territory infarction: clinical course and prognostic signs. Arch Neurol. 1996 Apr;53(4):309-15.
2. Ropper AH, Shafran B. Brain edema after stroke. Clinical syndrome and intracranial pressure. Arch Neurol. 1984 Jan;41(1):26-9.
3. Schwab S, Schwarz S, Spranger M, Keller E, Bertram M, Hacke W. Moderate hypothermia in the treatment of patients with severe middle cerebral artery infarction. Stroke. 1998 Dec;29(12):2461-6.
4. Morley NC, Berge E, Cruz-Flores S, Whittle IR. Surgical decompression for cerebral oedema in acute ischaemic stroke. Cochrane Database Syst Rev. 2002(3):CD003435.
5. Murtha LA, McLeod DD, McCann SK, Pepperall D, Chung S, Levi CR, et al. Short-duration hypothermia after ischemic stroke prevents delayed intracranial pressure rise. Int J Stroke. 2014 Jul;9(5):553-9.
6. van der Worp HB, Sena ES, Donnan GA, Howells DW, Macleod MR. Hypothermia in animal models of acute ischaemic stroke: a systematic review and meta-analysis. Brain. 2007 Dec;130(Pt 12):3063-74.
7. Tokutomi T, Morimoto K, Miyagi T, Yamaguchi S, Ishikawa K, Shigemori M. Optimal temperature for the management of severe traumatic brain injury: effect of hypothermia on intracranial pressure, systemic and intracranial hemodynamics, and metabolism. Neurosurgery. 2003 Jan;52(1):102-11; discussion 11-2.
8. Jalan R, SW OD, Deutz NE, Lee A, Hayes PC. Moderate hypothermia for uncontrolled intracranial hypertension in acute liver failure. Lancet. 1999 Oct 2;354(9185):1164-8.
9. Hemmen TM, Raman R, Guluma KZ, Meyer BC, Gomes JA, Cruz-Flores S, et al. Intravenous thrombolysis plus hypothermia for acute treatment of ischemic stroke (ICTuS-L): final results. Stroke. 2010 Oct;41(10):2265-70.
10. Schwab S, Georgiadis D, Berrouschot J, Schellinger PD, Graffagnino C, Mayer SA. Feasibility and safety of moderate hypothermia after massive hemispheric infarction. Stroke. 2001 Sep;32(9):2033-5.
11. Murtha L, McLeod D, Spratt N. Epidural intracranial pressure measurement in rats using a fiber-optic pressure transducer. J Vis Exp. 2012(62).
12. Spratt NJ, Fernandez J, Chen M, Rewell S, Cox S, van Raay L, et al. Modification of the method of thread manufacture improves stroke induction rate and reduces mortality after thread-occlusion of the middle cerebral artery in young or aged rats. J Neurosci Methods. 2006 Sep 15;155(2):285-90.
13. Petullo D, Masonic K, Lincoln C, Wibberley L, Teliska M, Yao DL. Model development and behavioral assessment of focal cerebral ischemia in rats. Life Sci. 1999;64(13):1099-108.
14. Rewell SS, Fernandez JA, Cox SF, Spratt NJ, Hogan L, Aleksoska E, et al. Inducing stroke in aged, hypertensive, diabetic rats. J Cereb Blood Flow Metab. 2010 Apr;30(4):729-33.
15. McLeod DD, Parsons MW, Levi CR, Beautement S, Buxton D, Roworth B, et al. Establishing a rodent stroke perfusion computed tomography model. Int J Stroke. 2011 Aug;6(4):284-9.
16. Length R. Java Applets for Power and Sample Size [Computer software]. 2006-9 Retrieved January 20, 2012, from http://www.stat.uiowa.edu/~rlenth/Power.
17. Murtha LA, Yang Q, Parsons MW, Levi CR, Beard DJ, Spratt NJ, et al. Cerebrospinal fluid is drained primarily via the spinal canal and olfactory route in young and aged spontaneously hypertensive rats. Fluids Barriers CNS. 2014;11:12.
18. Mann JD, Butler AB, Rosenthal JE, Maffeo CJ, Johnson RN, Bass NH. Regulation of intracranial pressure in rat, dog, and man. Ann Neurol. 1978 Feb;3(2):156-65.
19. Monro A. Observations on the structure and functions of the nervous system : illustrated with tables. Edinburgh: Printed for, and sold by, William Creech; and Joseph Johnson, London; 1783.

20. Kellie G. An account of the appearances observed in the dissection of two of three individuals presumed to have perished in the storm of the 3d, and whose bodies were discovered in the vicinity of Leith on the morning of the 4th, November 1821 : with some reflections on the pathology of the brain. Edinburgh?: s.n.; 1824.
21. Kotwica Z, Hardemark HG, Persson L. Intracranial pressure changes following middle cerebral artery occlusion in rats. Res Exp Med (Berl). 1991;191(2):99-104.
22. Kotwica Z, Persson L, Thuomas KA. The effects of brain edema on intracranial pressure in focal cerebral ischemia. An experimental study in a rat using magnetic resonance imaging. Zentralbl Neurochir. 1989;50(2):68-71.
23. Aries MJ, Elting JW, De Keyser J, Kremer BP, Vroomen PC. Cerebral autoregulation in stroke: a review of transcranial Doppler studies. Stroke. 2010 Nov;41(11):2697-704.
24. Hillis AE, Kane A, Tuffiash E, Ulatowski JA, Barker PB, Beauchamp NJ, et al. Reperfusion of specific brain regions by raising blood pressure restores selective language functions in subacute stroke. Brain Lang. 2001 Dec;79(3):495-510.
25. Hillis AE, Ulatowski JA, Barker PB, Torbey M, Ziai W, Beauchamp NJ, et al. A pilot randomized trial of induced blood pressure elevation: effects on function and focal perfusion in acute and subacute stroke. Cerebrovasc Dis. 2003;16(3):236-46.
26. Mistri AK, Robinson TG, Potter JF. Pressor therapy in acute ischemic stroke: systematic review. Stroke. 2006 Jun;37(6):1565-71.
27. Schwarz S, Georgiadis D, Aschoff A, Schwab S. Effects of induced hypertension on intracranial pressure and flow velocities of the middle cerebral arteries in patients with large hemispheric stroke. Stroke. 2002 Apr;33(4):998-1004.
28. Shin HK, Nishimura M, Jones PB, Ay H, Boas DA, Moskowitz MA, et al. Mild induced hypertension improves blood flow and oxygen metabolism in transient focal cerebral ischemia. Stroke. 2008 May;39(5):1548-55.
29. Han JH, Wong KS. Is counterpulsation a potential therapy for ischemic stroke? Cerebrovasc Dis. 2008;26(2):97-105.
30. Shuaib A, Bornstein NM, Diener HC, Dillon W, Fisher M, Hammer MD, et al. Partial aortic occlusion for cerebral perfusion augmentation: safety and efficacy of NeuroFlo in Acute Ischemic Stroke trial. Stroke. 2011 Jun;42(6):1680-90.
31. Den Hertog HM, van der Worp HB, Tseng MC, Dippel DW. Cooling therapy for acute stroke. Cochrane Database Syst Rev. 2009(1):CD001247.
32. Guluma KZ, Hemmen TM, Olsen SE, Rapp KS, Lyden PD. A trial of therapeutic hypothermia via endovascular approach in awake patients with acute ischemic stroke: methodology. Acad Emerg Med. 2006 Aug;13(8):820-7.

Table 1. Physiological Parameters

		Study I		Study II		Study III	
		0 h	24 h	0 h	24 h	0 h	24 h
Temp. *(°C)*	Normo.	37.1 ± 0.2	37.3 ± 0.4	37.4 ± 0.6	36.8 ± 0.2	37.6 ± 1.2	38.0 ± 0.5
	Hypo.	37.4 ± 0.0	37.4 ± 0.3	37.0 ± 0.2	36.9 ± 0.2	36.6 ± 0.7	38.1 ± 0.6†
RR *(BPM)*	Normo.	62.2 ± 10.2	60.6 ± 9.1	~	~	65.6 ± 17.9	61.0 ± 12.6
	Hypo.	66.0 ± 5.7	56.6 ± 11	~	~	58.0 ± 11.4	60.7 ± 21.2
HR *(BPM)*	Normo.	380 ± 32	399 ± 39	373 ± 22	397 ± 19	376 ± 43	401 ± 26
	Hypo.	400 ± 46	406 ± 27	386 ± 15	418 ± 7.0*†	393 ± 25	382 ± 32
MAP *(mmHg)*	Normo.	100 ± 9.4	112 ±10.1	90.1 ± 8.1	93.8 ± 9.2	97.2 ± 13.6	96.0 ± 11.0
	Hypo.	107 ± 10.3	128 ± 12.2	93.0 ± 7.6	94.9 ± 6.4	98.4 ± 10.3	109 ± 17
SpO_2 *(%)*	Normo.	99.0 ± 0.7	99.4 ± 0.9	99.2 ± 0.0	98.3 ± 2.0	98.7 ± 1.5	98.6 ± 1.4
	Hypo.	97.8 ± 1.6	99.3 ± 0.5	98.2 ± 1.2	99.0 ± 0.5	96.0 ± 3.9	98.7 ± 0.8
paO_2 *(mmHg)*	Normo.	138 ± 18	174 ± 63	165 ± 3	152 ± 48	~	~
	Hypo.	111 ± 21	155 ± 27	128 ± 28	152 ± 15	~	~
$paCO_2$ *(mmHg)*	Normo.	46.2 ± 5.6	48.0 ± 4.6	33.9 ± 2.8	25.8 ± 5.6	~	~
	Hypo.	48.4 ± 5.0	52.8 ± 9.5	46.1 ± 12.3	34.3 ±12.8	~	~
pH	Normo.	7.41 ± 0.04	7.44 ± 0.04	7.48 ± 0.03	7.48 ± 0.02	~	~
	Hypo.	7.39 ± 0.04	7.43 ± 0.04	7.42 ± 0.10	7.44 ± 0.11	~	~

Study I- n = 6/group; Study II- n = 6/group; Study III- n = 6 hypothermia, n = 3 concurrent + n = 10 historical controls; Temp. = temperature; RR = respiratory rate; HR = heart rate; BPM = breaths (RR) or beats (HR) per minute; MAP = mean arterial pressure; SpO_2 = oxygen saturation; paO_2 = arterial partial pressure of oxygen; $paCO_2$ = arterial partial pressure of carbon dioxide. 0h =immediately prior to MCAo *$p < 0.05$ versus normothermia; †$p < 0.05$ versus 0 h.

Table 2. Correlations between intracranial pressure change (24 hour – baseline) and infarct volume (%HLV), edema volume (%HLV) and neurological deficit score

		Infarct Volume		Edema Volume		Neuro. Score	
		r^2	*p*-Value	r^2	*p*-Value	r	*p*-Value
Study I	*Normo.*	~	~	0.21	0.37	0.23	0.65
	Hypo.	~	~	0.05	0.67	-0.18	0.67
Study II	*Normo.*	0.03	0.72	0.07	0.6	-0.29	0.56
	Hypo.	0.36	0.21	0.33	0.23	0.26	0.67
Study III	*Normo.*	< 0.01	0.83	< 0.01	0.87	0.39	0.19
	Hypo.	0.21	0.36	0.24	0.33	-0.47	0.3
Pooled Analysis	*Normo.*	0.01	0.68	0.09	0.15	0.39	0.06
	Hypo.	< 0.01	0.98	< 0.01	0.79	0.02	0.95

Titles and Legends to Figures

Figure 1. Study I - moderate hypothermia (32.5 °C), Wistar rats **A.** Intracranial pressure (ICP) 0 - 3.5 hours and 24 - 25 hours post-stroke in hypothermia-treated (open circles) and normothermia (closed circles) animals, the shaded region represents the cooling interval; MCAo is between the dotted vertical lines **B.** Cerebral perfusion pressure (CPP). CPP was calculated as arterial pressure minus ICP **C.** Brain-water content measured with wet-dry weight calculations for ipsilateral and contralateral hemispheres in hypothermia-treated (open circles) and normothermia (closed circles) animals. **A.** and **B.** data plotted as mean ± SD. **C.** Individual animals, mean ± SD. $*p < 0.0001$, for t-tests between respective hypothermia (open circles) and normothermia (closed circles) groups.

Figure 2. Study II - moderate hypothermia (32.5 °C), Sprague-Dawley rats **A.** Intracranial pressure (ICP) at baseline (pre-stroke, 0 hours) and 24 hours post-stroke in hypothermia-treated (open circles) and normothermia (closed circles) animals **B.** Cerebral perfusion pressure (CPP). CPP was calculated as arterial pressure minus ICP **C.** Infarct volume measured with T_2-weighted magnetic resonance imaging (MRI) **D.** Cerebral edema volume measured with T_2-weighted MRI. Individual animal data plotted, and mean ± SD. $*p < 0.0001$, $\dagger p < 0.05$ for t-tests between respective hypothermia (open circles) and normothermia (closed circles) groups.

Figure 3. Representative magnetic resonance imaging (MRI) scans at 24 hours post-stroke. **A.** Gadolinium contrast was infused intravenously and a T_1-weighted MRI scan was obtained to determine the area of blood-brain-barrier (BBB) breakdown. The area of BBB breakdown is depicted by the area of pallor. **B.** This area was traced and overlaid onto the same slice on the T_2-weighted MRI scan (yellow line). The area of hyperintensity of the T_2-weighted scan is representative of infarct.

Figure 4. Study III - mild hypothermia (35 °C), Wistar rats **A.** Intracranial pressure (ICP) 0 - 3.5 hours and 24 - 25 hours post-stroke in hypothermia-treated (open circles) and normothermia (concurrent controls, closed circles; historical controls, closed squares) animals; the shaded region represents the cooling interval; MCAo is between the dotted vertical lines **B.** Cerebral perfusion pressure (CPP). CPP was calculated as arterial pressure minus ICP **C.** Infarct volume measured with H&E histology **D.** Cerebral edema volume measured with H&E histology. **A.** and **B.** mean ± SD. **C.** and **D.** Individual animals, mean ± SD. $^*p < 0.0001$, $^\dagger p < 0.05$ for t-tests between respective hypothermia (open circles) and normothermia (closed circles/squares) groups.

Figure 5. Change in intracranial pressure (ICP) versus infarct volume (%HLV), cerebral edema volume (%HLV), and neurological score. Study I is represented by triangles; Study II is represented by squares; Study III is represented by circles. Normothermia closed shapes, hypothermia open shapes. To account for minor differences in baseline ICP between Wistar and Sprague-Dawley rats, data are presented as (delta) ICP. No significant correlation of ICP

with infarct volume (%HLV), edema volume (%HLV) or neurological deficit scores was seen in any study: **A.** Normothermia: $r^2 = 0.01$, $p = 0.68$; hypothermia: $r^2 < 0.01$, $p = 0.98$. **B.** Normothermia: $r^2 = 0.09$, $p = 0.15$; hypothermia: $r^2 < 0.01$, $p = 0.79$. **C.** Normothermia: $r = 0.38$, $p = 0.06$; hypothermia: $r = -0.02$, $p = 0.95$.

Supplementary Figure. A representative T_2-weighted magnetic resonance imaging (MRI) scan for each animal in the normothermia and hypothermia groups in Study II. The area of infarct is depicted by the area of hyperintensity.

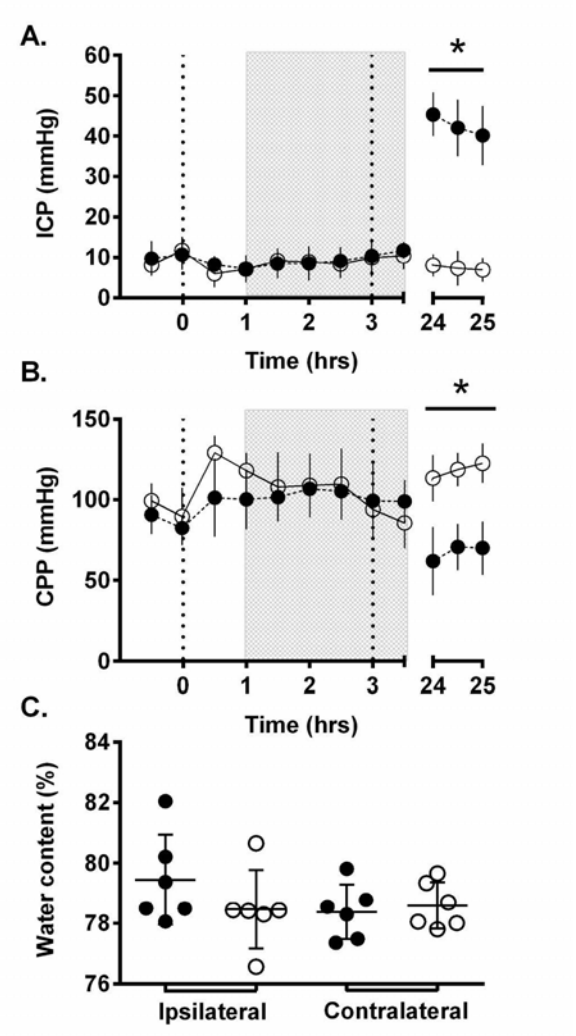

Figure 1. Study I - moderate hypothermia (32.5 °C), Wistar rats A. Intracranial pressure (ICP) 0 - 3.5 hours and 24 - 25 hours post-stroke in hypothermia-treated (open circles) and normothermia (closed circles) animals, the shaded region represents the cooling interval; MCAo is between the dotted vertical lines B. Cerebral perfusion pressure (CPP). CPP was calculated as arterial pressure minus ICP C. Brain-water content measured with wet-dry weight calculations for ipsilateral and contralateral hemispheres in hypothermia-treated (open circles) and normothermia (closed circles) animals. A. and B. data plotted as mean ± SD. C. Individual animals, mean ± SD. *p < 0.0001, for t-tests between respective hypothermia (open circles) and normothermia (closed circles) groups.
142x265mm (300 x 300 DPI)

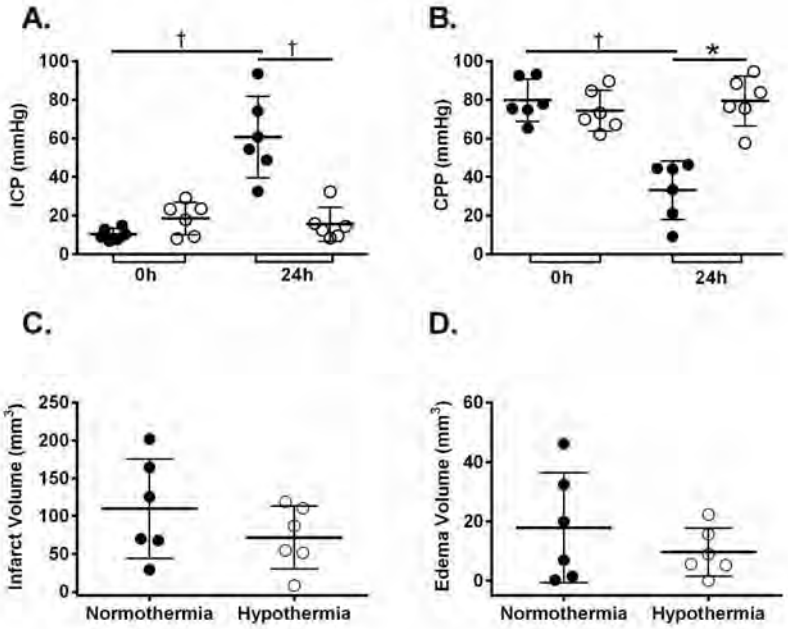

Figure 2. Study II - moderate hypothermia (32.5 °C), Sprague-Dawley rats A. Intracranial pressure (ICP) at baseline (pre-stroke, 0 hours) and 24 hours post-stroke in hypothermia-treated (open circles) and normothermia (closed circles) animals B. Cerebral perfusion pressure (CPP). CPP was calculated as arterial pressure minus ICP C. Infarct volume measured with T2-weighted magnetic resonance imaging (MRI) D. Cerebral edema volume measured with T2-weighted MRI. Individual animal data plotted, and mean ± SD. *p < 0.0001, †p < 0.05 for t-tests between respective hypothermia (open circles) and normothermia (closed circles) groups.
206x155mm (300 x 300 DPI)

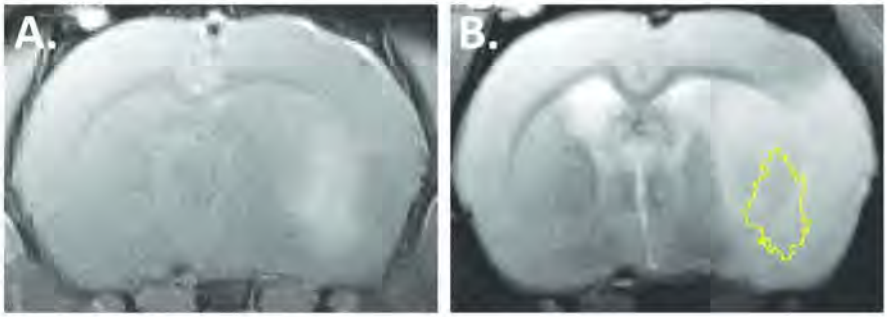

Figure 3. Representative magnetic resonance imaging (MRI) scans at 24 hours post-stroke. A. Gadolinium contrast was infused intravenously and a T1-weighted MRI scan was obtained to determine the area of blood-brain-barrier (BBB) breakdown. The area of BBB breakdown is depicted by the area of pallor. B. This area was traced and overlaid onto the same slice on the T2-weighted MRI scan (yellow line). The area of hyperintensity of the T2-weighted scan is representative of infarct.
182x64mm (300 x 300 DPI)

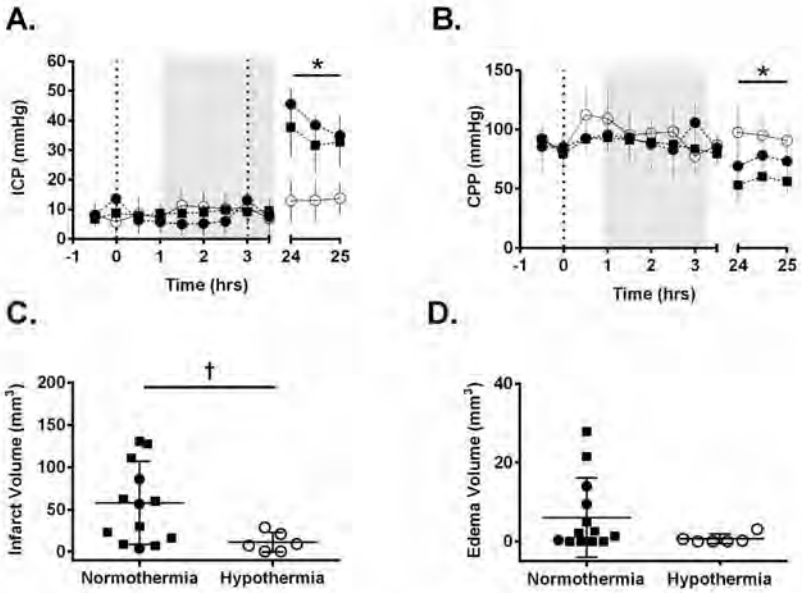

Figure 4. Study III - mild hypothermia (35 °C), Wistar rats A. Intracranial pressure (ICP) 0 - 3.5 hours and 24 - 25 hours post-stroke in hypothermia-treated (open circles) and normothermia (concurrent controls, closed circles; historical controls, closed squares) animals; the shaded region represents the cooling interval; MCAo is between the dotted vertical lines B. Cerebral perfusion pressure (CPP). CPP was calculated as arterial pressure minus ICP C. Infarct volume measured with H&E histology D. Cerebral edema volume measured with H&E histology. A. and B. mean ± SD. C. and D. Individual animals, mean ± SD. *p < 0.0001, †p < 0.05 for t-tests between respective hypothermia (open circles) and normothermia (closed circles/squares) groups.
198x142mm (300 x 300 DPI)

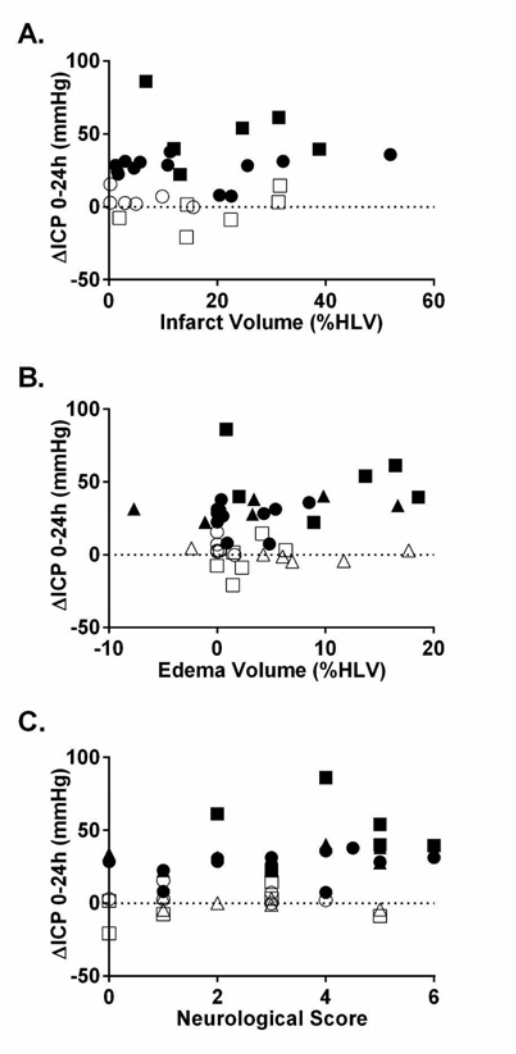

Figure 5. Change in intracranial pressure (ICP) versus infarct volume (%HLV), cerebral edema volume (%HLV), and neurological score. Study I is represented by triangles; Study II is represented by squares; Study III is represented by circles. Normothermia closed shapes, hypothermia open shapes. To account for minor differences in baseline ICP between Wistar and Sprague-Dawley rats, data are presented as (delta) ICP. No significant correlation of ICP with infarct volume (%HLV), edema volume (%HLV) or neurological deficit scores was seen in any study: A. Normothermia: r2 = 0.01, p = 0.68; hypothermia: r2 < 0.01, p = 0.98. B. Normothermia: r2 = 0.09, p = 0.15; hypothermia: r2< 0.01, p = 0.79. C. Normothermia: r = 0.38, p = 0.06; hypothermia: r = -0.02, p = 0.95.
128x266mm (300 x 300 DPI)

CHAPTER 6

PUBLICATION 4

Beard D, McLeod D, Logan C, **Murtha L**, Imtiaz M, van Helden D, Spratt N. Intracranial pressure elevation reduced flow through collateral vessels and the penetrating arterioles they supply. A possible explanation for 'Collateral Failure' in Stroke-in-Progression. Submitted to *JCBFM* - Awaiting Review. (2014).

6.1 INTRODUCTION

I have demonstrated in the previous publication that oedema cannot be the sole mechanism responsible for ICP elevation after small experimental ischaemic stroke. These data raise the important question- if ICP elevation also occurs in patients with small strokes, does it matter?

A subset of ischaemic stroke patients who initially present with minor symptoms, deteriorate 24-48 hours post-stroke, as outlined in Chapter 1. This neurological deterioration, known as stroke-in-progression, has recently been linked to a decline in the function of the leptomeningeal collateral vessels which supply blood to the ischaemic penumbra. To date, the cause of 'collateral failure' in this subset of patients is unknown. Although a good collateral supply has been linked to better outcome post-stroke, the functional dynamics of these vessels before, during and after stroke are still poorly understood. Furthermore, there is conflicting data in experimental literature as

to the flow dynamics of the collateral vessels and penetrating arterioles, and very little data investigating the importance of diameter versus blood flow velocity. Understanding the fundamental dynamics of collateral blood flow is essential to further develop therapies for stroke-in-progression patients.

Under normal circumstances cerebral blood flow is controlled by local autoregulation. Within the ischaemic penumbra these autoregulatory mechanisms progressively fail and cerebral perfusion via collateral blood vessels becomes cerebral perfusion pressure (CPP) dependent (CPP = MAP – ICP). Current therapies aimed at improving collateral circulation post-stroke have focused primarily on manipulating blood pressure. The ICP factor of the equation has largely been neglected. I have demonstrated in Publications 2 and 3 that ICP was dramatically elevated at 24 hours post-stroke and thus CPP was reduced to detrimental levels (CPP = 50-55 mmHg). Furthermore, the clinical data obtained for the CATCH study[81,84] strongly highlighted the similarities in timing between the ICP elevation seen in our stroke model and clinical deterioration in stroke-in-progression, i.e. 63% of patients with stroke-in-progression deteriorated on their first full day in hospital. Direct evidence that ICP elevation causes collateral blood flow reduction would provide a new mechanism to explain stroke-in-progression, a problem that has caused great angst amongst treating doctors for many years. The aims of this study were therefore, to determine the dynamics of collateral vessels post-stroke and to determine the effect of ICP elevation on collateral vessel blood flow.

6.2 CONTRIBUTIONS

"As co-authors of the paper: Beard D, McLeod D, Logan C, **Murtha L**, Imtiaz M, van Helden D, Spratt N. Intracranial pressure elevation reduced flow through collateral vessels and the penetrating arterioles they supply. A possible explanation for 'Collateral Failure' in Stroke-in-Progression. Submitted to *JCBFM* - Awaiting Review. (2014), we confirm that Lucy Murtha has made the following contributions: 30% conception and design of research; 5% experimental procedures; 10% analysis and interpretation of the findings; 20% writing of the paper and critical appraisal of content."

Mr Daniel Beard

Signed Date: 04.08.2014

Dr Damian McLeod

Signed Date: 05.08.2014

Ms Caitlin Logan

Signed Date: 07.08.2014

Mr Mohammad Imtiaz

Signed Date: 05.08.2014

Dr Dirk van Helden

Signed Date: 05.08.2014

Dr Neil Spratt

Signed Date: 04.08.2014

FACULTY ASSISTANT DEAN (RESEARCH TRAINING)

Professor Robert Callister

Signed Date: 03.09.2014

Journal of
Cerebral Blood Flow
& Metabolism

Intracranial Pressure Elevation Reduces Flow through Collateral Vessels and the Penetrating Arterioles they supply. A possible explanation for 'Collateral Failure' in Stroke-in-Progression

Journal:	*Journal of Cerebral Blood Flow and Metabolism*
Manuscript ID:	Draft
Manuscript Type:	Original Article
Date Submitted by the Author:	n/a
Complete List of Authors:	Beard, Daniel; University of Newcastle and Hunter Medical Research Institute., School of Biomedical Sciences and Pharmacy McLeod, Damian; University of Newcastle and Hunter Medical Research Institute., School of Biomedical Sciences and Pharmacy Logan, Caitlin; University of Newcastle and Hunter Medical Research Institute., School of Biomedical Sciences and Pharmacy Murtha, Lucy; University of Newcastle and Hunter Medical Research Institute., School of Biomedical Sciences and Pharmacy Imtiaz, Mohammad; University of Newcastle and Hunter Medical Research Institute, School of Biomedical Sciences and Pharmacy ; Victor Chang Cardiac Research Institute, Computational Cardiology Laboratory van Helden, Dirk; University of Newcastle and Hunter Medical Research Institute., School of Biomedical Sciences and Pharmacy Spratt, Neil; University of Newcastle and Hunter Medical Research Institute., School of Biomedical Sciences and Pharmacy; John Hunter Hospital, Department of Neurology
Keywords:	Cerebral Blood Flow, Cerebral Hemodynamics, Brain Ischemia, Brain Imaging, Experimental, Focal Ischemia, Acute Stroke, Animal Models, Arterioles, Basic Science, Cerebral blood flow measurement, cerebrovascular disease, Cranial windows, Hemodynamics, Imaging, Microscopy, Physiology, Pial Vessels

Intracranial Pressure Elevation Reduces Flow through Collateral Vessels and the Penetrating Arterioles they supply. A possible explanation for 'Collateral Failure' in Stroke-in-Progression.

Daniel J Beard (BSc Hons)[a], Damian D McLeod PhD[a], Caitlin L Logan (BSc Hons)[a], Lucy A Murtha (BSc Hons)[a], Mohammad S Imtiaz PhD[a,c], Dirk F van Helden PhD[a], Neil J Spratt FRACP PhD[a, b].

a. University of Newcastle School of Biomedical Sciences and Pharmacy and Hunter Medical Research Institute, Callaghan, NSW, Australia
b. Hunter New England Local Health District, New Lambton Heights, NSW, Australia
c. Victor Chang Cardiac Research Institute, Darlinghurst, NSW, Australia

Corresponding author: Neil Spratt

Department of Neurology, John Hunter Hospital, Locked Bag 1, Hunter Region Mail Centre, NSW 2310, Australia.

Ph: +61 2 49216171, fax: +61 2 49217903 email: Neil.Spratt@hnehealth.nsw.gov.au

Acknowledgements

We would like to thank the Faculty of Health Stores Workshop of the University of Newcastle for manufacture of bespoke surgical and anesthetic equipment. We would also like to thank Associate Professor Patrick McElduff for his help with the statistical analysis in this project. This work was supported in part by a NHMRC Project Grant, APP 1033461, the Hunter Medical Research Institute from funds donated by the Greater Building Society, and by the National Stroke Foundation (Australia). D. Beard and L. Murtha were both supported by an Australian Postgraduate Award. N. Spratt was supported by a NHMRC career development fellowship, #1035465.

Running Headline: Intracranial Pressure and Collaterals

Abstract

Recent imaging studies indicate that reduced blood flow through leptomeningeal collateral vessels ('collateral failure') is associated with stroke-in-progression, whereas the primary vessel occlusion remains stable. The cause for 'collateral failure' is not known. We recently demonstrated that intracranial pressure (ICP) rises dramatically but transiently 24 hours after even minor experimental stroke. We hypothesised that ICP elevation would reduce collateral blood flow. Our aims were to investigate the regulation of flow through leptomeningeal collateral vessels and the parenchymal arterioles arising from them during stroke-reperfusion, and determine the effect of ICP elevation on flow. Wistar rats were subjected to intraluminal middle cerebral artery occlusion (MCAo). Individual leptomeningeal collateral and associated penetrating arteriole blood flow was quantified using fluorescent microspheres. ICP was artificially raised in stepwise increments during MCAo. Baseline bidirectional flow changed to MCA-directed flow and increased by >450% immediately after MCA occlusion. Collateral diameter changed minimally. ICP increase was strongly correlated with collateral and penetrating arteriole blood flow reductions. Changes in collateral flow post-stroke appear to be primarily driven by the pressure drop across the collateral vessel, not vessel diameter. ICP elevation reduces cerebral perfusion pressure and collateral flow, and is the possible explanation for 'collateral failure' in stroke-in-progression.

Key Words

Collateral Failure, Experimental Stroke, Intracranial Pressure, Leptomeningeal Collaterals, Stroke-in-progression, Wistar Rat

Introduction

The term stroke-in-progression has been used to describe patients who present with mild or rapidly improving symptoms and then show a decline in neurological function within 24 to 72 hours after stroke onset.[1] It occurs in approximately 10-40% of patients[2] and has a poor prognosis, with over 50% of patients requiring assistance with daily tasks at 3 months.[3] Until recently the assumed pathophysiology of stroke-in-progression was that patients experience clinical improvement then subsequent deterioration due to spontaneous reperfusion, then rethrombosis of the initially occluded artery.[4] This is the basis for the frequent use of anticoagulants such as heparin in these patients, despite lack of evidence of clinical benefit.[5] Recent use of sequential advanced imaging has permitted identification of patients with early infarct expansion as the cause for their neurological deterioration, and for these patients to be distinguished from those with a 2nd stroke (in a separate arterial territory) and those with deterioration from other factors such as brain swelling. Such studies have shown fluctuating symptoms occur in patients with infarct expansion despite stable arterial occlusion.[6] Infarct expansion typically occurs within the first day post-admission, and is associated with reduced flow through leptomeningeal collateral vessels.[7,8]

Leptomeningeal collaterals provide anastomoses between adjacent arterial territories, and permit retrograde residual perfusion of the ischemic penumbra after stroke.[9] They also provide perfusion to watershed penetrating arterioles under normal circumstances.[10,11] Good collateral supply is strongly associated with better clinical outcome post-stroke.[12] However, failure of initially good leptomeningeal collateral flow has been recognised as occurring in some patients.[7] Proposed mechanisms include, collateral vessel thrombosis[13], venous steal[14], Reversed Robin Hood Syndrome[15] and blood pressure fluctuations secondary to autonomic dysfunction[16]. However evidence has not been strong for any of these mechanisms. Recent

data obtained by our group indicates that there is a transient but dramatic elevation of intracranial pressure (ICP) 24 hours after minor experimental stroke.[17] Perhaps surprisingly, we can find no published data regarding ICP in patients with small strokes. We hypothesise that a similar transient elevation in ICP 24 hours after minor stroke may occur in patients and cause 'collateral failure' leading to neurological deterioration in stroke-in-progression. The aims of this study were to 1. Investigate the key regulators of collateral and associated penetrating arterial blood flow during stroke and reperfusion. 2. Investigate changes in Anterior Cerebral Artery - Middle Cerebral Artery (ACA-MCA) watershed perfusion during stroke and reperfusion. 3. Determine the effect of intracranial pressure elevation on leptomeningeal collateral and watershed penetrating arteriole blood flow during stroke.

Materials and Methods

Ethics Statement

All animal experiments were performed on male outbred Wistar rats (aged 7-12 weeks, body weight 300-500g; ASU breeding facility University of Newcastle, Australia) were approved by the Animal Care and Ethics Committee of the University of Newcastle (Protocols # A-2011-131 and # A-2011-112) and were in accordance with the requirements of the Australian Code of Practice for the Care and Use of Animals for Scientific Purposes. The studies were conducted and the manuscript prepared in accordance with the ARRIVE guidelines.[18]

In Vitro Microsphere Flow Validation

The fluorescent microsphere method for blood flow calculation was validated *in vitro* by comparison with the weighed volume of blood through the same system over a 10 minute time interval. Fluorescent microspheres (1 μm in diameter) (Molecular Probes, Eugene, USA) diluted in heparinised rat blood (0.03% w/v) were infused via an automated syringe driver (Pump 11 Elite, Harvard Apparatus, Holliston, USA) through polyurethane tubing (internal diameter 127 μm). Multiple flow rates (0.25-10 μl/min) were tested. At each rate, the end of the tubing was positioned inside an Eppendorf tube. Eppendorf tubes were weighed prior to the experiment and reweighed after exactly 10 minutes infusion to calculate the volume of fluid in the tube, i.e. 'Measured Blood flow' (Q_m), calculated in μl/min. Microsphere flow (Q_{micro}) was imaged at the midpoint of the 10 minute collection interval. Microspheres passing through the tube were recorded at 300 frames per second with a digital camera (Genie HM640, Teledyne Dalsa, Waterloo, Canada) connected to a 10x objective fluorescent microscope (BX60, Olympus, Tokyo, Japan). Microsphere blood flow was

calculated using the following equation: Blood Flow = πr^2 . v, where v is microsphere velocity in μm/s and r is the radius (half the diameter) of the vessel (tubing) in μm.

Experimental Protocols

Study I

In Study I we investigated the key regulators of collateral blood flow during middle cerebral artery occlusion and reperfusion. Animals underwent baseline recordings of collateral and watershed penetrating arteriole blood flow prior to induction of experimental stroke (90 minutes middle cerebral artery occlusion (MCAo), n = 6). Collateral and watershed penetrating arteriole blood flow recordings were taken every 10 minutes throughout occlusion and every 5 minutes for 15 minutes post-reperfusion (Figure 1A).

Study II

The aim of Study II was to investigate perfusion changes in the watershed region supplied by the ACA-MCA collaterals using computed tomography perfusion (CTP) imaging. Animals were subject to either permanent MCAo (n = 6), or 1 h (n = 8) or 2 h (n = 7) temporary MCA occlusion. CTP scans were taken at baseline and immediately following MCAo. For temporary strokes CTP scans were taken every 30 minutes during occlusion, immediately following reperfusion and at 30 minutes after reperfusion. For permanent strokes CTP scans were taken every 30 minutes out to 2 h post-occlusion (Figure 1B).

Study III

The aim of Study III was to determine the effect of ICP elevation on collateral and penetrating arteriole flow during MCAo. After baseline measurements (collateral and penetrating arteriole flow, intracranial pressure (ICP) and mean arterial pressure (MAP)), rats were subjected to permanent middle cerebral artery occlusion (n = 6). A post-occlusion baseline collateral and penetrating arteriole flow recording was taken 30 minutes post-MCAo. Then, artificial ICP elevation was commenced by infusing artificial cerebrospinal fluid (aCSF) (SDR Scientific, Sydney, Australia) into the lateral ventricle at a starting rate of 4 ul/min. The rate of aCSF infusion was gradually increased to raise ICP in 5 mmHg increments (infusion rates needed for each 5mmHg increase are presented in Supplementary Table 1). At each 5 mmHg increment a recording of collateral and penetrating flow was made. These incremental increases in ICP continued until ICP reached approximately 30 mmHg above baseline (Figure 1C and 2E), equivalent to the values seen 24 h post stroke in this model.[17]

Anesthesia and Monitoring

The anesthetic and monitoring protocols were as previously reported.[19] Rats were anesthetised with 5% isoflurane in O_2/N_2 (1:3) and maintained with 1-2% isoflurane. Core temperature was maintained at 37 $^{\circ}$C by a thermocouple rectal probe (RET-2, Physitemp Instruments Inc., Clifton, USA) and warming plate (HP-1M, Physitemp). Incision sites were shaved, cleaned and injected subcutaneously with 2 mg/kg 0.05% Bupivacaine (Pfizer, Sydney, Australia). Blood gasses were monitored intermittently throughout Study I and at baseline in Study III from 0.1 ml blood samples taken from a right femoral arterial line. This line was also used for continuous arterial pressure monitoring. Heart rate and respiratory rate

were calculated from the clearly discernible cardiac and respiratory waveforms on the arterial pressure tracing.[20]

Surgical Procedures

Middle Cerebral Artery Occlusion

Male outbred Wistar rats underwent MCAo using the silicone-tipped intraluminal thread occlusion method, using 4-0 monofilament occluding threads with 3.5 mm length x 0.35 mm diameter silicone tips, as previously reported [21,22]. For CT studies, final thread advancement to produce MCAo was performed on the CT scanning table, as previously reported.[19]

Collateral and Watershed Penetrating Arteriole Blood Flow Calculation

A jugular venous line was placed for the constant infusion of microspheres, used to quantify collateral and associated penetrating arteriole blood flow.[22,23] A portion of the right parietal bone overlying the MCA-ACA watershed territory was removed using a high speed dental drill (Forte 100, Saeshen, Daegu, Korea) to create a cranial window extending 5 mm caudal x 5 mm lateral from a point at bregma and 1 mm lateral to midline (Figure 2A). Care was taken to leave the dura intact. The hole was filled with aCSF and sealed with a glass cover slip. A laser Doppler probe (LDF) (Moore Instruments, Sussex, UK) was placed just lateral to the cranial window to monitor the tissue perfusion of the MCA territory (Figure 2A). MCAo was confirmed by >50% drop in LDF signal. Pre-specified exclusion criteria were lack of LDF drop, sub-optimal cranial window or subarachnoid hemorrhage on post-mortem.

Placement of Intracranial Pressure (ICP) Monitor and Intraventricular catheter

Two hollow poly-ethyl ether ketone (PEEK) screws (Solid Spot LLC, Santa Clara, CA, USA) of 2 mm diameter x 5 mm length were inserted for monitoring of epidural ICP and for insertion of an intraventricular catheter for artificial elevation of ICP by aCSF infusion (Figure 2A), according to our published method, [17,20]. ICP was measured using a fibre optic pressure transducer (420-LP, SAMBA Sensors, Sweden) [17] sealed into a saline-filled screw with biocompatible caulking material (Silagum, DMG Dental, Hamburg, Germany). Recent studies indicate negligible differences between ICP measurements taken epidurally or intraparenchymally in rats and the epidural method avoids brain trauma and the risk of creating a CSF leak [24,25]. Probe location was validated by ensuring clear cardiac and respiratory waveforms and responsiveness of signal to abdominal compression [20]. In the more rostral screw an intraventricular catheter was inserted 8 mm, so that the tip was in the lateral ventricle (Figure 2A). The catheter was also sealed into the screw with caulking material prior to aCSF infusion.

Collateral and Penetrating Arteriole Blood Flow Measurements

Fluorescently labelled microspheres (1 μm diameter, 0.2% w/v) (Molecular Probes, Eugene, USA) were continuously infused through the jugular line (4 ml/hour). Transit of these microspheres through the terminal branches of the ACA, MCA and collaterals was visualised and recorded. In each experiment one collateral vessel was visualised. The collateral vessel selected was the first vessel in which fluorescent microspheres could be visualised flowing in the characteristic bidirectional pattern previously reported.[10,11] The penetrating arteriole at the confluence of the bidirectional baseline collateral vessel flow (i.e. the watershed territory)

was used to demarcate the ACA and MCA portions of the vessel (Figure 2B, and Supplementary Video 1). Tracking of microspheres and calculation of blood flow was performed as for the *in vitro* microsphere flow validation (Figure 2C). Blood flow was calculated in both the ACA and MCA portions of the collateral vessel at each time point. To calculate penetrating arteriole flow the following equations were used, dependent on the type of flow:

1. During bidirectional flow, penetrating arteriole flow = ACA flow + MCA flow
2. During unidirectional flow, penetrating arteriole flow = proximal flow – distal flow

(Proximal and distal flow were defined relative to the direction of flow, Figure 2B)

CTP Watershed Image Acquisition, Processing and Analysis

Detailed methods and computed tomography perfusion (CTP) data have previously been reported for this cohort of animals[19,22,23], however the watershed territory perfusion was not previously analyzed. Imaging was performed using a Siemens 64 slice CT scanner (Siemens, Erlangen, Germany) with a 512 x 512 matrix, 50 mm field of view (FOV) with twelve 2.4 mm slices. Radio-opaque contrast for perfusion imaging was injected through a jugular venous catheter.[19]

Post-processing of perfusion data was performed using MIStar imaging software (Apollo Medical Imaging Technology, Melbourne, Australia), as previously described[19] with some minor modifications. In brief, cerebral blood flow (CBF) maps were generated from CTP images. The 2.4 mm CTP slice at 0 mm bregma was analyzed for each animal. Two 1x1 mm regions of interest (ROIs; 1 superficial, 1 deep relative to skull) were generated and placed 2.5 mm lateral to the sagittal sinus (corresponding to the location of the penetrating arterioles

that are supplied by the leptomeningeal collaterals imaged in Study I) on the ipsilateral (right) and contralateral (left) cortex (Figure 2D). This allowed assessment of perfusion changes in the watershed territory between the ACA and MCA. The CBF from the superficial and deep ROIs was then averaged.

Statistics

Statistical tests were performed using Graphpad Prism 5.04 (La Jolla, USA) unless otherwise stated. Linear regression analysis was performed to assess the correlation between microsphere blood flow and measured blood flow *in vitro*. Accuracy was calculated using the standard error of the estimate (SEE) divided by the mean. Changes in collateral blood flow, blood flow velocity, collateral vessel diameter, penetrating arteriole blood flow, CTP-determined watershed perfusion and physiological variables (study I and II) were assessed using repeated measures one-way ANOVA with post-hoc Dunnett's test. Changes in collateral blood flow, blood flow velocity, and collateral vessel diameter during ICP elevation was also assessed using one-way ANOVA with post-hoc Dunnett's test. Physiological variables (Study III) were assed using a paired t-test. Collateral blood flow velocity, collateral diameter and ICP were all separately correlated with collateral blood flow by repeated measures linear regression using Stata 13 (StataCorp, Texas, USA). Further, ICP was correlated with blood flow velocity and collateral vessel diameter using the same method. We planned study III with 6 animals. We anticipated ICP elevation would reduce collateral flow by 35% with a standard deviation of 0.25. We were able to reject the null hypothesis that ICP does not reduce collateral flow with probability (power) 0.80. The type I error probability associated with the test of this null hypothesis (alpha) was 0.05. Data is presented as mean ± standard deviation (SD). Statistical significance was accepted at $p < 0.05$.

Results

In Vitro Microsphere Blood Flow Validation

Regression analysis indicated that the relationship between measured blood flow (Q_m) and microsphere blood flow (Q_{micro}) was significant and linear ($r^2 = 0.99$, $p < 0.0001$). There were no significant differences between the regression line and the line of identity with respect to the intercept or slope. The Q_{micro} calculation was accurate to 9.1% (Supplementary Figure 1).

Study 1 - Key Determinants of Collateral Blood Flow during MCAo and Reperfusion

7 animals were excluded in total. Reasons for exclusion were: subarachnoid haemorrhage (n = 1) or sub-optimal cranial window (n = 6). Heart rate was significantly higher than baseline during MCAo and during reperfusion (389 ± 22 BPM baseline and 451 ± 74 BPM and 471 ± 64 BPM during MCAo and reperfusion, respectively, both $p < 0.05$ vs. baseline). All other physiological variables were within normal physiological range[26], and did not vary significantly from baseline (Table 1). Following MCAo, flow within the MCA side of the collateral vessel reversed (Supplementary Video 2). Flow across the entire collateral vessel increased dramatically, to 696 ± 331 nl/min and 453 ± 179 nl/min on the ACA and MCA sides of the vessel, respectively (699% and 458% of baseline, both $p < 0.01$, Figure 3A). Further gradual increase in flow occurred, peaking 80 min post-MCAo (1066 ± 469 nl/min and 825 ± 617 nl/min, 1071% and 834% of baseline, respectively, both $p < 0.001$, Figure 3A).

Reperfusion produced variable blood flow responses. Three different patterns were observed (Figure 3B). 1. Return to bidirectional flow; 2. A complete reversal of retrograde flow so that flow was from MCA to ACA side (Supplementary video 3); 3. Persistent ACA to MCA flow. Responses varied between animals and in individual animals at different time points post

reperfusion. There was an immediate reduction of flow upon reperfusion, regardless of direction of flow (from 924 ± 353 nl/min pre-reperfusion to 316 ± 424 nl/min post-reperfusion on the ACA side of collateral vessels and from 697 ± 334 nl/min to 337 ± 243 nl/min on the MCA sides, both $p < 0.01$; Figure 3A).

The velocity of collateral blood flow increased significantly immediately post-MCAo to 10336 ± 6965 μm/s and 7041± 5443 μm/s on the ACA and MCA sides of the collateral vessel, respectively (600% and 395% of baseline, respectively, both $p < 0.001$). Velocity remained significantly above baseline throughout MCAo and peaked 80 minutes post-MCAo (Figure 4A). Collateral vessels exhibited a gradual increase in diameter following MCAo to 44.1 ± 6 μm and 45.2 ± 6 μm on the ACA and MCA side of the vessel respectively (125% and 126% of baseline, respectively, $p < 0.05$ v. baseline at all time points) (Figure 4B). Collateral blood flow velocity was strongly correlated, and collateral vessel diameter weakly correlated with collateral blood flow (within subject $r = 0.86$ and 0.36, respectively, both $p < 0.0001$; Figures 4C and 4D).

Study I and II - Watershed Penetrating Arteriole Flow and Tissue Perfusion during MCAo and Reperfusion

Study I - Microsphere Technique

Mean penetrating arteriole blood flow remained relatively constant throughout MCAo-reperfusion. It was 198 ± 83 nl/min at baseline, and ranged from 186 ± 170 nl/min to 312 ± 217 nl/min during MCAo, and from 219 ± 123 nl/min to 266 ± 71 nl/min during reperfusion, with no clear trend of change over time (Figure 5A).

Study II - CTP Technique

All physiological variables were within normal physiological range[26], and did not vary significantly from baseline (Table 1). Mean watershed cerebral blood flow in the ipsilateral and contralateral cortex remained relatively constant throughout occlusion and reperfusion in all three experimental groups (Figure 5B-G). Representative CTP maps are shown in Supplementary Figure 3.

Study III - Effect of Intracranial Pressure Elevation on Collateral and Watershed Blood Flow

2 animals were excluded in total. Reason for exclusion was: sub-optimal cranial window (n=2). During ICP elevation heart rate (368 ± 22 BPM vs 420 ± 47 BPM, $p < 0.01$) and ICP (12 ± 9 mmHg vs 27 ± 11 mmHg, $p < 0.001$) were significantly higher than baseline. Cerebral perfusion pressure (72 ± 21 mmHg vs 56 ± 21 mmHg, $p < 0.0001$) was significantly lower than baseline. All other physiological variables were within the normal physiological range[26], and did not vary significantly from baseline (Table 1). Progressive elevation of ICP above baseline significantly reduced collateral blood flow (1337 ± 900 nl/min at baseline (30 min post-MCAo) vs 915 ± 640 nl/min) at 10 mmHg and 605 ± 872 nl/min at 30 mmHg, $p<0.05$, Figure 6A). Penetrating arteriole flow decreased dramatically even with a small increase of ICP to 5 mmHg above baseline. Flow reductions were statistically significant at ICP's of 5, 10 and 20 mmHg above baseline (40 ± 31, 75 ± 88 and 30 ± 56 nl/min respectively, versus 303 ± 210 nl/min at post-MCAo baseline, $p < 0.05$, Figure 6B). There was a significant inverse correlation between ICP and both collateral blood flow and

penetrating arteriole flow (within subject $r = -0.62$, $p < 0.0001$; and $r = -0.40$, $p = 0.04$, respectively, Figures 6C and D).

Elevation of ICP to between 15 and 30 mmHg above baseline significantly reduced collateral blood flow velocity (10393 ± 4533 μm/s at baseline vs 6939 ± 4508 μm/s at 15 mmHg, and 4668 ± 4611 μm/s at 30 mmHg, $p < 0.05$; Figure 6E). Elevation of ICP did not significantly alter vessel diameter (47 ± 13 μm at baseline vs 50 ± 18 μm at 15 mmHg, and 40 ± 16 μm at 30 mmHg; Figure 6F). There was a significant inverse correlation between ICP and collateral blood flow velocity (within subject $r = -0.69$, $p < 0.0001$) but no significant correlation with diameter (within subject $r = 0$) (Figure 6G and 6H, respectively).

Discussion

In this study we have made several key findings that shed new light on the regulators of leptomeningeal collateral flow and advance our understanding of the potential cause of 'collateral failure' seen in patients with stroke-in-progression. Changes in collateral blood flow after stroke were associated with only modest changes in vessel diameter, but large changes in blood flow velocity. This suggests that a change in the pressure drop across the collateral vessel is the key factor affecting flow during MCA occlusion and reperfusion, rather than collateral diameter changes. Blood flow through penetrating arterioles supplied by collaterals was maintained during ischemia-reperfusion. Maintenance of tissue perfusion to the watershed territory supplied by these vessels was confirmed using whole-brain CT perfusion imaging. Artificial ICP elevation caused a progressive reduction in collateral blood flow and a dramatic immediate reduction in penetrating arteriole blood flow.

Collateral vessels had slow bidirectional flow at baseline. Bidirectional flow has previously been observed in the leptomeningeal collateral circulation of mice.[10,11] We show here that this also occurs in rats. At odds with these findings are the results from studies using laser speckle imaging that reported no flow under basal conditions suggesting these vessels don't "open up" until major vessels occlusion occurs.[27,28] The likely explanation for these findings is that laser speckle imaging is unable to detect baseline flow in collateral vessels due to either its bidirectional nature or relatively low velocity. We also found that collateral blood flow continued following reperfusion, although at much lower velocities, and the direction varied both between and within animals over time. Again these findings are in contrast to those of obtained with the laser speckle technique[27], likely for similar reasons. Taken together these results suggest that under basal conditions leptomeningeal collaterals are well perfused and play a vital role in supplying the watershed region located between the two vascular

territories.

Immediately following MCAo collateral flow became unidirectional, towards the ischemic MCA territory. Flow increased dramatically, however counter to our expectations vessel diameter changes were only modest. Collateral vessels have larger diameters relative to vessels with similar flow velocities elsewhere in the cerebral circulation.[29] The importance of this larger diameter becomes apparent during experimental stroke, when there are many-fold increases in velocity and absolute blood flow as flow becomes unidirectional towards the occluded territory.[10] This aspect of the structure of collateral vessels appears optimized to maintain stable baseline perfusion, while allowing for rapid increases of retrograde flow following arterial occlusion. The indication that vessel diameter changes had a relatively modest impact on the flow increase post-MCAo suggests that the cerebral perfusion pressure (CPP) driven pressure differential across the collateral vessel is the major driver of collateral blood flow during stroke.[30] This is quite different to flow regulation of vascular beds under physiological conditions, where vessel diameter is the key regulator of flow. The distinction is important conceptually, in optimizing our efforts to manipulate collateral flow therapeutically.

Flow through the penetrating vessels arising from collaterals, and perfusion of the ipsilateral and contralateral watershed remained relatively constant throughout stroke. Consistent with our results, Toriumi *et al*[11] showed that red cell velocity in penetrating arterioles associated with collateral vessels did not significantly change from baseline following MCAo. However in contrast to these findings, Shih *et al*[31] reported a reduction in red blood cell (RBC) flux in penetrating arterioles (driven by a reduction in RBC velocity) during MCAo. The likely explanation for these apparent discrepancies is that Shih *et al*[31] did not specify whether the penetrating arterioles measured in their study arose directly from the collateral vessels, or

from within the ischemic MCA territory. In the latter case, a reduction in flow would be anticipated. Sustained flow through the collateral-supplied watershed penetrating arterioles most likely gives rise to an area of oligemic tissue that borders the penumbra in stroke patients.[32]

Intracranial pressure elevation caused a significant linear reduction in collateral blood flow. The idea that alterations in cerebral perfusion pressure can alter perfusion of the ischemic penumbra is long-established.[33] Most of this perfusion travels via collateral vessels.[12] A number of recent studies in animal models of stroke have sucessfully enhanced collateral flow by increasing CPP using pressor therapy or partial aortic occlusion to increase blood pressure within the cerebral arteries.[34,35] A number of small clinical studies have attempted to enhance perfusion to the penumbra using pressor therapy. However, the efficacy of these approaches are yet to demonstrated in large randomised tials.[36] The effects of ICP on collateral perfusion are less often considered. We provide the first empirical evidence that elevation of ICP to levels equivalent to those occurring naturally after experimental stroke causes a significant stepwise reduction in CPP and collateral blood flow.[17] Although we were unable to directly measure the pressure gradient between the adjacent territtories, our data strongly suggests that elevation of ICP, by reducing CPP reduced the driving pressure across the collateral vessel leading to a stepwise reduction in blood flow velocity and flow.

As soon as ICP was elevated to as little as 5 mmHg above baseline, watershed penetrating arteriole flow decreased dramatically and remained low thereafter. This result may be explained by the distinct responses of pial arteries and arterioles versus parenchymal arterioles to ischemia. Parenchymal arterioles are known as the "bottleneck" of perfusion to the cortex. Parenchymal arterioles have been shown to maintain basal tone even after 2 h temporary MCA occlusion - reperfusion, whereas the pial arteries lose tone after even short

durations of ischemia.[37] Therefore small reductions in CPP will have a much greater effect on pial arterioles, since a greater driving pressure (CPP) is required to maintain flow across high resistance vessels. The lack of further flow reductions with further ICP elevation may in part represent the counteracting effects of penetrating parenchymal arteriolar vasodilation (over a many minutes timescale) concurrent with progressive experimental ICP elevation. Conversely, the maximally dilated MCA pial vasculature downstream of the collateral vessel is a low resistance circuit.[38] Therefore, incremental changes in CPP result in a linear reduction in collateral blood flow. This apparent selective sensitivity of the watershed parenchymal arterioles arising from collateral vessels to changes in perfusion pressure is a potential contributor to the selective sensitivity of this region to infarction in the setting of vessel stenosis, in which local fluctuations in perfusion pressure are also implicated.

Recent serial advanced imaging studies have revealed that patients with stroke in progression have persistent arterial occlusion and good collateral status at baseline and the subsequent infarct expansion is associated with reduced collateral status or 'collateral failure'.[6,7]. ICP is known to increase in patients with large malignant infarctions (>80% of the MCA territory) [39], however because ICP monitoring is invasive it is not performed in patients with small strokes. We do not know whether these patients experience a transient ICP rise similar to that seen in rats with experimental stroke.[17] Clinical data obtained for the CATCH study strongly highlighted the similarities in timing between the ICP elevation seen in our stroke model and clinical deterioration in stroke-in-progression - 53% of patients with stroke-in-progression deteriorated on day 1 (first full day in hospital).[8] The findings of the current study suggest that ICP elevation is a very plausible mechanism for the 'collateral failure' seen in stroke-in-progression patients.

Our method for collateral blood flow quantification permits a degree of real-time quantification not available with other currently available techniques, and this provided us

with tremendous insights regarding the regulation of collateral flow during stroke-reperfusion and the response to ICP elevation. However measurements were limited to a single collateral vessel in each animal. To date there is no method to quantify total collateral blood flow through all collateral vessels in real time. However, we used CT perfusion imaging of tissue perfusion as a surrogate for this to confirm our findings regarding penetrating arteriole flow to the watershed territories.

In conclusion, we have shown that leptomeningeal collateral vessels provide retrograde perfusion of the occluded arterial territory during stroke, while maintaining stable perfusion to the watershed territory. Change in collateral vessel diameter had little effect on changes in flow, which appeared to be primarily driven by changes in the pressure drop across the collateral vessel following arterial occlusion. Supporting the key role of this pressure differential, incremental elevation of ICP caused a stepwise reduction in collateral blood flow. Coupled with our recent findings showing a dramatic but transient ICP elevation after minor experimental stroke, and human imaging studies indicating that 'collateral failure' rather than thrombus extension is the likely mechanism for most stroke-in-progression, these findings have important potential clinical implications. They suggest that ICP elevation is a likely explanation for 'collateral failure' and may be the responsible mechanism for stroke-in-progression.

Supplementary information is available at the Journal of Cerebral Blood Flow & Metabolism website- www.nature.com/jcbfm

Conflicts of Interest/Disclosures: None

References

1. Davalos AC, J. Progressing Stroke In: Fisher MB, J., editor. Current Review of Cerebrovascular Disease: Springer; 2001.
2. Ali LK, Saver JL. The ischemic stroke patient who worsens: new assessment and management approaches. Rev Neurol Dis. 2007;4(2):85-91.
3. Coutts SB, Modi J, Patel SK, Aram H, Demchuk AM, Goyal M, et al. What causes disability after transient ischemic attack and minor stroke?: Results from the CT and MRI in the Triage of TIA and minor Cerebrovascular Events to Identify High Risk Patients (CATCH) Study. Stroke. 2012;43(11):3018-22.
4. Caplan LR. Treatment of "progressive" stroke. Stroke. 1991;22(5):694-5.
5. Roden-Jullig A, Britton M. Effectiveness of heparin treatment for progressing ischaemic stroke: before and after study. J Intern Med. 2000;248(4):287-91.
6. Asdaghi N, Hameed B, Saini M, Jeerakathil T, Emery D, Butcher K. Acute perfusion and diffusion abnormalities predict early new MRI lesions 1 week after minor stroke and transient ischemic attack. Stroke. 2011;42(8):2191-5.
7. Campbell BC, Christensen S, Tress BM, Churilov L, Desmond PM, Parsons MW, et al. Failure of collateral blood flow is associated with infarct growth in ischemic stroke. J Cereb Blood Flow Metab. 2013;33(8):1168-72.
8. Coutts SB, Modi J, Patel SK, Demchuk AM, Goyal M, Hill MD. CT/CT angiography and MRI findings predict recurrent stroke after transient ischemic attack and minor stroke: results of the prospective CATCH study. Stroke. 2012;43(4):1013-7.
9. Brozici M, van der Zwan A, Hillen B. Anatomy and functionality of leptomeningeal anastomoses: a review. Stroke. 2003;34(11):2750-62.
10. Chalothorn D, Faber JE. Formation and maturation of the native cerebral collateral circulation. J Mol Cell Cardiol. 2010;49(2):251-9.
11. Toriumi H, Tatarishvili J, Tomita M, Tomita Y, Unekawa M, Suzuki N. Dually supplied T-junctions in arteriolo-arteriolar anastomosis in mice: key to local hemodynamic homeostasis in normal and ischemic states? Stroke. 2009;40(10):3378-83.
12. Miteff F, Levi CR, Bateman GA, Spratt N, McElduff P, Parsons MW. The independent predictive utility of computed tomography angiographic collateral status in acute ischaemic stroke. Brain. 2009;132(Pt 8):2231-8.
13. Liebeskind DS. Collateral circulation. Stroke. 2003;34(9):2279-84.
14. Pranevicius O, Pranevicius M, Pranevicius H, Liebeskind DS. Transition to collateral flow after arterial occlusion predisposes to cerebral venous steal. Stroke. 2012;43(2):575-9.
15. Alexandrov AV, Sharma VK, Lao AY, Tsivgoulis G, Malkoff MD, Alexandrov AW. Reversed Robin Hood syndrome in acute ischemic stroke patients. Stroke. 2007;38(11):3045-8.
16. Palamarchuk I, Kimpinski K, Lippert C, Hachinski V. Nocturnal deterioration after ischemic stroke and autonomic dysfunction: hypothesis and implications. Cerebrovasc Dis. 2013;36(5-6):454-61.
17. Murtha LA, McLeod DD, McCann SK, Pepperall D, Chung S, Levi CR, et al. Short-duration hypothermia after ischemic stroke prevents delayed intracranial pressure rise. Int J Stroke. 2014;9(5):553-9.
18. Kilkenny C, Browne W, Cuthill IC, Emerson M, Altman DG. Animal research: reporting in vivo experiments--the ARRIVE guidelines. J Cereb Blood Flow Metab. 2011;31(4):991-3.
19. McLeod DD, Parsons MW, Levi CR, Beautement S, Buxton D, Roworth B, et al. Establishing a rodent stroke perfusion computed tomography model. Int J Stroke. 2011;6(4):284-9.
20. Murtha L, McLeod D, Spratt N. Epidural intracranial pressure measurement in rats using a fiber-optic pressure transducer. J Vis Exp. 2012 (62).

21. Spratt NJ, Fernandez J, Chen M, Rewell S, Cox S, van Raay L, et al. Modification of the method of thread manufacture improves stroke induction rate and reduces mortality after thread-occlusion of the middle cerebral artery in young or aged rats. J Neurosci Methods. 2006;155(2):285-90.
22. McLeod DD, Beard DJ, Parsons MW, Levi CR, Calford MB, Spratt NJ. Inadvertent occlusion of the anterior choroidal artery explains infarct variability in the middle cerebral artery thread occlusion stroke model. PloS one. 2013;8(9):e75779.
23. McLeod DD, Parsons MW, Hood R, Hiles B, Allen J, McCann SK, et al. Perfusion computed tomography thresholds defining ischemic penumbra and infarct core: studies in a rat stroke model. Int J Stroke. 2013 Oct 21.
24. Hiploylee C, Colbourne F. Intracranial pressure measured in freely moving rats for days after intracerebral hemorrhage. Exp Neurol. 2014;255:49-55.
25. Uldall M, Juhler M, Skjolding AD, Kruuse C, Jansen-Olesen I, Jensen R. A novel method for long-term monitoring of intracranial pressure in rats. J Neurosci Methods 2014;227:1-9.
26. Sharp PE. The Laboratory Rat. CRC Press; 2013.
27. Armitage GA, Todd KG, Shuaib A, Winship IR. Laser speckle contrast imaging of collateral blood flow during acute ischemic stroke. J Cereb Blood Flow Metab 2010;30(8):1432-6.
28. Wang Z, Luo W, Zhou F, Li P, Luo Q. Dynamic change of collateral flow varying with distribution of regional blood flow in acute ischemic rat cortex. J Biomed Opt 2012;17(12):125001.
29. Rovainen CM, Woolsey TA, Blocher NC, Wang DB, Robinson OF. Blood flow in single surface arterioles and venules on the mouse somatosensory cortex measured with videomicroscopy, fluorescent dextrans, nonoccluding fluorescent beads, and computer-assisted image analysis. J Cereb Blood Flow Metab 1993;13(3):359-71.
30. Alexandrov AW. Hyperacute ischemic stroke management: reperfusion and evolving therapies. Crit Care Nurs Clin North Am. 2009;21(4):451-70.
31. Shih AY, Friedman B, Drew PJ, Tsai PS, Lyden PD, Kleinfeld D. Active dilation of penetrating arterioles restores red blood cell flux to penumbral neocortex after focal stroke. J Cereb Blood Flow Metab. 2009;29(4):738-51.
32. Furlan M, Marchal G, Viader F, Derlon JM, Baron JC. Spontaneous neurological recovery after stroke and the fate of the ischemic penumbra. Ann Neurol 1996;40(2):216-26.
33. Urrutia VC, Wityk RJ. Blood pressure management in acute stroke. Neurol Clin 2008;26(2):565-83, x-xi.
34. Shin HK, Nishimura M, Jones PB, Ay H, Boas DA, Moskowitz MA, et al. Mild induced hypertension improves blood flow and oxygen metabolism in transient focal cerebral ischemia. Stroke. 2008;39(5):1548-55.
35. Winship IR, Armitage GA, Ramakrishnan G, Dong B, Todd KG, Shuaib A. Augmenting collateral blood flow during ischemic stroke via transient aortic occlusion. J Cereb Blood Flow Metab. 2014;34(1):61-71.
36. Mistri AK, Robinson TG, Potter JF. Pressor therapy in acute ischemic stroke: systematic review. Stroke. 2006;37(6):1565-71.
37. Cipolla MJ, Sweet JG, Gokina NI, White SL, Nelson MT. Mechanisms of enhanced basal tone of brain parenchymal arterioles during early postischemic reperfusion: role of ET-1-induced peroxynitrite generation. J Cereb Blood Flow Metab. 2013;33(10):1486-92.
38. Cipolla MJ, Lessov N, Hammer ES, Curry AB. Threshold duration of ischemia for myogenic tone in middle cerebral arteries: effect on vascular smooth muscle actin. Stroke. 2001;32(7):1658-64.
39. Hacke W, Schwab S, Horn M, Spranger M, De Georgia M, von Kummer R. 'Malignant' middle cerebral artery territory infarction: clinical course and prognostic signs. Arch Neurol 1996;53(4):309-15.

Titles and Legends to Figures

Figure 1. Experimental timelines. A. Study I. Collateral and penetrating arteriole blood flow was measured during 90 min MCAo and 15 min reperfusion. **B.** Study II. CTP imaging (vertical dotted lines) was carried out to measure whole brain perfusion changes during both permanent and temporary (1h and 2h) MCAo. Following baseline CTP scans, scans were taken every 30 min during MCAo. Further scans were taken immediately after reperfusion (R) and at 30 min post-reperfusion. Images obtained from these scans were then used to assess changes in watershed perfusion during occlusion and reperfusion. **C.** Study III. ICP was artificially elevated by fluid infusion into the lateral ventricles and effects on collateral blood flow were determined. MCAo = middle cerebral artery occlusion; CTP = computed tomography perfusion; P_a = arterial pressure; ABG = arterial blood gas; ICP = intracranial pressure; Q_c = collateral blood flow; CPP = cerebral perfusion pressure.

Figure 2. Surgical and Experimental Procedures. A. Schematic of skull surgery and monitoring: cranial window used to measure collateral flow (Q_c), laser Doppler flow (LDF) probe to measure middle cerebral artery (MCA) perfusion, intraventricular catheter (IVC) for infusion of artificial cerebrospinal fluid (aCSF) and intracranial pressure (ICP) probe location. **B.** Schematic of collateral blood flow direction before and after middle cerebral artery occlusion (MCAo). The penetrating arteriole at the confluence of the bidirectional collateral vessel blood flow (top panel) was used to demarcate the anterior (ACA) and middle (MCA) cerebral artery portions of the vessel (vertical line). This same landmark was also

used following MCA occlusion (bottom panel). Blood flow was measured in both ACA and MCA portions of the vessel at each imaging time point. **C.** Calculation of collateral vessel flow. Image shows two merged frames, taken 3.3 ms apart. A leptomeningeal collateral vessel and larger bridging veins are seen. Arrows show the location of a microsphere at 2 time points – distance travelled between frames is used to calculate velocity; lines show locations of vessel diameter measurements. **D.** Representative CTP cerebral blood flow map at bregma. Two ROIs were fitted (white boxes) 2.5 mm lateral to midline of the right (ipsilateral) hemisphere corresponding to the location of the penetrating arterioles that are supplied by the leptomeningeal collaterals imaged in Study I. Perfusion was measured by taking the average CBF within these ROIs. **E.** Representative ICP trace. ICP was increased by infusion of aCSF into the left lateral ventricle of a rat post-stroke. The infusion rate was increased stepwise from 4-40 μL/min. This resulted in an increase in ICP with no significant change in arterial blood pressure, so cerebral perfusion pressure (CPP) (not shown) mirrored ICP changes.

Figure 3. Leptomeningeal collateral flow increases during ischemia and decreases during reperfusion. **A.** Collateral blood flow; blood flow in the anterior cerebral artery (ACA) segment of the collateral vessel (solid columns) and blood flow in the MCA segment of the collateral vessel (hollow columns) during MCA occlusion (M) and post-reperfusion (R); **$p < 0.001$ compared to baseline (B); # $p < 0.05$, ## $p < 0.01$, ### $p < 0.001$ for time-points post-reperfusion compared to 90 min MCAo ($n = 6$). **B.** Individual animal analysis of direction and magnitude of blood flow through the MCA segment of collateral vessels during reperfusion (nl/min). Squares = unidirectional flow, Circles = bidirectional flow.

Figure 4. Collateral flow change is strongly correlated with blood flow velocity changes and only weakly correlated with vessel diameter. A. Blood flow velocity, and B. Collateral vessel diameter, in the anterior cerebral artery (ACA, solid columns) and middle cerebral artery (MCA, hollow columns) segments of the collateral vessels. B = baseline; M = MCAo, R = post-reperfusion. *p < 0.05, **p < 0.01, **p < 0.001 for MCAo time points compared to baseline; # p <0.05, ## p < 0.01, ### p < 0.001 for post-reperfusion time points compared to 90 min MCAo. Linear regression analysis of collateral blood flow versus blood flow velocity (C), and vessel diameter (D). Data points include measurements from both the ACA and MCA sides of each collateral vessel, recorded at each time point. Separate data symbols and regression lines are shown for each animal (n = 6).

Figure 5. Penetrating arteriole blood flow and watershed-region tissue perfusion remain constant throughout MCA occlusion and reperfusion. A. Blood flow in the watershed penetrating arterioles arising from collateral vessels calculated using fluorescent microspheres. Ipsilateral and contralateral watershed tissue perfusion assessed using serial CTP CBF during MCA occlusion ± reperfusion, during 1 hr MCAo (**B and C**), 2 hr MCAo (**D and E**) and permanent MCAo (**F and G**). B = baseline; M = MCAo, R = reperfusion.

Figure 6. Artificial elevation of intracranial pressure (ICP) reduces both collateral and penetrating arteriole flow. The reduction in collateral flow is primarily driven by a significant reduction in blood flow velocity in the collateral vessel, not changes in vessel diameter. A. Collateral blood flow and B. Penetrating arteriole flow, at baseline and at each incremental increase of ICP. *p < 0.05, **p < 0.01 compared baseline. Linear regression analysis of ICP versus: C. collateral blood flow, and D. penetrating arteriole blood flow, during ICP elevation E. Collateral blood flow velocity and F. Collateral vessel diameter, at

baseline and at each incremental increase of ICP. *p < 0.05, for comparison with baseline. Linear regression analysis of ICP versus: G. collateral blood flow velocity, and H. collateral vessel diameter, during ICP elevation (data points are measurements recorded at each time point, n = 6 animals for collateral flow, collateral blood flow velocity and collateral vessel diameter; n = 4 animals for penetrating arteriole flow, individual regression lines are shown).

Tables

Table 1. Physiological Parameters

Study I

	Baseline	MCAo	Reperfusion
RR (BPM)	53 ± 7	60 ± 13	60 ±10
HR (BPM)	389 ± 22	451 ± 74**	471 ± 64*
MAP (mmHg)	80 ± 15	92 ± 15	79 ± 9
pO_2 (mmHg)	124 ± 49	148 ± 59	171 ± 71
pCO_2 (mmHg)	44 ± 12	42 ± 7	45 ± 5
pH	7.38 ± 0.07	7.39 ± 0.01	7.41 ± 0.03

Study II (CTP 1hr MCAo)

	Baseline	MCAo	Reperfusion
RR (BPM)	63 ± 15	66 ± 6	69 ± 15
HR (BPM)	378 ± 40	395 ± 33	360 ± 46

Study II (CTP 2hr MCAo)

	Baseline	MCAo	Reperfusion
RR (BPM)	59 ± 5	60 ± 7	67 ± 17
HR (BPM)	381 ± 44	387 ± 34	379 ± 35

Study II (CTP pMCAo)

	Baseline	MCAo
RR (BPM)	58 ± 10	66 ± 11
HR (BPM)	381 ± 46	371 ± 41

Study III

	Baseline	ICP Elevation
MAP (mmHg)	84 ± 15	85 ± 11
ICP (mmHg)	12 ± 9	27 ± 11***
CPP (mmHg)	72 ± 21	56 ± 21****
RR (BPM)	58 ± 7	62 ± 8
HR (BPM)	368 ± 22	420 ± 47**
pO_2 (mmHg)	184 ± 42	-
pCO_2 (mmHg)	45 ± 14	-
pH	7.40 ± 0.04	-

MAP = mean arterial pressure; ICP = intracranial pressure; CPP = cerebral perfusion pressure; RR = respiratory rate; HR = heart rate; pO_2 = partial pressure of oxygen; pCO_2 = partial pressure of carbon dioxide. *p < 0.05, ***p < 0.001, ****p < 0.0001, versus baseline.

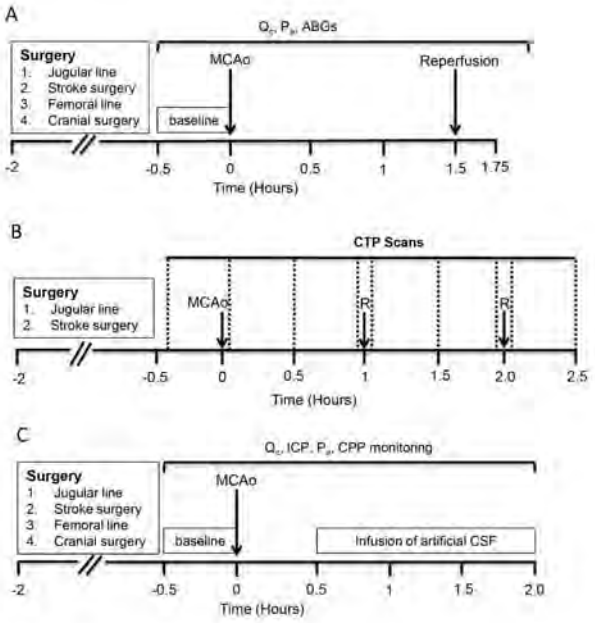

Figure 1. Experimental timelines. A. Study I. Collateral and penetrating arteriole blood flow was measured during 90 min MCAo and 15 min reperfusion. B. Study II. CTP imaging (vertical dotted lines) was carried out to measure whole brain perfusion changes during both permanent and temporary (1h and 2h) MCAo. Following baseline CTP scans, scans were taken every 30 min during MCAo. Further scans were taken immediately after reperfusion (R) and at 30 min post-reperfusion. Images obtained from these scans were then used to assess changes in watershed perfusion during occlusion and reperfusion. C. Study III. ICP was artificially elevated by fluid infusion into the lateral ventricles and effects on collateral blood flow were determined. MCAo = middle cerebral artery occlusion; CTP = computed tomography perfusion; Pa = arterial pressure; ABG = arterial blood gas; ICP = intracranial pressure; Qc = collateral blood flow; CPP = cerebral perfusion pressure.
254x190mm (300 x 300 DPI)

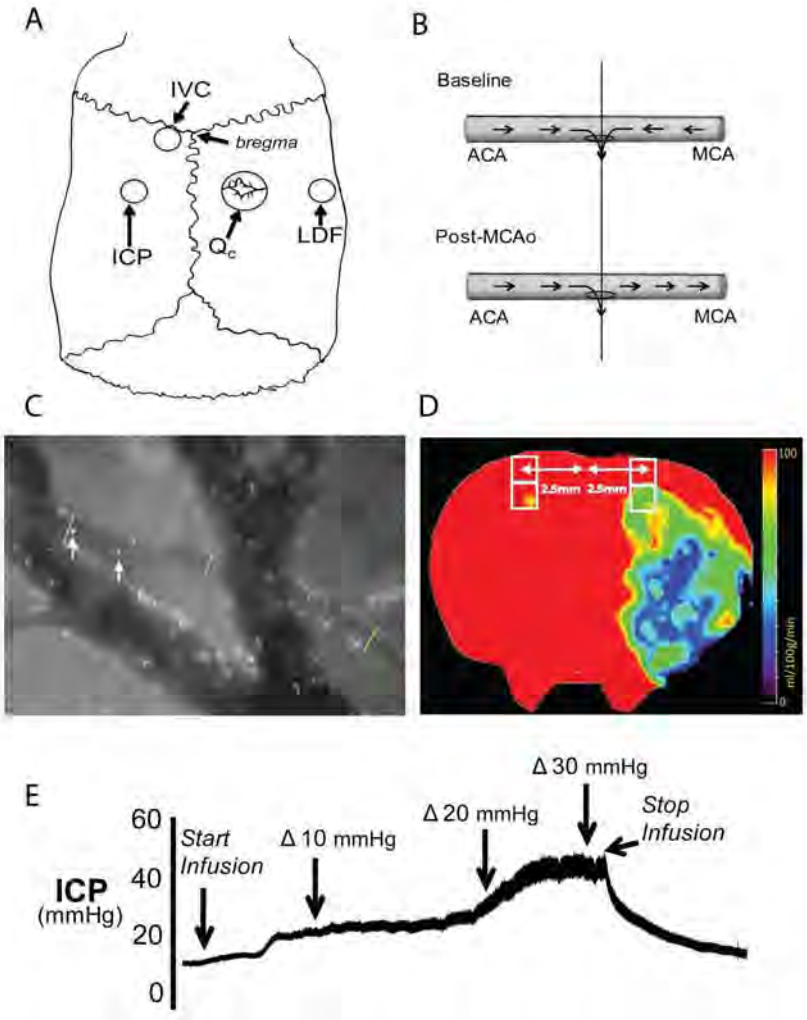

Figure 2. Surgical and Experimental Procedures. A. Schematic of skull surgery and monitoring: cranial window used to measure collateral flow (Qc), laser Doppler flow (LDF) probe to measure middle cerebral artery (MCA) perfusion, intraventricular catheter (IVC) for infusion of artificial cerebrospinal fluid (aCSF) and intracranial pressure (ICP) probe location. B. Schematic of collateral blood flow direction before and after middle cerebral artery occlusion (MCAo). The penetrating arteriole at the confluence of the bidirectional collateral vessel blood flow (top panel) was used to demarcate the anterior (ACA) and middle (MCA) cerebral artery portions of the vessel (vertical line). This same landmark was also used following MCA occlusion (bottom panel). Blood flow was measured in both ACA and MCA portions of the vessel at each imaging time point. C. Calculation of collateral vessel flow. Image shows two merged frames, taken 3.3 ms apart. A leptomeningeal collateral vessel and larger bridging veins are seen. Arrows show the location of a microsphere at 2 time points – distance travelled between frames is used to calculate velocity; lines show locations of vessel diameter measurements. D. Representative CTP cerebral blood flow map at bregma. Two ROIs were fitted (white boxes) 2.5 mm lateral to midline of the right (ipsilateral) hemisphere corresponding

to the location of the penetrating arterioles that are supplied by the leptomeningeal collaterals imaged in Study I. Perfusion was measured by taking the average CBF within these ROIs. E. Representative ICP trace. ICP was increased by infusion of aCSF into the left lateral ventricle of a rat post-stroke. The infusion rate was increased stepwise from 4-40 µL/min. This resulted in an increase in ICP with no significant change in arterial blood pressure, so cerebral perfusion pressure (CPP) (not shown) mirrored ICP changes.
212x281mm (300 x 300 DPI)

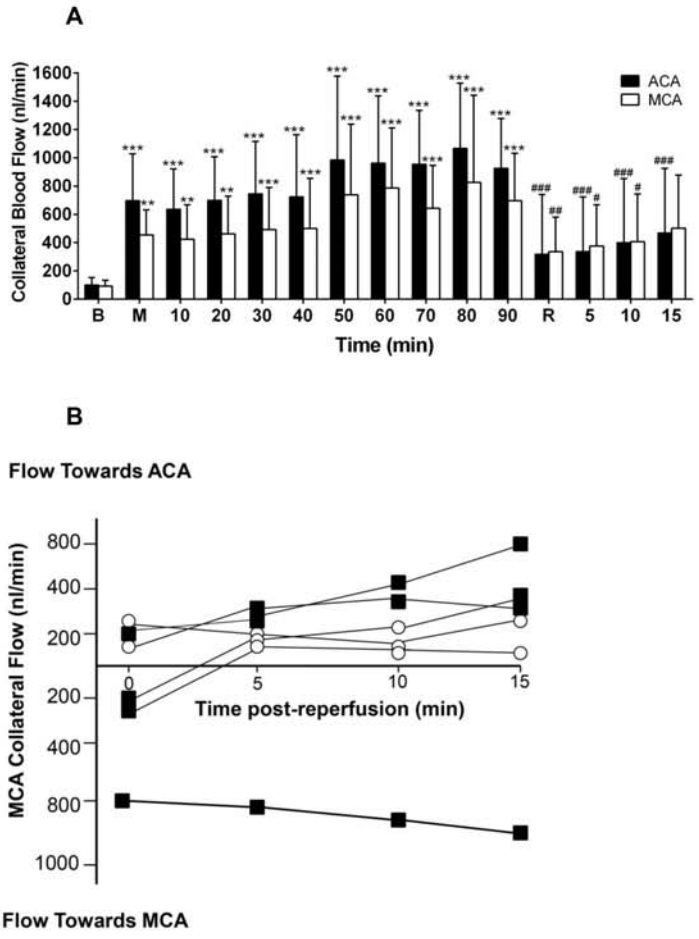

Figure 3. Leptomeningeal collateral flow increases during ischemia and decreases during reperfusion. A. Collateral blood flow; blood flow in the anterior cerebral artery (ACA) segment of the collateral vessel (solid columns) and blood flow in the MCA segment of the collateral vessel (hollow columns) during MCA occlusion (M) and post-reperfusion (R); **p < 0.001 compared to baseline (B); # p < 0.05, ## p < 0.01, ### p < 0.001 for time-points post-reperfusion compared to 90 min MCAo (n = 6). B. Individual animal analysis of direction and magnitude of blood flow through the MCA segment of collateral vessels during reperfusion (nl/min). Squares = unidirectional flow, Circles = bidirectional flow.
190x275mm (300 x 300 DPI)

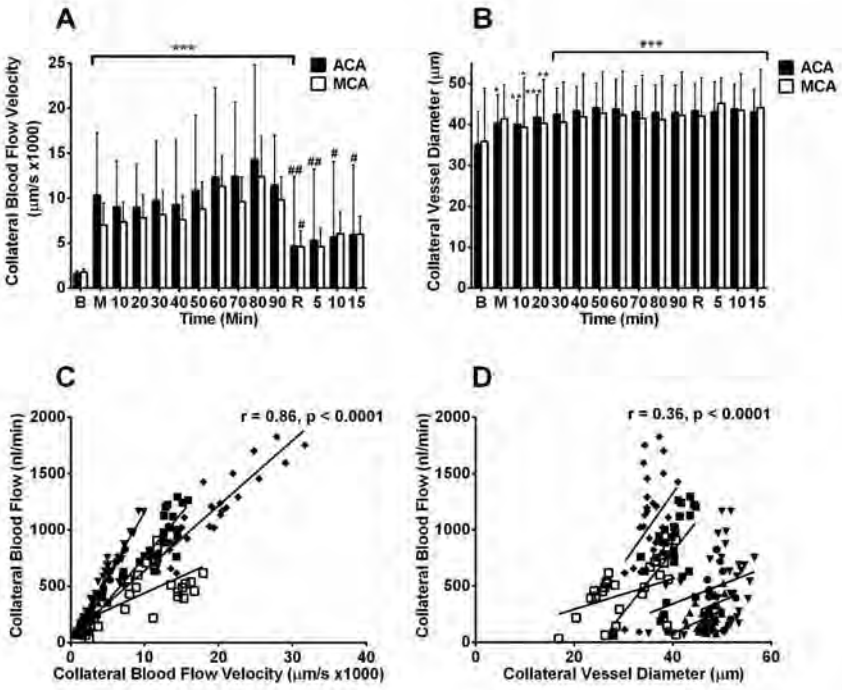

Figure 4. Collateral flow change is strongly correlated with blood flow velocity changes and only weakly correlated with vessel diameter. A. Blood flow velocity, and B. Collateral vessel diameter, in the anterior cerebral artery (ACA, solid columns) and middle cerebral artery (MCA, hollow columns) segments of the collateral vessels. B = baseline; M = MCAo, R = post-reperfusion. *p < 0.05, **p < 0.01, **p < 0.001 for MCAo time points compared to baseline; # p <0.05, ## p < 0.01, ### p < 0.001 for post-reperfusion time points compared to 90 min MCAo. Linear regression analysis of collateral blood flow versus blood flow velocity (C), and vessel diameter (D). Data points include measurements from both the ACA and MCA sides of each collateral vessel, recorded at each time point. Separate data symbols and regression lines are shown for each animal (n = 6).
214x175mm (300 x 300 DPI)

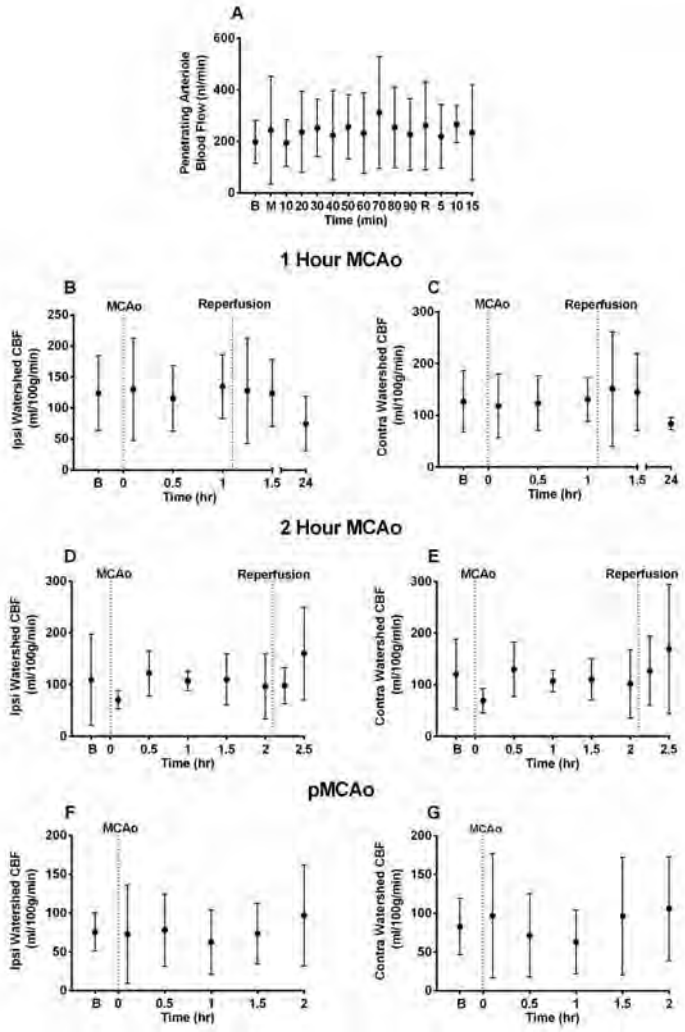

Figure 5. Penetrating arteriole blood flow and watershed-region tissue perfusion remain constant throughout MCA occlusion and reperfusion. A. Blood flow in the watershed penetrating arterioles arising from collateral vessels calculated using fluorescent microspheres. Ipsilateral and contralateral watershed tissue perfusion assessed using serial CTP CBF during MCA occlusion ± reperfusion, during 1 hr MCAo (B and C), 2 hr MCAo (D and E) and permanent MCAo (F and G). B = baseline; M = MCAo, R = reperfusion.
205x294mm (300 x 300 DPI)

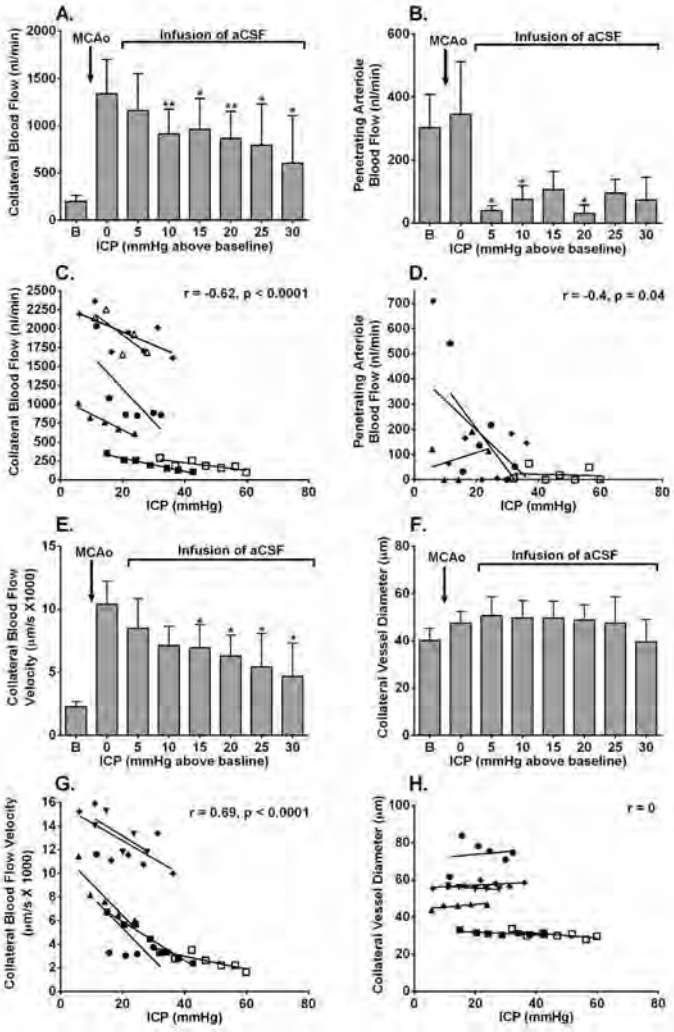

Figure 6. Artificial elevation of intracranial pressure (ICP) reduces both collateral and penetrating arteriole flow. The reduction in collateral flow is primarily driven by a significant reduction in blood flow velocity in the collateral vessel, not changes in vessel diameter. A. Collateral blood flow and B. Penetrating arteriole flow, at baseline and at each incremental increase of ICP. *p < 0.05, **p < 0.01 compared baseline. Linear regression analysis of ICP versus: C. collateral blood flow, and D. penetrating arteriole blood flow, during ICP elevation E. Collateral blood flow velocity and F. Collateral vessel diameter, at baseline and at each incremental increase of ICP. *p < 0.05, for comparison with baseline. Linear regression analysis of ICP versus: G. collateral blood flow velocity, and H. collateral vessel diameter, during ICP elevation (data points are measurements recorded at each time point, n = 6 animals for collateral flow, collateral blood flow velocity and collateral vessel diameter; n = 4 animals for penetrating arteriole flow, individual regression lines are shown).
206x297mm (300 x 300 DPI)

CHAPTER 7

DISCUSSION

The results that I have demonstrated in this thesis are both novel and potentially very important for the outcome of future stroke patients. Firstly, using the epidural, fibre-optic intracranial pressure (ICP) measurement developed for this project, I showed that ICP was dramatically elevated at 24 hours following minor strokes; this result was confirmed in three strains of rat and raises the possibility that a similar rise might be occurring in patients with small strokes. Secondly, I showed that cerebral oedema was not the primary mechanism involved in ICP elevation post-stroke; this result was confirmed using three different methods of oedema calculation and challenges almost a century of scientific wisdom about ICP elevation post-stroke. Thirdly, I showed that this rise in ICP was completely prevented following short-duration mild and moderate hypothermia induced shortly after stroke; this result raises the possibility that short-duration, mild hypothermia may be a safer, easier and more effective method of cooling than the long durations that are currently induced in clinical trials. Finally, I demonstrated that collateral blood flow was dramatically increased following stroke and that a strong inverse correlation was seen between ICP elevation and collateral blood flow reduction; this result suggests that ICP elevation is the likely cause of the 'collateral failure' seen in stroke-in-progression patients.

Epidural, fibre-optic ICP measurement is more reliable and safer than previous experimental models.

Very few animal studies have investigated ICP post-stroke. It is likely that this is largely due to the difficulty in measuring ICP in rats as well as the mechanical tissue damage that results from existing techniques. In this thesis, I demonstrated that ICP could be easily and reliably measured in rats over multiple days without tissue damage or loss of signal fidelity. The fact that the ICP probe can be removed and reinserted multiple times is important in stroke research. Clinical and animal studies suggest that ICP elevates 24-48 hours post-stroke[14-19]. In order to measure baseline ICP pre-stroke as well as serial measurements post-stroke, the ability to re-insert the ICP probe multiple times is an important factor. In the clinical setting, intraventricular placement of ICP probes is considered 'gold standard'. Similar to our method, this involves the insertion of a hollow screw into the skull in which an ICP probe is inserted. Although intraventricular placement is invasive, with a higher risk of infection, it is commonly used in the clinical setting for its secondary purpose of removing cerebrospinal fluid (CSF) to reduce ICP. In animal models, removal of CSF is often not performed. Two recent studies have demonstrated that epidural placement of ICP probes correlates strongly with intraparenchymal[146] and intraventricular[142] placement and was shown to have a lower risk of hydrocephalus and infection. ICP elevation is an important complication of multiple neurological diseases and this technique has the potential to be used in many models of ICP measurement. The development of an easy, reliable and 'safe' measurement of ICP in rats may allow for greater research into the currently understudied area of ICP regulation following neurological injury.

ICP is dramatically elevated following small stroke

The dramatic ICP rise that was seen in Publications 2 and 3 was observed despite small infarct sizes. As mentioned in Chapter 1, little is known about ICP dynamics in patients with small strokes; however it is assumed that these patients do not have an ICP rise. The counterintuitive nature of the ICP response is perhaps the reason such a seemingly basic, yet crucial pathophysiological response has passed unnoticed until now – almost no-one had thought to look. Without direct measurement, elevated ICP is hard to diagnose. The clinical signs of increased ICP are minimal. Headache is a common complaint following stroke and papilloedema (optic disk swelling) takes days to develop. Although thousands of animal studies have investigated various sizes of stroke, including small strokes, very few have concurrently measured ICP. A study from Kotwica *et al.* (1991)[27] demonstrated an ICP peak in Sprague-Dawley rats at 24 hours after small stroke. Interestingly, the magnitude of the ICP peaks recorded in this study were far less than the ICP elevations seen in our study using Sprague-Dawley rats (10-15 mmHg vs. 60 mmHg, respectively) despite similar infarct sizes (9-15% vs. 21%; percentage of contralateral hemisphere). Even following large strokes (25-36%; percentage of contralateral hemisphere), Kotwica demonstrated an ICP peak far less than that shown in our small strokes. This was also seen in the Silasi *et al.* (2009)[26] study, which recorded an average of 25 mmHg at 24 hours following large stroke (infarct 228 ± 36 mm^3; approximately 45% of contralateral hemisphere) in Sprague-Dawley rats. Differences in ICP measurement techniques may explain the differences in ICP magnitude between the studies. Both Kotwica and Silasi measured ICP for 5-15 days post-stroke. Preliminary ICP telemetry studies from our laboratory have

suggested that without a very tight and reliable seal around the catheter, CSF can leak from the system, resulting in ICP recordings that are falsely low. It is therefore plausible that levels of ICP elevation in these studies were slightly higher than actually reported.

I have convincingly demonstrated that ICP is dramatically elevated at 24 hours after small stroke, and raises the possibility that ICP may in fact increase in patients with small infarct volumes. Since ICP has a direct relationship to cerebral perfusion pressure (CPP = Mean arterial pressure - ICP), even minor changes in ICP may have potentially detrimental effects on perfusion to the CPP-dependent ischaemic penumbra. It has been shown that an ICP >25 mmHg is detrimental to outcome following large stroke[16,20]. If the same mechanism is occurring in small stroke, neurological outcome could be affected. There is also an argument of biological plausibility. It is now known that major pathophysiological responses to stroke that were identified in rodents, were preserved in humans once the required studies were performed. Cortical spreading depression is an illustrative example. Despite scepticism amongst clinicians for many years, once the necessary study was performed in humans, it exactly replicated the experimental findings[147]. Similarly, it was long thought that the efficacy and safety data of rodent model thrombolysis (tPA) studies could not be directly translated. A meta-analysis investigating these factors actually demonstrated empirical evidence that animal models of tPA post-stroke can yield similar results to clinical trials. It is therefore plausible that ICP is elevated in patients with small strokes.

Cerebral oedema is not the only cause of ICP elevation

I have demonstrated in Publications 2 and 3 that a mechanism other than oedema is the primary mechanism involved in ICP elevation seen post-stroke in these rats. This result challenges nearly a century of accepted wisdom, however, on review of the experimental and clinical literature, there are no studies demonstrating a direct causative relationship between oedema and ICP elevation post-stroke. One experimental study demonstrated an increase in cerebral oedema and ICP over 24 hours following large stroke, however, since ICP and oedema were performed in different animal cohorts, no direct correlation was reported[29]. Certainly, following large 'malignant' ischaemic strokes, cerebral oedema and mass effect are common, as is increased ICP. In these patients it should be asked- what came first, the chicken or the egg? A small clinical study actually demonstrated that brain herniation preceded dramatic ICP elevations post-stroke[16] and another demonstrated that only 5 of 19 'malignant' stroke patients had severe ICP elevations[19]. The assumption that cerebral oedema is the primary cause of ICP elevation post-stroke seems to be due to the fact that ICP changes have only been investigated in patients with large strokes and large volumes of oedema[14,15,18]. Understanding the fundamental mechanisms driving ICP elevation is important not only for stroke, but potentially for many other neurological conditions in which increased ICP is a complication. If a factor other than oedema is contributing to ICP elevation, research into this area could provide further insight into the scientific knowledge of these conditions. A better understanding of the basic factors governing ICP elevation may also reveal pathophysiological factors that have

gone unnoticed until now, which may potentially lead to alternative, much needed, treatments.

If ICP is elevated in patients with small strokes and minimal oedema, another mechanism must be responsible. So the question remains, if cerebral oedema is not responsible for ICP elevation post-stroke- what is? According to the Monro-Kellie doctrine[47,48], if cerebral oedema is not driving ICP elevation, it is likely that cerebral blood volume (CBV) or CSF is playing a key role. CBV and CSF are not factors that have been thought to be linked to increased ICP post-stroke, and so there are few studies investigating these parameters. CBV has been linked to increases in ICP in other pathological conditions, as explained in Chapter 1, and is most commonly the result of venous obstruction. A simple method to determine if CBV changes are involved in ICP elevation post-stroke would be to perform serial perfusion computed tomography scans before and after stroke. In humans, the contrast medium used to perform these scans is toxic, and thus, is used sparingly. An animal model would be preferable, and these studies are currently underway in our laboratory. CSF may also play a role in ICP elevation. Increased CSF volume, either by increased CSF production or decreased CSF absorption, as well as changes in CSF composition may be important factors in ICP regulation. To date, these factors have not been investigated post-stroke in relation to ICP. Investigating these factors *in vivo* is inherently difficult. In humans, CSF dynamics are difficult to quantify, and in rodents the volumes of CSF are minute. Our laboratory has developed several methods to investigate these factors. Firstly, using a low viscosity casting resin injected into the lateral ventricles of the rat, CSF volume can be compared in stroke and non-stroke animals. Secondly, using contrast-enhanced

perfusion CT scans (see Appendix), CSF dynamics can be visualised *in vivo* and changes between stroke and non-stroke determined. Finally, by transfusing CSF from a stroke rat into a naïve control rat, it can be determined if changes in CSF composition affect ICP elevation. These exciting studies are currently underway. Investigating the fundamental biology is essential to understanding the role of this unknown ICP elevating mechanism in neurological disease and to the development of alternative therapeutic approaches.

Short-duration hypothermia prevents ICP rise

The effect size that was seen between hypothermia-treated and normothermic animals in Publications 2 and 3 was enormous. Both moderate and mild hypothermia acted in a 'switch-like' manner to completely prevent the dramatic ICP elevations seen in normothermic animals. Such a profound effect is highly unusual in biology and has potentially important clinical implications. The current paradigm in clinical hypothermia is to lower ICP many hours after it has already increased[44,54]. A common mantra in stroke research is 'time is brain' – the longer it takes to treatment onset, the further the unsalvageable core will expand into the ischaemic penumbra. When it comes to thrombolysis treatment, data has shown that earlier treatment is associated with bigger proportional benefits[11]. Why then, do the majority of clinical studies delay hypothermia until ICP is already elevated (and infarct has expanded)? The exciting prospect of this study is that ICP was not affected during the short duration of cooling, but instead prevented the rise from occurring in the first place. What is so surprising is that such a short duration of cooling could have such a long-lived and profound effect,

exerting preventative effects 20 hours before the rise was seen in non-cooled animals. Moreover, cooling before ICP was elevated prevented any increase in ICP during rewarming.

To date, no short-duration hypothermia studies have been conducted in humans. The idea that 'less is more' is counterintuitive. However, it may not be so surprising when the history of hypothermia is considered. Although hypothermia has been known to cause death since the time of Hippocrates, "cold causes fits, tetanus, gangrene and feverish shivering fits … Cold is bad for the bones, teeth, nerves, brain and the spinal cord…"[148], the knowledge that hypothermia was protective came about many centuries later with the observation of soldiers with battle wounds in cold countries. It was assumed that since these soldiers survived their wounds following extreme hypothermia - colder must be better. Thermometers, however, were not a common clinical tool until the mid-19th century and once utilised in the clinical setting, with the invention of evidence-based medicine, it became apparent that moderate hypothermia was safer and more effective than deep hypothermia. Could it not be possible then, that shorter is also safer and more beneficial than longer hypothermia?

Translation of therapeutic hypothermia into the clinical setting is the ultimate goal of this research. Before that is feasible, however, more experimental studies need to be conducted. Determining the optimal dose, duration, time-window and induction method of hypothermia is of vital importance for successful translation from bench to bedside. In humans, dose and duration data is lacking. Several small clinical trials have suggested that surface cooling to 33-35 °C in awake stroke patients for >24 hours is

feasible and safe[17,18,149], however these studies were too small to provide reasonable efficacy data. Despite overwhelming animal data indicating that short-duration cooling is effective, the vast majority of hypothermia trials cool for 24-72 hours or longer. There is also no clinical data regarding a treatment time-window in stroke, although a trial in cardiac arrest patients demonstrated improved outcome out to 8 hours[91]. Although no other experimental studies have investigated hypothermia and ICP post-stroke, the results of this thesis have mirrored the results of the van der Worp *et al.* (2007) meta-analysis[114], which suggested that cooling to 35 °C before or shortly after stroke for less than 6 hours is beneficial for infarct reduction. An interesting phenomenon that I demonstrated in Publication 3 was the suggestion of a small ICP rise at 24 hours in the mild hypothermia-treated animals (35 °C). This elevation was not statistically significant (~5 mmHg increase) and the effect size between the hypothermia-treated and normothermic animals was still large (~20 mmHg between groups at 24 hours), but the data suggests that cooling to 35 °C may be close to the limit for the 'switch-like' effect. If a short duration of mild cooling, induced shortly after stroke, were all that is needed to *prevent* ICP rise and further neurological deterioration, the application in the clinical setting would be much easier. Without the need for intensive care, this modality could become widespread, greatly increasing the number of patients that could benefit from this exciting treatment.

There are typically two ways of inducing hypothermia: surface and endovascular cooling. Our studies, like the majority of animal studies, demonstrated benefit with the use of surface cooling. Data that directly compares the efficacy of the two methods is lacking in both the clinical setting and experimental studies. To date, the only

successful large-scale clinical trials have all used the non-invasive method of surface cooling[90-92]. Although endovascular cooling is invasive, it is a faster method of hypothermia induction than surface cooling and is better tolerated by patients, and thus, has become a popular cooling method. However, there is no data to date to suggest that endovascular cooling provides better outcomes post-stroke. Some physiological responses, such as shivering, are linked to skin temperature rather than to body core temperature. Our more recent pilot data shows prevention of ICP elevation with short-duration skin cooling. An intriguing thought that arises from this data is the possibility that it is the drop in skin temperature rather than the drop in core temperature that may be the mechanism involved in preventing ICP. Of course, this hypothesis requires further pre-clinical testing, however if skin cooling does prevent ICP the clinical implications would be huge. The use of hypothermia in the clinical setting would become very easy, cheap and very widely accessible.

It is clear that for hypothermia to become a widely used therapeutic modality in the clinical setting, further investigations into dose, duration, time-window and induction methods are needed. The translation of these results into the clinical setting, however, may not be direct, since humans take much longer to cool/rewarm than rodents. Stroke research does not currently have a good record of translation from bench to bedside[7]. To combat this, the STAIR guidelines suggest, amongst other things, that experimental efficacy is obtained in multiple species. To translate experimental hypothermia more effectively, it may be wise to investigate these factors in a larger animal model of ischaemic stroke, such as primates[150,151], canines[152,153] or sheep[154,155]. Conducting dose and duration response experiments and delaying cooling by several

hours in a larger animal model of stroke, may give further and potentially more translatable insight into the effects of hypothermia on ICP.

Leptomeningeal collateral blood flow is increased following stroke but reduced by increases in ICP

In Publication 4, I demonstrated that leptomeningeal collateral blood flow increased by > 450% following the occlusion of the middle cerebral artery and that incremental increases in ICP significantly reduced this flow. The correlation between ICP increase and collateral blood flow was strong. This data, coupled with the data of Publications 2 and 3, which demonstrated large ICP increases following small strokes, suggests that ICP elevation plays a key role in the 'collateral failure' that is seen in a subset of ischaemic stroke patients with stroke-in-progression. This result may potentially have a huge impact on the outcome of these patients; however there are still questions that remain unanswered.

Does naturally occurring ICP elevation reduce collateral flow and penumbral perfusion post-stroke? I demonstrated a strong inverse relationship between artificial ICP elevation and collateral blood flow in Publication 4. Until recently, it was assumed that patients suffering from stroke-in-progression showed initial clinical improvement due to spontaneous reperfusion and that the subsequent deterioration was the result of a reformation of the clot. Very recent imaging data strongly suggests that the vessel does not recannalise and that the deterioration may be the result of leptomeningeal collateral blood vessel failure[83-85]. The cause of this 'collateral failure' is currently

unknown; however, based on the data presented in this thesis, ICP elevation seems to play a critical role. It is therefore important to confirm that the natural rise in ICP that is seen post-stroke results in a similar decline in collateral flow and perfusion of the ischaemic penumbra. As mentioned above, there have been multiple examples of pathophysiological stroke response preservation between rodents and humans. If natural ICP elevation reduces collateral flow in rats, it may be likely that the same response is occurring in man. This could revolutionise the understanding of stroke-in-progression and greatly improve the potential for treatment.

Does preventing ICP elevation with short-duration hypothermia also prevent collateral blood flow reduction? There are currently no available treatments for patients suffering from stroke-in-progression. Due to the potentially mistaken interpretation of the pathophysiology, patients are still commonly treated with anticoagulants such as heparin. In Publications 2 and 3, I demonstrated that a short duration of hypothermia completely prevented the dramatic elevation in ICP that was seen post-stroke. The obvious extension to these results is to determine whether preventing the ICP elevation with short-duration hypothermia also prevents the reduction in collateral flow and cerebral perfusion. These studies, which are currently in the pilot study stage, may provide the first direct evidence that naturally occurring ICP elevation post-stroke causes collateral flow reduction and that a relatively cheap, simple and safe treatment of short-duration hypothermia might prevent this phenomenon from occurring.

Does ICP elevation cause infarct expansion? Several international teams have reported imaging findings from stroke patients indicating that 'failure' of collateral vessels is the

main cause of infarct expansion. Although collateral failure has been associated with neurological deterioration, the possibility that collateral flow reduction is an effect of infarct expansion, rather than the cause has not been excluded. I hypothesise, based on data presented in this thesis, that ICP elevation is the major contributor to this 'collateral failure'. Therefore, investigating whether increases in ICP result in infarct expansion using serial magnetic resonance imaging in rats, will provide the first direct evidence that infarct expansion occurs as a result of ICP elevation. If confirmed, it would represent a radical rethinking of the causes of stroke-in-progression and would also have clear and immediate therapeutic implications (short-duration hypothermia). Successful investigations of these factors will allow greater insight into the enigmatic condition of stroke-in-progression.

Currently there is no way to know if a patient with minor stroke will go on to develop stroke-in-progression. If the studies outlined above demonstrate that ICP elevation results in infarct expansion, then measuring ICP in patients with minor stoke may be key to detecting early changes in these patients. There is currently no available data regarding ICP in patients with minor stroke and unless a reliable non-invasive measure of ICP measurement becomes available, such data is likely to remain unobtainable for ethical reasons. Transcranial Doppler ultrasound, tympanic membrane displacement, and ocular measurements are non-invasive techniques that are currently being investigated[156-161], however further development of these techniques is required. Non-invasive ICP measurement would allow ICP data to be collected in a range of patients and may provide valuable insight into the mechanisms involved in stroke, stroke-in-progression, and multiple other neuropathologies in which ICP elevation is a

complication. The concepts that ICP may rise after minor stroke (regardless of oedema), that short-duration hypothermia may prevent this rise and that such a rise could be the cause of collateral failure and contribute to stroke-in-progression are all radically new, and further clinical and pre-clinical investigations are imperative.

CHAPTER 8

CONCLUSIONS

The data in this thesis have demonstrated several novel, important, and paradigm-shifting results:

1. Intracranial pressure can be reliably and repeatedly measured using a fibre-optic pressure transducer placed above the dura in the rat.
2. Intracranial pressure is dramatically elevated 24 hours following small experimental ischaemic stroke.
3. Cerebral oedema is not the primary mechanism causing this intracranial pressure elevation.
4. A short duration of mild and moderate hypothermia, induced shortly after stroke (many hours before intracranial pressure is elevated), completely prevents intracranial pressure rise at 24 hours.
5. Leptomeningeal collateral blood flow increases significantly following experimental ischaemic stroke.
6. Intracranial pressure elevations significantly reduce leptomeningeal collateral blood flow.

These findings may have big clinical implications. They suggest that ICP may be elevated not only in large strokes as previously thought, but also in patients with smaller strokes (which make up the majority of stroke patients). They also suggest that

this rise is not the result of cerebral oedema like previously assumed, but that other factors may be involved. This mechanism may be important not only in stroke, but perhaps also in other neurological conditions. These results suggest that a major rethink of ICP regulation post-stroke is needed. The finding of a sustained effect on ICP resulting from a brief period of mild hypothermia may eliminate the problems of rewarming injury resulting from ICP elevation and revolutionise and extend the application of hypothermia, which is the only neuroprotective therapy with proven benefit in human brain ischaemia. Because of its relative simplicity (compared to long-duration hypothermia), short-duration hypothermia is a much more appealing alternative treatment approach in the relatively large number of patients in whom thrombolysis is currently contraindicated, or as an adjunct treatment for the substantial number of patients in whom reperfusion is unsuccessful. Lastly, I have shown here that ICP elevation is the likely mechanism involved in the 'collateral failure' seen in stroke-in-progression patients. This is a potentially new pathophysiological mechanism to explain a problem that has caused great angst amongst treating doctors for many years. The outcomes of this research are important both in terms of increasing understanding of human disease and in terms of potential therapeutic application. This evidence warrants a rethink of current approaches to treatment of stroke. I anticipate that the outcomes of these studies will ultimately save lives and prevent severe disability in patients suffering from stroke.

CHAPTER 9

REFERENCES

---

1 Mackay, J. & Mensah, G. Atlas of Heart Disease and Stroke. *World Health Organization* (2004).

2 Australian Institue of Health and Welfare. Australia's health 2014. Australia's health series no.14. **Cat. no. AUS178** (2014).

3 Deloitte Access Economics. The economic impact of stroke in Australia. *National Stroke Foundation of Australia* (2013).

4 AIHW. Stroke and its management in Australia: an update. *Cardiovascular Disease Series* **37** (2013).

5 Rothwell, P. M. *et al.* Change in stroke incidence, mortality, case-fatality, severity, and risk factors in Oxfordshire, UK from 1981 to 2004 (Oxford Vascular Study). *Lancet* **363**, 1925-1933, doi:10.1016/S0140-6736(04)16405-2 S0140673604164052 [pii] (2004).

6 Donnan, G. A., Baron, J. C., Davis, S. M. & Sharp, F. R. *The Ischemic Penumbra: Pathophysiology, Imaging and Therapy*. Vol. 1 (Informa Healthcare, 2007).

7 O'Collins, V. E. *et al.* 1,026 experimental treatments in acute stroke. *Ann Neurol* **59**, 467-477, doi:10.1002/ana.20741 (2006).

8 Sandercock, P. A., Counsell, C., Tseng, M. C. & Cecconi, E. Oral antiplatelet therapy for acute ischaemic stroke. *Cochrane Database Syst Rev* **3**, CD000029, doi:10.1002/14651858.CD000029.pub3 (2014).

9 Langhorne, P., Williams, B. O., Gilchrist, W. & Howie, K. Do stroke units save lives? *Lancet* **342**, 395-398, doi:0140-6736(93)92813-9 [pii] (1993).

10 Gilligan, A. K. *et al.* Stroke units, tissue plasminogen activator, aspirin and neuroprotection: which stroke intervention could provide the greatest community benefit? *Cerebrovasc Dis* **20**, 239-244, doi:87705 [pii] 10.1159/000087705 (2005).

11 Emberson, J. *et al.* Effect of treatment delay, age, and stroke severity on the effects of intravenous thrombolysis with alteplase for acute ischaemic stroke: a meta-analysis of individual patient data from randomised trials. *Lancet*, doi:S0140-6736(14)60584-5 [pii] 10.1016/S0140-6736(14)60584-5 (2014).

12 Quain, D. A. *et al.* Improving access to acute stroke therapies: a controlled trial of organised pre-hospital and emergency care. *Med J Aust* **189**, 429-433, doi:qua10056_fm [pii] (2008).

13 Hofmeijer, J. *et al.* Surgical decompression for space-occupying cerebral infarction (the Hemicraniectomy After Middle Cerebral Artery infarction with Life-threatening Edema Trial [HAMLET]): a multicentre, open, randomised trial. *Lancet Neurol* **8**, 326-333, doi:10.1016/S1474-4422(09)70047-X S1474-4422(09)70047-X [pii] (2009).

14 Hacke, W. *et al.* 'Malignant' middle cerebral artery territory infarction: clinical course and prognostic signs. *Arch Neurol* **53**, 309-315 (1996).

15 Ropper, A. H. & Shafran, B. Brain edema after stroke. Clinical syndrome and intracranial pressure. *Arch Neurol* **41**, 26-29 (1984).

16 Schwab, S., Aschoff, A., Spranger, M., Albert, F. & Hacke, W. The value of intracranial pressure monitoring in acute hemispheric stroke. *Neurology* **47**, 393-398 (1996).

17 Schwab, S. *et al.* Feasibility and safety of moderate hypothermia after massive hemispheric infarction. *Stroke* **32**, 2033-2035 (2001).

18 Schwab, S. *et al.* Moderate hypothermia in the treatment of patients with severe middle cerebral artery infarction. *Stroke* **29**, 2461-2466 (1998).

19 Frank, J. I. Large hemispheric infarction, deterioration, and intracranial pressure. *Neurology* **45**, 1286-1290 (1995).

20 Balestreri, M. *et al.* Impact of intracranial pressure and cerebral perfusion pressure on severe disability and mortality after head injury. *Neurocrit Care* **4**, 8-13, doi:NCC:4:1:008 [pii] 10.1385/NCC:4:1:008 (2006).

21 Citerio, G. & Andrews, P. J. Intracranial pressure. Part two: Clinical applications and technology. *Intensive Care Med* **30**, 1882-1885, doi:10.1007/s00134-004-2377-3 (2004).

22 Monro, A. *Observations on the structure and functions of the nervous system : illustrated with tables*. (Printed for, and sold by, William Creech; and Joseph Johnson, London, 1783).

23 Kellie, G. *An account of the appearances observed in the dissection of two of three individuals presumed to have perished in the storm of the 3d, and whose bodies were discovered in the vicinity of Leith on the morning of the 4th, November 1821 : with some reflections on the pathology of the brain*. (s.n., 1824).

24 Dunn, L. T. Raised intracranial pressure. *J Neurol Neurosurg Psychiatry* **73 Suppl 1**, i23-27 (2002).

25 Steiner, L. A. & Andrews, P. J. Monitoring the injured brain: ICP and CBF. *Br J Anaesth* **97**, 26-38, doi:ael110 [pii] 10.1093/bja/ael110 (2006).

26 Silasi, G., MacLellan, C. L. & Colbourne, F. Use of telemetry blood pressure transmitters to measure intracranial pressure (ICP) in freely moving rats. *Curr Neurovasc Res* **6**, 62-69 (2009).

27 Kotwica, Z., Hardemark, H. G. & Persson, L. Intracranial pressure changes following middle cerebral artery occlusion in rats. *Res Exp Med (Berl)* **191**, 99-104 (1991).

28 Verlooy, J., Selosse, P., Van Reempts, J., Haseldonckx, M. & Borgers, M. Fiberoptic intracranial pressure monitoring in rats. *J Neurosci Methods* **31**, 1-6, doi:0165-0270(90)90002-W [pii] (1990).

29 Kotwica, Z., Persson, L. & Thuomas, K. A. The effects of brain edema on intracranial pressure in focal cerebral ischemia. An experimental study in a rat using magnetic resonance imaging. *Zentralbl Neurochir* **50**, 68-71 (1989).

30 Chiu, C. *et al.* Temporal course of cerebrospinal fluid dynamics and amyloid accumulation in the aging rat brain from three to thirty months. *Fluids Barriers CNS* **9**, 3, doi:10.1186/2045-8118-9-3 2045-8118-9-3 [pii] (2012).

31 Al-Sarraf, H. & Philip, L. Effect of hypertension on the integrity of blood brain and blood CSF barriers, cerebral blood flow and CSF secretion in the rat. *Brain Res* **975**, 179-188, doi:S0006899303026325 [pii] (2003).

32 Al-Sarraf, H. & Philip, L. Increased brain uptake and CSF clearance of 14C-glutamate in spontaneously hypertensive rats. *Brain Res* **994**, 181-187, doi:S0006899303037521 [pii] (2003).

33 Tripathi, R. Tracing the bulk outflow route of cerebrospinal fluid by transmission and scanning electron microscopy. *Brain Res* **80**, 503-506, doi:0006-8993(74)91033-6 [pii] (1974).

34 Tripathi, B. J. & Tripathi, R. C. Vacuolar transcellular channels as a drainage pathway for cerebrospinal fluid. *J Physiol* **239**, 195-206 (1974).

35 Welch, K. & Friedman, V. The cerebrospinal fluid valves. *Brain* **83**, 454-469 (1960).

36 Cserr, H. F., Harling-Berg, C. J. & Knopf, P. M. Drainage of brain extracellular fluid into blood and deep cervical lymph and its immunological significance. *Brain Pathol* **2**, 269-276 (1992).

37 Zakharov, A. *et al.* Integrating the roles of extracranial lymphatics and intracranial veins in cerebrospinal fluid absorption in sheep. *Microvasc Res* **67**, 96-104, doi:S0026286203000736 [pii] (2004).

38 Kida, S., Pantazis, A. & Weller, R. O. CSF drains directly from the subarachnoid space into nasal lymphatics in the rat. Anatomy, histology and immunological significance. *Neuropathol Appl Neurobiol* **19**, 480-488 (1993).

39 Carare, R. O., Hawkes, C. A. & Weller, R. O. Afferent and efferent immunological pathways of the brain. Anatomy, function and failure. *Brain Behav Immun* **36**, 9-14, doi:10.1016/j.bbi.2013.10.012 S0889-1591(13)00511-4 [pii] (2014).

40 Silver, I., Li, B., Szalai, J. & Johnston, M. Relationship between intracranial pressure and cervical lymphatic pressure and flow rates in sheep. *Am J Physiol* **277**, R1712-1717 (1999).

41 Mollanji, R., Bozanovic-Sosic, R., Zakharov, A., Makarian, L. & Johnston, M. G. Blocking cerebrospinal fluid absorption through the cribriform plate increases resting intracranial pressure. *Am J Physiol Regul Integr Comp Physiol* **282**, R1593-1599, doi:10.1152/ajpregu.00695.2001 (2002).

42 Johnston, M., Zakharov, A., Papaiconomou, C., Salmasi, G. & Armstrong, D. Evidence of connections between cerebrospinal fluid and nasal lymphatic vessels in humans, non-human primates and other mammalian species. *Cerebrospinal Fluid Res* **1**, 2, doi:1743-8454-1-2 [pii] 10.1186/1743-8454-1-2 (2004).

43 Wagshul, M. E. *et al.* Ventricular dilation and elevated aqueductal pulsations in a new experimental model of communicating hydrocephalus. *Exp Neurol* **218**, 33-40, doi:10.1016/j.expneurol.2009.03.034 S0014-4886(09)00124-1 [pii] (2009).

44 Bateman, G. A. The pathophysiology of idiopathic normal pressure hydrocephalus: cerebral ischemia or altered venous hemodynamics? *AJNR Am J Neuroradiol* **29**, 198-203, doi:ajnr.A0739 [pii] 10.3174/ajnr.A0739 (2008).

45 Preuss, M. *et al.* Updated physiology and pathophysiology of CSF circulation--the pulsatile vector theory. *Childs Nerv Syst* **29**, 1811-1825, doi:10.1007/s00381-013-2219-0 (2013).

46 Killer, H. E. *et al.* Cerebrospinal fluid dynamics between the intracranial and the subarachnoid space of the optic nerve. Is it always bidirectional? *Brain* **130**, 514-520, doi:awl324 [pii]10.1093/brain/awl324 (2007).

47 Shapira, Y., Artru, A. A. & Lam, A. M. Changes in the rate of formation and resistance to reabsorption of cerebrospinal fluid during deliberate hypotension induced with adenosine or hemorrhage. *Anesthesiology* **76**, 432-439 (1992).

48 Paradot, G., Baledent, O., Gondry-Jouet, C., Meyer, M. E. & Le Gars, D. [Cerebrospinal fluid flow imaging in the meningeal hemorrhage]. *Neurochirurgie* **52**, 323-329, doi:MDOI-NCHIR-09-2006-52-4-0028-3770-101019-200604252 [pii] (2006).

49 Brinker, T., Seifert, V. & Stolke, D. Acute changes in the dynamics of the cerebrospinal fluid system during experimental subarachnoid hemorrhage. *Neurosurgery* **27**, 369-372 (1990).

50 Johanson, C., Stopa, E., Baird, A. & Sharma, H. Traumatic brain injury and recovery mechanisms: peptide modulation of periventricular neurogenic regions by the choroid plexus-CSF nexus. *J Neural Transm* **118**, 115-133, doi:10.1007/s00702-010-0498-0 (2011).

51 Schmid Daners, M. *et al.* Age-specific characteristics and coupling of cerebral arterial inflow and cerebrospinal fluid dynamics. *PLoS One* **7**, e37502, doi:10.1371/journal.pone.0037502 PONE-D-12-02706 [pii] (2012).

52 Stoquart-ElSankari, S. *et al.* Aging effects on cerebral blood and cerebrospinal fluid flows. *J Cereb Blood Flow Metab* **27**, 1563-1572, doi:9600462 [pii] 10.1038/sj.jcbfm.9600462 (2007).

53 Goldsmith, P., Burn, D. J., Coulthard, A. & Jenkins, A. Extrinsic cerebral venous sinus obstruction resulting in intracranial hypertension. *Postgrad Med J* **75**, 550-551 (1999).

54 Lam, B. L., Schatz, N. J., Glaser, J. S. & Bowen, B. C. Pseudotumor cerebri from cranial venous obstruction. *Ophthalmology* **99**, 706-712 (1992).

55 Purvin, V. A., Trobe, J. D. & Kosmorsky, G. Neuro-ophthalmic features of cerebral venous obstruction. *Archives of Neurology* **52**, 880-885, doi:10.1001/archneur.1995.00540330058015 (1995).

56 Wen, D. Y., Hardten, D. R., Wirtschafter, J. D., Sung, J. H. & Haines, S. J. Elevated intracranial pressure from cerebral venous obstruction by Masson's vegetant intravascular hemangioendothelioma. Case report. *J Neurosurg* **75**, 787-790, doi:10.3171/jns.1991.75.5.0787 (1991).

57 Biousse, V., Ameri, A. & Bousser, M. G. Isolated intracranial hypertension as the only sign of cerebral venous thrombosis. *Neurology* **53**, 1537-1542 (1999).

58 Masuhr, F., Mehraein, S. & Einhaupl, K. Cerebral venous and sinus thrombosis. *J Neurol* **251**, 11-23, doi:10.1007/s00415-004-0321-7 (2004).

59 Engelborghs, K. *et al.* Impaired autoregulation of cerebral blood flow in an experimental model of traumatic brain injury. *J Neurotrauma* **17**, 667-677, doi:10.1089/089771500415418 (2000).

60 Urrutia, V. C. & Wityk, R. J. Blood pressure management in acute stroke. *Neurol Clin* **26**, 565-583, x-xi, doi:10.1016/j.ncl.2008.02.002 S0733-8619(08)00022-4 [pii] (2008).

61 Liebeskind, D. S. *et al.* Collaterals at angiography and outcomes in the Interventional Management of Stroke (IMS) III trial. *Stroke* **45**, 759-764, doi:10.1161/STROKEAHA.113.004072 STROKEAHA.113.004072 [pii] (2014).

62 Christoforidis, G. A., Mohammad, Y., Kehagias, D., Avutu, B. & Slivka, A. P. Angiographic assessment of pial collaterals as a prognostic indicator following intra-arterial thrombolysis for acute ischemic stroke. *AJNR Am J Neuroradiol* **26**, 1789-1797, doi:26/7/1789 [pii] (2005).

63 Bang, O. Y. *et al.* Impact of collateral flow on tissue fate in acute ischaemic stroke. *J Neurol Neurosurg Psychiatry* **79**, 625-629, doi:jnnp.2007.132100 [pii] 10.1136/jnnp.2007.132100 (2008).

64 Roberts, H. C. *et al.* Computed tomographic findings in patients undergoing intra-arterial thrombolysis for acute ischemic stroke due to middle cerebral artery occlusion: results from the PROACT II trial. *Stroke* **33**, 1557-1565 (2002).

65 Miteff, F. *et al.* The independent predictive utility of computed tomography angiographic collateral status in acute ischaemic stroke. *Brain* **132**, 2231-2238, doi:10.1093/brain/awp155 awp155 [pii] (2009).

66 Bang, O. Y. *et al.* Collateral flow predicts response to endovascular therapy for acute ischemic stroke. *Stroke* **42**, 693-699, doi:10.1161/STROKEAHA.110.595256 STROKEAHA.110.595256 [pii] (2011).

67 Shuaib, A. *et al.* Partial aortic occlusion for cerebral perfusion augmentation: safety and efficacy of NeuroFlo in Acute Ischemic Stroke trial. *Stroke* **42**, 1680-1690, doi:10.1161/STROKEAHA.110.609933 STROKEAHA.110.609933 [pii] (2011).

68 Wityk, R. J. Blood pressure augmentation in acute ischemic stroke. *J Neurol Sci* **261**, 63-73 (2007).

69 Shin, H. K. *et al.* Mild induced hypertension improves blood flow and oxygen metabolism in transient focal cerebral ischemia. *Stroke* **39**, 1548-1555 (2008).

70 Winship, I. R. *et al.* Augmenting collateral blood flow during ischemic stroke via transient aortic occlusion. *J Cereb Blood Flow Metab*, doi:10.1038/jcbfm.2013.162 (2013).

71 Terpolilli, N. A. *et al.* Inhalation of nitric oxide prevents ischemic brain damage in experimental stroke by selective dilatation of collateral arterioles. *Circ Res* **110**, 727-738, doi:10.1161/CIRCRESAHA.111.253419 CIRCRESAHA.111.253419 [pii] (2012).

72 Coyle, P. Diameter and length changes in cerebral collaterals after middle cerebral artery occlusion in the young rat. *Anat Rec* **210**, 357-364, doi:10.1002/ar.1092100211 (1984).

73 Coyle, P. & Jokelainen, P. T. Differential outcome to middle cerebral artery occlusion in spontaneously hypertensive stroke-prone rats (SHRSP) and Wistar Kyoto (WKY) rats. *Stroke* **14**, 605-611 (1983).

74 Zhang, H., Prabhakar, P., Sealock, R. & Faber, J. E. Wide genetic variation in the native pial collateral circulation is a major determinant of variation in severity of stroke. *J Cereb Blood Flow Metab* **30**, 923-934, doi:10.1038/jcbfm.2010.10 jcbfm201010 [pii] (2010).

75 Toriumi, H. *et al.* Dually supplied T-junctions in arteriolo-arteriolar anastomosis in mice: key to local hemodynamic homeostasis in normal and ischemic states? *Stroke* **40**, 3378-3383, doi:10.1161/STROKEAHA.109.558577 STROKEAHA.109.558577 [pii] (2009).

76 Chalothorn, D. & Faber, J. E. Formation and maturation of the native cerebral collateral circulation. *J Mol Cell Cardiol* **49**, 251-259, doi:10.1016/j.yjmcc.2010.03.014 S0022-2828(10)00107-0 [pii] (2010).

77 Armitage, G. A., Todd, K. G., Shuaib, A. & Winship, I. R. Laser speckle contrast imaging of collateral blood flow during acute ischemic stroke. *J Cereb Blood Flow Metab* **30**, 1432-1436, doi:10.1038/jcbfm.2010.73 jcbfm201073 [pii] (2010).

78 Shih, A. Y. *et al.* Active dilation of penetrating arterioles restores red blood cell flux to penumbral neocortex after focal stroke. *J Cereb Blood Flow Metab* **29**, 738-751, doi:10.1038/jcbfm.2008.166 jcbfm2008166 [pii] (2009).

79 Ali, L. K. & Saver, J. L. The ischemic stroke patient who worsens: new assessment and management approaches. *Rev Neurol Dis* **4**, 85-91 (2007).

80 Coutts, S. B. *et al.* CT/CT angiography and MRI findings predict recurrent stroke after transient ischemic attack and minor stroke: results of the prospective CATCH study. *Stroke* **43**, 1013-1017, doi:10.1161/STROKEAHA.111.637421 STROKEAHA.111.637421 [pii] (2012).

81 Coutts, S. B. *et al.* What causes disability after transient ischemic attack and minor stroke?: Results from the CT and MRI in the Triage of TIA and minor Cerebrovascular Events to Identify High Risk Patients (CATCH) Study. *Stroke* **43**, 3018-3022, doi:10.1161/STROKEAHA.112.665141 STROKEAHA.112.665141 [pii] (2012).

82 Caplan, L. R. Treatment of "progressive" stroke. *Stroke* **22**, 694-695 (1991).

83 Asdaghi, N. *et al.* Acute perfusion and diffusion abnormalities predict early new MRI lesions 1 week after minor stroke and transient ischemic attack. *Stroke* **42**, 2191-2195, doi:10.1161/STROKEAHA.110.611376 STROKEAHA.110.611376 [pii] (2011).

84 Coutts, S. B. *et al.* CT/CT angiography and MRI findings predict recurrent stroke after transient ischemic attack and minor stroke: results of the prospective CATCH study. *Stroke* **43**, 1013-1017, doi:10.1161/STROKEAHA.111.637421 (2012).

85 Campbell, B. C. *et al.* Failure of collateral blood flow is associated with infarct growth in ischemic stroke. *J Cereb Blood Flow Metab* **33**, 1168-1172, doi:10.1038/jcbfm.2013.77 (2013).

86 Liebeskind, D. S. Collateral circulation. *Stroke* **34**, 2279-2284 (2003).

87 Pranevicius, O., Pranevicius, M., Pranevicius, H. & Liebeskind, D. S. Transition to collateral flow after arterial occlusion predisposes to cerebral venous steal. *Stroke* **43**, 575-579, doi:10.1161/STROKEAHA.111.635037 (2012).

88 Alexandrov, A. V. *et al.* Reversed Robin Hood syndrome in acute ischemic stroke patients. *Stroke* **38**, 3045-3048, doi:10.1161/STROKEAHA.107.482810 (2007).

89 Palamarchuk, I., Kimpinski, K., Lippert, C. & Hachinski, V. Nocturnal deterioration after ischemic stroke and autonomic dysfunction: hypothesis and implications. *Cerebrovasc Dis* **36**, 454-461, doi:10.1159/000356093 (2013).

90 Bernard, S. A. *et al.* Treatment of comatose survivors of out-of-hospital cardiac arrest with induced hypothermia. *N Engl J Med* **346**, 557-563, doi:10.1056/NEJMoa003289 346/8/557 [pii] (2002).

91 Hypothermia After Cardiac Arrest Study Group. Mild therapeutic hypothermia to improve the neurologic outcome after cardiac arrest. *N Engl J Med* **346**, 549-556, doi:10.1056/NEJMoa012689 346/8/549 [pii] (2002).

92 Shankaran, S. *et al.* Whole-body hypothermia for neonates with hypoxic-ischemic encephalopathy. *N Engl J Med* **353**, 1574-1584, doi:353/15/1574 [pii] 10.1056/NEJMcps050929 (2005).

93 Fay, T. Observations on prolonged human refrigeration. *New York State Journal of Medicine* **40**, 347-348 (1940).

94 Fay, T. Observations on generalized refrigeration in cases of severe cerebral trauma. *Association for Research in Nervous and Mental Disease* **24**, 611-619 (1943).

95 Bigelow, W. G., Callaghan, J. C. & Hopps, J. A. General hypothermia for experimental intracardiac surgery; the use of electrophrenic respirations, an artificial pacemaker for

cardiac standstill, and radio-frequency rewarming in general hypothermia. *Trans Meet Am Surg Assoc Am Surg Assoc* **68**, 211-219 (1950).

96 Botterell, E. H., Lougheed, W. M., Morley, T. P. & Vandewater, S. L. Hypothermia in the surgical treatment of ruptured intracranial aneurysms. *J Neurosurg* **15**, 4-18, doi:10.3171/jns.1958.15.1.0004 (1958).

97 Botterell, E. H., Lougheed, W. M., Scott, J. W. & Vandewater, S. L. Hypothermia, and interruption of carotid, or carotid and vertebral circulation, in the surgical management of intracranial aneurysms. *J Neurosurg* **13**, 1-42, doi:10.3171/jns.1956.13.1.0001 (1956).

98 Marion, D. W., Obrist, W. D., Carlier, P. M., Penrod, L. E. & Darby, J. M. The use of moderate therapeutic hypothermia for patients with severe head injuries: a preliminary report. *J Neurosurg* **79**, 354-362, doi:10.3171/jns.1993.79.3.0354 (1993).

99 Marion, D. W. *et al.* Treatment of traumatic brain injury with moderate hypothermia. *N Engl J Med* **336**, 540-546, doi:10.1056/NEJM199702203360803 (1997).

100 Winters, S. A. *et al.* Assessment of risk factors for post-rewarming "rebound hyperthermia" in cardiac arrest patients undergoing therapeutic hypothermia. *Resuscitation* **84**, 1245-1249, doi:10.1016/j.resuscitation.2013.03.027 S0300-9572(13)00197-4 [pii] (2013).

101 Mulder, M. *et al.* Awakening and Withdrawal of Life-Sustaining Treatment in Cardiac Arrest Survivors Treated With Therapeutic Hypothermia. *Crit Care Med*, doi:10.1097/CCM.0000000000000540 (2014).

102 Yoo, J. S. *et al.* Surgical repair of descending thoracic and thoracoabdominal aortic aneurysm involving the distal arch: Open proximal anastomosis under deep hypothermia versus arch clamping technique. *J Thorac Cardiovasc Surg*, doi:S0022-5223(14)00892-7 [pii] 10.1016/j.jtcvs.2014.06.068 (2014).

103 Gluckman, P. D. *et al.* Selective head cooling with mild systemic hypothermia after neonatal encephalopathy: multicentre randomised trial. *Lancet* **365**, 663-670, doi:S014067360517946X [pii] 10.1016/S0140-6736(05)17946-X (2005).

104 Azzopardi, D. V. *et al.* Moderate hypothermia to treat perinatal asphyxial encephalopathy. *N Engl J Med* **361**, 1349-1358, doi:361/14/1349 [pii] 10.1056/NEJMoa0900854 (2009).

105 Azzopardi, D. *et al.* Effects of hypothermia for perinatal asphyxia on childhood outcomes. *N Engl J Med* **371**, 140-149, doi:10.1056/NEJMoa1315788 (2014).

106 Joy, R., Pournami, F., Bethou, A., Bhat, V. B. & Bobby, Z. Effect of therapeutic hypothermia on oxidative stress and outcome in term neonates with perinatal asphyxia: a randomized controlled trial. *J Trop Pediatr* **59**, 17-22, doi:10.1093/tropej/fms036 fms036 [pii] (2013).

107 Shiozaki, T. *et al.* Effect of mild hypothermia on uncontrollable intracranial hypertension after severe head injury. *J Neurosurg* **79**, 363-368, doi:10.3171/jns.1993.79.3.0363 (1993).

108 Clifton, G. L. *et al.* A phase II study of moderate hypothermia in severe brain injury. *J Neurotrauma* **10**, 263-271; discussion 273 (1993).

109 Maekawa, T., Yamashita, S., Nagao, S., Hayashi, N. & Ohashi, Y. Prolonged mild therapeutic hypothermia versus fever control with tight hemodynamic monitoring and slow rewarming in patients with severe traumatic brain injury: a randomized controlled trial. *J Neurotrauma*, doi:10.1089/neu.2013.3197 (2014).

110 Stravitz, R. T. *et al.* Therapeutic hypothermia for acute liver failure: toward a randomized, controlled trial in patients with advanced hepatic encephalopathy. *Neurocritical care* **9**, 90-96 (2008).

111 Jacobs, S., Hunt, R., Tarnow-Mordi, W., Inder, T. & Davis, P. Cooling for newborns with hypoxic ischaemic encephalopathy. *Cochrane Database Syst Rev*, CD003311, doi:10.1002/14651858.CD003311.pub2 (2007).

112 Polderman, K. H. Induced hypothermia and fever control for prevention and treatment of neurological injuries. *Lancet* **371**, 1955-1969, doi:10.1016/S0140-6736(08)60837-5 S0140-6736(08)60837-5 [pii] (2008).

113 Polderman, K. H. Hypothermia and neurological outcome after cardiac arrest: state of the art. *Eur J Anaesthesiol Suppl* **42**, 23-30, doi:10.1017/S026502150700333X S026502150700333X [pii] (2008).

114 van der Worp, H. B., Sena, E. S., Donnan, G. A., Howells, D. W. & Macleod, M. R. Hypothermia in animal models of acute ischaemic stroke: a systematic review and meta-analysis. *Brain* **130**, 3063-3074, doi:awm083 [pii] 10.1093/brain/awm083 (2007).

115 Clark, D. L., Penner, M., Orellana-Jordan, I. M. & Colbourne, F. Comparison of 12, 24 and 48 h of systemic hypothermia on outcome after permanent focal ischemia in rat. *Exp Neurol* **212**, 386-392, doi:10.1016/j.expneurol.2008.04.016 S0014-4886(08)00169-6 [pii] (2008).

116 Corbett, D., Hamilton, M. & Colbourne, F. Persistent neuroprotection with prolonged postischemic hypothermia in adult rats subjected to transient middle cerebral artery

occlusion. *Exp Neurol* **163**, 200-206, doi:10.1006/exnr.2000.7369 S0014-4886(00)97369-2 [pii] (2000).

117 Markarian, G. Z., Lee, J. H., Stein, D. J. & Hong, S. C. Mild hypothermia: therapeutic window after experimental cerebral ischemia. *Neurosurgery* **38**, 542-550; discussion 551 (1996).

118 Geurts, M., Macleod, M. R., Kollmar, R., Kremer, P. H. & van der Worp, H. B. Therapeutic Hypothermia and the Risk of Infection: A Systematic Review and Meta-Analysis. *Crit Care Med*, doi:10.1097/CCM.0b013e3182a276e8 (2013).

119 Stockmann, H., Krannich, A., Schroeder, T. & Storm, C. Therapeutic temperature management after cardiac arrest and the risk of bleeding: Systematic review and meta-analysis. *Resuscitation*, doi:S0300-9572(14)00683-2 [pii] 10.1016/j.resuscitation.2014.07.018 (2014).

120 Lakhan, S. E. & Pamplona, F. Application of mild therapeutic hypothermia on stroke: a systematic review and meta-analysis. *Stroke Res Treat* **2012**, 295906, doi:10.1155/2012/295906 (2012).

121 Georgiou, A. P. & Manara, A. R. Role of therapeutic hypothermia in improving outcome after traumatic brain injury: a systematic review. *Br J Anaesth* **110**, 357-367, doi:10.1093/bja/aes500 aes500 [pii] (2013).

122 Polderman, K. H. Mechanisms of action, physiological effects, and complications of hypothermia. *Crit Care Med* **37**, S186-202, doi:10.1097/CCM.0b013e3181aa5241 00003246-200907001-00002 [pii] (2009).

123 Hemmen, T. M. *et al.* Intravenous thrombolysis plus hypothermia for acute treatment of ischemic stroke (ICTuS-L): final results. *Stroke* **41**, 2265-2270, doi:10.1161/STROKEAHA.110.592295 STROKEAHA.110.592295 [pii] (2010).

124 Jalan, R., SW, O. D., Deutz, N. E., Lee, A. & Hayes, P. C. Moderate hypothermia for uncontrolled intracranial hypertension in acute liver failure. *Lancet* **354**, 1164-1168, doi:S0140673698124406 [pii] (1999).

125 Tokutomi, T. *et al.* Optimal temperature for the management of severe traumatic brain injury: effect of hypothermia on intracranial pressure, systemic and intracranial hemodynamics, and metabolism. *Neurosurgery* **52**, 102-111; discussion 111-102 (2003).

126 Tokutomi, T. *et al.* Effect of 35 degrees C hypothermia on intracranial pressure and clinical outcome in patients with severe traumatic brain injury. *J Trauma* **66**, 166-173, doi:10.1097/TA.0b013e318157dbec 00005373-200901000-00021 [pii] (2009).

127 Polderman, K. H., Tjong Tjin Joe, R., Peerdeman, S. M., Vandertop, W. P. & Girbes, A. R. Effects of therapeutic hypothermia on intracranial pressure and outcome in patients with severe head injury. *Intensive Care Med* **28**, 1563-1573, doi:10.1007/s00134-002-1511-3 (2002).

128 Metz, C. *et al.* Moderate hypothermia in patients with severe head injury: cerebral and extracerebral effects. *J Neurosurg* **85**, 533-541, doi:10.3171/jns.1996.85.4.0533 (1996).

129 Berger, C., Xia, F., Kohrmann, M. & Schwab, S. Hypothermia in acute stroke--slow versus fast rewarming an experimental study in rats. *Exp Neurol* **204**, 131-137, doi:S0014-4886(06)00587-5 [pii] 10.1016/j.expneurol.2006.10.002 (2007).

130 Hatashita, S. & Hoff, J. T. Role of a hydrostatic pressure gradient in the formation of early ischemic brain edema. *J Cereb Blood Flow Metab* **6**, 546-552 (1986).

131 Howells, D. W. *et al.* Different strokes for different folks: the rich diversity of animal models of focal cerebral ischemia. *J Cereb Blood Flow Metab* **30**, 1412-1431, doi:10.1038/jcbfm.2010.66 jcbfm201066 [pii] (2010).

132 Oliff, H. S., Weber, E., Eilon, G. & Marek, P. The role of strain/vendor differences on the outcome of focal ischemia induced by intraluminal middle cerebral artery occlusion in the rat. *Brain Res* **675**, 20-26, doi:0006-8993(95)00033-M [pii] (1995).

133 Oliff, H. S., Weber, E., Miyazaki, B. & Marek, P. Infarct volume varies with rat strain and vendor in focal cerebral ischemia induced by transcranial middle cerebral artery occlusion. *Brain Res* **699**, 329-331, doi:0006-8993(95)01045-W [pii] (1995).

134 McLeod, D. *et al.* Perfusion computed tomography thresholds defining ischaemic penumbra and infarct core: studies in a rat stroke model. *International Journal of Stroke* **(Accepted for publication, 29 April 2013)** (2013).

135 Andrews, B. T., Levy, M., McIntosh, T. K. & Pitts, L. H. An epidural intracranial pressure monitor for experimental use in the rat. *Neurol Res* **10**, 123-126 (1988).

136 Barth, K. N., Onesti, S. T., Krauss, W. E. & Solomon, R. A. A simple and reliable technique to monitor intracranial pressure in the rat: technical note. *Neurosurgery* **30**, 138-140 (1992).

137 Jallo, J. *et al.* A chronic model to simultaneously measure intracranial pressure, cerebral blood flow, and study the pial microvasculature. *J Neurosci Methods* **75**, 155-160, doi:S0165-0270(97)00064-2 [pii] (1997).

138 Kusaka, G., Calvert, J. W., Smelley, C., Nanda, A. & Zhang, J. H. New lumbar method for monitoring cerebrospinal fluid pressure in rats. *J Neurosci Methods* **135**, 121-127, doi:10.1016/j.jneumeth.2003.12.013 S0165027003004242 [pii] (2004).

139 Mandell, E. C. & Zimmermann, E. Continuous measurement of cerebrospinal fluid pressure in unrestrained rats. *Physiol Behav* **24**, 399-402, doi:0031-9384(80)90105-5 [pii] (1980).

140 Morimoto, Y., Warner, D. S. & Pearlstein, R. D. Acute changes in intracranial pressure and pressure-volume index after forebrain ischemia in normoglycemic and hyperglycemic rats. *Stroke* **27**, 1405-1409; discussion 1410 (1996).

141 Shahrokhi, N., Khaksari, M., Soltani, Z., Mahmoodi, M. & Nakhaee, N. Effect of sex steroid hormones on brain edema, intracranial pressure, and neurologic outcomes after traumatic brain injury. *Can J Physiol Pharmacol* **88**, 414-421, doi:10.1139/y09-126 y09-126 [pii] (2010).

142 Uldall, M. *et al.* A novel method for long-term monitoring of intracranial pressure in rats. *J Neurosci Methods* **227**, 1-9, doi:10.1016/j.jneumeth.2014.01.036 S0165-0270(14)00054-5 [pii] (2014).

143 Jiang, J. & Tyssebotn, I. Measurement of cerebrospinal fluid pressure in conscious rats. *Undersea Hyperb Med* **24**, 39-43 (1997).

144 Goren, S., Kahveci, N., Alkan, T., Goren, B. & Korfali, E. The effects of sevoflurane and isoflurane on intracranial pressure and cerebral perfusion pressure after diffuse brain injury in rats. *J Neurosurg Anesthesiol* **13**, 113-119 (2001).

145 Jennische, E. *et al.* The peptide AF-16 abolishes sickness and death at experimental encephalitis by reducing increase of intracranial pressure. *Brain Res* **1227**, 189-197, doi:10.1016/j.brainres.2008.05.083 S0006-8993(08)01362-0 [pii] (2008).

146 Hiploylee, C. & Colbourne, F. Intracranial pressure measured in freely moving rats for days after intracerebral hemorrhage. *Exp Neurol* **255**, 49-55, doi:10.1016/j.expneurol.2014.02.017 S0014-4886(14)00062-4 [pii] (2014).

147 Dohmen, C. *et al.* Spreading depolarizations occur in human ischemic stroke with high incidence. *Ann Neurol* **63**, 720-728, doi:10.1002/ana.21390 (2008).

148 Lloyd, G. E. R. *Hippocratic writings*. [New] ed edn, (Penguin, 1978).

149 Kammersgaard, L. P. *et al.* Feasibility and safety of inducing modest hypothermia in awake patients with acute stroke through surface cooling: A case-control study: the Copenhagen Stroke Study. *Stroke* **31**, 2251-2256 (2000).

150 Sasaki, M., Honmou, O., Radtke, C. & Kocsis, J. D. Development of a middle cerebral artery occlusion model in the nonhuman primate and a safety study of i.v. infusion of human mesenchymal stem cells. *PLoS One* **6**, e26577, doi:10.1371/journal.pone.0026577 PONE-D-11-12121 [pii] (2011).

151 de Crespigny, A. J. *et al.* Acute studies of a new primate model of reversible middle cerebral artery occlusion. *J Stroke Cerebrovasc Dis* **14**, 80-87, doi:S1052-3057(04)00183-1 [pii] 10.1016/j.jstrokecerebrovasdis.2004.12.005 (2005).

152 Christoforidis, G. A. *et al.* An endovascular canine middle cerebral artery occlusion model for the study of leptomeningeal collateral recruitment. *Invest Radiol* **46**, 34-40, doi:10.1097/RLI.0b013e3181f0cbc7 (2011).

153 Kang, B. T. *et al.* Canine model of ischemic stroke with permanent middle cerebral artery occlusion: clinical and histopathological findings. *J Vet Sci* **8**, 369-376, doi:200712369 [pii] (2007).

154 Wells, A. J. *et al.* A surgical model of permanent and transient middle cerebral artery stroke in the sheep. *PLoS One* **7**, e42157, doi:10.1371/journal.pone.0042157 PONE-D-11-08927 [pii] (2012).

155 Boltze, J. *et al.* Permanent middle cerebral artery occlusion in sheep: a novel large animal model of focal cerebral ischemia. *J Cereb Blood Flow Metab* **28**, 1951-1964, doi:10.1038/jcbfm.2008.89 jcbfm200889 [pii] (2008).

156 Schmidt, B. *et al.* Adaptive noninvasive assessment of intracranial pressure and cerebral autoregulation. *Stroke* **34**, 84-89 (2003).

157 Shimbles, S., Dodd, C., Banister, K., Mendelow, A. D. & Chambers, I. R. Clinical comparison of tympanic membrane displacement with invasive intracranial pressure measurements. *Physiol Meas* **26**, 1085-1092, doi:S0967-3334(05)02360-9 [pii] 10.1088/0967-3334/26/6/017 (2005).

158 Querfurth, H. W. *et al.* Ophthalmodynamometry for ICP prediction and pilot test on Mt. Everest. *BMC Neurol* **10**, 106, doi:10.1186/1471-2377-10-106 1471-2377-10-106 [pii] (2010).

159 Firsching, R. *et al.* Noninvasive assessment of intracranial pressure with venous ophthalmodynamometry. Clinical article. *J Neurosurg* **115**, 371-374, doi:10.3171/2011.3.JNS101275 (2011).

160 Frumin, E. *et al.* Prospective analysis of single operator sonographic optic nerve sheath diameter measurement for diagnosis of elevated intracranial pressure. *West J Emerg Med* **15**, 217-220, doi:10.5811/westjem.2013.9.16191 wjem-15-217 [pii] (2014).

161 Ragauskas, A. *et al.* Improved diagnostic value of a TCD-based non-invasive ICP measurement method compared with the sonographic ONSD method for detecting elevated intracranial pressure. *Neurol Res* **36**, 607-614, doi:10.1179/1743132813Y.0000000308 (2014).

APPENDIX A-1

PUBLICATION 5

Murtha L, Yang Q, Parsons M, Levi C, Beard D, Spratt N, McLeod D. Cerebrospinal fluid is drained primarily via the spinal canal and olfactory route in young and aged spontaneously hypertensive rats. *Fluids Barriers CNS*. 11:12, doi:10.1186/2045-8118-11-12. (2014).

Murtha et al. Fluids and Barriers of the CNS 2014, 11:12
http://www.fluidsbarrierscns.com/content/11/1/12

FLUIDS AND BARRIERS OF THE CNS

RESEARCH Open Access

Cerebrospinal fluid is drained primarily via the spinal canal and olfactory route in young and aged spontaneously hypertensive rats

Lucy A Murtha[1], Qing Yang[2], Mark W Parsons[3], Christopher R Levi[3], Daniel J Beard[1], Neil J Spratt[1,3†] and Damian D McLeod[1*†]

Abstract

Background: Many aspects of CSF dynamics are poorly understood due to the difficulties involved in quantification and visualization. In particular, there is debate surrounding the route of CSF drainage. Our aim was to quantify CSF flow, volume, and drainage route dynamics *in vivo* in young and aged spontaneously hypertensive rats (SHR) using a novel contrast-enhanced computed tomography (CT) method.

Methods: ICP was recorded in young (2–5 months) and aged (16 months) SHR. Contrast was administered into the lateral ventricles bilaterally and sequential CT imaging was used to visualize the entire intracranial CSF system and CSF drainage routes. A customized contrast decay software module was used to quantify CSF flow at multiple locations.

Results: ICP was significantly higher in aged rats than in young rats (11.52 ± 2.36 mmHg, versus 7.04 ± 2.89 mmHg, $p = 0.03$). Contrast was observed throughout the entire intracranial CSF system and was seen to enter the spinal canal and cross the cribriform plate into the olfactory mucosa within 9.1 ± 6.1 and 22.2 ± 7.1 minutes, respectively. No contrast was observed adjacent to the sagittal sinus. There were no significant differences between young and aged rats in either contrast distribution times or CSF flow rates. Mean flow rates (combined young and aged) were 3.0 ± 1.5 μL/min at the cerebral aqueduct; 3.5 ± 1.4 μL/min at the 3rd ventricle; and 2.8 ± 0.9 μL/min at the 4th ventricle. Intracranial CSF volumes (and as percentage total brain volume) were 204 ± 97 μL (8.8 ± 4.3%) in the young and 275 ± 35 μL (10.8 ± 1.9%) in the aged animals (NS).

Conclusions: We have demonstrated a contrast-enhanced CT technique for measuring and visualising CSF dynamics *in vivo*. These results indicate substantial drainage of CSF via spinal and olfactory routes, but there was little evidence of drainage via sagittal sinus arachnoid granulations in either young or aged animals. The data suggests that spinal and olfactory routes are the primary routes of CSF drainage and that sagittal sinus arachnoid granulations play a minor role, even in aged rats with higher ICP.

Keywords: Computed tomography, Cerebrospinal fluid dynamics, Contrast, Spontaneously hypertensive rat, Intracranial pressure (ICP), Age, CSF, SHR

* Correspondence: Damian.Mcleod@newcastle.edu.au
†Equal contributors
[1]University of Newcastle and Hunter Medical Research Institute, University of Newcastle: School of Biomedical Sciences & Pharmacy, Medical Sciences Building, Callaghan, NSW 2308, Australia
Full list of author information is available at the end of the article

Background

Cerebrospinal fluid (CSF) dynamics are thought to be altered in many pathological conditions including hydrocephalus [1,2], idiopathic intracranial hypertension [3,4], intracerebral haemorrhage [5], subarachnoid haemorrhage [6,7], large hemispheric stroke [8,9], traumatic brain injury [10], and in the aging brain [11,12]. However, relatively little is known about the exact mechanisms of changes in CSF dynamics and drainage in these conditions due to difficulties in quantification.

The role and location of CSF drainage has been studied in both animals and humans. Traditional interpretation has been that most CSF drains into the venous sinuses via arachnoid granulations [13-15]. The primary site of CSF reabsorption, however, has become a contentious issue over the last decade. The importance of the olfactory perineural pathways and the cervical lymphatics [16-19] in reabsorbing CSF has been studied in several species, including humans. Postmortem lymphatic vascular casting [20-22] and radioactive albumin clearance methods [17,23-25] have demonstrated the major contribution of these pathways in CSF drainage. Furthermore, physiological studies by Johnston's group, suggested that the arachnoid granulations may only come into play when intracranial pressure is elevated and that lymphatic drainage routes may play a major role [26,27], especially in neonates where arachnoid granulations are sparse [28]. Both human and animal studies indicate that the spinal route, either via spinal arachnoid granulations or via lymphatics around spinal nerve root dural sheaths may also be important [29-35]. These lymphatic routes may have important immunological significance [19].

To investigate CSF dynamics and drainage within the entire rat brain we developed a novel contrast-enhanced computed tomography (CT) technique to image the rat CSF system in three-dimensions. One unique feature of this technique is that the dynamic nature of CSF drainage can be observed *in vivo*. We chose to compare young and aged spontaneously hypertensive rats (SHR) because their cerebral ventricular volume is thought to increase with age [36,37], which, in addition to the hypertension, may affect CSF dynamics. In addition, this effect may also influence physiological variables such as intracranial pressure, for example, elevated ICP is seen in some hydrocephalus patients [1,2]. Using our novel contrast-enhanced CT method, we hypothesized that the aged SHRs would have altered CSF dynamics and drainage and a higher baseline ICP when compared to the young SHRs.

Methods

All animal experiments were conducted in accordance with the Australian Code of Practice for the Care and Use of Animals for Scientific Purposes and were approved by The University of Newcastle Animal Care and Ethics Committee. Experiments were performed on two cohorts of male spontaneously hypertensive rats (SHR) (Animal Resources Centre, Western Australia). One group weighed 200-360 g, aged 2–5 months (n = 5); the other group weighed 360-400 g, aged 16 months (n = 5). Due to ethical constraints, we calculated the sample size required to detect a difference in baseline ICP between two different rat strains (Wistar and Long Evans; data previously published [38]). Using an alpha of 0.05 and Power of 0.80, a sample size of 5 animals per group was required to detect a 4.2 mmHg difference between baseline ICP in the two rat strains.

Surgery and physiological monitoring

Animals were anaesthetised with isoflurane (5% induction, 2% maintenance) in 50:50%, N_2:O_2 via a facemask. It has previously been reported in dogs that isoflurane causes no significant change in the rate of CSF production [39]. Respiratory rate was regularly monitored and core temperature was maintained at 37°C via a thermocouple rectal probe and warming plate for the duration of surgical anaesthesia. Incision sites were shaved, cleaned and injected subcutaneously with 2 mg/kg 0.05% Bupivacaine (Pfizer, Australia). To measure arterial blood pressure under anaesthetic, a fibreoptic microcatheter (SAMBA Sensors, Sweden) was briefly inserted into the saphenous branch of the femoral artery, and a steady state baseline arterial blood pressure trace was recorded.

Intracranial pressure (ICP) was recorded prior to scanning using a SAMBA microcatheter as previously described [40] with minor changes. Briefly, animals were placed in the ear bars of a custom-built CT-compatible stereotaxic frame. Hollow poly-ether-ether-ketone (PEEK) screws (Solid Spot LLC, Santa Clara, CA, USA) of 2 mm in diameter × 5 mm in length were inserted bilaterally 0.3 mm caudal and 1.5 mm lateral to Bregma. The ICP probe was inserted into the right screw and an airtight seal made by surrounding both screws in a biocompatiable caulking material (Silagum, DMG Dental, Hamburg, Germany). The probe was removed prior to scanning.

Computed tomography (CT) imaging

Following baseline arterial pressure and ICP measurement, animals remained on the same base plate and stereotaxic frame, which was positioned on the CT scanner table. All imaging was performed using a 64-slice clinical CT scanner (Siemens, Erlangen, Germany) [41,42]. The CSF imaging protocol was developed specifically for the current study. Each CT-CSF imaging sequence used 0.6 mm slice thickness with coronal plane image acquisition, and a total of 90 slices captured from the rat nose to the cervical vertebrae (C2). Two 1 ml syringes and two PE-10 intraventricular catheters were then preloaded with

a 1:4 dilution of Ultravist 300 mg/mL (Bayer HealthCare Pharmaceuticals Inc.) in 0.9% saline. This dilution was chosen to reduce the viscosity and make it closer to that of CSF. Care was taken to ensure that no air bubbles were present within the catheters. The catheter tips were inserted 3.5 mm below the skull into each lateral ventricle via the bilateral screws used for ICP monitoring, and a head CT scan performed (baseline scan) to ensure that catheter tips were positioned within each lateral ventricle. Using an automated syringe driver (Harvard Apparatus, Pump 11 Elite, MA, USA), contrast was injected into each ventricle at 2 μL/min for 10 minutes, with a CT scan performed every minute from the start of infusion. The infusion rate of 2 μL/min was chosen to reduce the possibility of the infusion affecting the CSF production (rodent CSF production rate previously reported as 2.66-2.84 μL/min [43]). Following the cessation of infusion, serial CT scans were performed every 5 minutes for 60 minutes (Figure 1, an additional movie file shows this in more detail [see Additional file 1]).

Processing CT images

For each animal, serial CT images were loaded into MiStar software (Apollo Medical Imaging Technology Pty Ltd, Melbourne, Australia). Motion correction was performed, and the resulting images were subtracted from the baseline non-contrast image.

3D reconstruction of CT images: rat CSF system

A representative 3D reconstruction of the rat CSF system was created by generating a Maximum Intensity Projection (MIP).The MIP was loaded into the MiStar fusion 3D render module. Thresholds were applied to the 3D render to highlight the CSF system.

Visual inspection of contrast time-course throughout CSF system

The time taken for injected contrast to reach specific anatomical landmarks within the CSF system was quantified in each animal. The anatomical landmarks included the cerebral aqueduct, 3rd ventricle, 4th ventricle, spinal canal, basal cisterns and cribriform plate. The contrast window range was set to 0–250 Hounsfield Units (HU) for each animal sequence to prevent the false detection of signal noise at each image time-point. The time taken for the contrast to reach each landmark was calculated by analysing each sequential image.

CSF flow rate calculations

Contrast-enhanced CT images were processed using the MiStar software decay module specifically written for rat imaging. CSF flow rate measured at the cerebral aqueduct was used to estimate CSF production. Flow rates were also calculated elsewhere within the CSF system. A small region-of-interest (ROI) with 6 voxels was positioned within the centre of the aqueduct on the 10 minute time-point scan (post-infusion). The total change in Hounsfield Units for voxels within the ROI was plotted over time, and an exponential decay curve was fitted to the first five decay data points. The exponential decay rate constant is directly proportional to flow within the ROI. This principle was applied to each voxel to generate the Decay Rate Map, measured in ml/min/100 L (which was then converted to μl/min/100 ml). The ROI was then co-registered with the Decay Rate Map to obtain the flow value. Flow was converted into μl/min by multiplication with volume (slice thickness × area of ROI). The process was repeated (with the same fixed ROI) at the 3rd ventricle and 4th ventricle of each animal.

Brain and intracranial CSF volume calculation

Twenty five 0.6 mm coronal CT slices were analysed slice-by-slice to calculate brain and CSF volume. On each slice, a threshold of 100 HU was set and ROI software tools were used to define the area of total brain tissue (using baseline scans) or contrast-enhanced CSF within the cranium. On each slice, the volume was calculated as slice thickness × area of ROI. The combined sum of the ROI volumes was calculated.

Statistics

Statistical tests were performed using GraphPad Prism Version 6 for Windows (GraphPad Software, USA). Two-tailed Student's t-test was used to compare differences in CSF production rate, and CSF volumes between young and aged groups. Significance was accepted at the $p < 0.05$ level. T-tests are also reported for physiological variables for illustrative purposes, with p-values uncorrected for use of multiple comparisons. Unless otherwise stated, data is expressed as mean ± standard deviation (±SD).

Results

Physiological variables

Arterial blood pressure (systolic/diastolic) was measured in 3 young animals and 5 aged animals. Mean arterial blood pressure was lower in the young versus the aged animals (94 ± 32 mmHg vs. 160 ± 22 mmHg, $p = 0.01$). Intracranial pressure (ICP) was measured in all animals and traces revealed consistent pulse and respiratory waveforms. A significantly higher ICP was found in aged rats, 11.52 ± 2.36 mmHg, versus 7.04 ± 2.89 mmHg in the younger animals, $p = 0.03$. Cerebral perfusion pressure (mean arterial blood pressure - intracranial pressure) was significantly lower in the young versus the aged animals (86 ± 32 mmHg vs. 148 ± 20 mmHg, $p = 0.02$).

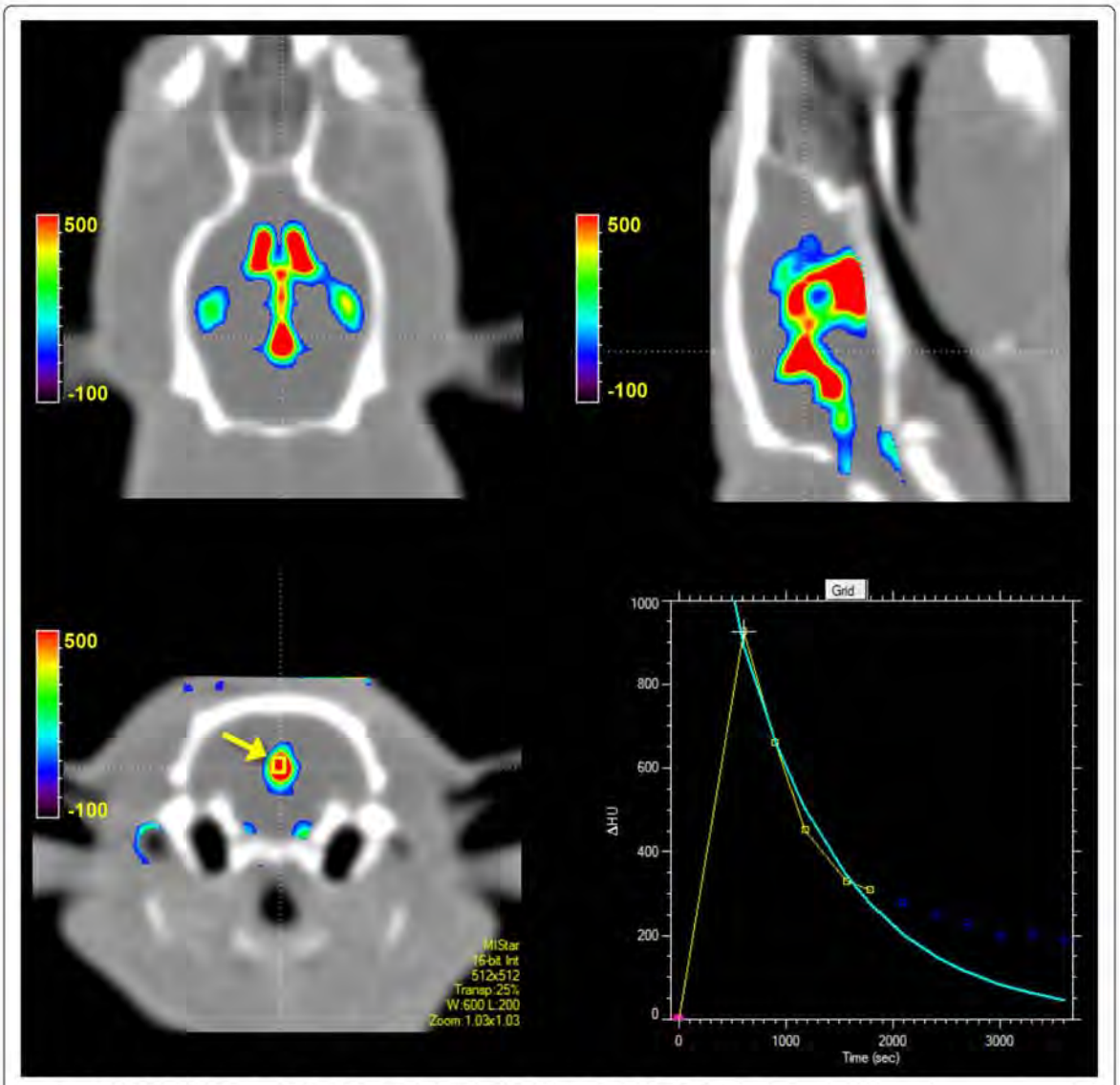

Figure 1 Calculating cerebrospinal fluid flow through the cerebral aqueduct of the rat. Radio-opaque contrast (20 μl) was simultaneously injected into each lateral ventricle at 2 μl/min for 10 min while plain CT images (0.6 mm slice thickness) were taken over 60 minutes. A small region-of-interest (ROI) (yellow box, arrow) was positioned within the centre of the aqueduct and the decay rate used to generate flow maps. An additional movie file shows this in more detail [see Additional file 1].

Cerebrospinal fluid drainage pathways and time course

CSF was observed to drain into the spinal canal (subarachnoid space) and via the olfactory pathway (through the cribriform plate), the optic nerves, and the cervical lymph nodes in all animals (Figure 2, an additional movie file shows this in more detail [see Additional file 2]). Contrast-enhanced CSF was observed at the cerebral aqueduct 3.2 ± 0.8 minutes post-injection in both cohorts. It was first observed to enter the 3rd ventricle 1.8 ± 0.4 minutes and 1.6 ± 0.5 minutes post-injection in the young and aged respectively, the 4th ventricle at 4.4 ± 2.2 minutes and 3.8 ± 0.8 minutes post-injection, the spinal canal at 11.5 ± 9.1 minutes and 7.2 ± 0.8 minutes post-injection, and the basal cisterns at 18.5 ± 6.8 minutes and 14.0 ± 4.2 minutes post-injection in the young and the aged respectively (Figure 3). Contrast could be observed leaving the cranial vault at the cribriform plate 23.8 ± 6.3 minutes post-injection in the young and 21 ± 8.2 minutes in the aged (Figure 3). No contrast-enhanced CSF was observed at the sagittal sinus [Additional file 1].

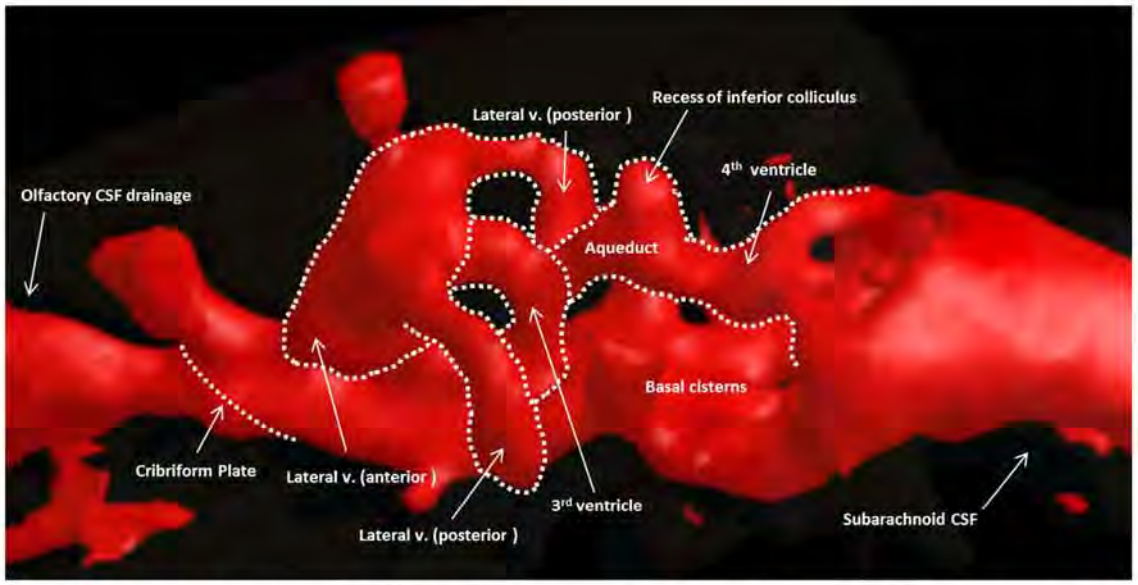

Figure 2 Cerebrospinal fluid (CSF) system in a rat imaged with contrast-enhanced computed tomography (CT). Images show a 3D render reconstruction of CT images after 20 μL of radio-opaque contrast was injected into each lateral ventricle via cannulae guided through hollow screws inserted into the skull. Anatomical landmarks of the CSF system in the rat are based on a stereotaxic rat atlas [61]. Basal cisterns are not depicted in the rat atlas, but their location at the base of the brain is indicated by presence of contrast enhanced CSF in this location. An additional movie file shows this in more detail [see Additional file 2].

Cerebrospinal fluid production and flow rates and total intracranial CSF volume

CSF flow was able to be quantified at multiple sites within the ventricular system, but flow quantification in the extraventricular locations was not possible due to respiratory motion artifact (spinal canal) and contrast dilution, resulting in reduced signal-to-noise ratio and partial volume averaging error caused by the extensive surface area of each drainage route. CSF production rates, as measured by CSF flow rate at the cerebral aqueduct, were 3.14 ± 2.1 μL/min and 2.79 ± 0.57 μL/min in the young and the aged, respectively. CSF flow rates were 3.74 ± 1.93 μL/min and 3.19 ± 0.70 μL/min at the 3rd ventricle and 2.89 ± 0.21 μL/min and 2.70 ± 1.29 μL/min at the 4th ventricle (Figure 4A- 4C). The total intracranial CSF volume was 204 ± 97 μL in the young and 275 ± 35 μL in the aged cohort (Figure 4D). None of these values differed significantly between the young vs. aged cohorts.

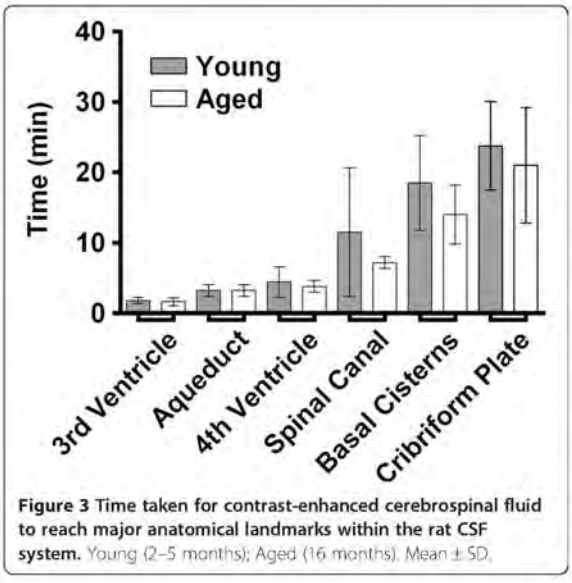

Figure 3 Time taken for contrast-enhanced cerebrospinal fluid to reach major anatomical landmarks within the rat CSF system. Young (2–5 months); Aged (16 months). Mean ± SD.

Brain volume

Brain volume was 2157 ± 314 mm^3 and 2366 ± 233 mm^3 in the young and aged rats, respectively (Figure 5). CSF volumes (and as percentage of brain volume) were 204 ± 97 μL (8.8 ± 4.3%) in the young and 275 ± 35 μL (10.8 ± 1.9%) in the aged animals. These values were not significantly different.

Discussion

This study used young and aged SHRs to demonstrate a new technique for the measurement of CSF flow, volume and drainage *in vivo*. The results of this study suggest that sagittal sinus arachnoid granulations are not the primary route of CSF drainage and that CSF is primarily

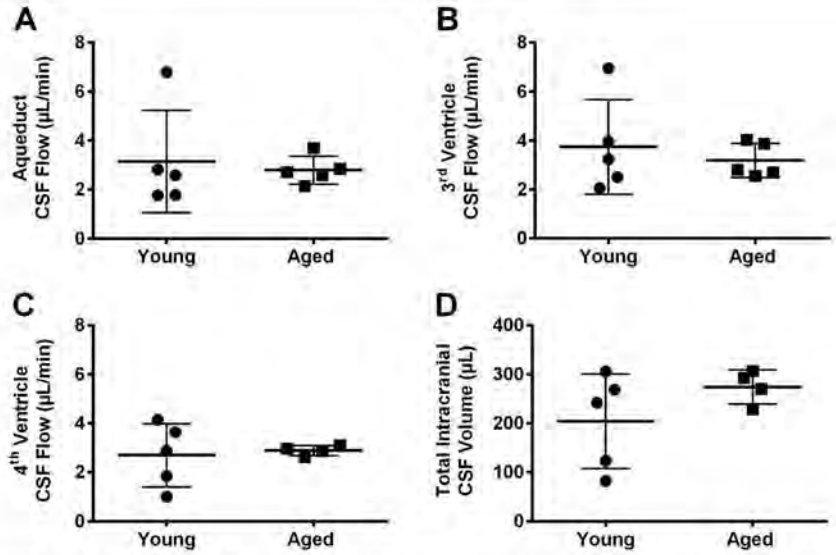

Figure 4 Cerebrospinal fluid (CSF) dynamics in the rat. (A) Flow rate through the cerebral aqueduct; **(B)** Flow rate through the 3rd ventricle; **(C)** Flow rate through the 4th ventricle; **(D)** Total intracranial CSF volume, in young (2–5 months) versus aged (16 months) spontaneously hypertensive rats. Data presented as individual data points with mean ± SD.

absorbed via the spinal and olfactory routes. The time taken for contrast-enhanced CSF to reach each drainage route did not differ between the young and aged animals. Our novel CT method also allowed for measurement of CSF flow and volume and found that there was little difference between young and aged animals, despite a higher ICP in the aged animals. This method provides an alternative avenue for the investigation of the pathophysiological perturbations occurring in disorders of CSF regulation and abnormal intracranial pressure.

There is increasing recognition of the importance of altered CSF and brain interstitial fluid dynamics with age, not only in conditions such as normal pressure hydrocephalus but also in dementias such as Alzheimer's disease [44,45]. Despite this, most CSF-related research occurs in young animals. In the current study we investigated CSF dynamics in an aged population of SHRs, since this strain is known to develop hypertension, ventriculomegaly and cerebral volume loss with age [36,37]. We found little difference in the absolute CSF flow rates or total brain volume between young (2–5 months) and aged (16 months) rats. These data are similar to findings in a previous study of normotensive rats (without ventriculomegaly) aged from 3–30 months. Chiu et al. found that peak CSF production occurs at 10 months before steadily decreasing over time to almost baseline values [43]. Furthermore, the values they reported in 12–20 month rats ranged from 2.66-2.84 µL/min, which were comparable to our reported values in 16 month aged rats and to previously reported values in 3–4 months old rats in other studies [46,47]. It is also interesting to note that the CSF flow rates, when measured at different anatomical locations within the CSF ventricular system, did not vary greatly. The lack of a significant difference in *in vivo* CSF volumes between young and aged SHRs is inconsistent with previous *in vitro* studies, and most likely due to a lack of statistical power to detect a difference in this variable. This was contributed to by small animal numbers and in particular by the significant between-animal variability in the younger cohort. The point estimate of a 26% difference is in keeping with previous published data [36,37]. Additionally, it may be that changes would be more apparent in 'elderly' (≈2 years) animals, than in at 16 months of age. This age was chosen to avoid the

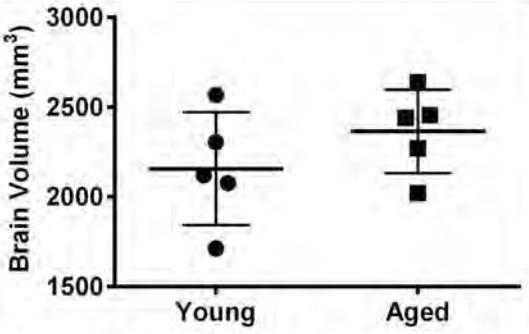

Figure 5 Total brain volume calculated from baseline non-contrast images. Young (2–5 months); Aged (16 months). Mean ± SD.

tumours and mortality that increase beyond 18 months in this strain. Our data also demonstrated a significantly higher intracranial pressure (ICP) and cerebral perfusion pressure (CPP) in the aged rats when compared to the young. This is consistent with findings in humans [48,49] and in other rat strains [50]. Additionally, the greater variability in CPP in the young animals may have contributed to the greater variance in CSF data, i.e. there was a greater percentage of variance (relative to the mean) in mean arterial pressure, and in ICP, in the young vs. aged. It is plausible that greater variance in CPP resulted in greater variance in CSF flow and drainage parameters, as changes in CPP may affect CSF production and drainage.

Although the ICP was higher in aged animals, we could not see any contrast adjacent to or filling the sagittal sinus to indicate drainage of the CSF via arachnoid granulations, even at the later time points. There was, however, clear evidence of passage of contrast into the spinal canal, olfactory cavity, along the ophthalmic nerves and into cervical lymph nodes. Our findings support recent studies that the primary route of CSF drainage in most mammalian species is via perineural sheaths. In anatomical studies using a coloured tracer and anatomical dissection, CSF drainage into nasal lymphatics via the olfactory nerves and cribriform plate has been demonstrated in sheep, pigs, rabbits, rats, mice and monkeys [16,17,20-25]. Additionally presence of this route has been shown in human cadavers [20]. Many studies have also demonstrated spinal lymphatic CSF drainage using tracers in several mammalian species including humans [22,23,26,35,51]. It was calculated that the rate of spinal CSF absorption was between 38–76% of CSF production in healthy individuals (higher during activity) [35]. At least in the sheep, the venous sinus arachnoid granulation pathway of CSF absorption appears to be a secondary pathway only recruited at high intracranial pressures, for example after a neurological injury [17,28].

The calculation of CSF volume is technically challenging and many techniques have been tried, with varying success. Values obtained in this study correspond well to some published data in rats using quite different techniques, including volumes of 233–240 μL in young SHRs using the ventriculo-cisternal dilution method [46,47] and volumes from 275–441 μL in Fischer 344/BN rats using magnetic resonance imaging [43]. However, some published studies report much higher volumes. Lai et al. (1983) reported a mean CSF volume of 580 μL in rats using the formula 'CSF volume = CSF formation rate/CSF turnover rate' [52]. They assumed that the CSF turnover rate was constant amongst species [53], and used the human CSF turnover rate of 0.38% per minute (obtained using ventriculo-lumbar perfusion method from 12 children with subacute sclerosing panencephalitis and pontine glioma) [54], to calculate CSF volume. We are not sure that this assumption is well justified. However, despite these potential limitations, the rat CSF volume and turnover rate from that paper appear to have become the accepted values in reviews of the field, perhaps due to the paucity of other available data [55-57].

Our novel CT method provides several possible advantages, and some limitations, when compared with other techniques such as the ventriculo-cisternal dilution and post-mortem dye-tracer methods. First among these is that it does not require an intracisternal draining catheter, with potential resultant effects on ICP and possibly on CSF production, if homeostatic mechanisms are evoked. Secondly, the ability to image the entire CSF system simultaneously and sequentially gives a more complete understanding of the dynamics of CSF flow and drainage. We were able to monitor the major physiological parameters thought to influence CSF production rate, that is, ICP [58], blood pressure [59], and temperature [60]. Additionally, flow rates, whole brain volume, and CSF volume calculations were obtained from the same study. Some unavoidable limitations also exist with the CT method, and particular points of the analysis require great care. In particular, partial volume averaging effects are a known potential problem when measuring values from a very small structure such as the cerebral aqueduct. Great care must be taken to identify the midpoint of the region of contrast enhancement for placement of a small region-of-interest. An additional limitation is that although we could observe and quantify the time taken for contrast-enhanced CSF to reach the drainage pathways *in vivo*, we have been unable to reliably quantify the volume of CSF draining via these routes.

Conclusions

We have provided *in vivo* data using CT imaging of CSF distribution over time, which indicates that the primary route of CSF drainage in young and aged rats is via the spinal and olfactory lymphatics, and that drainage into the sagittal sinus arachnoid granulations plays at most a minor role. The CT technique we developed provides an alternative to ventriculo-cisternal dilution methods for measurement of CSF flow through the cerebral aqueduct, the widely accepted surrogate measure for CSF production. It avoids the need to puncture the cisterna magna and permits visualisation and timing of CSF distribution and drainage, quantification of CSF flow elsewhere within the ventricular system and measurement of total brain and intracranial CSF volumes. Interestingly, this study of young and aged SHRs suggest that CSF production rates and volumes are quite similar, and do not change dramatically with age. The information gathered using our novel contrast-enhanced CT method may provide much needed insight into the CSF dynamics and drainage involved in many neurological diseases.

Additional files

Additional file 1: Contrast-enhanced cerebrospinal fluid flow through the cranium over 60 minutes. Radio-opaque contrast (20 μl) was simultaneously injected into each lateral ventricle at 2 μl/min for 10 min while plain CT images (0.6 mm slice thickness) were taken over 60 minutes. File format: mov.

Additional file 2: 3D render reconstruction of cerebrospinal fluid system of the rat. The computed tomography images of one rat were loaded in MiStar software and subtracted from the baseline non-contrast image. A Maximum Instensity Projection was generation and loaded into the MiStar fusion 3D render module. File format: mov.

Abbreviations

CSF: Cerebrospinal fluid; CT: Computed tomography; HU: Hounsfield Units; ICP: Intracranial pressure; MIP: Maximum Intensity Projection; ROI: Region of interest; SHR: Spontaneously hypertensive rat.

Competing interests

The authors declare that they have no competing interests.

Authors' contributions

LM and DM carried out the surgical and computed tomography components of the study, analysed and interpreted the data, performed statistical analysis and drafted the manuscript. QY designed MiStar software decay module specifically written for this project. DB and NS participated in the design of the study and helped draft the manuscript. DM, NS, LM, MP and CL, conceived the study, and participated in its design and coordination. All authors read and approved the final manuscript.

Authors' information

LM- B. Biomed Sci. (Hons), PhD Candidate (Human Physiology).
QY- PhD (Physics).
MP- PhD, FRACP (Neurology).
CL- MBBS, B Med Sci (Hons), FRACP (Neurology).
DB- B. Biomed Sci. (Hons), PhD Candidate (Human Physiology).
NS- MBBS, PhD, FRACP (Neurology).
DM- PhD (Human Physiology).

Acknowledgements

We would like to thank the radiographers David Buxton and Marc Heaton (Hunter Health Imaging, John Hunter Hospital) for CT imaging assistance and the Faculty of Health Workshop of the University of Newcastle for manufacture of surgical and anesthetic equipment. Dr. Spratt was supported by an Australian National Health & Medical Research Council (NHMRC) Career Development Fellowship (APP1035465). Aspects of this work were supported by the NHMRC (Project Grant APP1033461), Hunter Medical Research Institute and National Stroke Foundation (Australia) research grants.

Author details

[1]University of Newcastle and Hunter Medical Research Institute, University of Newcastle: School of Biomedical Sciences & Pharmacy, Medical Sciences Building, Callaghan, NSW 2308, Australia. [2]Apollo Medical Imaging Technology Pty Ltd, Suite 611, 365 Little Collins Street, Melbourne, Vic 3000, Australia. [3]Hunter New England Local Health District: Department of Neurology, John Hunter Hospital, Locked Bag 1, Hunter Region M.C, NSW 2310, Australia.

Received: 4 April 2014 Accepted: 27 May 2014
Published: 6 June 2014

References

1. Wagshul ME, McAllister JP, Rashid S, Li J, Egnor MR, Walker ML, Yu M, Smith SD, Zhang G, Chen JJ, Benveniste H: **Ventricular dilation and elevated aqueductal pulsations in a new experimental model of communicating hydrocephalus.** *Exp Neurol* 2009, **218**:33–40.
2. Bateman GA: **The pathophysiology of idiopathic normal pressure hydrocephalus: cerebral ischemia or altered venous hemodynamics?** *AJNR Am J Neuroradiol* 2008, **29**:198–203.
3. Preuss M, Hoffmann KT, Reiss-Zimmermann M, Hirsch W, Merkenschlager A, Meixensberger J, Dengl M: **Updated physiology and pathophysiology of CSF circulation–the pulsatile vector theory.** *Childs Nerv Syst* 2013, **29**:1811–1825.
4. Killer HE, Jaggi GP, Flammer J, Miller NR, Huber AR, Mironov A: **Cerebrospinal fluid dynamics between the intracranial and the subarachnoid space of the optic nerve. Is it always bidirectional?** *Brain* 2007, **130**:514–520.
5. Shapira Y, Artru AA, Lam AM: **Changes in the rate of formation and resistance to reabsorption of cerebrospinal fluid during deliberate hypotension induced with adenosine or hemorrhage.** *Anesthesiology* 1992, **76**:432–439.
6. Paradot G, Baledent O, Gondry-Jouet C, Meyer ME, Le Gars D: **[Cerebrospinal fluid flow imaging in the meningeal hemorrhage].** *Neurochirurgie* 2006, **52**:323–329.
7. Brinker T, Seifert V, Stolke D: **Acute changes in the dynamics of the cerebrospinal fluid system during experimental subarachnoid hemorrhage.** *Neurosurgery* 1990, **27**:369–372.
8. Schwab S, Schellinger P, Aschoff A, Albert F, Spranger M, Hacke W: **[Epidural cerebrospinal fluid pressure measurement and therapy of intracranial hypertension in "malignant" middle cerebral artery infarct].** *Nervenarzt* 1996, **67**:659–666.
9. Minnerup J, Wersching H, Ringelstein EB, Heindel W, Niederstadt T, Schilling M, Schabitz WR, Kemmling A: **Prediction of malignant middle cerebral artery infarction using computed tomography-based intracranial volume reserve measurements.** *Stroke* 2011, **42**:3403–3409.
10. Johanson C, Stopa E, Baird A, Sharma H: **Traumatic brain injury and recovery mechanisms: peptide modulation of periventricular neurogenic regions by the choroid plexus-CSF nexus.** *J Neural Transm* 2011, **118**:115–133.
11. Schmid Daners M, Knobloch V, Soellinger M, Boesiger P, Seifert B, Guzzella L, Kurtcuoglu V: **Age-specific characteristics and coupling of cerebral arterial inflow and cerebrospinal fluid dynamics.** *PLoS One* 2012, **7**:e37502.
12. Stoquart-ElSankari S, Baledent O, Gondry-Jouet C, Makki M, Godefroy O, Meyer ME: **Aging effects on cerebral blood and cerebrospinal fluid flows.** *J Cereb Blood Flow Metab* 2007, **27**:1563–1572.
13. Tripathi R: **Tracing the bulk outflow route of cerebrospinal fluid by transmission and scanning electron microscopy.** *Brain Res* 1974, **80**:503–506.
14. Tripathi BJ, Tripathi RC: **Vacuolar transcellular channels as a drainage pathway for cerebrospinal fluid.** *J Physiol* 1974, **239**:195–206.
15. Welch K, Friedman V: **The cerebrospinal fluid valves.** *Brain* 1960, **83**:454–469.
16. Cserr HF, Harling-Berg CJ, Knopf PM: **Drainage of brain extracellular fluid into blood and deep cervical lymph and its immunological significance.** *Brain Pathol* 1992, **2**:269–276.
17. Zakharov A, Papaiconomou C, Koh L, Djenic J, Bozanovic-Sosic R, Johnston M: **Integrating the roles of extracranial lymphatics and intracranial veins in cerebrospinal fluid absorption in sheep.** *Microvasc Res* 2004, **67**:96–104.
18. Kida S, Pantazis A, Weller RO: **CSF drains directly from the subarachnoid space into nasal lymphatics in the rat. Anatomy, histology and immunological significance.** *Neuropathol Appl Neurobiol* 1993, **19**:480–488.
19. Carare RO, Hawkes CA, Weller RO: **Afferent and efferent immunological pathways of the brain. Anatomy, function and failure.** *Brain Behav Immun* 2014, **36**:9–14.
20. Johnston M, Zakharov A, Papaiconomou C, Salmasi G, Armstrong D: **Evidence of connections between cerebrospinal fluid and nasal lymphatic vessels in humans, non-human primates and other mammalian species.** *Cerebrospinal Fluid Res* 2004, **1**:2.
21. Nagra G, Koh L, Zakharov A, Armstrong D, Johnston M: **Quantification of cerebrospinal fluid transport across the cribriform plate into lymphatics in rats.** *Am J Physiol Regul Integr Comp Physiol* 2006, **291**:R1383–R1389.
22. Johnston M, Zakharov A, Koh L, Armstrong D: **Subarachnoid injection of Microfil reveals connections between cerebrospinal fluid and nasal lymphatics in the non-human primate.** *Neuropathol Appl Neurobiol* 2005, **31**:632–640.
23. Boulton M, Young A, Hay J, Armstrong D, Flessner M, Schwartz M, Johnston M: **Drainage of CSF through lymphatic pathways and arachnoid villi in sheep: measurement of 125I-albumin clearance.** *Neuropathol Appl Neurobiol* 1996, **22**:325–333.
24. Boulton M, Flessner M, Armstrong D, Mohamed R, Hay J, Johnston M: **Contribution of extracranial lymphatics and arachnoid villi to the clearance of a CSF tracer in the rat.** *Am J Physiol* 1999, **276**:R818–R823.

25. Boulton M, Flessner M, Armstrong D, Hay J, Johnston M: **Lymphatic drainage of the CNS: effects of lymphatic diversion/ligation on CSF protein transport to plasma.** *Am J Physiol* 1997, **272**:R1613–R1619.
26. Silver I, Li B, Szalai J, Johnston M: **Relationship between intracranial pressure and cervical lymphatic pressure and flow rates in sheep.** *Am J Physiol* 1999, **277**:R1712–R1717.
27. Mollanji R, Bozanovic-Sosic R, Zakharov A, Makarian L, Johnston MG: **Blocking cerebrospinal fluid absorption through the cribriform plate increases resting intracranial pressure.** *Am J Physiol Regul Integr Comp Physiol* 2002, **282**:R1593–R1599.
28. Papaïconomou C, Zakharov A, Azizi N, Djenic J, Johnston M: **Reassessment of the pathways responsible for cerebrospinal fluid absorption in the neonate.** *Childs Nerv Syst* 2004, **20**:29–36.
29. Welch K, Pollay M: **The spinal arachnoid villi of the monkeys Cercopithecus aethiops sabaeus and Macaca irus.** *Anat Rec* 1963, **145**:43–48.
30. Gomez DG, Chambers AA, Di Benedetto AT, Potts DG: **The spinal cerebrospinal fluid absorptive pathways.** *Neuroradiology* 1974, **8**:61–66.
31. Kido DK, Gomez DG, Pavese AM Jr, Potts DG: **Human spinal arachnoid villi and granulations.** *Neuroradiology* 1976, 11:221–228.
32. Tubbs RS, Hansasuta A, Stetler W, Kelly DR, Blevins D, Humphrey R, Chua GD, Shoja MM, Loukas M, Oakes WJ: **Human spinal arachnoid villi revisited: immunohistological study and review of the literature.** *J Neurosurg Spine* 2007, **7**:328–331.
33. Marmarou A, Shulman K, LaMorgese J: **Compartmental analysis of compliance and outflow resistance of the cerebrospinal fluid system.** *J Neurosurg* 1975, **43**:523–534.
34. Bozanovic-Sosic R, Mollanji R, Johnston MG: **Spinal and cranial contributions to total cerebrospinal fluid transport.** *Am J Physiol Regul Integr Comp Physiol* 2001, **281**:R909–R916.
35. Edsbagge M, Tisell M, Jacobsson L, Wikkelso C: **Spinal CSF absorption in healthy individuals.** *Am J Physiol Regul Integr Comp Physiol* 2004, **287**:R1450–R1455.
36. Ritter S, Dinh TT: **Progressive postnatal dilation of brain ventricles in spontaneously hypertensive rats.** *Brain Res* 1986, **370**:327–332.
37. Ritter S, Dinh TT, Stone S, Ross N: **Cerebroventricular dilation in spontaneously hypertensive rats (SHRs) is not attenuated by reduction of blood pressure.** *Brain Res* 1988, **450**:354–359.
38. Murtha LA, McLeod DD, McCann SK, Pepperall D, Chung S, Levi CR, Calford MB, Spratt NJ: **Short-duration hypothermia after ischemic stroke prevents delayed intracranial pressure rise.** *Int J Stroke* 2013. doi:10.1111/ijs.12181.
39. Artru AA: **Isoflurane does not increase the rate of CSF production in the dog.** *Anesthesiology* 1984, **60**:193–197.
40. Murtha L, McLeod D, Spratt N: **Epidural intracranial pressure measurement in rats using a fiber-optic pressure transducer.** *J Vis Exp* 2012, **62**:e3689. doi:10.3791/3689.
41. McLeod D, Parsons M, Hood R, Hiles B, Allen J, McCann S, Murtha L, Calford M, Levi C, Spratt N: **Perfusion computed tomography thresholds defining ischaemic penumbra and infarct core: studies in a rat stroke model.** *Int J Stroke* 2013. doi: 10.1111/ijs.12147.
42. McLeod DD, Parsons MW, Levi CR, Beautement S, Buxton D, Roworth B, Spratt NJ: **Establishing a rodent stroke perfusion computed tomography model.** *Int J Stroke* 2011, **6**:284–289.
43. Chiu C, Miller MC, Caralopoulos IN, Worden MS, Brinker T, Gordon ZN, Johanson CE, Silverberg GD: **Temporal course of cerebrospinal fluid dynamics and amyloid accumulation in the aging rat brain from three to thirty months.** *Fluids Barriers CNS* 2012, **9**:3.
44. Xie L, Kang H, Xu Q, Chen MJ, Liao Y, Thiyagarajan M, O'Donnell J, Christensen DJ, Nicholson C, Iliff JJ, Takano T, Deane R, Nedergaard M: **Sleep drives metabolite clearance from the adult brain.** *Science* 2013, **342**:373–377.
45. Sykova E, Vorisek I, Antonova T, Mazel T, Meyer-Luehmann M, Jucker M, Hajek M, Ort M, Bures J: **Changes in extracellular space size and geometry in APP23 transgenic mice: a model of Alzheimer's disease.** *Proc Natl Acad Sci U S A* 2005, **102**:479–484.
46. Al-Sarraf H, Philip L: **Effect of hypertension on the integrity of blood brain and blood CSF barriers, cerebral blood flow and CSF secretion in the rat.** *Brain Res* 2003, **975**:179–188.
47. Al-Sarraf H, Philip L: **Increased brain uptake and CSF clearance of 14C-glutamate in spontaneously hypertensive rats.** *Brain Res* 2003, **994**:181–187.
48. Dunn LT: **Raised intracranial pressure.** *J Neurol Neurosurg Psychiatry* 2002, **73**(Suppl 1):i23–i27.
49. Rangel Castilla L, Gopinath S, Robertson CS: **Management of intracranial hypertension.** *Neurol Clin* 2008, **26**:521–541. x.
50. Hawkins BE, Cowart JC, Parsley MA, Capra BA, Eidson KA, Hellmich HL, Dewitt DS, Prough DS: **Effects of trauma, hemorrhage and resuscitation in aged rats.** *Brain Res* 2013, **1496**:28–35.
51. Ghersi-Egea JF, Finnegan W, Chen JL, Fenstermacher JD: **Rapid distribution of intraventricularly administered sucrose into cerebrospinal fluid cisterns via subarachnoid velae in rat.** *Neuroscience* 1996, **75**:1271–1288.
52. Lai YL, Smith PM, Lamm WJ, Hildebrandt J: **Sampling and analysis of cerebrospinal fluid for chronic studies in awake rats.** *J Appl Physiol* 1983, **54**:1754–1757.
53. Cserr HF: **Physiology of the choroid plexus.** *Physiol Rev* 1971, **51**:273–311.
54. Cutler RW, Page L, Galicich J, Watters GV: **Formation and absorption of cerebrospinal fluid in man.** *Brain* 1968, **91**:707–720.
55. Johanson CE, Duncan JA 3rd, Klinge PM, Brinker T, Stopa EG, Silverberg GD: **Multiplicity of cerebrospinal fluid functions: New challenges in health and disease.** *Cerebrospinal Fluid Res* 2008, **5**:10.
56. Preston JE: **Ageing choroid plexus-cerebrospinal fluid system.** *Microsc Res Tech* 2001, **52**:31–37.
57. Redzic ZB, Preston JE, Duncan JA, Chodobski A, Szmydynger-Chodobska J: **The choroid plexus-cerebrospinal fluid system: from development to aging.** *Curr Top Dev Biol* 2005, **71**:1–52.
58. Hochwald GM, Sahar A: **Effect of spinal fluid pressure on cerebrospinal fluid formation.** *Exp Neurol* 1971, **32**:30–40.
59. Carey ME, Vela AR: **Effect of systemic arterial hypotension on the rate of cerebrospinal fluid formation in dogs.** *J Neurosurg* 1974, **41**:350–355.
60. Snodgrass SR, Lorenzo AV: **Temperature and cerebrospinal fluid production rate.** *Am J Physiol* 1972, **222**:1524–1527.
61. Paxinos G, Watson C: *The rat brain in stereotaxic coordinates.* 4th edition. San Diego: Academic Press; 1998.

doi:10.1186/2045-8118-11-12
Cite this article as: Murtha *et al.*: Cerebrospinal fluid is drained primarily via the spinal canal and olfactory route in young and aged spontaneously hypertensive rats. *Fluids and Barriers of the CNS* 2014 **11**:12.

APPENDIX A-2

PUBLICATION 6

McLeod D, Parsons M, Hood R, Hiles B, Allen J, McCann S, **Murtha L**, Calford M, Levi C, Spratt N. Perfusion computed tomography thresholds defining ischemic penumbra and infarct core: studies in a rat stroke model. *Int J Stroke*. doi: 10.1111/ijs.12147. (2013). [E-Pub ahead of print]

Perfusion computed tomography thresholds defining ischemic penumbra and infarct core: studies in a rat stroke model

D. D. McLeod[1]*, M. W. Parsons[2], R. Hood[1], B. Hiles[1], J. Allen[1], S. K. McCann[1], L. Murtha[1], M. B. Calford[1], C. R. Levi[2], and N. J. Spratt[1,2]

Background **Perfusion computed tomography is becoming more widely used as a clinical imaging tool to predict potentially salvageable tissue (ischemic penumbra) after ischemic stroke and guide reperfusion therapies.**
Aims **The study aims to determine whether there are important changes in perfusion computed tomography thresholds defining ischemic penumbra and infarct core over time following stroke.**
Methods **Permanent middle cerebral artery occlusion was performed in adult outbred Wistar rats ($n = 6$) and serial perfusion computed tomography scans were taken every 30 mins for 2 h. To define infarction thresholds at 1 h and 2 h post-stroke, separate groups of rats underwent 1 h ($n = 6$) and 2 h ($n = 6$) of middle cerebral artery occlusion followed by reperfusion. Infarct volumes were defined by histology at 24 h. Co-registration with perfusion computed tomography maps (cerebral blood flow, cerebral blood volume, and mean transit time) permitted pixel-based analysis of thresholds defining infarction, using receiver operating characteristic curves.**
Results **Relative cerebral blood flow was the perfusion computed tomography parameter that most accurately predicted penumbra (area under the curve = 0·698) and also infarct core (area under the curve = 0·750). A relative cerebral blood flow threshold of < 75% of mean contralateral cerebral blood flow most accurately predicted penumbral tissue at 0·5 h (area under the curve = 0·660), 1 h (area under the curve = 0·659), 1·5 h (area under the curve = 0·636), and 2 h (area under the curve = 0·664) after stroke onset. A relative cerebral blood flow threshold of < 55% of mean contralateral most accurately predicted infarct core at 1 h (area under the curve = 0·765) and at 2 h (area under the curve = 0·689) after middle cerebral artery occlusion.**
Conclusions **The data provide perfusion computed tomography defined relative cerebral blood flow thresholds for infarct core and ischemic penumbra within the first two hours after experimental stroke in rats. These thresholds were shown to be stable to define the volume of infarct core and penumbra within this time window.**
Key words: infarct core, ischemic penumbra, perfusion computed tomography

Correspondence: Damian McLeod*, School of Biomedical Sciences & Pharmacy, The University of Newcastle, University Drive, Callaghan, NSW 2308, Australia.
E-mail: damian.mcleod@newcastle.edu.au
[1]Discipline of Human Physiology, School of Biomedical Sciences & Pharmacy, Faculty of Health, and Hunter Medical Research Institute, University of Newcastle, Callaghan, New South Wales, Australia
[2]Department of Neurology, John Hunter Hospital, Hunter Region M.C., New South Wales, Australia

Conflicts of interest: None declared.

DOI: 10.1111/ijs.12147

Introduction

Perfusion computed tomography (CTP) imaging of stroke patients is used to determine the volume of tissue at risk of infarction that may be salvageable by early reperfusion (ischemic penumbra). CTP thresholds defining ischemic penumbra and infarct core have most recently been established by co-registration of acute CTP maps with follow-up magnetic resonance imaging (MRI) diffusion-weighted lesion volume (DWI) at 24 h to define ischemic penumbra (patients without reperfusion), and infarct core (patients with major reperfusion) (1). CTP would offer several possible advantages over current methods to define perfusion following experimental stroke. In particular, it is performed *in vivo*, yet provides whole brain coverage, and the potential for quantification of flow, unlike the case with methods such as laser Doppler flowmetry and MR perfusion. Moreover, experimental studies provide an opportunity to test the time dependency of CTP parameters, as repeated scanning is feasible and ethically justifiable. This permits studies of the evolution of penumbra and the accuracy over time of thresholds used to define it – both key questions in stroke research. The aims of the current study were: (1) to determine the most accurate CTP parameters for prediction of ischemic penumbra and infarct core within two-hours of stroke onset in Wistar rats; (2) using these parameters, to determine the most accurate thresholds for ischemic penumbra at 0·5, 1, 1·5 and 2 h; and infarct core at one and two-hours following stroke.

Methods

Summary of experimental plan

CTP imaging was performed on rats at serial time-points before and after intraluminal thread occlusion of the middle cerebral artery (MCA). Three different occlusion durations (1 h, 2 h, and permanent MCA occlusion) were chosen to determine CTP thresholds for ischemic penumbra and infarct core at multiple time-points in the acute phase after stroke. CTP maps were co-registered with 24 h histopathology, and pixel-based receiver operating characteristic (ROC) curve analysis was used to determine the most accurate thresholds to predict penumbra and infarct core.

Surgical procedures

All surgical and experimental protocols were in accordance with the Australian Code of Practice for the Care and Use of Animals for Scientific Purposes and were approved by the University of Newcastle Animal Care and Ethics Committee. Male outbred Wistar rats underwent MCA occlusion (MCAo) using the silicone-tipped intraluminal thread occlusion method (2).

Animals were anesthetized with isoflurane (5% induction, 1·5–2·5% maintenance) and a 50:50 mix of nitrous oxide and oxygen via facemask. Animals were subject to either permanent MCAo ($n = 6$) or 1 h or 2 h temporary MCAo ($n = 6$ each), with reperfusion achieved by gentle withdrawal of the occluding thread. Details of thread insertion for MCAo on the CT scanning table have been previously reported (3). All animals had a jugular venous catheter inserted for injection of radio-opaque contrast during imaging.

Temperature was monitored with a rectal probe thermometer and maintained at 37 °C with a homeothermic heat mat during surgery and imaging. Heart rate, SpO_2, and respiratory rate were monitored throughout surgical anesthesia.

CT Imaging procedures

After surgical preparation, the animals were placed in a standardized prone position on a custom-built CT-compatible board with anesthetic nosepiece attached, and positioned on the CT scanner table. Jugular venous catheters were connected to an automatic injector (Stellant, Medrad, Warrendale, PA, USA), and preloaded with contrast (Ultravist, 300 mg/ml; Bayer, Schering Pharma AG, Leverkusen, Germany). The concentration of isoflurane was kept at 1·0–1·5% with 50:50 nitrous oxide : oxygen throughout the CT imaging protocol.

All imaging was performed with a Siemens 64 slice CT scanner (Siemens, Erlangen, Germany) with a 512 × 512 matrix; 50 mm field-of-view and 12 2·4 mm slices were obtained per scan. The development and optimization of the scanning procedure has been previously described (3). Briefly, for each CTP scan, the flow rate of contrast was 0·5 ml/s with a total injection volume of 2 ml. Scanning parameters were: 100 kVp, 218 mAs, and 0·5 s rotation speed. Sixty images at an interval of 0·5 s were acquired over 30 s for each of the 12 slices while the CT scanner table remained stationary.

A baseline head CTP scan was taken of all animals prior to MCAo, immediately following MCAo, at 30 min intervals post-MCAo until reperfusion, immediately after reperfusion, and at 30 min post-reperfusion. Animals in the permanent MCAo group had their final scans at 2 h post-MCAo.

Image processing

Postprocessing of perfusion data was performed using MIStar imaging software (Apollo Medical Imaging Technology, Melbourne, Victoria, Australia), as previously described (3). In brief, the software automatically detected the arterial input function (AIF) and venous output function from the internal carotid and sagittal sinus, respectively, and corrected any partial volume averaging by scaling the peak of the AIF to the peak height of the venous time attenuation curve. These were checked manually. The software then used singular value decomposition with delay correction (1) to deconvolve the corrected AIF with individual time attenuation curves (residue function) from each voxel, and produced perfusion maps for cerebral blood flow (CBF), cerebral blood volume (CBV), and mean transit time (MTT), which were calculated by the equation: MTT = CBV/CBF. Delay time (DT) maps were also generated in the study, as per McLeod *et al.* (3); however, the parameter was not used in the current study because our preliminary studies indicated that DT was not a reliable measure due to the rapid cerebral circulation time in the rat.

Histology

At 24 h following MCA occlusion, all rats were euthanized and perfused transcardially with saline followed by 4% paraformaldehyde before histological processing, hemotoxylin-eosin staining (3). Sections were scanned at 20× objective on a digital slide scanner (Aperio Technologies Inc., Vista, CA, USA), regions of infarction were traced on the Aperio Imagescope software, and infarct volumes were quantified as previously described (3).

Co-registration of histology with CTP maps

From the 12 CTP map slices processed at each scan time-point, three 2·4 mm CTP slices covered the MCA territory. The middle slice, located closest to bregma, was used for subsequent analyses, as it had the smallest volume of major blood vessels on perfusion maps. Details of the co-registration process have been reported previously (3); an example is shown in Fig. 1. The size of the infarct on the coronal bregma slice was measured as the number of pixels within the co-registered histological infarct core (Fig. 1). The potential for repeated contrast injections to influence perfusion variables was also quantified. Background radio-intensity values (Δ HU) were measured from the pre-stroke CTP scan (prior to 1st contrast injection) in the 2 h MCAo-reperfusion group, and again just prior to the final scan (i.e. 30 min after the last of eight contrast doses in three hours).

Statistics

Infarct volume quantification

Infarct volumes (mean ± SEM) for the permanent MCAo group, and 1 h and 2 h MCAo-reperfusion groups were calculated. One-way analysis of variance (ANOVA) was performed to test the effect of MCAo duration on infarct volume (Graphpad Prism 5, GraphPad Software, Inc., La Jolla, CA, USA). Post hoc two-tailed multiple comparisons tests (Bonferroni) were performed if occlusion duration had a significant effect at a level of $P < 0·05$.

Quantifying the effect of repeated doses of contrast on background radio-density

The mean Δ HU of regions-of-interest (ROIs) encompassing the ipsilateral and contralateral hemispheres (coronal bregma CT slice) was quantified from baseline images (prior to contrast injection) at the pre-stroke scan time-point, and at the final scan time-point (30 min following reperfusion) in the 2 h MCAo-reperfusion group. Two-way ANOVA was performed to test the effect of time and hemisphere on background radio-density units (Δ HU). Post hoc Bonferroni tests were performed if time or hemisphere had a significant effect ($P < 0·05$).

ROC curve analysis

ROC curve analysis was used to test the predictive performance of perfusion CT in relation to the co-registered histological infarct core at 24 h. The tracing of histological infarct core was considered to be the 'true' lesion, and the pixels in which the histological lesion and perfusion CT lesion overlapped were considered to be 'true positive'. Pixels not within the histology or perfusion CT lesion were considered to be 'true negative'. Pixels within the

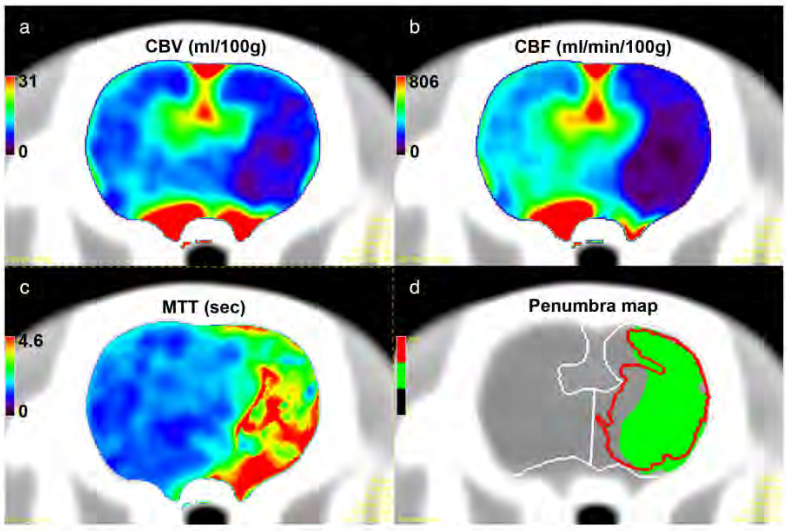

Fig. 1 CTP maps from a rat two hours post-MCAo: (a) cerebral blood volume, CBV; (b) cerebral blood flow, CBF; (c) mean transit time, MTT; (d) penumbra map. Penumbra map shows co-registered histological infarct (infarct ROI, red outline) and contralateral (left) and ipsilateral (right) hemisphere ROIs (white outlines). Pixels with CBF < 75% of contralateral mean CBF are shown in green. Note: large blood vessels of the sagittal sinus, internal carotids, and anterior cerebral artery were excluded from the analysis. At each threshold tested, the receiver operator characteristic (ROC) Analysis involves identification of true positive pixels – green pixels within the red – outlined infarct ROI; true negative – the gray pixels outside the infarct ROI but within the ipsilateral ROI (right hemisphere); false positive – green pixels outside infarct ROI and within ipsilateral ROI; false negative – gray pixels within the infarct ROI. CTP, perfusion computed tomography; MCAo, middle cerebral artery occlusion; ROI, region of interest.

Table 1 Range and increments of relative CTP thresholds tested

CTP parameter	Range (%)	Increments (%)
CBF	0–100	5
CBV	0–100	5
MTT	100–200	5

CTP, perfusion computed tomography; CBF, cerebral blood flow; CBV, cerebral blood volume; MTT, mean transit time.

perfusion CT lesion but not within the histology infarct lesion were assigned as 'false positive', and pixels within the histology lesion but not within the perfusion CT lesion were assigned as 'false negative' (Fig. 1).

To prevent a large true negative value biasing the true negative to false positive ratio when calculating specificity, only hemispheric (ischemic side) brain pixels were analyzed, rather than both hemispheres. As previously reported (1), without this correction, the false negative values would have a much greater influence upon the area under the curve (AUC) than the false positives, producing results that could substantially overestimate the true lesion volume.

Sensitivity [true positive/(true positive + false negative)] and specificity [true negative/(true negative + false positive)] were calculated for each perfusion map (CBF, CBV, and MTT) at each threshold increment tested (Table 1). The true positivity rate (sensitivity) was plotted against the false positive rate (1 – specificity) to generate ROC curves at each threshold increment. The AUC and 95% confidence intervals were then calculated for each threshold increment.

CTP thresholds (i.e. percentage of mean contralateral hemisphere CBF, CBV, and MTT) have not been previously determined in an animal model of ischemic stroke. Previous animal experiments have generally used absolute CBF thresholds, and have demonstrated that penumbra and infarct core change over the first few hours from stroke onset as the infarct core expands into the penumbra (4,5). However, a recent study in human ischemic stroke using CTP (1) showed that relative thresholds were more accurate than absolute thresholds in defining the volume of the ischemic penumbra and infarct core. Therefore, relative perfusion thresholds were tested in the current study.

Histologically defined infarction at 24 h was used to define the extent of critically hypoperfused tissue (incorporating penumbra and core) in animals without reperfusion, and infarct core in animals with reperfusion. To calculate the most accurate CTP parameter for predicting the penumbra threshold, data from all scan time-points in permanent MCAo animals were pooled and an ROC curve analysis was performed to determine the AUCs for CBF, CBV, and MTT. The CTP parameter with the highest AUC was then used to define the most accurate penumbra threshold for that parameter at each scan time-point.

The infarct core was defined as infarcted tissue on 24 h histology in temporary MCAo animals (i.e. tissue not salvaged by reperfusion). Co-registered CTP data from the 1 h scan time-point, just prior to reperfusion (1 h MCAo-reperfusion group), were used to define CTP infarction thresholds at one hour after stroke. Data at the 2 h scan time-point (2 h MCAo-reperfusion group) were used to define infarction thresholds at two hours post-stroke onset. To calculate the most accurate overall CTP parameter for predicting infarct core within two hours of stroke onset, specificity and

sensitivity data from both MCAo-reperfusion groups were pooled and an ROC curve analysis was performed to determine the AUCs for CBF, CBV, and MTT. The CTP parameter with the highest AUC was then used to define the most accurate infarction thresholds at each time-point.

Lesion size validation

To internally validate the ROC results, a lesion size analysis was performed to compare the perfusion CT threshold-derived lesion sizes to the relevant co-registered 24 h histology infarct size, in the permanent and reperfusion MCAo groups. Penumbra thresholds were applied to co-registered CTP maps at each scan time-point in the permanent MCAo group. The 1 h infarction threshold was applied to both the 0.5 and 1 h CTP scans (1 h MCAo-reperfusion group); the two hour infarction threshold was applied to the 0·5, 1, 1·5, and 2 h scan points (2 h MCAo-reperfusion group). The one hour and two hour thresholds for infarct core were also applied to the permanent MCAo group. One-way repeated measures ANOVA (RM ANOVA) was performed on each of the data sets to test the effect of time on lesion size. Post hoc two-tailed multiple comparison tests were performed if time had a significant effect at a level of $P < 0{\cdot}05$.

Results

Infarct volumes determined via histopathology

Infarct volumes (mean ± SEM) for the 1 h, 2 h MCAo-reperfusion, and permanent MCAo groups were 18·5 ± 9·07 mm^3, 24·4 ± 8·78 mm^3, and 113·9 ± 20·21 mm^3, respectively. One-way ANOVA showed a significant effect of MCAo duration on infarct volume ($P = 0{\cdot}004$). Post-hoc Bonferroni tests did not show a significant difference in infarct volumes between the 1 h and 2 h MCAo-reperfusion groups ($P > 0{\cdot}05$). There was a significant difference in infarct volumes between the 1 h MCAo-reperfusion group and the permanent MCAo group ($P < 0{\cdot}001$), and a significant difference between the 2 h MCAo-reperfusion and permanent MCAo group ($P < 0{\cdot}01$).

Background radio-density quantification

There was no significant change in precontrast radio-density between baseline and final scans in the 2 h MCAo-reperfusion group ($n = 6$). The Δ HU (mean ± SEM) of the contralateral hemisphere ROI in the pre-stroke control scan, and the final scan, were 102 ± 1·9 and 102 ± 2·2, respectively. Ipsilateral baseline Δ HU values at control, and prior to the final scan, were 104 ± 1·6 and 104 ± 2·9, respectively.

Confirming MCA occlusion on CTP maps

Control CTP scans (prior to MCAo) from all animals showed no evidence of a perfusion lesion in any animal. Successful vessel occlusion was confirmed by evidence of a perfusion lesion on CTP maps processed from the scan performed immediately after MCAo. Absence of a perfusion lesion on any of the CTP maps was taken to indicate inadequate vessel occlusion ($n = 3$), in which case the occluding thread was gently advanced, and another CTP scan was performed. Perfusion lesions were seen on CTP maps at all subsequent scan times during vessel occlusion, indicating no cases of inadvertent MCA reperfusion. The lesion location (cranial to caudal distribution) varied within the MCA territory between animals. In animals that were reperfused, the 30-min post-reperfusion CTP maps showed that two out of the six rats in the 1 h MCAo-reperfusion group had a minimal perfusion lesion on CTP maps (four of six had no visible lesion); six of six rats in the 2 h MCAo-reperfusion group had a minimal perfusion lesion.

Defining the most accurate CTP parameter for penumbra and infarct core prediction

Pooled ROC curve analysis data from the permanent MCAo group indicated that relative CBF (rCBF) was the CTP parameter that most accurately predicted the ischemic penumbra (including core) within two hours of stroke onset (Fig. 2a). Pooled data from the 1 h and 2 h MCAo-reperfusion groups indicated that rCBF was also the most accurate parameter for prediction of infarct core within two hours of stroke onset (Fig. 2b).

Defining the most accurate rCBF thresholds for penumbra and infarct core over time

The same rCBF threshold (< 75% of mean contralateral hemisphere CBF) most accurately predicted the outer border of penumbra (including core) at each different scan time-point in the permanent MCAo group (Table 2). This indicates that there is little change in rCBF thresholds predicting ischemic penumbra within two hours of stroke onset.

Infarct core was most accurately predicted by the CBF threshold of < 55% of mean contralateral CBF at both the one hour (1 h MCAo-reperfusion group) and two hour (2 h MCAo-reperfusion group) time-points (Table 3).

Applying CBF thresholds to CBF maps for lesion size validation

At each scan time-point following MCAo, CTP-predicted lesion sizes were calculated after applying the penumbra threshold (CBF < 75% of mean contralateral hemisphere) to the permanent MCAo group CBF maps at the 0·5, 1, 1·5, and 2 h scan time-points and compared with the co-registered 24 h infarct size. One-way

Table 2 Most accurate relative penumbral thresholds that predicted the stroke lesion at each scan time-point after MCAo

Time (hours post-MCAo)	CBF threshold (% of contralateral)	AUC	95% CIs
0·5	CBF < 75%	0·66	0·765; 0·555
	CBV < 75%	0·56	0·696; 0·422
	MTT < 135%	0·58	0·692; 0·464
1·0	CBF < 75%	0·66	0·762; 0·551
	CBV < 70%	0·63	0·752; 0·511
	MTT < 120%	0·60	0·706; 0·493
1·5	CBF < 75%	0·64	0·760; 0·512
	CBV < 75%	0·59	0·716; 0·462
	MTT < 135%	0·59	0·694; 0·475
2·0	CBF < 75%	0·66	0·791; 0·537
	CBV < 75%	0·62	0·743; 0·505
	MTT < 140%	0·57	0·700; 0·443

AUC, area under the curve; CBF, cerebral blood flow; CBV, cerebral blood volume; CI, confidence interval; MCAo, middle cerebral artery occlusion; MTT, mean transit time.

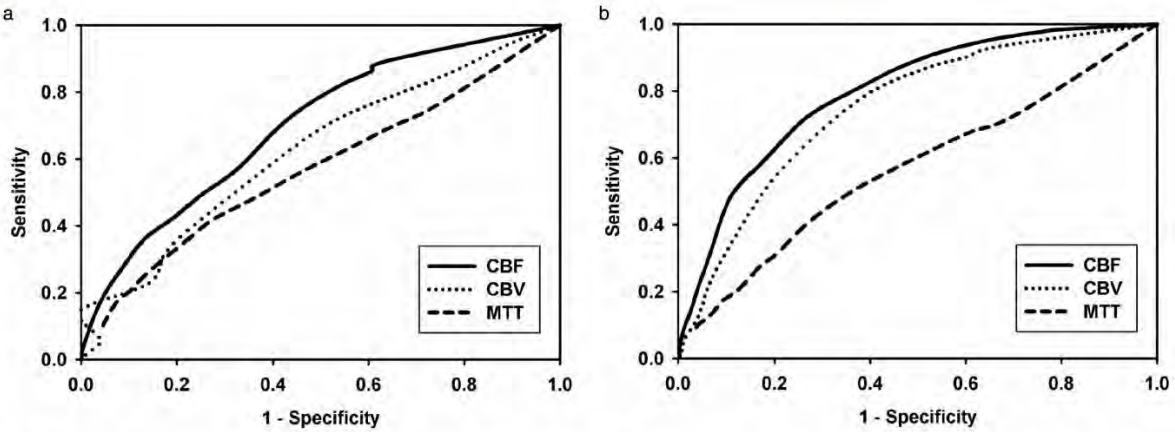

Fig. 2 ROC curves for penumbra and infarct core. (a) The tissue that progressed to infarction in permanent MCAo animals (penumbra) was best predicted by rCBF (AUC = 0·698), followed by rCBV (AUC = 0·618), then rMTT (AUC = 0·568). Penumbra ROC curve analysis includes data from all scan time-points from permanent MCAo group ($n = 6$). (b) The CTP parameter that most accurately predicted infarct core at 24 h in animals with MCA reperfusion was rCBF (AUC = 0·796), followed by rCBV (AUC = 0·750), then rMTT (AUC = 0·569). Infarct core ROC curve analysis includes data from the 1 h ($n = 6$) and 2 h ($n = 6$) MCAo-reperfusion groups. AUC, area under the curve; MCA, middle cerebral artery; MCAo, middle cerebral artery occlusion; rCBF, regional cerebral blood flow; rCBV, regional cerebral blood volume; rMTT, regional mean transit time.

Table 3 Most accurate relative CTP thresholds for infarct core prediction at one hour and two hours after MCAo

Time (hours post-MCAo)	CBF threshold (% of contralateral)	AUC	95% CIs
1	CBF < 55%	0·77	0·888; 0·641
	CBV < 75%	0·69	0·822; 0·548
	MTT < 130%	0·60	0·741; 0·453
2	CBF < 55%	0·69	0·759; 0·619
	CBV < 70%	0·71	0·779; 0·649
	MTT < 145%	0·55	0·640; 0·459

AUC, area under the curve; CBF, cerebral blood flow; CBV, cerebral blood volume; CI, confidence interval; CTP, perfusion computed tomography; MCAo, middle cerebral artery occlusion; MTT, mean transit time.

RM ANOVA did not show any significant effect of time on lesion size ($P = 0·37$) (Fig. 3a).

CTP-predicted infarct core lesion sizes were calculated after applying the CBF threshold (CBF < 55% of contralateral hemisphere) to the 1 h MCAo-reperfusion group CBF maps at the 0·5 and 1 h scan time-points. Mean lesion sizes were plotted against the co-registered infarct size at 24 h (Fig. 3b). One-way RM ANOVA did not show any significant effect of time on infarct core lesion size ($P = 0·09$). Similarly, when the infarction threshold was applied to the 2 h MCAo-reperfusion group, CBF maps at the 0·5, 1, 1·5, and 2 h time-points, one-way RM ANOVA did not show a significant effect of time on infarct core lesion size ($P = 0·08$) (Fig. 3c).

When both the penumbra threshold (CBF < 75% of contralateral) and infarction threshold (CBF < 55% of contralateral) were applied to the permanent MCAo group CBF maps at each scan time-point, the lesion size histograms were plotted overlying each other to show the separate 'Penumbra' size and 'Core' size at each time-point (Fig. 4). One-way RM ANOVA showed that time had no effect on 'Penumbra' size ($P = 0·53$). The data indicate that the predicted penumbra becomes incorporated into the infarct core at 24 h (Fig. 4).

Discussion

This is the first rodent stroke study to use CTP thresholds and histological infarct outcomes to define the ischemic penumbra and infarct core at serial time-points after stroke. The CTP parameter that most accurately predicted the penumbra and infarct core within two hours of stroke onset was rCBF. The rCBF thresholds of < 75% and < 55% most accurately predicted the penumbra and infarct core, respectively, at each imaging time-point up to two hours after stroke. The rCBF penumbra and core thresholds were stable during the acute phase following stroke in this model.

The stability of the rCBF penumbra threshold over time is consistent with the literature. For example, MRI perfusion imaging methods have demonstrated that the penumbra threshold defining the CBF lesion volume does not change significantly within the first three hours after permanent MCAo in rats (6). The stability of the infarction threshold is not surprising, given that there was no significant difference in infarct volumes between the 1 h and 2 h MCAo-reperfusion groups. By applying the rCBF penumbra and core thresholds to the permanent MCAo group, however, we confirmed in our model the well-established finding that the penumbra becomes incorporated into the infarct core after ischemic stroke (4,5).

The current findings provide new information that may be used to investigate potential acute treatment strategies following ischemic stroke. Serial CTP scanning in the rat stroke model allows investigation of whole brain hemodynamics over time, an advantage over other methods of perfusion monitoring that only allow monitoring of a small cortical region. An additional strength of this study was the use of pixel-based analysis,

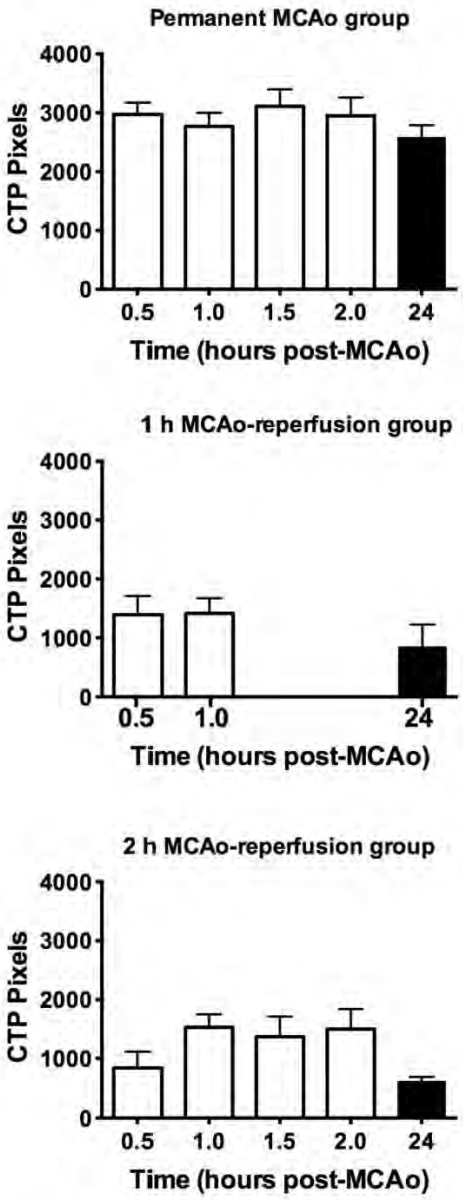

Fig. 3 Calculated penumbra and infarct core sizes over time. (a) Lesion sizes calculated using the most accurate penumbra threshold (CBF < 75% of mean contralateral) at different time-points (hollow columns), compared with that from the co-registered histology (dark column). (b and c) Lesion sizes for infarct core calculated using the CBF < 55% of mean contralateral threshold applied to the 1 h (b) and 2 h (c) MCAo-reperfusion animals ($n = 6$ in each group), and compared with the co-registered 24 h histology (dark columns). Data are mean + SEM. CBF, cerebral blood flow;MCAo, middle cerebral artery occlusion.

permitting analysis of subjects with highly variable lesion sizes, and also closely mimicking clinical studies. The use of a rat model limited spatial resolution somewhat; however, this was partially compensated for by the ability to use a much smaller field of view, and achieve whole brain coverage.

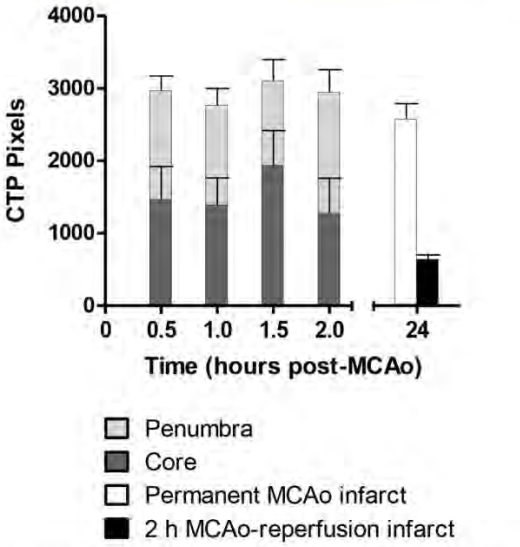

Fig. 4 CTP-predicted penumbra and infarct core lesion size plotted at each scan time-point in permanent MCAo animals ($n = 6$), calculated by applying the penumbra threshold (CBF < 75% of mean contralateral) and infarction threshold (CBF < 55% of mean contralateral) to CBF maps at each scan time-point. Data are mean + SEM. The permanent MCAo group infarct size at 24 h is plotted as 'Permanent MCAo infarct'; the 2 h MCAo-reperfusion group infarct size at 24 h is plotted as '2 h MCAo-reperfusion infarct'. Overlapping histograms at each scan time-point allow visualization of the 'Penumbra' and 'Core' size at each scan time-point. The predicted penumbra becomes incorporated into the infarct core at 24 h (white bar). The difference between the 'permanent MCAo infarct' and the '2 h MCAo-reperfusion infarct' indicates the amount of tissue that was predicted to be salvaged if reperfusion occurred immediately after the 2 h scan time-point. The resulting infarct from the 2 h MCAo animals is included for comparison (separate cohort, $n = 6$). CBF, cerebral blood flow; CTP, perfusion computed tomography; MCAo, middle cerebral artery occlusion.

Persistent perfusion lesions were seen following withdrawal of the occluding thread in several animals. The cause of the observed perfusion lesions for up to 30 min following reperfusion is most likely due to small vessel nonreperfusion (also known as 'no-reflow') due to swelling of endothelial cells with subsequent formation of microthrombi within vessels of the infarct core (7–9).

The rCBF thresholds of < 75% and < 55% most accurately predicted the penumbra and infarct core in rats, whereas the best rCBF thresholds were < 50% and < 40%, respectively, using similar methodology in humans (1). There are several possible explanations for these differences, for example, circulation time is significantly faster in the rat, and by necessity the studies were done under light anesthesia. Thresholds obtained in the present study were also somewhat higher than those obtained in previous rodent stroke studies using techniques such as CBF autoradiography (10).

Inadequate clearance of radio-opaque contrast was largely excluded as a cause of potential overestimation of rCBF thresholds, as no change was seen in radio-density even after multiple doses of radiocontrast. This indicates that 30 min between CTP

scan time-points is adequate for renal clearance of intravenous radio-opaque contrast in rats.

There were some limitations to this study. As mentioned, the use of one hour and two hour temporary MCAo durations may have been suboptimal for determining the effect of time on the infarction threshold because infarct volumes in both duration groups were small and not significantly different. The small infarcts are consistent with previous reports of small and variable infarct volumes following MCAo in outbred Wistar rats from some suppliers (11,12). An important potential source of inaccuracy is the co-registration of histology and CTP maps. This was done based on stereotaxic coordinates from a rat atlas. Although the brain hemispheres and infarcted tissue are accurately demarcated from high-resolution scanned images, there is inevitable brain shrinkage that occurs due to histological fixation and processing. As a result, any differences in the coronal sectioning in any of the x, y, or z planes between the histology section and CTP map may result in co-registration errors. Unfortunately, there is currently no perfect method for co-registration of histological sections with *in vivo* imaging sets. Co-registration errors combined with small sample sizes in each experimental group are mostly likely responsible for the absence of a distinct threshold on the ROC curves and suboptimal AUCs. Given the issues of co-registration and resolution, segmentation for separate analysis of gray and white matter compartments was not attempted. However, the well-known differences in baseline perfusion and infarction thresholds between gray and white matter are likely to be of less importance in this experimental study than in human imaging, because white matter comprises only 14% of the rat brain (versus 50% in humans) (13). Blood pressure and intracranial pressure were not monitored during CTP imaging, and thus changes in cerebral perfusion pressure during imaging cannot be ruled out as a source of error that may have led to an overestimation of rCBF penumbra and infarction thresholds.

The current study provides the first evidence of the impact of time on CTP-defined penumbra and infarction thresholds in a rat ischemic stroke model. Our data show the stability of relative CBF thresholds predicting penumbra and infarct core within the first two hours from stroke. The data suggest that a single set of relative CTP thresholds may be used to define penumbra and infarct core within two hours of ischemic stroke onset in rats.

Acknowledgements

We would like to thank radiographers Marc Heaton, David Buxton, and Stephen Beautement (Hunter Health Imaging, John Hunter Hospital); Qing Yang (Apollo Medical Imaging Technology, Melbourne Australia); Debbie Pepperall; Sunyoung Chung; and the University of Newcastle Faculty of Health Workshop team for their technical expertise throughout the study. This study was supported by grants from the Australian National Health & Medical Research Council (NHMRC stroke program grant 454417), The National Stroke Foundation, and the Hunter Medical Research Institute.

References

1 Bivard A, Spratt N, Levi C, Parsons M. Perfusion computer tomography: imaging and clinical validation in acute ischaemic stroke. *Brain* 2011; **134**(Pt 11):3408–16.
2 Spratt NJ, Fernandez J, Chen M *et al.* Modification of the method of thread manufacture improves stroke induction rate and reduces mortality after thread-occlusion of the middle cerebral artery in young or aged rats. *J Neurosci Methods* 2006; **155**:285–90.
3 McLeod DD, Parsons MW, Levi CR *et al.* Establishing a rodent stroke perfusion computed tomography model. International journal of stroke: official journal of the International Stroke. *Society* 2011; **6**:284–9.
4 Astrup J, Siesjo BK, Symon L. Thresholds in cerebral ischemia: the ischemic penumbra. *Stroke* 1981; **12**:723–5.
5 Hossmann KA. Viability thresholds and the penumbra of focal ischemia. *Ann Neurol* 1994; **36**:557–65.
6 Henninger N, Fisher M. Stimulating circle of Willis nerve fibers preserves the diffusion-perfusion mismatch in experimental stroke. *Stroke* 2007; **38**:2779–86.
7 Ames A, 3rd, Wright RL, Kowada M, Thurston JM, Majno G. Cerebral ischemia. II. The no-reflow phenomenon. *Am J Pathol* 1968; **52**:437–53.
8 Liu S, Connor J, Peterson S, Shuttleworth CW, Liu KJ. Direct visualization of trapped erythrocytes in rat brain after focal ischemia and reperfusion. *J Cerebral Blood Flow Metab* 2002; **22**:1222–30.
9 Mori E, del Zoppo GJ, Chambers JD, Copeland BR, Arfors KE. Inhibition of polymorphonuclear leukocyte adherence suppresses no-reflow after focal cerebral ischemia in baboons. *Stroke* 1992; **23**:712–8.
10 Touzani O, Baron JC. Duration and thresholds of the ischemic penumbra in different species; in Donnan GA, Baron JC, Davis SM, Sharp FR (eds). The Ischemic Penumbra. New York, Informa Healthcare USA, Inc., 2007:37–58.
11 Oliff HS, Weber E, Eilon G, Marek P. The role of strain/vendor differences on the outcome of focal ischemia induced by intraluminal middle cerebral artery occlusion in the rat. *Brain Res* 1995; **675**:20–6.
12 Ma J, Zhao L, Nowak TS, Jr. Selective, reversible occlusion of the middle cerebral artery in rats by an intraluminal approach optimized filament design and methodology. *J Neurosci Methods* 2006; **156**:76–83.
13 Zhang K, Sejnowski TJ. A universal scaling law between gray matter and white matter of cerebral cortex. *Proc Natl Acad Sci U S A* 2000; **97**:5621–6.

APPENDIX B

COPYRIGHT PERMISSIONS

I warrant that I have obtained, where necessary, permission from the copyright owners to use any third party copyright material reproduced in the thesis, or to use any of my own published work in which the copyright is held by another party.

Figure 2

Permission to copy and communicate this work has been granted by Oxford University press

Figure 3

Permission to copy and communicate this work has been granted by Oxford University press

Publication 1

Murtha L, McLeod D, Spratt N. Epidural intracranial pressure measurement in rats using a fiber-optic pressure transducer. *J Vis Exp*. e3689, doi:10.3791/3689. (2012).

Publication 2

Murtha L, McLeod D, McCann S, Pepperall D, McCann S, Chung S, Levi C, Calford M, Spratt N. Short-duration hypothermia after ischemic stroke prevents delayed intracranial pressure rise. *Int J Stroke.* 9, 553-559, doi:10.1111/ijs.12181. (2014).

Publication 5

Murtha L, Yang Q, Parsons M, Levi C, Beard D, Spratt N, McLeod D. Cerebrospinal fluid is drained primarily via the spinal canal and olfactory route in young and aged spontaneously hypertensive rats. *Fluids Barriers CNS*. 11:12, doi:10.1186/2045-8118-11-12. (2014).

Publication 6

McLeod D, Parsons M, Hood R, Hiles B, Allen J, McCann S, Murtha L, Calford M, Levi C, Spratt N. Perfusion computed tomography thresholds defining ischemic penumbra and infarct core: studies in a rat stroke model. *Int J Stroke*. doi: 10.1111/ijs.12147. (2013). [E-Pub ahead of print]

OXFORD UNIVERSITY PRESS LICENSE TERMS AND CONDITIONS

Sep 11, 2014

This is a License Agreement between Lucy A Murtha ("You") and Oxford University Press ("Oxford University Press") provided by Copyright Clearance Center ("CCC"). The license consists of your order details, the terms and conditions provided by Oxford University Press, and the payment terms and conditions.

All payments must be made in full to CCC. For payment instructions, please see information listed at the bottom of this form.

License Number	3466220041672
License date	Sep 11, 2014
Licensed content publisher	Oxford University Press
Licensed content publication	Brain
Licensed content title	The independent predictive utility of computed tomography angiographic collateral status in acute ischaemic stroke:
Licensed content author	Ferdinand Miteff, Christopher R. Levi, Grant A. Bateman, Neil Spratt, Patrick McElduff, Mark W. Parsons
Licensed content date	08/01/2009
Type of Use	Thesis/Dissertation
Institution name	None
Title of your work	THE EFFECTS AND MECHANISMS OF THERAPEUTIC HYPOTHERMIA ON INTRACRANIAL PRESSURE REGULATION FOLLOWING ISCHAEMIC STROKE IN RATS
Publisher of your work	n/a
Expected publication date	Sep 2014
Permissions cost	0.00 USD
Value added tax	0.00 USD
Total	0.00 USD
Total	0.00 USD
Terms and Conditions	

STANDARD TERMS AND CONDITIONS FOR REPRODUCTION OF MATERIAL FROM AN OXFORD UNIVERSITY PRESS JOURNAL

1. Use of the material is restricted to the type of use specified in your order details.

2. This permission covers the use of the material in the English language in the following territory: world. If you have requested additional permission to translate this material, the terms and conditions of this reuse will be set out in clause 12.

3. This permission is limited to the particular use authorized in (1) above and does not allow you to sanction its use elsewhere in any other format other than specified above, nor does it apply to quotations, images, artistic works etc that have been reproduced from other sources

which may be part of the material to be used.

4. No alteration, omission or addition is made to the material without our written consent. Permission must be re-cleared with Oxford University Press if/when you decide to reprint.

5. The following credit line appears wherever the material is used: author, title, journal, year, volume, issue number, pagination, by permission of Oxford University Press or the sponsoring society if the journal is a society journal. Where a journal is being published on behalf of a learned society, the details of that society must be included in the credit line.

6. For the reproduction of a full article from an Oxford University Press journal for whatever purpose, the corresponding author of the material concerned should be informed of the proposed use. Contact details for the corresponding authors of all Oxford University Press journal contact can be found alongside either the abstract or full text of the article concerned, accessible from www.oxfordjournals.org Should there be a problem clearing these rights, please contact journals.permissions@oup.com

7. If the credit line or acknowledgement in our publication indicates that any of the figures, images or photos was reproduced, drawn or modified from an earlier source it will be necessary for you to clear this permission with the original publisher as well. If this permission has not been obtained, please note that this material cannot be included in your publication/photocopies.

8. While you may exercise the rights licensed immediately upon issuance of the license at the end of the licensing process for the transaction, provided that you have disclosed complete and accurate details of your proposed use, no license is finally effective unless and until full payment is received from you (either by Oxford University Press or by Copyright Clearance Center (CCC)) as provided in CCC's Billing and Payment terms and conditions. If full payment is not received on a timely basis, then any license preliminarily granted shall be deemed automatically revoked and shall be void as if never granted. Further, in the event that you breach any of these terms and conditions or any of CCC's Billing and Payment terms and conditions, the license is automatically revoked and shall be void as if never granted. Use of materials as described in a revoked license, as well as any use of the materials beyond the scope of an unrevoked license, may constitute copyright infringement and Oxford University Press reserves the right to take any and all action to protect its copyright in the materials.

9. This license is personal to you and may not be sublicensed, assigned or transferred by you to any other person without Oxford University Press's written permission.

10. Oxford University Press reserves all rights not specifically granted in the combination of (i) the license details provided by you and accepted in the course of this licensing transaction, (ii) these terms and conditions and (iii) CCC's Billing and Payment terms and conditions.

11. You hereby indemnify and agree to hold harmless Oxford University Press and CCC, and their respective officers, directors, employs and agents, from and against any and all claims arising out of your use of the licensed material other than as specifically authorized pursuant to this license.

12. Other Terms and Conditions:

v1.4

You will be invoiced within 48 hours of this transaction date. You may pay your invoice by credit card upon receipt of the invoice for this transaction. Please follow instructions

provided at that time.
To pay for this transaction now; please remit a copy of this document along with your payment. Payment should be in the form of a check or money order referencing your account number and this invoice number RLNK501400937.
Make payments to "COPYRIGHT CLEARANCE CENTER" and send to:

Copyright Clearance Center
Dept 001
P.O. Box 843006
Boston, MA 02284-3006
Please disregard electronic and mailed copies if you remit payment in advance.
Questions? customercare@copyright.com or +1-855-239-3415 (toll free in the US) or +1-978-646-2777.

Gratis licenses (referencing $0 in the Total field) are free. Please retain this printable license for your reference. No payment is required.

OXFORD UNIVERSITY PRESS LICENSE TERMS AND CONDITIONS

Sep 11, 2014

This is a License Agreement between Lucy A Murtha ("You") and Oxford University Press ("Oxford University Press") provided by Copyright Clearance Center ("CCC"). The license consists of your order details, the terms and conditions provided by Oxford University Press, and the payment terms and conditions.

All payments must be made in full to CCC. For payment instructions, please see information listed at the bottom of this form.

License Number	3466220264534
License date	Sep 11, 2014
Licensed content publisher	Oxford University Press
Licensed content publication	Brain
Licensed content title	Hypothermia in animal models of acute ischaemic stroke: a systematic review and meta-analysis:
Licensed content author	H. Bart van der Worp, Emily S. Sena, Geoffrey A. Donnan, David W. Howells, Malcolm R. Macleod
Licensed content date	12/01/2007
Type of Use	Thesis/Dissertation
Institution name	None
Title of your work	THE EFFECTS AND MECHANISMS OF THERAPEUTIC HYPOTHERMIA ON INTRACRANIAL PRESSURE REGULATION FOLLOWING ISCHAEMIC STROKE IN RATS
Publisher of your work	n/a
Expected publication date	Sep 2014
Permissions cost	0.00 USD
Value added tax	0.00 USD
Total	0.00 USD
Total	0.00 USD
Terms and Conditions	

STANDARD TERMS AND CONDITIONS FOR REPRODUCTION OF MATERIAL FROM AN OXFORD UNIVERSITY PRESS JOURNAL

1. Use of the material is restricted to the type of use specified in your order details.

2. This permission covers the use of the material in the English language in the following territory: world. If you have requested additional permission to translate this material, the terms and conditions of this reuse will be set out in clause 12.

3. This permission is limited to the particular use authorized in (1) above and does not allow you to sanction its use elsewhere in any other format other than specified above, nor does it apply to quotations, images, artistic works etc that have been reproduced from other sources

which may be part of the material to be used.

4. No alteration, omission or addition is made to the material without our written consent. Permission must be re-cleared with Oxford University Press if/when you decide to reprint.

5. The following credit line appears wherever the material is used: author, title, journal, year, volume, issue number, pagination, by permission of Oxford University Press or the sponsoring society if the journal is a society journal. Where a journal is being published on behalf of a learned society, the details of that society must be included in the credit line.

6. For the reproduction of a full article from an Oxford University Press journal for whatever purpose, the corresponding author of the material concerned should be informed of the proposed use. Contact details for the corresponding authors of all Oxford University Press journal contact can be found alongside either the abstract or full text of the article concerned, accessible from www.oxfordjournals.org Should there be a problem clearing these rights, please contact journals.permissions@oup.com

7. If the credit line or acknowledgement in our publication indicates that any of the figures, images or photos was reproduced, drawn or modified from an earlier source it will be necessary for you to clear this permission with the original publisher as well. If this permission has not been obtained, please note that this material cannot be included in your publication/photocopies.

8. While you may exercise the rights licensed immediately upon issuance of the license at the end of the licensing process for the transaction, provided that you have disclosed complete and accurate details of your proposed use, no license is finally effective unless and until full payment is received from you (either by Oxford University Press or by Copyright Clearance Center (CCC)) as provided in CCC's Billing and Payment terms and conditions. If full payment is not received on a timely basis, then any license preliminarily granted shall be deemed automatically revoked and shall be void as if never granted. Further, in the event that you breach any of these terms and conditions or any of CCC's Billing and Payment terms and conditions, the license is automatically revoked and shall be void as if never granted. Use of materials as described in a revoked license, as well as any use of the materials beyond the scope of an unrevoked license, may constitute copyright infringement and Oxford University Press reserves the right to take any and all action to protect its copyright in the materials.

9. This license is personal to you and may not be sublicensed, assigned or transferred by you to any other person without Oxford University Press's written permission.

10. Oxford University Press reserves all rights not specifically granted in the combination of (i) the license details provided by you and accepted in the course of this licensing transaction, (ii) these terms and conditions and (iii) CCC's Billing and Payment terms and conditions.

11. You hereby indemnify and agree to hold harmless Oxford University Press and CCC, and their respective officers, directors, employs and agents, from and against any and all claims arising out of your use of the licensed material other than as specifically authorized pursuant to this license.

12. Other Terms and Conditions:

v1.4

You will be invoiced within 48 hours of this transaction date. You may pay your invoice by credit card upon receipt of the invoice for this transaction. Please follow instructions

provided at that time.
To pay for this transaction now; please remit a copy of this document along with your payment. Payment should be in the form of a check or money order referencing your account number and this invoice number RLNK501400939.
Make payments to "COPYRIGHT CLEARANCE CENTER" and send to:

Copyright Clearance Center
Dept 001
P.O. Box 843006
Boston, MA 02284-3006
Please disregard electronic and mailed copies if you remit payment in advance.
Questions? customercare@copyright.com or +1-855-239-3415 (toll free in the US) or +1-978-646-2777.

Gratis licenses (referencing $0 in the Total field) are free. Please retain this printable license for your reference. No payment is required.

Re: Copyright Permission

Ward Parry <ward.parry@jove.com>

Fri 1/08/2014 11:31 PM

To: Lucy Murtha <Lucy.Murtha@uon.edu.au>;

Hi Lucy,

That is fine.

Best,
Ward

On Thu, Jul 31, 2014 at 10:15 PM, Lucy Murtha <Lucy.Murtha@uon.edu.au> wrote:

> To whom it may concern,
>
> I am contacting you to seek written permission to copy and communicate the following material within the electronic version of my Doctor of Philosophy thesis:
>
> **Murtha L**, McLeod D, Spratt N. Epidural intracranial pressure measurement in rats using a fiber-optic pressure transducer. *J Vis Exp*. e3689, doi:10.3791/3689. (2012).
>
> If you are not the rights holder for this material I would be grateful if you would advise me who to contact. The thesis will be made available on the internet via the University of Newcastle's online digital repository http://ogma.newcastle.edu.au:8080/vital/access/manager/Index.
>
> Kind regards,
>
> Lucy
>
> Lucy Murtha, PhD Candidate
> Translation Stroke Research Group
> School of Biomedical Sciences & Pharmacy

Rm 504, Medical Sciences Building
The University of Newcastle
University Drive, Callaghan
NSW 2308 Australia
Ph: +61 2 4921 7303

--
Ward Parry
Director of Library Relations
JoVE
1 Alewife Center, Suite 200, Cambridge, MA 02140
tel: 617-229-7013

JOHN WILEY AND SONS LICENSE TERMS AND CONDITIONS

Jul 31, 2014

This is a License Agreement between Lucy A Murtha ("You") and John Wiley and Sons ("John Wiley and Sons") provided by Copyright Clearance Center ("CCC"). The license consists of your order details, the terms and conditions provided by John Wiley and Sons, and the payment terms and conditions.

All payments must be made in full to CCC. For payment instructions, please see information listed at the bottom of this form.

License Number	3439640009414
License date	Jul 31, 2014
Licensed content publisher	John Wiley and Sons
Licensed content publication	International Journal of Stroke
Licensed content title	Short-duration hypothermia after ischemic stroke prevents delayed intracranial pressure rise
Licensed copyright line	© 2013 The Authors. International Journal of Stroke © 2013 World Stroke Organization
Licensed content author	L. A. Murtha,D. D. McLeod,S. K. McCann,D. Pepperall,S. Chung,C. R. Levi,M. B. Calford,N. J. Spratt
Licensed content date	Sep 12, 2013
Start page	553
End page	559
Type of use	Dissertation/Thesis
Requestor type	Author of this Wiley article
Format	Print and electronic
Portion	Full article
Will you be translating?	No
Title of your thesis / dissertation	THE EFFECTS AND MECHANISMS OF THERAPEUTIC HYPOTHERMIA ON INTRACRANIAL PRESSURE REGULATION FOLLOWING ISCHAEMIC STROKE IN RATS
Expected completion date	Sep 2014
Expected size (number of pages)	70
Total	0.00 USD
Terms and Conditions	

TERMS AND CONDITIONS

This copyrighted material is owned by or exclusively licensed to John Wiley & Sons, Inc. or one of its group companies (each a"Wiley Company") or handled on behalf of a society with which a Wiley Company has exclusive publishing rights in relation to a particular work (collectively "WILEY"). By clicking accept in connection with completing this licensing transaction, you

agree that the following terms and conditions apply to this transaction (along with the billing and payment terms and conditions established by the Copyright Clearance Center Inc., ("CCC's Billing and Payment terms and conditions"), at the time that you opened your Rightslink account (these are available at any time at http://myaccount.copyright.com).

Terms and Conditions

- The materials you have requested permission to reproduce or reuse (the "Wiley Materials") are protected by copyright.

- You are hereby granted a personal, non-exclusive, non-sub licensable (on a stand-alone basis), non-transferable, worldwide, limited license to reproduce the Wiley Materials for the purpose specified in the licensing process. This license is for a one-time use only and limited to any maximum distribution number specified in the license. The first instance of republication or reuse granted by this licence must be completed within two years of the date of the grant of this licence (although copies prepared before the end date may be distributed thereafter). The Wiley Materials shall not be used in any other manner or for any other purpose, beyond what is granted in the license. Permission is granted subject to an appropriate acknowledgement given to the author, title of the material/book/journal and the publisher. You shall also duplicate the copyright notice that appears in the Wiley publication in your use of the Wiley Material. Permission is also granted on the understanding that nowhere in the text is a previously published source acknowledged for all or part of this Wiley Material. Any third party content is expressly excluded from this permission.

- With respect to the Wiley Materials, all rights are reserved. Except as expressly granted by the terms of the license, no part of the Wiley Materials may be copied, modified, adapted (except for minor reformatting required by the new Publication), translated, reproduced, transferred or distributed, in any form or by any means, and no derivative works may be made based on the Wiley Materials without the prior permission of the respective copyright owner. You may not alter, remove or suppress in any manner any copyright, trademark or other notices displayed by the Wiley Materials. You may not license, rent, sell, loan, lease, pledge, offer as security, transfer or assign the Wiley Materials on a stand-alone basis, or any of the rights granted to you hereunder to any other person.

- The Wiley Materials and all of the intellectual property rights therein shall at all times remain the exclusive property of John Wiley & Sons Inc, the Wiley Companies, or their respective licensors, and your interest therein is only that of having possession of and the right to reproduce the Wiley Materials pursuant to Section 2 herein during the continuance of this Agreement. You agree that you own no right, title or interest in or to the Wiley Materials or any of the intellectual property rights therein. You shall have no rights hereunder other than the license as provided for above in Section 2. No right, license or interest to any trademark, trade name, service mark or other branding ("Marks") of WILEY or its licensors is granted hereunder, and you agree that you shall not assert any such right, license or interest with respect thereto.

- NEITHER WILEY NOR ITS LICENSORS MAKES ANY WARRANTY OR REPRESENTATION OF ANY KIND TO YOU OR ANY THIRD PARTY, EXPRESS, IMPLIED OR STATUTORY, WITH RESPECT TO THE MATERIALS OR THE

ACCURACY OF ANY INFORMATION CONTAINED IN THE MATERIALS, INCLUDING, WITHOUT LIMITATION, ANY IMPLIED WARRANTY OF MERCHANTABILITY, ACCURACY, SATISFACTORY QUALITY, FITNESS FOR A PARTICULAR PURPOSE, USABILITY, INTEGRATION OR NON-INFRINGEMENT AND ALL SUCH WARRANTIES ARE HEREBY EXCLUDED BY WILEY AND ITS LICENSORS AND WAIVED BY YOU

- WILEY shall have the right to terminate this Agreement immediately upon breach of this Agreement by you.
- You shall indemnify, defend and hold harmless WILEY, its Licensors and their respective directors, officers, agents and employees, from and against any actual or threatened claims, demands, causes of action or proceedings arising from any breach of this Agreement by you.
- IN NO EVENT SHALL WILEY OR ITS LICENSORS BE LIABLE TO YOU OR ANY OTHER PARTY OR ANY OTHER PERSON OR ENTITY FOR ANY SPECIAL, CONSEQUENTIAL, INCIDENTAL, INDIRECT, EXEMPLARY OR PUNITIVE DAMAGES, HOWEVER CAUSED, ARISING OUT OF OR IN CONNECTION WITH THE DOWNLOADING, PROVISIONING, VIEWING OR USE OF THE MATERIALS REGARDLESS OF THE FORM OF ACTION, WHETHER FOR BREACH OF CONTRACT, BREACH OF WARRANTY, TORT, NEGLIGENCE, INFRINGEMENT OR OTHERWISE (INCLUDING, WITHOUT LIMITATION, DAMAGES BASED ON LOSS OF PROFITS, DATA, FILES, USE, BUSINESS OPPORTUNITY OR CLAIMS OF THIRD PARTIES), AND WHETHER OR NOT THE PARTY HAS BEEN ADVISED OF THE POSSIBILITY OF SUCH DAMAGES. THIS LIMITATION SHALL APPLY NOTWITHSTANDING ANY FAILURE OF ESSENTIAL PURPOSE OF ANY LIMITED REMEDY PROVIDED HEREIN.
- Should any provision of this Agreement be held by a court of competent jurisdiction to be illegal, invalid, or unenforceable, that provision shall be deemed amended to achieve as nearly as possible the same economic effect as the original provision, and the legality, validity and enforceability of the remaining provisions of this Agreement shall not be affected or impaired thereby.
- The failure of either party to enforce any term or condition of this Agreement shall not constitute a waiver of either party's right to enforce each and every term and condition of this Agreement. No breach under this agreement shall be deemed waived or excused by either party unless such waiver or consent is in writing signed by the party granting such waiver or consent. The waiver by or consent of a party to a breach of any provision of this Agreement shall not operate or be construed as a waiver of or consent to any other or subsequent breach by such other party.
- This Agreement may not be assigned (including by operation of law or otherwise) by you without WILEY's prior written consent.
- Any fee required for this permission shall be non-refundable after thirty (30) days from receipt by the CCC.
- These terms and conditions together with CCC's Billing and Payment terms and conditions

(which are incorporated herein) form the entire agreement between you and WILEY concerning this licensing transaction and (in the absence of fraud) supersedes all prior agreements and representations of the parties, oral or written. This Agreement may not be amended except in writing signed by both parties. This Agreement shall be binding upon and inure to the benefit of the parties' successors, legal representatives, and authorized assigns.

- In the event of any conflict between your obligations established by these terms and conditions and those established by CCC's Billing and Payment terms and conditions, these terms and conditions shall prevail.
- WILEY expressly reserves all rights not specifically granted in the combination of (i) the license details provided by you and accepted in the course of this licensing transaction, (ii) these terms and conditions and (iii) CCC's Billing and Payment terms and conditions.
- This Agreement will be void if the Type of Use, Format, Circulation, or Requestor Type was misrepresented during the licensing process.
- This Agreement shall be governed by and construed in accordance with the laws of the State of New York, USA, without regards to such state's conflict of law rules. Any legal action, suit or proceeding arising out of or relating to these Terms and Conditions or the breach thereof shall be instituted in a court of competent jurisdiction in New York County in the State of New York in the United States of America and each party hereby consents and submits to the personal jurisdiction of such court, waives any objection to venue in such court and consents to service of process by registered or certified mail, return receipt requested, at the last known address of such party.

WILEY OPEN ACCESS TERMS AND CONDITIONS

Wiley Publishes Open Access Articles in fully Open Access Journals and in Subscription journals offering Online Open. Although most of the fully Open Access journals publish open access articles under the terms of the Creative Commons Attribution (CC BY) License only, the subscription journals and a few of the Open Access Journals offer a choice of Creative Commons Licenses:: Creative Commons Attribution (CC-BY) license Creative Commons Attribution Non-Commercial (CC-BY-NC) license and Creative Commons Attribution Non-Commercial-NoDerivs (CC-BY-NC-ND) License. The license type is clearly identified on the article.

Copyright in any research article in a journal published as Open Access under a Creative Commons License is retained by the author(s). Authors grant Wiley a license to publish the article and identify itself as the original publisher. Authors also grant any third party the right to use the article freely as long as its integrity is maintained and its original authors, citation details and publisher are identified as follows: [Title of Article/Author/Journal Title and Volume/Issue. Copyright (c) [year] [copyright owner as specified in the Journal]. Links to the final article on Wiley's website are encouraged where applicable.

The Creative Commons Attribution License

The Creative Commons Attribution License (CC-BY) allows users to copy, distribute and transmit an article, adapt the article and make commercial use of the article. The CC-BY license permits commercial and non-commercial re-use of an open access article, as long as the author is properly

attributed.

The Creative Commons Attribution License does not affect the moral rights of authors, including without limitation the right not to have their work subjected to derogatory treatment. It also does not affect any other rights held by authors or third parties in the article, including without limitation the rights of privacy and publicity. Use of the article must not assert or imply, whether implicitly or explicitly, any connection with, endorsement or sponsorship of such use by the author, publisher or any other party associated with the article.

For any reuse or distribution, users must include the copyright notice and make clear to others that the article is made available under a Creative Commons Attribution license, linking to the relevant Creative Commons web page.

To the fullest extent permitted by applicable law, the article is made available as is and without representation or warranties of any kind whether express, implied, statutory or otherwise and including, without limitation, warranties of title, merchantability, fitness for a particular purpose, non-infringement, absence of defects, accuracy, or the presence or absence of errors.

Creative Commons Attribution Non-Commercial License

The Creative Commons Attribution Non-Commercial (CC-BY-NC) License permits use, distribution and reproduction in any medium, provided the original work is properly cited and is not used for commercial purposes.(see below)

Creative Commons Attribution-Non-Commercial-NoDerivs License

The Creative Commons Attribution Non-Commercial-NoDerivs License (CC-BY-NC-ND) permits use, distribution and reproduction in any medium, provided the original work is properly cited, is not used for commercial purposes and no modifications or adaptations are made. (see below)

Use by non-commercial users

For non-commercial and non-promotional purposes, individual users may access, download, copy, display and redistribute to colleagues Wiley Open Access articles, as well as adapt, translate, text- and data-mine the content subject to the following conditions:

- The authors' moral rights are not compromised. These rights include the right of "paternity" (also known as "attribution" - the right for the author to be identified as such) and "integrity" (the right for the author not to have the work altered in such a way that the author's reputation or integrity may be impugned).
- Where content in the article is identified as belonging to a third party, it is the obligation of the user to ensure that any reuse complies with the copyright policies of the owner of that content.
- If article content is copied, downloaded or otherwise reused for non-commercial research and education purposes, a link to the appropriate bibliographic citation (authors, journal, article title, volume, issue, page numbers, DOI and the link to the definitive published version on **Wiley Online Library**) should be maintained. Copyright notices and disclaimers must not be deleted.

- Any translations, for which a prior translation agreement with Wiley has not been agreed, must prominently display the statement: "This is an unofficial translation of an article that appeared in a Wiley publication. The publisher has not endorsed this translation."

Use by commercial "for-profit" organisations

Use of Wiley Open Access articles for commercial, promotional, or marketing purposes requires further explicit permission from Wiley and will be subject to a fee. Commercial purposes include:

- Copying or downloading of articles, or linking to such articles for further redistribution, sale or licensing;
- Copying, downloading or posting by a site or service that incorporates advertising with such content;
- The inclusion or incorporation of article content in other works or services (other than normal quotations with an appropriate citation) that is then available for sale or licensing, for a fee (for example, a compilation produced for marketing purposes, inclusion in a sales pack)
- Use of article content (other than normal quotations with appropriate citation) by for-profit organisations for promotional purposes
- Linking to article content in e-mails redistributed for promotional, marketing or educational purposes;
- Use for the purposes of monetary reward by means of sale, resale, licence, loan, transfer or other form of commercial exploitation such as marketing products
- Print reprints of Wiley Open Access articles can be purchased from: corporatesales@wiley.com

Further details can be found on Wiley Online Library
http://olabout.wiley.com/WileyCDA/Section/id-410895.html

Other Terms and Conditions:

v1.9

You will be invoiced within 48 hours of this transaction date. You may pay your invoice by credit card upon receipt of the invoice for this transaction. Please follow instructions provided at that time.
To pay for this transaction now; please remit a copy of this document along with your payment. Payment should be in the form of a check or money order referencing your account number and this invoice number RLNK501366664.
Make payments to "COPYRIGHT CLEARANCE CENTER" and send to:

00533900 re:Copyright Permission

"Micah Magante" <info@biomedcentral.com>

Fri 1/08/2014 4:34 PM

To Lucy Murtha <Lucy.Murtha@uon.edu.au>;

Dear Dr Lucy

Thank you for contacting BioMed Central.

Copyright on any research article in all journals published by BioMed Central is retained by the author(s).

Authors grant BioMed Central a license to publish the article and identify itself as the original publisher.

Authors also grant any third party the right to use the article freely as long as its integrity is maintained and its original authors, citation details and publisher are identified.

The BioMed Central Copyright and License Agreement (identical to the Creative Commons Attribution License) formalizes these and other terms and conditions of publishing research articles.

For more information please go to:
http://www.biomedcentral.com/info/about/copyright

If you have any questions please do not hesitate to contact me.

Best wishes

Jorge Menil Jr
Customer Services
info@biomedcentral.com
www.biomedcentral.com
----------Your Question/Comment ----------

To whom it may concern,

I am contacting you to seek written permission to copy and communicate the following material within the electronic version of my Doctor of Philosophy thesis:

Murtha L, Yang Q, Parsons M, Levi C, Beard D, Spratt N, McLeod D. Cerebrospinal fluid is drained primarily via the spinal canal and olfactory route in young and aged spontaneously hypertensive rats. Fluids Barriers CNS. 11:12, doi:10.1186/2045-8118-11-12. (2014).

If you are not the rights holder for this material I would be grateful if you would advise me who to contact. The thesis will be made available on the internet via the University of Newcastle's online digital repository
http://ogma.newcastle.edu.au:8080/vital/access/manager/Index

Kind regards,

Lucy

Lucy Murtha, PhD Candidate
Translation Stroke Research Group
School of Biomedical Sciences & Pharmacy
Rm 504, Medical Sciences Building
The University of Newcastle
University Drive, Callaghan
NSW 2308 Australia
Ph: +61 2 4921 7303

ref:_00D20CUt._50020d8JNMAA2:ref

JOHN WILEY AND SONS LICENSE TERMS AND CONDITIONS

Jul 31, 2014

This is a License Agreement between Lucy A Murtha ("You") and John Wiley and Sons ("John Wiley and Sons") provided by Copyright Clearance Center ("CCC"). The license consists of your order details, the terms and conditions provided by John Wiley and Sons, and the payment terms and conditions.

All payments must be made in full to CCC. For payment instructions, please see information listed at the bottom of this form.

License Number	3439661393281
License date	Jul 31, 2014
Licensed content publisher	John Wiley and Sons
Licensed content publication	International Journal of Stroke
Licensed content title	Perfusion computed tomography thresholds defining ischemic penumbra and infarct core: studies in a rat stroke model
Licensed copyright line	© 2013 The Authors. International Journal of Stroke © 2013 World Stroke Organization
Licensed content author	D. D. McLeod,M. W. Parsons,R. Hood,B. Hiles,J. Allen,S. K. McCann,L. Murtha,M. B. Calford,C. R. Levi,N. J. Spratt
Licensed content date	Oct 21, 2013
Start page	n/a
End page	n/a
Type of use	Dissertation/Thesis
Requestor type	Author of this Wiley article
Format	Print and electronic
Portion	Full article
Will you be translating?	No
Title of your thesis / dissertation	THE EFFECTS AND MECHANISMS OF THERAPEUTIC HYPOTHERMIA ON INTRACRANIAL PRESSURE REGULATION FOLLOWING ISCHAEMIC STROKE IN RATS
Expected completion date	Sep 2014
Expected size (number of pages)	70
Total	0.00 USD
Terms and Conditions	

TERMS AND CONDITIONS

This copyrighted material is owned by or exclusively licensed to John Wiley & Sons, Inc. or one of its group companies (each a"Wiley Company") or handled on behalf of a society with which a Wiley Company has exclusive publishing rights in relation to a particular work (collectively "WILEY"). By clicking accept in connection with completing this licensing transaction, you

agree that the following terms and conditions apply to this transaction (along with the billing and payment terms and conditions established by the Copyright Clearance Center Inc., ("CCC's Billing and Payment terms and conditions"), at the time that you opened your Rightslink account (these are available at any time at http://myaccount.copyright.com).

Terms and Conditions

- The materials you have requested permission to reproduce or reuse (the "Wiley Materials") are protected by copyright.

- You are hereby granted a personal, non-exclusive, non-sub licensable (on a stand-alone basis), non-transferable, worldwide, limited license to reproduce the Wiley Materials for the purpose specified in the licensing process. This license is for a one-time use only and limited to any maximum distribution number specified in the license. The first instance of republication or reuse granted by this licence must be completed within two years of the date of the grant of this licence (although copies prepared before the end date may be distributed thereafter). The Wiley Materials shall not be used in any other manner or for any other purpose, beyond what is granted in the license. Permission is granted subject to an appropriate acknowledgement given to the author, title of the material/book/journal and the publisher. You shall also duplicate the copyright notice that appears in the Wiley publication in your use of the Wiley Material. Permission is also granted on the understanding that nowhere in the text is a previously published source acknowledged for all or part of this Wiley Material. Any third party content is expressly excluded from this permission.

- With respect to the Wiley Materials, all rights are reserved. Except as expressly granted by the terms of the license, no part of the Wiley Materials may be copied, modified, adapted (except for minor reformatting required by the new Publication), translated, reproduced, transferred or distributed, in any form or by any means, and no derivative works may be made based on the Wiley Materials without the prior permission of the respective copyright owner. You may not alter, remove or suppress in any manner any copyright, trademark or other notices displayed by the Wiley Materials. You may not license, rent, sell, loan, lease, pledge, offer as security, transfer or assign the Wiley Materials on a stand-alone basis, or any of the rights granted to you hereunder to any other person.

- The Wiley Materials and all of the intellectual property rights therein shall at all times remain the exclusive property of John Wiley & Sons Inc, the Wiley Companies, or their respective licensors, and your interest therein is only that of having possession of and the right to reproduce the Wiley Materials pursuant to Section 2 herein during the continuance of this Agreement. You agree that you own no right, title or interest in or to the Wiley Materials or any of the intellectual property rights therein. You shall have no rights hereunder other than the license as provided for above in Section 2. No right, license or interest to any trademark, trade name, service mark or other branding ("Marks") of WILEY or its licensors is granted hereunder, and you agree that you shall not assert any such right, license or interest with respect thereto.

- NEITHER WILEY NOR ITS LICENSORS MAKES ANY WARRANTY OR REPRESENTATION OF ANY KIND TO YOU OR ANY THIRD PARTY, EXPRESS, IMPLIED OR STATUTORY, WITH RESPECT TO THE MATERIALS OR THE

ACCURACY OF ANY INFORMATION CONTAINED IN THE MATERIALS, INCLUDING, WITHOUT LIMITATION, ANY IMPLIED WARRANTY OF MERCHANTABILITY, ACCURACY, SATISFACTORY QUALITY, FITNESS FOR A PARTICULAR PURPOSE, USABILITY, INTEGRATION OR NON-INFRINGEMENT AND ALL SUCH WARRANTIES ARE HEREBY EXCLUDED BY WILEY AND ITS LICENSORS AND WAIVED BY YOU

- WILEY shall have the right to terminate this Agreement immediately upon breach of this Agreement by you.
- You shall indemnify, defend and hold harmless WILEY, its Licensors and their respective directors, officers, agents and employees, from and against any actual or threatened claims, demands, causes of action or proceedings arising from any breach of this Agreement by you.
- IN NO EVENT SHALL WILEY OR ITS LICENSORS BE LIABLE TO YOU OR ANY OTHER PARTY OR ANY OTHER PERSON OR ENTITY FOR ANY SPECIAL, CONSEQUENTIAL, INCIDENTAL, INDIRECT, EXEMPLARY OR PUNITIVE DAMAGES, HOWEVER CAUSED, ARISING OUT OF OR IN CONNECTION WITH THE DOWNLOADING, PROVISIONING, VIEWING OR USE OF THE MATERIALS REGARDLESS OF THE FORM OF ACTION, WHETHER FOR BREACH OF CONTRACT, BREACH OF WARRANTY, TORT, NEGLIGENCE, INFRINGEMENT OR OTHERWISE (INCLUDING, WITHOUT LIMITATION, DAMAGES BASED ON LOSS OF PROFITS, DATA, FILES, USE, BUSINESS OPPORTUNITY OR CLAIMS OF THIRD PARTIES), AND WHETHER OR NOT THE PARTY HAS BEEN ADVISED OF THE POSSIBILITY OF SUCH DAMAGES. THIS LIMITATION SHALL APPLY NOTWITHSTANDING ANY FAILURE OF ESSENTIAL PURPOSE OF ANY LIMITED REMEDY PROVIDED HEREIN.
- Should any provision of this Agreement be held by a court of competent jurisdiction to be illegal, invalid, or unenforceable, that provision shall be deemed amended to achieve as nearly as possible the same economic effect as the original provision, and the legality, validity and enforceability of the remaining provisions of this Agreement shall not be affected or impaired thereby.
- The failure of either party to enforce any term or condition of this Agreement shall not constitute a waiver of either party's right to enforce each and every term and condition of this Agreement. No breach under this agreement shall be deemed waived or excused by either party unless such waiver or consent is in writing signed by the party granting such waiver or consent. The waiver by or consent of a party to a breach of any provision of this Agreement shall not operate or be construed as a waiver of or consent to any other or subsequent breach by such other party.
- This Agreement may not be assigned (including by operation of law or otherwise) by you without WILEY's prior written consent.
- Any fee required for this permission shall be non-refundable after thirty (30) days from receipt by the CCC.
- These terms and conditions together with CCC's Billing and Payment terms and conditions

(which are incorporated herein) form the entire agreement between you and WILEY concerning this licensing transaction and (in the absence of fraud) supersedes all prior agreements and representations of the parties, oral or written. This Agreement may not be amended except in writing signed by both parties. This Agreement shall be binding upon and inure to the benefit of the parties' successors, legal representatives, and authorized assigns.

- In the event of any conflict between your obligations established by these terms and conditions and those established by CCC's Billing and Payment terms and conditions, these terms and conditions shall prevail.
- WILEY expressly reserves all rights not specifically granted in the combination of (i) the license details provided by you and accepted in the course of this licensing transaction, (ii) these terms and conditions and (iii) CCC's Billing and Payment terms and conditions.
- This Agreement will be void if the Type of Use, Format, Circulation, or Requestor Type was misrepresented during the licensing process.
- This Agreement shall be governed by and construed in accordance with the laws of the State of New York, USA, without regards to such state's conflict of law rules. Any legal action, suit or proceeding arising out of or relating to these Terms and Conditions or the breach thereof shall be instituted in a court of competent jurisdiction in New York County in the State of New York in the United States of America and each party hereby consents and submits to the personal jurisdiction of such court, waives any objection to venue in such court and consents to service of process by registered or certified mail, return receipt requested, at the last known address of such party.

WILEY OPEN ACCESS TERMS AND CONDITIONS

Wiley Publishes Open Access Articles in fully Open Access Journals and in Subscription journals offering Online Open. Although most of the fully Open Access journals publish open access articles under the terms of the Creative Commons Attribution (CC BY) License only, the subscription journals and a few of the Open Access Journals offer a choice of Creative Commons Licenses:: Creative Commons Attribution (CC-BY) license Creative Commons Attribution Non-Commercial (CC-BY-NC) license and Creative Commons Attribution Non-Commercial-NoDerivs (CC-BY-NC-ND) License. The license type is clearly identified on the article.

Copyright in any research article in a journal published as Open Access under a Creative Commons License is retained by the author(s). Authors grant Wiley a license to publish the article and identify itself as the original publisher. Authors also grant any third party the right to use the article freely as long as its integrity is maintained and its original authors, citation details and publisher are identified as follows: [Title of Article/Author/Journal Title and Volume/Issue. Copyright (c) [year] [copyright owner as specified in the Journal]. Links to the final article on Wiley's website are encouraged where applicable.

The Creative Commons Attribution License

The Creative Commons Attribution License (CC-BY) allows users to copy, distribute and transmit an article, adapt the article and make commercial use of the article. The CC-BY license permits commercial and non-commercial re-use of an open access article, as long as the author is properly

attributed.

The Creative Commons Attribution License does not affect the moral rights of authors, including without limitation the right not to have their work subjected to derogatory treatment. It also does not affect any other rights held by authors or third parties in the article, including without limitation the rights of privacy and publicity. Use of the article must not assert or imply, whether implicitly or explicitly, any connection with, endorsement or sponsorship of such use by the author, publisher or any other party associated with the article.

For any reuse or distribution, users must include the copyright notice and make clear to others that the article is made available under a Creative Commons Attribution license, linking to the relevant Creative Commons web page.

To the fullest extent permitted by applicable law, the article is made available as is and without representation or warranties of any kind whether express, implied, statutory or otherwise and including, without limitation, warranties of title, merchantability, fitness for a particular purpose, non-infringement, absence of defects, accuracy, or the presence or absence of errors.

Creative Commons Attribution Non-Commercial License

The Creative Commons Attribution Non-Commercial (CC-BY-NC) License permits use, distribution and reproduction in any medium, provided the original work is properly cited and is not used for commercial purposes.(see below)

Creative Commons Attribution-Non-Commercial-NoDerivs License

The Creative Commons Attribution Non-Commercial-NoDerivs License (CC-BY-NC-ND) permits use, distribution and reproduction in any medium, provided the original work is properly cited, is not used for commercial purposes and no modifications or adaptations are made. (see below)

Use by non-commercial users

For non-commercial and non-promotional purposes, individual users may access, download, copy, display and redistribute to colleagues Wiley Open Access articles, as well as adapt, translate, text- and data-mine the content subject to the following conditions:

- The authors' moral rights are not compromised. These rights include the right of "paternity" (also known as "attribution" - the right for the author to be identified as such) and "integrity" (the right for the author not to have the work altered in such a way that the author's reputation or integrity may be impugned).
- Where content in the article is identified as belonging to a third party, it is the obligation of the user to ensure that any reuse complies with the copyright policies of the owner of that content.
- If article content is copied, downloaded or otherwise reused for non-commercial research and education purposes, a link to the appropriate bibliographic citation (authors, journal, article title, volume, issue, page numbers, DOI and the link to the definitive published version on **Wiley Online Library**) should be maintained. Copyright notices and disclaimers must not be deleted.

- Any translations, for which a prior translation agreement with Wiley has not been agreed, must prominently display the statement: "This is an unofficial translation of an article that appeared in a Wiley publication. The publisher has not endorsed this translation."

Use by commercial "for-profit" organisations

Use of Wiley Open Access articles for commercial, promotional, or marketing purposes requires further explicit permission from Wiley and will be subject to a fee. Commercial purposes include:

- Copying or downloading of articles, or linking to such articles for further redistribution, sale or licensing;
- Copying, downloading or posting by a site or service that incorporates advertising with such content;
- The inclusion or incorporation of article content in other works or services (other than normal quotations with an appropriate citation) that is then available for sale or licensing, for a fee (for example, a compilation produced for marketing purposes, inclusion in a sales pack)
- Use of article content (other than normal quotations with appropriate citation) by for-profit organisations for promotional purposes
- Linking to article content in e-mails redistributed for promotional, marketing or educational purposes;
- Use for the purposes of monetary reward by means of sale, resale, licence, loan, transfer or other form of commercial exploitation such as marketing products
- Print reprints of Wiley Open Access articles can be purchased from: corporatesales@wiley.com

Further details can be found on Wiley Online Library
http://olabout.wiley.com/WileyCDA/Section/id-410895.html

Other Terms and Conditions:

v1.9

You will be invoiced within 48 hours of this transaction date. You may pay your invoice by credit card upon receipt of the invoice for this transaction. Please follow instructions provided at that time.
To pay for this transaction now; please remit a copy of this document along with your payment. Payment should be in the form of a check or money order referencing your account number and this invoice number RLNK501366699.
Make payments to "COPYRIGHT CLEARANCE CENTER" and send to: